Clinical pharmacology and bioanalysis of antileishmanial drugs

Towards improved treatment strategies for leishmaniasis

Clinical pharmacology and bioanalysis of antileishmanial drugs

Towards improved treatment strategies for leishmaniasis

Klinische farmacologie en bioanalyse van antileishmaniale geneesmiddelen

Op weg naar verbeterde behandelstrategieën voor leishmaniasis

(met een samenvatting in het Nederlands)

Proefschrift

ter verkrijging van de graad van doctor aan de Universiteit Utrecht op gezag van de rector magnificus, prof.dr. G.J. van der Zwaan, ingevolge het besluit van het college voor promoties in het openbaar te verdedigen op woensdag 21 juni 2017 des middags te 2.30 uur

door

Antonia Elisabeth Kip

geboren op 27 juni 1987 te Eindhoven

CONTENTS

PREFACE

Leishmaniasis is a tropical infectious disease particularly affecting poor and neglected patients in remote areas. Leishmaniasis is caused by the intracellular protozoan parasite *Leishmania*, transmitted to humans by the sandfly. There are over twenty different *Leishmania* species, causing different clinical presentations. Visceral leishmaniasis, classically known as kala-azar which is Hindi for black fever, is the most devastating and fatal form of leishmaniasis caused by a systemic infection of the liver, spleen and/or bone marrow. With 20,000-40,000 deaths per year, this condition is the second largest parasitic killer in the world [1]. An estimated 0.2-0.4 million visceral leishmaniasis cases occur annually, 90% of which in India, Bangladesh, Sudan, South Sudan, Ethiopia and Brazil [1]. A large proportion of visceral leishmaniasis patients, up to 60% in Sudan, experience parasite recurrence in the form of the skin infection post-kala-azar dermal leishmaniasis. The most common and more widely distributed clinical manifestation is the skin infection cutaneous leishmaniasis, with an estimated 0.7-1.2 million cases annually and highest occurrences in the Americas, the Mediterranean basin and the Middle East [1]. The disfigurement, ulceration and often permanent scarring as a result of cutaneous or post-kala-azar dermal leishmaniasis are frequently associated with stigmatization. The social stigma results in isolation and increased rates of depression and anxiety, and affects the individual's opportunity for education, employment and marriage.

Current treatment options for leishmaniasis are far from sufficient. Since the 1940s, pentavalent antimonials have been administered against leishmaniasis, with considerable toxicity. Newer treatment options such as liposomal amphotericin B and the oral drug miltefosine cause less severe side-effects, but their failure rates are unacceptably high in certain endemic regions, especially in East Africa for treatment of visceral leishmaniasis.

Since 2000 there has been a surge in research on new treatment solutions against tropical diseases, and in particular leishmaniasis, mainly due to the advent of public-private partnerships [2]. In addition to the identification of new chemical entities and subsequent drug development, it is key to optimize the antileishmanial treatment with existing drugs to provide the best possible treatment solutions to the neglected leishmaniasis patients.

This thesis investigates antileishmanial treatment optimization by clinical pharmacological research, with a specific focus on the treatment of particularly neglected pediatric and HIV co-infected patient populations.

Chapter 1 provides a comprehensive overview of the clinical pharmacokinetics of all systemically administered drugs for treatment of visceral and cutaneous leishmaniasis currently available. Additionally, this chapter identifies remaining gaps in knowledge and directions for research.

To investigate the pharmacokinetics of antileishmanial drugs, accurate, precise and reliable bioanalytical methods are required to determine drug concentrations. In the visceral leishmaniasis patient population, largely consisting of children, there is a need for non-invasive sampling methods. In addition, the remote leishmaniasis endemic areas call for ease of storage and transport and prolonged sample stability. The clinical pharmacokinetic studies described in this thesis focus mainly on the antileishmanial drug miltefosine. The development and validation of three bioanalytical methods to quantify miltefosine in different human matrices are described in **chapter 2**.

Chapter 2.1 describes the bioanalytical and clinical validation of a liquid chromatography-tandem mass spectrometry method to quantify miltefosine in dried blood spot (DBS) samples. DBS sampling is less invasive than venous blood sampling and DBS samples are easier and cheaper to store and transport. Hematocrit was found to be a potential factor influencing the accuracy of DBS methods and therefore volumetric absorptive microsampling was evaluated as an alternative to DBS sampling in **chapter 2.2**, having the potential to overcome this hematocrit effect.

Leishmania parasites reside within macrophages, which means intracellular drug concentrations within peripheral blood mononuclear cells (PBMCs) could be considered a better approximation of the parasite's exposure to the drug than drug plasma or whole blood concentrations. The development and validation of a method to quantify intracellular miltefosine in PBMCs is presented in **chapter 2.3**. The intracellular miltefosine kinetics has been described by a population pharmacokinetic model in **chapter 3.1**. In addition, this chapter describes the first exploration in correlating miltefosine plasma and intracellular drug exposure to treatment outcome in cutaneous leishmaniasis employing a population modelling approach.

In visceral leishmaniasis, several studies have described a lower miltefosine efficacy [3–5] and lower miltefosine exposure [6,7] in pediatric compared to adult patients. An improved allometric miltefosine dose has previously been proposed for children, in which patients with a smaller body size receive a relatively higher mg/kg dose compared to the 2.5 mg/kg standard dose [7]. **Chapter 3.2** describes the pharmacokinetics of the allometric miltefosine dosing regimen in its first clinical evaluation in East African pediatric visceral leishmaniasis patients, using population pharmacokinetic modelling. In **chapter 3.3**, the pharmacokinetics of the allometric dosing regimen are characterized in Bangladeshi post-kala-azar dermal leishmaniasis pediatric patients and linked to treatment outcome.

Current treatment options for visceral leishmaniasis patients co-infected with HIV are limited and efficacy is generally low with high relapse rates. Yet the pharmacokinetics of antileishmanial drugs has never been studied in this specific patient population. **Chapter 3.4** describes the first study of the pharmacokinetics of antileishmanial drugs miltefosine and liposomal amphotericin B, and concomitantly administered antiretroviral drugs, in Ethiopian visceral leishmaniasis patients co-infected with HIV.

Clinical evaluation of new drug (combination) regimens against visceral leishmaniasis, particularly in East Africa, is hampered by the frequent occurrence of relapses [8,9]. A follow-up of at least six months after treatment is necessary to determine final cure rates. To speed up the drug development process in antileishmanial treatment, identification of appropriate pharmacodynamic biomarkers that could serve as surrogate endpoints of long-term efficacy is essential. **Chapter 4.1** provides an overview of pharmacodynamic markers which could be further investigated for their use as biomarkers monitoring treatment outcome. Macrophage activation marker neopterin has been evaluated as longitudinal marker of treatment response for two antileishmanial regimens, which is described in **chapter 4.2**.

In **chapter 5**, conclusions of the presented research are discussed and placed in a broader perspective to provide directions for future efforts to further rationalize and optimize antileishmanial therapies, especially in the most vulnerable patient populations.

REFERENCES

1. Alvar J, Vélez ID, Bern C, Herrero M, Desjeux P, Cano J, et al. Leishmaniasis worldwide and global estimates of its incidence. PLoS One. 2012;7:e35671.

2. Moran M. A breakthrough in R&D for neglected diseases: New ways to get the drugs we need. PLoS Med. 2005;2:e302.

3. Ostyn B, Hasker E, Dorlo TPC, Rijal S, Sundar S, Dujardin J, et al. Failure of miltefosine treatment for visceral leishmaniasis in children and men in South-East Asia. PLoS One. 2014;9:e100220.

4. Wasunna M, Njenga S, Balasegaram M, Alexander N, Omollo R, Edwards T, et al. Efficacy and safety of AmBisome in combination with sodium stibogluconate or miltefosine and miltefosine monotherapy for African visceral leishmaniasis: phase II randomized trial. PLoS Negl. Trop. Dis. 2016;10:e0004880.

5. Bhattacharya SK, Sinha PK, Sundar S, Thakur CP, Jha TK, Pandey K, et al. Phase 4 trial of miltefosine for the treatment of Indian visceral leishmaniasis. J. Infect. Dis. 2007;196:591–8.

6. Dorlo TPC, Kip AE, Younis BM, Ellis SE, Alves F, Beijnen JH, et al. Reduced miltefosine exposure in East African visceral leishmaniasis patients affects the time to relapse of infection. 2017; Submitted for publication.

7. Dorlo TPC, Huitema ADR, Beijnen JH, De Vries PJ. Optimal dosing of miltefosine in children and adults with visceral leishmaniasis. Antimicrob. Agents Chemother. 2012;56:3864–72.

8. Rijal S, Ostyn B, Uranw S, Rai K, Bhattarai NR, Dorlo TPC, et al. Increasing failure of miltefosine in the treatment of kala-azar in nepal and the potential role of parasite drug resistance, reinfection, or noncompliance. Clin. Infect. Dis. 2013;56:1530–8.

9. Sundar S, Singh A, Rai M, Prajapati VK, Singh AK, Ostyn B, et al. Efficacy of miltefosine in the treatment of visceral leishmaniasis in India after a decade of use. Clin. Infect. Dis. 2012;55:543–50.

Chapter 1

Introduction

Chapter 1

Clinical pharmacokinetics of systemically administered antileishmanial drugs

A.E. Kip
J.H.M. Schellens
J.H. Beijnen
T.P.C. Dorlo

ABSTRACT

This review describes the pharmacokinetic properties of the systemically administered antileishmanial drugs pentavalent antimony, paromomycin, pentamidine, miltefosine and amphotericin B, including their absorption, distribution, metabolism and excretion and potential drug-drug interactions. This overview provides an understanding of their clinical pharmacokinetics, which could assist in rationalizing and optimizing treatment regimens especially in combining multiple antileishmanial drugs in an attempt to increase efficacy and shorten treatment duration.

Pentavalent antimony pharmacokinetics is characterized by rapid renal excretion of unchanged drug and long terminal half-life potentially due to intracellular conversion to trivalent antimony. Pentamidine is the only antileishmanial drug metabolized by cytochrome P450 enzymes. Paromomycin is excreted by the kidneys unchanged and is eliminated fastest of all antileishmanial drugs. Miltefosine pharmacokinetics is characterized by a long terminal half-life and extensive accumulation during treatment. Amphotericin B pharmacokinetics differs per drug formulation, with a fast renal and faecal excretion of amphotericin B deoxylate, but a much slower clearance of liposomal amphotericin B resulting in an approximately ten-fold higher exposure.

Amphotericin B and pentamidine pharmacokinetics have never been evaluated in leishmaniasis patients. Studies linking exposure to effect would be required to define target exposure levels in dose optimization, but have only been performed for miltefosine. Limited research has been conducted on exposure at the drug's site of action, such as skin exposure in cutaneous leishmaniasis patients. Pharmacokinetic data on special patient populations such as HIV co-infected patients are mostly lacking. More research in these areas will help improve clinical outcomes by informed dosing and combination of drugs.

INTRODUCTION

Leishmaniasis is a neglected tropical disease caused by the *Leishmania* parasite and can cause diverse clinical manifestations depending on the subspecies responsible for the infection and the host immune response. The two main types are the systemic disease visceral leishmaniasis (VL) and the skin infection cutaneous leishmaniasis (CL). Several drugs (Table 1) are currently used in clinical practice in treatment of both VL and CL [1,2], but clinical guidelines differ per region. Clinical results obtained in one area of endemicity cannot be extrapolated to other geographical areas as efficacies have been shown to vary widely between countries and parasite subspecies (reviewed in [3,4]).

Rising levels of resistance against antimonials, mostly in India, and potentially miltefosine is a great pitfall in the treatment of leishmaniasis patients [4,5]. Available treatment options are limited, especially in vulnerable patient populations such as paediatric leishmaniasis patients and HIV patients co-infected with VL. Therefore, several new combinations of drugs are currently being tested to improve the efficacy of anti-leishmanial therapies. Furthermore, combination therapies could possibly shorten treatment duration and thereby lower the costs of treatment.

Pharmacokinetics provides a scientific framework for choosing the appropriate (combination of) drugs and their dosage. The clinical pharmacokinetics of antileishmanial drugs, however, remains largely unexplored [6]. The aim of this review is to give a comprehensive overview of the pharmacokinetic (PK) characteristics relating to the absorption, distribution, metabolism and excretion (ADME) of antileishmanial drugs currently being used in the clinic, as a basis to further rationalize the therapy for leishmaniasis. Albeit the pharmacokinetics of miltefosine [7] and liposomal amphotericin B (L-AMB, with focus on treatment of fungal infections [8]) have previously been reviewed, our aim was to discuss all systemically administered antileishmanial drugs collectively in the context of leishmaniasis.

A summary is composed of all PK studies performed, providing the reported primary and secondary PK parameters in overview tables. The pharmacokinetics in special patient populations relevant in treatment of leishmaniasis will be described: paediatric patients, HIV co-infected patients, pregnant patients and patients with renal failure. Furthermore, potential drug-drug interactions between antileishmanial drugs, as well as between antileishmanial and antiretroviral drugs will be discussed. In case information in humans is lacking, *in vitro* and *in vivo* animal studies will be examined.

In this review we solely focus on systemically administered drugs, as the majority of these drugs are administered in both CL and VL. The systemic drugs included in this review (Table 1) are based on the WHO guidelines on Control of the Leishmaniases [2]: pentavalent antimony, paromomycin, pentamidine, miltefosine and amphotericin B (AMB). In addition to these ketoconazole has been mentioned in systemic treatment of New World CL species. Given the drug's limited clinical use and the U.S. Food and Drug Administration's and European Medicines Agency's decisions to suspend its oral use in skin infections due to severe hepatotoxicity [9], ketoconazole is not being discussed in this review.

With this review we aim to provide a more solid PK basis for a scientific approach to treatment design in future clinical studies investigating (combination) treatments against leishmaniasis. In addition, our aim was to identify knowledge gaps to guide future PK studies in this clinical area.

Table 1. Overview of antileishmanial drugs systemically administered in treatment of visceral and/or cutaneous leishmaniasis.

Antileishmanial drug	Formulations	IM/IV/ Oral	Distribution – Highest accumulation	Distribution - Skin	Metabolism	Excretion
Pentavalent antimonials	- Sodium stibugluconate (SSG) - Meglumine Antimoniate (MA)	IM/IV	Liver, thyroid, heart	Confirmed	Intracellular reduction to Sb^{III}	Renal clearance
Paromomycin	- Paromomycin sulphate	IM	Not reported	Not reported	Not metabolized	Renal clearance
Pentamidine	- Pentamidine dimesylate - Pentamidine isethionate	IM/IV	Kidney, liver, spleen, adrenal glands	Not reported	CYP1A1, (CYP2D6, CYP3A5 and CYP4A11)	Not excreted unchanged
Miltefosine	- Miltefosine	Oral	Not reported (rat/mice: kidney, liver, spleen, intestines, adrenal)	Not reported (in rats: Confirmed)	Intracellularly by phospholipase D	Not excreted unchanged (metabolized to endogenous compounds)
Amphotericin B[a]	- Amphotericin B deoxylate (D-AMB) - Liposomal amphotericin B (L-AMB)	IV	Liver, spleen	Not reported (in rats: Confirmed)	Metabolism not well studied. Liposomes engulfed by RES	D-AMB: urinary excretion (21%) / faecal excretion (43%) L-AMB: urinary excretion (5%) /faecal excretion (4%)

Only includes information in human subjects (unless indicated otherwise). IM: intramuscular, IV: intravenous, CYP: cytochrome P450.
[a]More lipid formulations exist of amphotericin B, but these are outside the scope of this review.

METHODS

PK studies were included in this review (Table 2 to Table 7) if PK parameters were reported in addition to drug concentrations. PK studies employing less sensitive bio-assays were excluded. Many PK studies have been conducted for AMB and for this reason we excluded studies with <10 subjects or patients, studies with continuous infusion, and studies on neonates <3 kg, based on their limited relevance in the context of the treatment of leishmaniasis. Studies on experimental formulations are excluded for all drugs, such as a PK study on the experimental generic SSG formulation "Ulamina" [10], as no records have been found of the commercialization of this formulation.

ADME AND CLINICAL PHARMACOKINETICS

Pentavalent antimonials
Pentavalent antimonials (Sb, pentavalent Sb/Sb^V) have been first-line treatment against CL and VL in the majority of endemic regions for decades, though increasing drug-resistance has compromised it efficacy [3,4]. Pentavalent antimonials are administered intramuscularly (IM) or intravenously (IV) in systemic treatment of both CL and VL. It is marketed in two formulations: sodium stibogluconate (SSG, marketed as Pentostam) and meglumine antimoniate (MA, marketed as Glucantime). The Sb content in the two antimonials is different with 85 mg Sb^V/mL in MA and 100 mg Sb^V/mL in SSG. Due to structural differences in these compounds, differences in PK could be expected. Unless indicated otherwise, results refer to SSG, as this

is the most widely studied compound. All PK studies used analytical methods that do not distinguish between different chemical forms of antimony (Sb^{III}, Sb^V, etc) [11]. The abbreviation Sb is used to refer to (total) antimony.

Despite being used in the clinic for decennia, Sb's mechanism of action is not well understood. Two main models currently exist: the pro-drug model and the active Sb^V model. According to the pro-drug model, Sb^V compounds are pro-drugs exerting its activity against the *Leishmania* parasite after reduction to Sb^{III} in host cells [12]. Sb^{III} finally induces apoptosis by the activation of oxidative stress and increase of intracellular Ca^{2+} [13,14]. In the active Sb^V model, Sb^V has intrinsic anti-leishmanial activity finally leading to the inhibition of DNA topoisomerase I [14]. Multiple studies identified an indirect effect of Sb on immune activation (overview in [15]). Most common side-effects of treatment with pentavalent antimony are myalgia/arthralgia, gastrointestinal problems and headache [16]. In addition, serious side effects have been reported such as cardiomyopathy, renal failure and reversible hepatic and pancreatic abnormalities [16,17].

ADME

After IM injection, Sb is absorbed quickly and the peak plasma concentration (C_{max}) is reached in between 0.5-2 hours (h) [11,18–20]. Absorption half-lives varied between 0.36 and 0.85 h [18,19]. In general, bioavailability is assumed to be close to 100% for IM injection.

Highest accumulation of Sb in human volunteers, after administration of radioactively labelled (Sb^{124}) sodium antimony mercapto-succinate, was recorded in the liver > thyroid > heart [21]. A full Sb tissue distribution study in rhesus monkeys on day 55 after receiving a 21-day MA treatment, showed highest Sb concentrations in the thyroid > nails > liver > gall bladder > spleen [22]. In rats, distribution at 24 h after a 21-day MA treatment was highest in the spleen > kidney > thyroid > liver [23]. No protein binding data were reported.

Sb is administered systemically in treatment of CL and several studies have investigated skin Sb distribution. Al-Jaser et al. identified a small delay in distribution to the skin with a time to C_{max} (t_{max}) of 2.1 h compared to ~1.5 h for whole blood [20]. Skin biopsies taken from both the CL lesion and unaffected skin from patients treated with ~10 mg/kg/day SSG for 10 days, indicated no difference in Sb distribution to affected versus healthy skin (mean±standard error of mean, SEM: C_{max} 5.02±1.43 and 6.56±2.01 µg/g, respectively) [20]. Studies in Brazilian CL patients reported higher tissue concentrations with high variability after 20 days of 10-20 mg Sb/kg/day (range 8.32-70.68 µg/g [24]) and 20 mg/kg/day (7.46±7.7 µg/g [25]). The wide spread in observed Sb tissue concentrations could possibly influence Sb efficacy in treatment of CL. However, no exposure-response studies were conducted relating skin exposure to treatment outcome.

The prevalent view is that Sb^V derived from Sb^V-based drugs is reduced to Sb^{III} intracellularly and subsequently released at slow rates, which partially explains the slow terminal elimination phase observed in total Sb. Current PK studies have focused on the analysis of total Sb (Table 2), but Miekeley et al. [26] used ICP-MS to analyze Sb^{III} and Sb^V separately. They reported the first evidence for *in vivo* conversion of MA into ion species Sb^V and Sb^{III} in humans. *In vitro*, two locations have been identified where this bioreduction could take place: the acidic compartment of mammalian cells such as the phagolysosome in which the *Leishmania* parasite resides, or the cytosol of the parasite itself [27].

Given the ten-fold higher toxicity of Sb^{III} species, the evaluation of Sb^{III} pharmacokinetics could play an important part in evaluating adverse effects and therapeutic action. Whilst the

Sb^{III} content was negligible in the original drug formulation, urine Sb^{III} concentrations of 111 µg/L were observed 11 days after the last MA injection. Also in monkeys, the proportion of Sb^{III} relative to total antimony, increased from 5% on day 1 to 50% on day 9, making it a major Sb plasma species during the slow terminal elimination phase [22].

Renal clearance is consistently documented to be the main route of Sb excretion [11,28]. The majority of Sb was eliminated via urine within 24 h after dosing with a short elimination half-life between 1.7 and 2.02 h [11,18,20,28,29]. Between 40%-80% of total dose given was retrieved in urine within 24 h of dosing [19,30]. The excess of the drug is excreted in nearly unaltered form in its formulation in complex with organic compound [26]. A significantly more rapid elimination could be observed in whole blood ($t_{1/2}$ = 3.04 h) compared to lesion tissue ($t_{1/2}$ = 6.88 h) [20].

<u>Clinical pharmacokinetics</u>
The pharmacokinetics of Sb (Table 2) administered IV or IM appeared similar: a two- or three-compartment model with bi-exponentional elimination with short half-life of approximately 2 h and a termimal elimination phase of 1-3 days was found for both IV [29] and IM data [11,18]. Miekeley et al. [26] - using the more sensitive ICP-MS for Sb analysis - reported an even slower terminal elimination half-life of >50 days, which could also be identified for monkeys (35.8 days) [22], hypothesized to be the intracellular conversion of Sb^V to Sb^{III}, and subsequent slow release [18].

C_{max} varied between 7.23-10.5 µg/mL for a 10 mg/kg daily dosing regimen [18,19,30] and was 38.8 µg/mL in adults receiving a 20 mg/kg dose daily. This non-linearity could possibly be explained by differences in formulation, as Chulay et al. reported a slightly higher C_{max} after MA administration (11.2 µg/mL, n=3) compared to SSG (9.4 µg/mL, n=2). However, interpretation is difficult due to the small sample size. Another possible explanation for these observations could be the lower clearance observed in the Colombian CL population. There were no significant differences in PK parameters between single dose and multiple dosing [19]. In Colombian CL patients, the pharmacokinetics appeared linear as the area under the concentration time curve from 0-24 h (AUC_{0-24h}) in children with a 50% increase in dose (20-30 mg/kg), increased 48% from 111 to 164 mg·h/L [11]. The Sb trough concentration (C_{trough}) gradually increased around four-fold during a 20-30 day treatment [11,18,28].

As mentioned previously, all PK studies used analytical methods that do not distinguish between different chemical forms of antimony (Sb^{III}, Sb^V, etc) [11]. Sb^{III} is assumed to be the active component in Sb treatment in the pro-drug model. As only a small proportion of total Sb consists of Sb^{III}, total Sb might not accurately reflect the pharmacokinetics of antimonials, especially as inter-patient differences could be expected in the intracellular reduction to Sb^{III}. This accentuates the relevance of studying the intracellular pharmacokinetics of Sb.

Paromomycin
Paromomycin, an aminoglycoside also known as aminosidine, is a highly hydrophilic and lipid insoluble antibiotic drug. Paromomycin is active against gram-positive and gram-negative bacteria, including *Mycobacterium tuberculosis*, and against some protozoa, including the *Leishmania* parasite. It is IM administered both as a monotherapy and as a shorter combination treatment together with SSG (reviewed in [31]). Paromomycin is formulated as the salt paromomycin sulphate, of which approximately 75% consists of the base although sulphate

Table 2. Pentavalent antimonials: primary and secondary pharmacokinetic parameters.

Author	Patients	Weight (kg)	Daily dose	Sampling day	C_{max} (µg/mL)	C_{trough} (µg/mL)	t_{max} (h)	k_a (h^{-1})	V/F (L)	CL/F (L/h)	AUC (mg·h/L)	$t_{1/2}$ (h)
Non-compartmental												
Cruz et al. [11][a]	Cutaneous leishmaniasis patients											
	Adults 20 mg/kg/day	62 (56–120)	20 mg/kg 20 days	Day 19	38.8±2.1	0.198±0.023	1.0 (1.0–2.0)	N/A	0.30±0.01[b,c]	0.106±0.006[b]	0–24h 190±10	$t_{1/2,\beta}$: 1.99±0.08 $t_{1/2,24-48h}$: 20.6±1.8
	Children 20 mg/kg/day	15 (13–18)	20 mg/kg 20 days	Day 19	32.7±0.9	0.113±0.015	0.875 (0.5–1.5)	N/A	0.39±0.03[b,c]	0.185±0.013[b]	0–24h 111±7	$t_{1/2,\beta}$: 1.48±0.02
	Children 30 mg/kg/day	17.5 (13–21)	20 mg/kg 19 days 30 mg/kg Day 20	Day 20	43.8±2.3	0.102±0.011	1.0 (1.0–1.5)	N/A	0.39±0.02[b,c]	0.186±0.012[b]	0–24h 164±10	$t_{1/2,\beta}$: 1.47±0.06 $t_{1/2,24-48h}$: 25.3±3.1
Zaghloul et al. [19][a]	Cutaneous leishmaniasis patients	66.4±8.7	First dose 300 mg (~5 mg/kg)	Day 1	6.4±1.4[d]	N/A	N/A	3.3[e]	239±32.6[f]	13.2 ±1.5	0–∞ 49.88±4.43[d]	$t_{1/2,\alpha}$: 0.41±0.15[g] $t_{1/2,\beta}$: 9.4±1.9[g]
			600 mg (~10 mg/kg) >3 weeks	N/A	7.23±1.58	N/A	1.7±0.19	1.9[e]	258±44.4[f]	12.86±1.58	0–∞ 65.4±8.3	$t_{1/2,\alpha}$: 1.68±1.3[g] $t_{1/2,\beta}$: 9.69±2.3[g]
Compartmental												
Al-Jaser et al. [30][a]	Cutaneous leishmaniasis patients	60–75	8–10 mg/kg 10 days	N/A	8.77±0.39	N/A	1.34±0.09	1.71±0.15	45.7±2.6	17.67±1.38	37.0±1.57	$t_{1/2,\alpha}$: 0.48±0.035 $t_{1/2,\beta}$: 1.85±0.072
Chulay et al. [18]	Visceral leishmaniasis patients	47.4±8.05	10 mg/kg 30 days	Day 1	10.5±1.2	0.062±0.018	2	0.8[e]	0.22±0.057[b]	N/A	N/A	$t_{1/2,\beta}$: 2.02±0.25 $t_{1/2,\gamma}$: 76±28
Pamplin et al. [29][a]	Cutaneous leishmaniasis patients	N/A	10 mg/kg 10 days	N/A	N/A	N/A	N/A	1.76	N/A	N/A	N/A	$t_{1/2,\alpha}$: 0.34±0.9 $t_{1/2,\beta}$: 1.72±0.6 $t_{1/2,\gamma}$: 32.8±3.8

Data provided as either a) mean±standard deviation or b) median (range), unless indicated otherwise. N/A: Not Available. C_{max}: peak plasma concentration, C_{trough}: trough plasma concentration, C_{trough}: trough plasma concentration 24 h after dose, t_{max}: time to C_{max}, k_a: absorption rate constant, V: volume of distribution, F: bioavailability, CL: clearance, AUC: area under the concentration-time curve, $t_{1/2}$: plasma half-life.
[a]Values reported as mean±standard error of the mean
[b]Per kg
[c]V_d, apparent volume of distribution during the β-elimination phase
[d]Data normalized to a 600 mg dose
[e]Documented as absorption $t_{1/2}$
[f]V is reported as V_{ss}, the steady state volume of distribution including both the central and peripheral compartment.
[g]Calculated with compartmental analysis, reported as distribution half-life (indicated as $t_{1/2,\alpha}$) and elimination half-life (indicated as $t_{1/2,\beta}$)

salt contents vary per batch [32].

Paromomycin inhibits protozoan protein synthesis by binding to the 30S ribosomal subunit resulting in the accumulation of abnormal 30S-50S ribosomal complexes and finally causing cell death. In the phase III clinical trial in Indian VL patients, the most common side-effects were injection site pain (55%), rise in hepatic transaminases (6%), ototoxicity (2%) and renal dysfunction (1%) [33].

ADME

Paromomycin is generally assumed and documented to be very poorly absorbed after oral administration [34,35]. However, like other aminoglycosides, it is rapidly absorbed from IM injection sites and its absorption is nearly 100% [32]. The t_{max} is reached within one or two hours after IM injection [33,36,37]. The absorption rate constant was found to be 2.11-2.65 h^{-1} for a 15 mg/kg dose, but 6.27 h^{-1} for the 12 mg/kg dosing [36,38], though variation in the latter is large (standard deviation, SD of 4.41 h^{-1}).

At physiological pH, paromomycin is polar, which limits its distribution towards the intracellular fluids and tissues. In dogs, protein binding is limited to 4% [39], similar to other aminoglycides' binding in human serum [40]. Protein binding of paromomycin in humans is mostly stated to be negligible, though one study reported 33% protein-bound paromomycin [41]. The one-compartmental population PK model with low distribution volume (V_d) of only 15.3 L that has been reported [38], is consistent with limited distribution and protein binding.

Paromomycin is not metabolized and is primarily excreted unchanged via glomerular filtration in the kidneys [32,41,42]. Elimination of paromomycin is fast: within four hours over 50% of the dose could be detected in urine [36]. The elimination half-life is between two and three hours [36,38].

Clinical pharmacokinetics

Two studies were performed on paromomycin pharmacokinetics (Table 3): one in healthy volunteers and one in a large population of Indian VL patients. Primary and secondary PK parameters were comparable between the two studies, indicating there were no specific disease effects of VL on the pharmacokinetics of paromomycin [36,38].

V_d was directly proportional to weight and was around 0.4 L/kg for both studies [37,39]. In the two studies, C_{max} was comparable (22-23 µg/mL versus 18-21 µg/mL), without differences between males and females. A similar C_{max} (mean±SD) was observed in healthy Sudanese subjects (19.5±7.6 µg/mL) [43]. Sudanese VL patients, however, had a much lower C_{max} of 5.6±4.2 µg/mL at 15 mg/kg and 7.8±4.9 µg/mL at 20 mg/kg [37]. This could imply differences in paromomycin pharmacokinetics in VL patients between regions, but interpretation is hampered by the small sample size in the Sudanese VL population (n=9).

There were no significant differences in dose-adjusted AUC until infinity ($AUC_{0-\infty}$) between dosing groups (12 mg/kg: 9.29±1.52 mg·h/L per kg; 15 mg/kg: 9.29±2.2 mg·h/L per kg), indicating linear pharmacokinetics at these dose levels. There was no evidence of drug accumulation or induction of metabolism upon multiple dosing [33]. C_{trough}, however, declined from 4.53±6.71 µg/mL on day 1 to 1.31±4.16 on day 21, but with high variation [33].

Paromomycin's site of action is intracellularly and resistance of parasites against paromomycin was found related to decreased drug uptake in resistant compared to wild-type strains [44]. This affirms the importance of evaluating intracellular PK of paromomycin in future PK studies.

Table 3. Paromomycin: primary and secondary pharmacokinetic parameters.

Author	Patients	Weight (kg)	Daily dose	Sampling day	C_{max} (µg/mL)	C_{trough} (µg/mL)	t_{max} (h)	k_a (h⁻¹)	V/F (L)	CL/F (L/h)	AUC (mg·h/mL)	$t_{1/2}$ (h)
Compartmental												
Kanyok et al. [36]	Healthy volunteers											
	12 mg/kg	68.2±14.0	12 mg/kg (9 mg/kg base) single-dose	Single-dose	21.6±2.3	<LLOQ	1.19±0.46	6.27±4.41	0.35±0.04[b,c]	7.1±0.78[d]	0–∞ 86.3±15.0	2.21±0.17
	15 mg/kg	70.7±13.0	15 mg/kg (11 mg/kg base) single-dose	Single-dose	23.4±3.9	<LLOQ	1.51±0.40	2.65±1.29	0.41±0.06[b,c]	7.6±1.94[d]	0–∞ 104.5±26.3	2.64±0.82
Kshirsagar et al. [38]	Visceral leishmaniasis patients	35.5±11.8[a]	15 mg/kg (11 mg/kg base) 21 days	Day 1	20.5±7.01	4.53±6.71	N/A	2.11 (7.68%)[e]	15.3 (2.27%)[e]	4.06 (3.05%)[e] IIV: 30.7%	N/A	2.62
				Day 21	18.3±8.86	1.31±4.16						

Data provided as mean±standard deviation, unless indicated otherwise. N/A: Not Available. C_{max}: peak plasma concentration, C_{trough}: trough plasma concentration 24 h after dose, t_{max}: time to C_{max}, k_a: absorption rate constant, V: volume of distribution, F: bioavailability, CL: clearance, AUC: area under the concentration-time curve, $t_{1/2}$: plasma half-life, <LLOQ: below lower limit of quantitation, IIV: inter-individual variability.

[a]Not provided on poster [38], but provided for 501 patients included in clinical results of trial [33]; used as proxy for 448 out of these 501 patients included in population PK model
[b]V_β, apparent volume of distribution during the β-elimination phase
[c]Per kg
[d]Per 1.73m², reported as 117.7 and 126.0 mL/min, converted to L/h.
[e]Mean (% SE)

Pentamidine

Pentamidine is a synthetic derivative of amidine, which was used to treat refractory VL in India in the 1980s. Since then it has been used as a second-line therapy against leishmaniasis, but has mainly been administered for treatment of sleeping sickness and *Pneumocystis carinii* infections in AIDS patients. The drug is given IM or, preferably, by IV. In the past, two lyophilized salts of pentamidine were marketed. However, since the 1990s the production of pentamidine dimesylate was ceased and pentamidine isethionate remained, which contains 1 g of base per 1.74 g of salt. As both formulations are salts dissolved in water, no differences were expected in their pharmacokinetics.

The mechanism of action of pentamidine is unclear, but the mitochondrion was found to be an important target of pentamidine action [45]. Pentamidine's use in treatment against leishmaniasis is mainly limited by its severe side effects: diabetes mellitus, severe hypoglycaemia, shock, myocarditis and renal toxicity [2].

ADME

Due to the two strongly basic amidine groups, oral bioavailability of pentamidine is low [46]. Therefore, pentamidine is administered IV or IM. The t_{max} after IM injection is approximately 1 hour [47].

The distribution of pentamidine was studied in biopsies of 22 deceased AIDS patients [48]. Organs with the highest accumulated pentamidine concentrations were the kidney, liver, spleen and adrenal glands. Radiolabelled pentamidine in humans is rapidly being taken up by the liver: 2.5 h after the commencing of IV infusion, 65% of the drug could be traced to the liver [49]. Pentamidine seemed to be excreted in bile, but the release from the liver is slow: 99% of the absorbed pentamidine in the liver is still present 24 h after IV infusion [49]. Pentamidine is approximately 70% protein-bound.

Pentamidine was extensively metabolized in isolated perfused rat liver [50]. *In vitro* cytochrome P450 (CYP) enzymes CYP2D6 and CYP1A1 were responsible for pentamidine metabolism in human liver microsomes [51]. Involvement of CYP1A1 in pentamidine metabolism was later confirmed in human liver microsomes, with additional involvement of CYP3A5 and CYP4A11, but involvement of CYP2D6 could not be identified [52]. No data could be found on pentamidine metabolites in humans [52].

Multiple studies found a low urinary excretion of pentamidine, between 2.1 and 5.5% or below 20% in the first 24 h after infusion [49,53–55]. Faecal excretion was found to be only one third of the amount excreted in urine [56].

Clinical pharmacokinetics

Pentamidine's distribution into tissues and slow excretion has already been described in 1970 [55]. Pentamidine pharmacokinetics is best described by two or three compartment models (Table 4). A rapid distribution phase was observed with a sharp 32% plasma concentration decrease within 10 minutes after end of infusion ($t_{1/2}$ ~5 min) [51,54].

Pentamidine pharmacokinetics has most extensively been studied in the 1980s and 1990s in heterogeneous patient populations. As can be seen from Supplementary table 1, included patients are often a mixture of male/female, child/adult, with/without renal failure, dialysis/no dialysis, AIDS patients/non-AIDS patients, with different dosages and sampling schemes. This possibly explains the wide variability in reported PK parameters. Regardless of the high variability, a consistently large V_d was observed, consistent with the 70% protein

Table 4. Pentamidine: primary and secondary pharmacokinetic parameters.

Author	Patients	Weight (kg)	Daily dose	Sampling day	C_{max} (ng/mL)	C_{trough} (ng/mL)	t_{max} (h)	V_1/F (L)	V_{ss}/F (L)	CL/F (L/h)	AUC (ng·h/mL)	$t_{1/2}$ (h)
Non-compartmental												
Bronner et al.[a] [47]	African trypanosomiasis patients	54 (34-66)	3.5-4.5 mg base/kg 10 days	Day 1	813±1,257	At 48h 14 (7-16)	~1 h[b]	N/A	N/A	N/A	0-48h 2,699±1,364[c]	$t_{1/2}$: 23±13 (n=7)
				Day 10	825±783	78 (57-92)	~1 h[b]	N/A	N/A	N/A	5,887±1,881[c]	$t_{1/2}$: 47±13 (n=9)
Bronner et al.[a] [51]	African trypanosomiasis patients	63 (50-84)	3.0-4.8 mg base/kg	Single-dose	393±168	N/A	End of infusion	N/A	11,817 ±4,510	67±21	0-168h 2,494±1,550	Terminal $t_{1/2}$: 11±5[c] days
Compartmental												
Conte et al. [53]	AIDS patients / P. carinii pneumonia	62±17	4.0 mg salt/kg, IM	Single-dose	209±48	6.55±3.51	0.67± 0.26	924±404	2,724 ±1,066	305±81	N/A	$t_{1/2\alpha}$: 0.90±0.18 $t_{1/2\beta}$: 9.4±2.0
			4.0 mg salt/kg, IV	Single-dose	612±371	2.90±1.44	N/A	140±93	821±535	248±91	N/A	$t_{1/2\alpha}$: 30±0.22 $t_{1/2\beta}$: 6.4±1.3
Conte et al.[d] [57]	AIDS patients / P. carinii pneumonia	64±8 (excl. 2 children)	4 mg/kg[e], various treatment lengths	Different	N/A	N/A	N/A	205±54	1,000 ±506	411±55	N/A	$t_{1/2}$: 6.2±1.2
Conte et al. [54]	AIDS patients / P. carinii pneumonia	66±10	3 mg/kg[e] 9-18 days	Day 1	282±72[f]	2.1±1.4	N/A	38.2±27.3	3,500 ±3,800	268±70	0-∞ 748±211	$t_{1/2\alpha}$: 1.2±0.6[g] $t_{1/2\beta}$: 29±25
	Volunteer hemodialysis patients	73±10	3 mg/kg[e] Single dose	Single-dose	275±184	1.1±0.8	N/A	218±295	12,400 ±3,900	592±472	578±407	$t_{1/2\alpha}$: 1.8±0.6[g] $t_{1/2\beta}$: 72.6±38.1
			4 mg/kg[e] Single dose	Single-dose	227±110	1.7±0.5	N/A	218±200	32,400± 45,300	329±58	747±158	$t_{1/2\alpha}$: 3.5±1.6[g] $t_{1/2\beta}$: 118±119
	P. carinii pneumonia patients	80±8	3-4 mg/kg[e] 12-21 days	Last dose	N/A	N/A	N/A	N/A	N/A	N/A	N/A	Terminal $t_{1/2}$: 12.0±2.3 days
Thomas et al. [49]	AIDS patients	60.2 (58-65)	~2.3 mg base/kg	Single-dose	N/A	N/A	N/A	26±8	825±458	73.6±35.8	0-∞ 2,500±1,700	$t_{1/2\alpha}$: 5.4±2.4 min $t_{1/2\beta}$: 11. 2±7.8

Data provided as either a) mean±standard deviation or b) median (range), unless indicated otherwise. N/A: Not Available. C_{max}: peak plasma concentration, C_{trough}: trough plasma concentration 24 h after dose, t_{max}: time to C_{max}, k_a: absorption rate constant, V: volume of distribution, F: bioavailability, CL: clearance, AUC: area under the concentration-time curve, $t_{1/2}$: plasma half-life
[a]All concentrations were reported in nmol/L and were translated into ng/mL with a molecular weight of 340.42 g/mol
[b]C_{max} for most patients reached within 1 hour. For 3 patients, C_{max} was noted 12-24 hours after the dose [47]
[c]Patients excluded if plasma concentration substantially increased after initial decrease, if concentrations below quantitation limit, if terminal slope very different
[d]Only reported for 5 adult patients, without renal failure (IV).
[e]Unclear whether dose is reported as base or salt
[f]Only including patients with extensive sampling scheme
[g]In addition to reported slower distribution phase, a rapid distribution to peripheral tissues (mean $0.07-0.19$ h^{-1}) was observed in the three-compartment model

1

binding. There is a large variability in documented elimination half-life of pentamidine, but a consistent 11-12 day terminal half-life was found [51,54] (Table 4). Pentamidine accumulates during treatment [47,54,57,58] and pre-dose C_{trough} levels increased from 14 ng/mL to 78 ng/mL during a 10-day once daily treatment [47].

It is widely assumed that the *Leishmania* infection inhibits hepatic drug metabolism, which was found to be mediated by NO in hamsters [59]. This could possibly affect pentamidine exposure in VL patients, as pentamidine is metabolized by CYP enzymes. However, to our knowledge, the pharmacokinetics of pentamidine have never been investigated in VL patients.

Miltefosine

Miltefosine is an alkylphosphocholine drug with a polar head and hydrophobic tail and has a critical micelle concentration of approximately 20 μg/mL (50 μM) [60]. Though originally developed as an anti-cancer drug, it has been licensed since 2002 in India for VL treatment and since 2004 in Germany for treatment of CL.

No definite mode of action is determined for miltefosine, but multiple hypotheses have emerged, such as: induction of apoptosis, disturbance of lipid-dependent cell signalling pathways, alteration of membrane composition and immunomodulatory effects [7]. Miltefosine is orally administered in standard treatment of 2.5 mg/kg daily for 28 days and this is well tolerated with mainly gastrointestinal side-effects.

ADME
Miltefosine is slowly absorbed upon oral administration. The k_a is ~9 day^{-1}, which corresponds to an absorption half-life of ~2 h. The t_{max} was reported to be between 8 and 24 h [61]. In East African VL patients, absorption appeared even slower indicating a possible disease-effect on the absorption of miltefosine [Dorlo et al., submitted for publication]. Bioavailability in rats and dogs was found to be 82 and 94%, respectively [7]. No data are available in humans, due to the hemolytic activity of miltefosine after IV infusion [62,63].

Pre-clinical *in vivo* studies in mice and rats, indicated a wide distribution of miltefosine and uptake in a range of different tissues. In rats, [^{14}C]-radioactively labelled miltefosine was predominantly found in the kidney > intestinal mucosa > liver > spleen [64]. Another study in rats showed similar distribution patterns after 18 days of oral miltefosine administration (kidney > adrenal > skin > spleen > small intestines) [65]. Radiolabelled miltefosine oral administration in mice resulted in accumulation in the kidney > liver > lung [66].

In humans, plasma protein binding was 96-98%, of which 97% bound to albumin [62]. Miltefosine accumulated in peripheral blood mononuclear cells (PBMCs), with an approximately two-fold higher PBMC compared to plasma concentration [67]. A 0.4 μg/mL miltefosine cerebrospinal fluid (CSF) concentration was measured after five days of miltefosine treatment in patients suffering from granulomatous amoebic encephalitis, suggesting a 2-4% miltefosine passage across the blood–brain barrier, although integrity of the barrier could not be guaranteed [68].

An *in vitro* evaluation of 15 different CYP enzymes revealed no oxidative metabolism of miltefosine [7,61] and no CYP3A isoenzyme induction was observed *in vivo* in rats [61]. Instead, miltefosine is most probably metabolized intracellularly by phospholipase D [64,66]. No metabolic conversion of miltefosine was observed by phospholipases A and B [64], and metabolism by phospholipase C is still debated [64,66]. After IV infusion with

Table 5. Miltefosine: primary and secondary pharmacokinetic parameters.

Author	Patients	Weight (kg)	Daily dose	C_{ss} (µg/mL)	k_a (day⁻¹)	t_{max} (h)	$V_{central}$/F (L)	CL/F (L/day)	$V_{peripheral}$/F (L)	Q (L/day)	AUC (µg·day/mL)	$t_{1/2}$ (days)
Non-compartmental												
Berman [61]	N/A	N/A	N/A	70[a]	N/A	8-24	N/A	N/A	N/A	N/A	N/A	$t_{1/2}$: 150-200 h
Castro et al. [100]	Adult cutaneous leishmaniasis patients	70.84± 11.73	2.11±0.32 mg/kg/day 28 days	31.9 (17.2-42.4)	N/A	N/A	N/A	N/A	N/A	N/A	628 (213-861) 880 (427-1206)[b]	$t_{1/2}$: 34.4 (9.5-46.15)
	Pediatric cutaneous leishmaniasis patients	26.22±7.62	2.27±0.16 mg/kg/day, 28 days	22.7 (17.0-29.3)	N/A	N/A	N/A	N/A	N/A	N/A	448 (304-583) 652 (438-832)[b]	$t_{1/2}$: 37.1 (7.4-47.0)
Compartmental												
Dorlo et al. [70]	Cutaneous leishmaniasis patients	85 (70-113)	150 mg 28 days	30.8 (median)	8.64 (10.1%)[c] IIV: 24.2%	N/A	39.6 (4%) IIV: 18.3%[d]	3.87 (5.3%) IIV: 23.2%[d]	1.65 (12.4%)	0.0375 (22.0%)	N/A	$t_{1/2}$: 7.05 (5.45-9.10) Terminal $t_{1/2}$: 30.9 (30.8-31.2)
Dorlo et al. [71]	Paediatric visceral leishmaniasis patients	15 (9-23)	1.5-2.5 mg/kg 28 days	N/A	9.98 (11.5%)[e] IIV: 18.4%	N/A	40.1 (4.5%)[f] IIV: 34.1%[d]	3.99 (3.5%)[f] IIV: 32.1%[d]	1.75 (8.2%)	0.0347 (18.3%)	N/A	$t_{1/2}$ (range): 4.99 - 7.18 Terminal $t_{1/2}$: 35.5
	Adult visceral leishmaniasis patients	36 (16-58)	50-150 mg 3-6 week									
	Cutaneous leishmaniasis patients[g]	85 (70-113)	150 mg 28 days									
Dorlo et al. [72][h]	Nepalese visceral leishmaniasis patents	40 (8-56)	Adults: >25 kg: 100 mg, ≤25 kg: 50 mg, 28 days Children: 2.5 mg/kg, to nearest 10 mg, 28 days	35.3 (11.6-120)	N/A	N/A	38.5 (4.5%)[f] IIV: 31.6%[d]	3.69 (3.4%)[f] IIV: 35.1%[d]	1.69 (8.6%)	0.0316 (16.6%)	724 (265-2,260) 1,140 (340-4,200)[b]	$t_{1/2}$: 6.26 (4.18-9.27) Terminal $t_{1/2}$: 48.9 (48.6-51.0)

Data provided as either a) median (range) or b) mean (coefficient of variation%), unless indicated otherwise. IIV: inter-individual variability. N/A: Not Available. C_{ss}: miltefosine accumulates during treatment and reaches steady state concentration (C_{ss}) last week of treatment; t_{max}: time to C_{max} within one dosing interval, k_a: absorption rate constant, V: volume of distribution, F: bioavailability, CL: clearance, AUC: area under the concentration–time curve, calculated from start to end of treatment (AUC_{0-D28}) unless indicated otherwise, $t_{1/2}$: plasma half-life. C_{trough}: not available for miltefosine.

[a] Unclear whether this is the mean C_{ss} or the max C_{ss}
[b] AUC from start of treatment to infinity ($AUC_{0-\infty}$)
[c] Reported as 0.36 h⁻¹
[d] IIV of clearance and volume of central compartment were correlated
[e] Reported as 0.416 h⁻¹
[f] Parameter scaled to a standardized fat-free mass of 53 kg. This corresponds to a theoretical weight of 70 kg.
[g] Same patients as described in Dorlo et al. [70]
[h] Parameters estimated with data of Nepalese VL patient cohort and additional information on previously described cohorts (Dorlo et al. [70]/ Dorlo et al. [71])

radioactive miltefosine in mice, most radioactivity in the liver was attributable to unchanged miltefosine (63%), with the main breakdown product being choline (32%), with low levels of phosphocholine (3%) and 1,2-diacylphosphatidylcholine (2%) [66].

The breakdown products of miltefosine are abundant endogenous compounds and are therefore difficult to quantify, e.g. choline is involved in the biosynthesis of cell membranes. Miltefosine is hardly excreted unchanged; excretion of miltefosine in urine accounts for only <0.2% of the administered dose at day 23 of treatment [61]. Faecal elimination has not been evaluated in humans, but slow faecal elimination of 10% of total miltefosine excretion has been reported in Beagle dogs [69].

Clinical pharmacokinetics

In contrast to older antileishmanial drugs, the pharmacokinetics of miltefosine has been studied more intensively (Table 5). The first reported population PK model of miltefosine identified a long terminal elimination phase with a half-life of 31 days [70], in addition to the initially reported 7 day elimination half-life [61]. Due to this long half-life, miltefosine accumulates during treatment to finally reach steady-state concentrations approximately in the last week of the 28-day treatment. In a more extensive population PK model, including data on both adult and pediatric patients with CL or VL, differences between patients in V_d and clearance could best be described by allometrically scaling these parameters by fat-free mass [71]. A lower exposure was found for children compared to adults while receiving the same 2.5 mg/kg dose (see "Pediatric patients").

Up to now, only one study has been published on the relationship between exposure and response in antileishmanial therapies [72]. A 1-day decrease of time the miltefosine plasma concentration was above the 10xEC50 (mean half maximal effective concentration), compared to the median of 30 days, was associated with a 1.08-fold increase in odds of treatment failure in VL [72]. Miltefosine has been found to accumulate intracellularly in PBMCs, which could influence miltefosine exposure at its site of action, though no significant correlation could be identified with treatment outcome in a non-compartmental analysis [67].

Amphotericin B

Amphotericin B (AMB) is a polyene antifungal, is poorly soluble in water and has a high affinity for sterol-containing membranes. The two main formulations are amphotericin B deoxylate (D-AMB) and liposome encapsulated amphotericin B (L-AMB). D-AMB has been developed in the 1950s and has been widely administered as an antifungal drug for the treatment of invasive fungal infections, but its dose-limiting nephrotoxicity and hypokalaemia hampers its use in the clinic. The lipid formulation L-AMB, incorporating AMB in a liposome bilayer, significantly reduced its renal toxicity and infusion-related toxicity. AMB binds to ergosterol in the cell membrane, subsequently leading to pore formation, fluid leakage and cell death. L-AMB side effects are mild infusion reactions and transient nephrotoxicity or thrombocytopenia

Other lipid-based formulations of AMB exist such AMB lipid complex (ABLC, Abelcet) or AMB colloidal dispersion (ABCD, Amphocil/Amphotec). In this review we will only focus on L-AMB (AmBisome®), since this is the most widely used lipid AMB formulation in leishmaniasis. Any findings regarding L-AMB cannot be extrapolated to other lipid formulations of AMB, as substantial differences exist in PK parameters between these formulations [8,73].

AMB exists in different forms in the plasma: protein-bound AMB, free AMB and upon

L-AMB administration also liposome-associated AMB. Up to now, all but one of the PK studies, only determined the total AMB concentration after destruction of the liposome with organic solvent and subsequent release of AMB. If not clarified otherwise, the abbreviation AMB refers to total AMB.

ADME
AMB is poorly absorbed after oral administration, due to the hydrophobicity of its polyene structure. Daily dosages of 2-5 grams resulted in (subtherapeutic) systemic concentrations of below 0.5 µg/mL (reviewed in [74]).

AMB is highly protein-bound (>90%) [75]. *In vitro* binding in human plasma, determined by ultrafiltration, showed that 95-99.5% of AMB was bound in plasma, with increasing percentages bound with increasing AMB concentrations [76].

Interestingly, a physiologically based PK model has recently been developed describing the biodistribution of AMB in tissues of mouse, rat and human [77]. To describe the data well, a saturable uptake of AMB in reticuloendothelial system organs, like the VL target sites spleen and liver, was required. Predicted human tissue data were in good correspondence with autopsy data from patients who received L-AMB therapy [78]. In three autopsy cases, highest AMB concentrations (after a total dose of 820-3,428 mg) were observed in the liver (92.8-291 µg/g) and spleen (150-291 µg/g), with lower concentrations in the kidney, thyroid, bone marrow and lung (<50 µg/g) [78]. Of the administered dose, 13.9-22.5% could be recovered from the liver [78]. This was in line with a larger autopsy study with seven L-AMB treated patients, where highest concentrations were found in the liver (102.81±68.72 µg/g) and spleen (60.32±29.75 µg/g) [79]. CSF levels were approximately 1,000-fold lower than concurrent serum levels [80]. Similar distribution patterns were observed after treatment with D-AMB [81], with highest accumulation in liver (up to 188 µg/g) and spleen (up to 190 µg/g) [81]. In total, 14-41% of the administered dose could be recovered from the liver (with a total maximum recovery of 51%) [81].

The same distribution (spleen and liver > kidneys > lungs) was also found in mice [82,83]. AMB concentrations were significantly lower in the liver and spleen of VL infected mice than in non-infected mice, hypothesized to be due to a loss in phagocytic activity in infected macrophages [84]. Disruption of normal liver function in VL might thus affect AMB exposure in VL patients.

D-AMB skin concentrations in rats were 30-50% of plasma concentrations and show a decrease over time parallel to these plasma concentrations [85]. Upon L-AMB administration, buccal mucosal AMB concentrations rise to concentrations 6-47 times higher than plasma concentrations [86].

Metabolism of amphotericin B has not been well studied and metabolites have up to now not been identified [74]. Pre-clinical studies reported that AMB is eliminated from the circulation by the urinary and biliary tract and by the reticuloendothelial system, the latter of which is also responsible for the clearance of L-AMB from the circulation (reviewed in [84]). One week after a single-dose, urinary excretion of unchanged AMB was 20.6% and 4.5% for D-AMB and L-AMB treated subjects, respectively [87]. During the same period, faecal excretion was 42.5% for D-AMB treated subjects, but only 4% for subjects treated with L-AMB. Possible explanations for the decrease in excretion of unchanged AMB in the liposomal formulation could either be a change in distribution of the AMB, prolongation of its residence time or increased metabolism.

Table 6. Amphotericin B: primary and secondary pharmacokinetic parameters based on non-compartmental analyses and individual based compartmental models.

Author	Patients	Weight (kg)	Daily dose	Sampling day	C_{max} (µg/mL)	V (L/kg)	V_{ss} (L/kg)	CL (mL/h/kg)	AUC (µg*h/mL)	$t_{1/2}$ (h)
L-AMB										
Gubbins et al. [86]	Peripheral Stem Cell Transplant (PSCT) patients	71.7±13.3	1.0 mg/kg 15 days	Day 1 / Day 7	8.1±4.2 / 13.5±9.1	0.19±0.14 / 0.16±0.20	N/A	15.6±10.8 / 10.6±10.6	112.2±75.3[a] / 333.7±548[a]	$t_{1/2}$: 9.7±3.1 / $t_{1/2}$: 13.0±11.8
		83.9±26.1	7.5 mg/kg weekly 2 weeks	Day 1-7 / Day 7-15	95.5±39.9 / 52.3±19.1	0.17±0.20 / 0.47±0.22	N/A	8.9±11.0 / 21.6±8.8	1,887±1,344[a] / 384.7±126.3[a]	$t_{1/2}$: 19.2±1.8 / $t_{1/2}$: 36.4±24.4
		87.5±27.1	15 mg/kg, single dose	Day 1-8	206.3±89.1	0.28±0.22	N/A	5.6±4.4	5,019±4,199[a]	$t_{1/2}$: 32.8±12.2
Walsh et al. [89]	Neutropenic patients	N/A	1.0 mg/kg Various durations	Day 1 / Last day	N/A	0.58±0.40 / 0.16±0.04	0.44±0.27 / 0.14±0.05	39±22 / 17±6	32±15[a] / 66±21[a]	$t_{1/2}$: 10.7±6.4 / $t_{1/2}$: 7.0±2.1
			2.5 mg/kg Various durations	Day 1 / Last day	N/A	0.69±0.85 / 0.18±0.13	0.40±0.37 / 0.16±0.09	51±44 / 22±15	71±36[a] / 213±196[a]	$t_{1/2}$: 8.1±2.3 / $t_{1/2}$: 6.3±2.0
			5.0 mg/kg Various durations	Day 1 / Last day	N/A	0.22±0.17 / 0.11±0.08	0.16±0.10 / 0.10±0.07	21±14 / 11±6	294±102[a] / 621±371[a]	$t_{1/2}$: 6.4±2.1 / $t_{1/2}$: 6.8±2.1
			7.5 mg/kg Various durations	Day 1 / Last day	N/A	0.26±0.15 / 0.20±0.07	0.18±0.10 / 0.17±0.05	25±22 / 20±7	534±429[a] / 417±155[a]	$t_{1/2}$: 8.5±3.9 / $t_{1/2}$: 6.9±0.9
Walsh et al. [88]	Immunocompromised patients with invasive fungal infections	N/A	7.5 mg/kg Various durations	Day 1 / Last 7	75.9±58.4 / 115.1±104.9	0.22±0.18 / 0.14±0.10	0.24±0.18 / 0.14±0.11	23±14 / 15±11	692±834 / 1,333±2,153	$t_{1/2}$: 6.8±1.9 / $t_{1/2}$: 6.0±0.8
			10.0 mg/kg Various durations	Day 1 / Last 7	119.6±69.8 / 164.7±119.7	0.23±0.24 / 0.16±0.17	0.22±0.23 / 0.14±0.14	18±19 / 12±12	1,062±971 / 1,919±2,056	$t_{1/2}$: 8.0±1.5 / $t_{1/2}$: 8.4±2.6
			12.5 mg/kg Various durations	Day 1 / Last 7	116.3±47.8 / 147.4±69.2	0.18±0.13 / 0.16±0.10	0.16±0.07 / 0.13±0.08	16±6 / 13±7	860±390 / 1,168±991	$t_{1/2}$: 7.1±3.5 / $t_{1/2}$: 8.2±2.5
			15.0 mg/kg Various durations	Day 1 / Last 7	105.1±30.9 / 178.6±49.0	0.33±0.12 / 0.18±0.09	0.23±0.09 / 0.14±0.06	25±8 / 14±7	554±30.9 / 1,152±617	$t_{1/2}$: 9.0±3.1 / $t_{1/2}$: 9.0±0.9

Table 6. Amphotericin B: primary and secondary pharmacokinetic parameters based on non-compartmental analyses and individual based compartmental models.

Author	Patients	Weight (kg)	Daily dose	Sampling day	C_{max} (µg/mL)	V (L/kg)	V_{ss} (L/kg)	CL (mL/h/kg)	AUC (µg*h/mL)	$t_{1/2}$ (h)
L-AMB + D-AMB										
Bekersky et al. [87]	Healthy volunteers L-AMB	79±11	2 mg/kg Single-dose	Single-dose	22.9±10	1.63±0.88	0.774±0.55	9.7±5.4	171±126 288±209[a]	$t_{1/2\alpha}$: 0.56±0.48 $t_{1/2\beta}$: 6.0±2.1 $t_{1/2\gamma}$: 152±116
	D-AMB	77±9	0.6 mg/kg Single-dose	Single-dose	1.43±0.2	2.34±0.20	1.81±0.24	13.1±2.0	13.9±2.0 46.6±7.2[a]	$t_{1/2\alpha}$: 0.17±0.14 $t_{1/2\beta}$: 6.8±1.6 $t_{1/2\gamma}$: 127±30
Heinemann et al. [95]	Critically ill patients L-AMB	72 (57-85)	1.2-4.2 mg/kg	Steady-state	14.4 (6.4-89.0)	0.42 (0.055-0.93)	N/A	1.20 (0.59-1.91) mL/min	171 (53.1-1,380)	$t_{1/2\alpha}$: 1.65 (1.25-5.22) $t_{1/2\beta}$: 13.1 (8.7-41.4)
	D-AMB	70 (50-120)	1.0 mg/kg	Steady-state	1.70 (1.45-2.07)	2.41 (1.12-4.32)	N/A	0.363 (0.036-0.942) mL/min	18.65 (9.73-28.30)	$t_{1/2\beta}$: 26.8 (9.9-37.0)
D-AMB										
Ayestaran et al. [132]	Neutropenic patients	64.4 (mean)	0.7-1 mg/kg	Day 1	2.83±1.17	N/A	0.56±0.15	33.0±14.3	29.0±15.5	$t_{1/2\alpha}$: 0.64±0.24 $t_{1/2\beta}$: 15.2±5.25
Benson et al. [133]	Pediatric patients	21.6±13.3	0.25-1.5 mg/kg	Various	1.64 (0.7-10.0)	0.71±0.23	N/A	21.0±1.8	N/A	$t_{1/2}$: 18.1±6.6
Kan et al. [134]	Healthy volunteers	74.2 (55-87)	0.1 mg/kg	Various	0.551±0.025	N/A	0.50±0.05	10±1	3.9±0.43	$t_{1/2}$: 30.8±4.1
			0.25 mg/kg	Various	0.984±0.056	N/A	0.74±0.13	10±1	8.7±0.76	$t_{1/2}$: 50.0±11.3
Koren et al. [102]	Infants/children	N/A	0.5-1 mg/kg	Various	N/A	0.378	N/A	26±5	N/A	$t_{1/2}$: 9.93±1.5

Data provided as either a) mean±standard deviation or b) median (range). N/A: Not Available. C_{max}: peak plasma concentration, V: volume of distribution, CL: clearance, AUC: area under the concentration-time curve, $t_{1/2}$: plasma half-life. AUC calculated 0 to 24 h after dose (AUC_{0-24h}), unless indicated otherwise. L-AMB: liposomal amphotericin B, D-AMB: amphotericin B deoxycholate. Trough plasma concentration not included, only documented for Bekersky et al. [87]

[a]Calculated from zero to infinity ($AUC_{0-\infty}$)

Clinical pharmacokinetics

The pharmacokinetics of L-AMB, best described by a two- or three-compartment model, has been studied in a wide range of dosages (Table 6 and Table 7), but has never been evaluated in leishmaniasis patients.

Variability (coefficient of variation, CV%) in PK parameters was much higher for L-AMB, compared to D-AMB (AUC$_{0-24h}$ CV% of 73.4 and 14.4%, respectively) [87]. High variability in AMB exposure, could potentially be caused by differences in the uptake of liposomes into non-blood compartments, or differences in drug release from the carrier liposomes. Interestingly, variability in exposure decreased with higher dosages, e.g. C$_{max}$ CV% decreased from 91% to 27% with increased dosing from 7.5 to 15 mg/kg, respectively [88].

Linear pharmacokinetics was reported up to a 7.5 mg/kg dose. At higher dosages, time-dependent non-linear L-AMB pharmacokinetics has been described [88,89]. Evaluating L-AMB dosages of 7.5 to 15.0 mg/kg, the highest C$_{max}$ and AUC levels were reached at 10 mg/kg, implying that (alternative) elimination mechanisms are induced or activated above this concentration [88]. Possibly, the uptake by the reticuloendothelial system is enhanced, which would simultaneously explain the high AMB concentration in the liver, spleen and bone marrow [88].

Considering these non-linearities and the high variability in PK parameters between patients, a non-compartmental analysis or individual-based compartmental analysis would not be appropriate to capture the PK profile of L-AMB. Five multi-compartmental population PK models have been developed for L-AMB [90–94]. The median weight in these studies varies widely (Supplementary table 1), since multiple studies only included pediatric patients [92,93]. Interestingly, a recent study reported a decrease in the V$_d$ over time during treatment [94]. Furthermore, body weight has been identified as a covariate on clearance and V$_d$ in most modelling studies [90,92–94], often allometrically scaled [92,94]

For most patients, C$_{trough}$ levels increased ~2.6-fold following multiple administrations, but for a portion of patients the increase was above 10-fold (exact treatment duration not reported) [93]. Walsh et al. did not find an increase in C$_{trough}$ after repeated dosing [89].

Encapsulation of AMB in liposomes alters the pharmacokinetics of the drug. A lower clearance and a lower V$_d$ was reported for L-AMB compared to D-AMB [87,95]. The C$_{max}$ (mean±SD) of unbound AMB was significantly lower for patients treated with 2 mg/kg L-AMB (0.016±0.004 μg/mL) than for patients treated with 0.6 mg/kg D-AMB (0.060±0.01 μg/mL) [76], explaining the decrease in side effects after L-AMB administration compared to D-AMB. Unbound AMB elimination was biphasic with a longer half-life than total AMB (initial half-life of 7.7±2.8 h, terminal half-life of 467±372 h [76]).

All AMB PK studies conducted were performed in often immunosuppressed patients with fungal infections and no study has been conducted in leishmaniasis patients up to now. As the spleen and liver physiology is severely damaged in VL, the uptake of L-AMB by the reticuloendothelial system might be altered, possibly changing the pharmacokinetics of AMB in VL patients. Furthermore, AMB pharmacokinetics has only been evaluated in plasma. Analyzing the intracellular AMB pharmacokinetics might give more reliable information on the AMB exposure of the parasite at the site of action.

Table 7. Amphotericin B: primary and secondary pharmacokinetic parameters derived from population-based compartmental studies.

Author	Patients	Weight (kg)	Daily dose	C_{max} (μg/mL)	C_{trough} (μg/mL)	$V_{central}$ (L)	CL (L/h)	$V_{peripheral}$ (L)	Q (L/h)	AUC (μg*h/mL)	$t_{1/2}$ (h)
Compartmental (population based)											
Hong et al. [92]	Paediatric patients with malignant disease (L-AMB)	28.8 (mean)	0.8-5.9 mg/kg	N/A	N/A	3.12 (40%)[a] IOV: 56%	0.44 (27%)[a] IIV: 10% IOV: 46%	18.0 (40%) IIV: 74%	0.73 (18%) IIV: 77%	N/A	Terminal $t_{1/2}$: 59.4±36.5
Hope et al. [90]	Patients with suspected invasive fungal infection (L-AMB)	68 (mean)	Intermittent: 10 mg/kg (day 1), 5 mg/kg (day 3/6) Conventional: 3 mg/kg 14 days	N/A	N/A	20.6±15.3	1.6±0.85	N/A	N/A	N/A	N/A
Würthewein et al. [91]	Allogeneic hematopoietic stem cell recipients (L-AMB)	72 (44-105)	3 mg/kg Median 10 days	18.0±8.6[b]	6.5±5.8[b]	19.2 (9%) IIV: 38%	1.22 (16%) IIV: 64%	52.8 (29%) IIV: 84%	2.18 (13%) IIV: 47%	228±159[b]	Terminal $t_{1/2}$: 54.3
Nath et al. [135][c]	Children with malignant disease (D-AMB)	23.3±1.3	1 mg/kg Up to 8 days	N/A	N/A	8.51 (38%)	0.79 (29%)	N/A	N/A	N/A	$t_{1/2,\lambda 1}$: 1.46±0.33 $t_{1/2,\lambda 2}$: 26.4±11.6
Ohata et al. [93]	Patients with invasive fungal infection (L-AMB)	27.1±14.1	2.5 mg/kg loading dose, subsequently 1.0 or 5.0 mg/kg	18.2±11[d] (Observed) 17.3±7.6[d] (Predicted)	N/A	3.43 (19%)[e] IIV: 100.2%	0.255 (16%)[e] IIV: 104.4%	6.97 (29%)[e] IIV: 238.5%	0.661 (45%)	N/A	N/A
Lestner et al. [94]	Immunocompromised children (L-AMB)	26.9±14.0	2.5, 5.0, 7.5 or 10.0 mg/kg	N/A	N/A	Initial[f] 10.7 (14.3%) Final[f] 2.3 (42.1%)	0.67 L/h/70 kg	N/A	N/A	N/A	N/A

Data provided as either a) mean±standard deviation b) median (range) or c) mean (coefficient of variation%), unless indicated otherwise. IIV: inter-individual variability. IOV: inter-occasion variability. NA: Not Available. C_{max}: peak plasma concentration, C_{trough}: trough plasma concentration 24 h after dose, V: volume of distribution, CL: clearance, AUC: area under the concentration-time curve, $t_{1/2}$: plasma half-life. L-AMB: liposomal amphotericin B, D-AMB: amphotericin B deoxycholate.

[a] Parameter scaled to a standardized weight of 21 kg
[b] At steady-state, exact definitions of C_{max} and C_{min} not provided in publication
[c] Posterior Bayesian estimates of the PK parameters for D-AMB, based on model including both D-AMB data and lipid emulsion data
[d] After single dose of 2.5 mg/kg daily
[e] Parameter scaled to a standardized weight of 23 kg
[f] A decrease was identified in $V_{central}$ between the first and last day of treatment, these were estimated separately.

SPECIFIC PATIENT POPULATIONS

Pediatric patients

Evaluation of the pharmacokinetics of anti-leishmanial drugs in the paediatric patient population is of particular importance, since 45% of the global leishmaniasis incidence consists of children under the age of 15 years old [96]. However, in the clinical development of antileishmanial drugs, PK studies in children have often been omitted. Children mostly receive the same mg/kg dosing regimen as adults, while it is generally accepted that this leads to lower exposure in children, as clearance and V_d are allometrically scaled by weight or fat-free mass [97]. For Sb, paromomycin, miltefosine and AMB, additional studies have been performed to gain more insight in the pharmacokinetics in children, to rationalize dosing in this vulnerable patient population. However, while differences in exposure between adult and paediatric patients were observed for Sb, miltefosine and AMB, specific paediatric dosages are currently only clinically being evaluated for miltefosine.

Children are relatively underexposed to miltefosine in comparison to adults and have a higher risk of relapse [71,72,98–100]. With a conventional linear 28-day 2.5 mg/kg daily dosing, only 71.4% of children reached an AUC from day 0-28 of treatment (AUC_{0-D28}) of 412 µg·day/mL, while 90% of adults reached this threshold [71]. Simulating a 28-day allometric dose regimen, where low-weight patients would receive a higher mg/kg daily dose, 95.6% and 97.3% of adults and children reached an AUC_{0-D28} of 412 µg·day/mL [71]. This allometric dose is currently being evaluated in pediatric VL patients aged 4-12 years old in Kenya and Uganda (NCT02431143), and pediatric post-kala-azar dermal leishmaniasis patients below 18 years old in Bangladesh (NCT02193022).

L-AMB pharmacokinetics has been characterized in pediatric patients in two population PK studies. Simulating different dosing regimens from 1-12.5 mg/kg daily for patients ranging 10-70 kg in weight, Hong et al. reported that children under 20 kg would require a higher mg/kg dose to achieve comparable steady state C_{max} levels [92]. However, weight could not be identified as covariate on clearance in Japanese pediatric patients [93]. Lower serum AMB concentrations were also observed in children (17 days to 15 years old) receiving D-AMB [101], and body weight was found to be correlated with clearance and V_d [101,102].

One study reported on Sb pharmacokinetics in children. In treating both adults and children with 20 mg Sb/kg daily, children reach only 58% of the AUC_{0-24h} that adults reach [11]. Changing the dose in children to 30 mg/kg increased paediatric exposure to 86% of adult exposure after 20 mg/kg. As expected, children have a higher weight-adjusted clearance (0.185 L/h/kg than adults (0.106 L/h/kg), indicating that elimination does not change in direct proportion to weight.

In a large-scale paromomycin phase III trial in India (313 adults and 188 children aged 5-14 years old), no significant differences were found in paromomycin pharmacokinetics between adults and children [33,38]. The C_{max} of children (18.3±8.26 µg/mL) was comparable to the C_{max} for subjects older than 30 years (19.1±9.75 µg/mL) [38]. However, the same study reported weight to be a significant covariate on V_d and clearance.

For pentamidine, concentration-time profiles were only available for two children (0.4 and 6 years old) and resembled the adult curves [57]. However, further investigation is required with larger sample size, to characterize pentamidine pharmacokinetics in pediatric patients.

HIV-VL co-infected patients

In 2-9% of VL cases, patients are co-infected with HIV, but this percentage rises up to 40% in specific patient populations (reviewed in [103]). Co-infection of HIV with VL results in rapid disease progression, more severe disease, and a poor treatment response. Treatment options are limited in HIV-positive VL patients, due to higher toxicity levels, generally low cure rates, high relapse rates, and higher fatality than in immunocompetent patients [103].

As antiretroviral and antileishmanial drugs are thus often administered concurrently, possible drug-drug interactions could take place and should be evaluated. The pharmacokinetics of antiretroviral (ARV) drugs has been reviewed previously [104]. Protease inhibitors are known inhibitors of CYP2D6 (ritonavir and darunavir) and CYP3A (ritonavir and lopinavir) and their combination with pentamidine should therefore be monitored, as pentamidine has *in vitro* been found to be metabolized by these CYP enzymes. As other antileishmanial drugs are not metabolized by CYP enzymes, interactions on this level are not expected. The pharmacokinetics of pentamidine have been studied in AIDS patients, but their specific ARV treatment was not reported [53,54,57].

Vice versa, selective inhibition of CYP enzymes was observed in rats treated with D-AMB, assumed to be due to an impairment of monooxygenases on the endoplasmic reticulum [105]. This inhibitory effect on CYP activity was confirmed in humans [106]. This could increase exposure to non-nucleoside reverse transcriptase inhibitors (NNRTIs), protease inhibitors and entry inhibitors as they are extensively metabolized by CYP enzymes. L-AMB did not affect CYP activity in rats [105].

Due to the high prevalence of nephrotoxicity upon D-AMB treatment, drug-drug interactions should be expected with mostly renally cleared nucleoside reverse transcriptase inhibitors (NRTIs) such as lamivudine and emtricitabine. Also concomitant use with other possibly nephrotoxic antiretrovirals, such as tenofovir, must be closely monitored for renal function. Drug-drug interactions have not been evaluated in L-AMB and are expected to be much less pronounced due to the decreased nephrotoxicity. Extra caution is also required when combining the renally cleared Sb and paromomycin with ARV drugs causing nephrotoxicity, such as tenofovir, as this could possibly affect antileishmanial drug exposure. Furthermore, as both pentamidine and nevirapine can be hepatotoxic, combination of these drugs should be monitored.

Miltefosine has *in vitro* been revealed to inhibit intestinal P-glycoprotein (P-gp) upon short-term exposure, suggesting a potential drug-drug interaction for substrates of intestinal P-gp [107], such as protease inhibitors darunavir, atazanavir and maraviroc. In addition, as miltefosine has been found to widen tight junctions and promotes its own paracellular transport, other oral (hydrophilic) compounds relying on paracellular transport such as lamivudine and zidovudine might also be increasingly absorbed influencing oral bioavailability [107].

The majority of ARV drugs, the NNRTIs, the protease inhibitors, the entry inhibitors and integrase inhibitors, are highly protein-bound. For antileishmanial drugs with high protein binding pentamidine (~70%), miltefosine (96-98%) and AMB (>90%), competition for protein binding could potentially take place. This could particularly be a problem in VL patients, who generally have severely lowered albumin levels [108,109].

Pentamidine pharmacokinetics has been evaluated in AIDS patients, but due to the large heterogeneity of patients within studies and between studies, no conclusions can be drawn on potential differences with non-HIV patients. D-AMB PK parameters in five HIV

patients [110], were in line with studies published for non-HIV patients (C_{max} 0.72 µg/mL after 0.3 mg/kg dosing and 9.48 mL/h/kg clearance). The pharmacokinetics of other antileishmanial drugs has not been evaluated in HIV patients or HIV co-infected VL patients.

In addition, ARV drug pharmacokinetics has not been evaluated in VL patients. VL causes a disruption of liver physiology potentially affecting exposure of co-infected patients to NNRTIs and protease inhibitors given their metabolism by liver (CYP) enzymes.

Therefore it is necessary to study the pharmacokinetics of these drugs in this difficult-to-treat patient population. One study has recently been performed investigating L-AMB in monotherapy and in combination therapy with miltefosine in HIV-VL co-infected patients in Ethiopia also receiving ARV treatment (NCT02011958), but results have not been published yet.

Pregnancy

Treatment options for pregnant women are particularly limited in leishmaniasis patients. The use of pentavalent antimonials, pentamidine and miltefosine is contraindicated in pregnancy (FDA category C, C and D, respectively) and thus the only treatment options are paromomycin (no category assigned) and amphotericin B (FDA category B) (reviewed in [111]). The physiological changes in pregnant women are known to possibly alter the absorption, distribution, metabolism and excretion of drugs and could thus potentially affect the exposure to drugs. Furthermore, long half-lives of antileishmanial drugs might also require the use of contraceptives in women of reproductive age.

Sb has been correlated with adverse pregnancy outcome (such as abortions, preterm births and stillbirths) [112–114]. Evidence for the mutagenic, carcinogenic and teratogenic effect of Sb is still scarce, but should probably be assumed [115]. Placental transfer of Sb was established in rats and Sb was transferred to pups via milk [116,117]. At a daily dose of 300 mg Sb/kg, fetal growth retardation and increased embryo lethality and skeleton anomalies were observed [116,118]. An obstacle in the wide-spread use of miltefosine in the clinic is its potential reproductive toxicity, reported as a result of pre-clinical *in vivo* studies in rats and rabbits [64]. Treatment of rats with 1-2 mg/kg miltefosine in early embryonic development and organogenesis, resulted in embryotoxic, fetotoxic and teratogenic risk, indicating placental transfer [64]. While pentamidine in theory could hold teratogenic properties due to its inhibition of protein an nucleic acid synthesis *in vitro*, rat studies found a feticidal but not teratogenic effect in doses similar to human recommended dosages [119].

Both miltefosine and pentamidine have long terminal half-lives. Miltefosine levels are still detectable in plasma up to six months after the end of treatment [70], and could thus still be harmful during pregnancy for long periods after end of treatment. A translational PK study rationalized the advised duration of contraceptive use after treatment to be 4 months after a 28-day miltefosine treatment, with a <0.1% probability of exceeding the NOAEL (no-observed-adverse-effect level) [120]. Pentamidine also has a relatively long terminal half-life of ~12 days, which could have implications for the contraceptive duration required, however this has not been studied.

Both paromomycin and AMB are not contraindicated in treatment of leishmaniasis patients. However, no studies have been performed on the pharmacokinetics of both antileishmanial drugs in pregnant or breastfeeding women. Animal studies (rat and rabbit) show that paromomycin is not teratogenic [32]. There are some worries about possible ototoxicity in the unborn child, as the aminoglycoside streptomycin has been reported to

have possibly caused cases of ototoxicity in the unborn child when administered to women during pregnancy [121]. No studies have been performed on the excretion of paromomycin into breast milk, however due to its poor lipid solubility and limited distribution, substantial excretion in breast milk is not expected. AMB has been found to cross the placenta in cord blood:maternal serum ratios between 0.38-1.51 (reviewed in [122]). Rodent and rabit studies showed no teratogenicity at 10 times the recommended human dose (reviewed in [122]).

Patients with renal impairment

The main route of elimination of both Sb and paromomycin is glomerular filtration, thus clearance is expected to be drastically impacted by renal impairment. Only a single report describes Sb pharmacokinetics in a VL patient suffering from acute renal failure (glomerular filtration rate of 16 mL/min). After treatment with 25 mg MA/kg daily, C_{max} was elevated (22.9 µg/mL), C_{trough} was particularly high at 9.3 µg/mL and the half-life was over seven times as high (15 h) as for patients with normal renal function. The paromomycin half-life was increased from 2.47 h for normal subjects, to 6.7 h for patients with a creatinine clearance of 30-60 ml/min and as high as 36.6 h for patients with a creatinine clearance of less than 10 ml/min [123]. In treating patients with renal impairment, Sb and paromomycin dose reductions are therefore advised.

For D-AMB, ~20% of the administered dose is renally excreted within one week. No PK parameters have been defined for patients with renal impairment, but a dose of 1 mg/kg D-AMB was well tolerated in a VL patient on hemodialysis [124]. No AMB could be identified in peritoneal dialysate [125], as expected due to high AMB protein binding.

For pentamidine, miltefosine and L-AMB no effect of renal impairment on PK parameters is expected, as only a small percentage is cleared by the kidneys (pentamidine/L-AMB <5% [53,54,57,87], miltefosine <0.2% [61],). Pentamidine PK parameters were indeed not significantly different in patients with impaired renal function, receiving hemodialysis or peritoneal dialysis, compared to patients with normal renal function [54,57]. No results have been published on miltefosine pharmacokinetics in patients with renal impairment, but haemodialysis did not affect steady-state miltefosine concentrations in two patients with terminal renal failure (Kip and Dorlo, unpublished data). Also after L-AMB administration, the AMB concentration-time profiles were not affected by hemodialysis nor hemofiltration [95,126], implying that AMB does not pass through extracorporal filtration membranes. In contrast, another study found a higher total AMB clearance in critically ill patients receiving continuous veno-venous hemofiltration (0.14 L/h/kg) compared to patients that do not (0.061 L/h/kg), though no significant differences in C_{max} and AUC_{0-24h} were observed [127].

DRUG-DRUG INTERACTIONS BETWEEN ANTILEISHMANIAL DRUGS

In specific patient populations and certain regions, the anti-leishmanial drugs currently available are not sufficient due to lack of efficacy, increasing drug resistance, parenteral administration or severe adverse effects. Combining several antileishmanial drugs could possibly solve these issues and improve on therapeutic outcome in leishmaniasis treatment. In addition, it could shorten treatment duration. In the clinical studies on combination therapies performed until now, no clinical PK evaluations of drug-drug interactions have been performed, whilst PK interactions could potentially affect the safety of and exposure to the independent drugs.

Caution is required in the combination of D-AMB with paromomycin or pentamidine due to the possibility of cumulative risk of nephrotoxicity. In addition, the metabolism of pentamidine could potentially be affected due to CYP inhibition by D-AMB [105]. Furthermore, as both Sb and paromomycin are renally excreted, their combination with nephrotoxic antileishmanials (especially D-AMB) should be monitored.

As described previously, miltefosine was found to be an intestinal P-gp inhibitor and AMB was reported to be a substrate for P-gp [128], although this has been contested [129]. As both miltefosine and AMB are amphiphilic molecules, AMB monomers were found to be incorporated in micellar formations of miltefosine, if miltefosine is present above its critical micelle concentration [130]. This could alter the drug distribution of both AMB and miltefosine. Further information on the pharmacokinetics of combined administration of miltefosine and AMB from a clinical study currently being conducted in Ethiopia (NCT02011958) can be found in chapter 3.4 of this thesis.

DIRECTIONS FOR FUTURE ADVANCEMENTS IN CLINICAL PHARMACOKINETIC RESEARCH IN LEISHMANIASIS

Until now clinical PK studies have only been performed in leishmaniasis patients for Sb, paromomycin and miltefosine. Performing these studies also for pentamidine and AMB is crucial in rationalizing treatment design, as VL could potentially affect the pharmacokinetics of pentamidine and AMB due to alterations in hepatic physiology and clinical conditions such as hypoalbuminemia.

For the drugs systemically administered in treatment of CL, limited information is available on the distribution of the drug towards the skin or skin lesions, which forms the target site of action. In addition, only one study evaluated intracellular drug concentrations. As the *Leishmania* parasite resides within macrophages, and most antileishmanial drugs exert their action intracellularly, future research should elaborate on intracellular drug exposure. Especially for Sb^V, which is converted into the active Sb^{III} intracellularly, these concentrations possibly more accurately reflect the effective drug concentration to which the parasite is exposed. Information on the intracellular drug pharmacokinetics could be attributable in establishing exposure-response relationships.

Furthermore, exposure-response studies linking the pharmacokinetics of antileishmanial drugs to treatment outcome have up to now only been performed for miltefosine [72][Dorlo et al., submitted for publication]. These studies are essential in the rationalization of the dose and schedule of antileishmanial treatment and the combination of different antileishmanial drugs.

More research is required in optimizing dosing regimens for paediatric patients. Though efforts have been made to specifically evaluate different dosing regimens in paediatric leishmaniasis patients, special dosing regimens are currently only being clinically evaluated for miltefosine, while an adjusted dosage has also been proposed for L-AMB [92].

Population PK modelling could be a valuable tool in future PK research, especially in drugs with large variability in exposure, such as L-AMB. Population PK modelling also provides the opportunity to evaluate the allometric scaling of body size on clearance and V_d. Furthermore, full PK analysis can be performed with relatively limited sampling. Sparse sampling is particularly convenient in PK studies of antileishmanial drugs, as approximately

half of the population is paediatric, requiring less intensive sampling schemes. Furthermore, clinical trials are often conducted in remote settings making sampling and follow-up difficult and consistent timing of sampling required for non-compartmental analysis is therefore challenging. For these sparse and non-heterogeneously collected PK sampling schedules, population PK modelling is especially valuable.

Regarding the PK sampling, there is room for improvement by employing newer collection techniques such as the less-invasive dried blood spot sampling [131]. Dried blood spot samples can be stored and shipped at room temperature, simplifying PK sampling and reducing costs, which is particularly valuable in remote and resource-poor VL and CL areas of endemicity.

FUNDING

CONFLICT OF INTEREST

Authors have no conflicts of interest to declare.

REFERENCES

1. Copeland NK, Aronson NE. Leishmaniasis: treatment updates and clinical practice guidelines review. Curr. Opin. Infect. Dis. 2015;28:426–37.

2. WHO. Control of the leishmaniases.WHO Technical Report Series #949. 2010. http://apps.who.int/iris/bitstream/10665/44412/1/WHO_TRS_949_eng.pdf. Accessed 7 Feb 2017.

3. Croft SL, Olliaro P. Leishmaniasis chemotherapy - challenges and opportunities. Clin. Microbiol. Infect. 2011;17:1478–83.

4. Sundar S, Singh A. Recent developments and future prospects in the treatment of visceral leishmaniasis. Ther. Adv. Infect. Dis. 2016;3:98–109.

5. Monge-Maillo B, López-Vélez R. Miltefosine for visceral and cutaneous leishmaniasis: Drug characteristics and evidence-based treatment recommendations. Clin. Infect. Dis. 2015;60:1398–404.

6. Verrest L, Dorlo TPC. Lack of clinical pharmacokinetic studies to optimize the treatment of neglected tropical diseases: a systematic review. Clin. Pharmacokinet. 2016; doi:10.1007/s40262-016-0467-3.

7. Dorlo TPC, Balasegaram M, Beijnen JH, de vries PJ. Miltefosine: A review of its pharmacology and therapeutic efficacy in the treatment of leishmaniasis. J. Antimicrob. Chemother. 2012;67:2576–97.

8. Stone NRH, Bicanic T, Salim R, Hope W. Liposomal amphotericin B (AmBisome®): a review of the pharmacokinetics, pharmacodynamics, clinical experience and future directions. Drugs. 2016;76:485–500.

9. US Food and Drug Administration FDA. FDA limits usage of Nizoral (ketoconazole) oral tablets due to potentially fatal liver injury and risk of drug interactions and adrenal gland problems. 2013. http://www.fda.gov/downloads/drugs/drugsafety/ucm362444.pdf. Accessed 7 Feb 2017.

10. Vásquez L, Scorza Dagert J V., Scorza J V., Vicuna-Fernández N, de Pena YP, López S, et al. Pharmacokinetics of experimental pentavalent antimony after intramuscular administration in adult volunteers. Curr. Ther. Res. 2006;67:193–203.

11. Cruz A, Rainey PM, Herwaldt BL, Stagni G, Palacios R, Trujillo R, et al. Pharmacokinetics of antimony in children treated for leishmaniasis with meglumine antimoniate. J. Infect. Dis. 2007;195:602–8.

12. Baiocco P, Colotti G, Franceschini S, Ilari A. Molecular basis of antimony treatment in Leishmaniasis. J. Med. Chem. 2009;52:2603–12.

13. Mookerjee Basu J, Mookerjee A, Sen P, Bhaumik S, Sen P, Banerjee S, et al. Sodium Antimony Gluconate induces generation of reactive oxygen species and nitric oxide via phosphoinositide 3-kinase and mitogen-activated protein kinase activation in Leishmania donovani-infected macrophages. Antimicrob. Agents Chemother. 2006;50:1788–97.

14. Frézard F, Demicheli C, Ribeiro RR. Pentavalent antimonials: New perspectives for old drugs. Molecules. 2009;14:2317–36.

15. Mookerjee Basu J, Mookerjee A, Banerjee R, Saha M, Singh S, Naskar K, et al. Inhibition of ABC transporters abolishes antimony resistance in Leishmania infection. Antimicrob. Agents Chemother. 2008;52:1080–93.

16. Oliveira LF, Schubach AO, Martins MM, Passos SL, Oliveira RV, Marzochi MC, et al. Systematic review of the adverse effects of cutaneous leishmaniasis treatment in the New World. Acta Trop. 2011;118:87–96.

17. Sundar S, Chakravarty J. Antimony toxicity. Int. J. Environ. Res. Public Health. 2010;7:4267–77.

18. Chulay JD, Fleckenstein L, Smith DH. Pharmacokinetics of antimony during treatment of visceral leishmaniasis with sodium stibogluconate or meglumine antimoniate. Trans. R. Soc. Trop. Med. Hyg. 1988;82:69–72.

19. Zaghloul IY, Radwan MA, Al Jaser MH, Al Issa R. Clinical efficacy and pharmacokinetics of antimony in cutaneous leishmaniasis patients treated with sodium stibogluconate. J. Clin. Pharmacol. 2010;50:1230–7.

20. Al Jaser M, El-Yazigi A, Kojan M, Croft SL. Skin uptake, distribution, and elimination of antimony following administration of sodium stibogluconate to patients with cutaneous leishmaniasis. Antimicrob. Agents Chemother. 1995;39:516–9.

21. Abdallah A, Saif M. Trace studies with antimony 124 in man. In: Wolstenholme, GEW, O'Connor, M, editors. Bilharziasis. London: Churchill. 1962. p. 287–309.

22. Friedrich K, Vieira FA, Porrozzi R, Marchevsky RS, Miekeley N, Grimaldi G, et al. Disposition of antimony in rhesus monkeys infected with Leishmania braziliensis and treated with meglumine antimoniate. J. Toxicol. Environ. Heal. Part A. 2012;75:63–75.

23. Coelho DR, Miranda ES, Saint'Pierre TD, Roma Paumgartten FJ. Tissue distribution of residual antimony in rats treated with multiple doses of meglumine antimoniate. Mem. Inst. Oswaldo Cruz. 2014;109:420–7.

24. Dorea JG, Merchan-Hamann E, Ryan DE, Holzbecher J. Retention of antimony in skin biopsies of Leishmaniasis patients after treatment with N-methylglucamine antimoniate. Clin. Chem. 1990;36:680–2.

25. Da Justa Neves DB, Caldas ED, Sampaio RNR.

Antimony in plasma and skin of patients with cutaneous leishmaniasis - Relationship with side effects after treatment with meglumine antimoniate. Trop. Med. Int. Heal. 2009;14:1515–22.

26. Miekeley N, Mortari SR, Schubach AO. Monitoring of total antimony and its species by ICP-MS and on-line ion chromatography in biological samples from patients treated for leishmaniasis. Anal. Bioanal. Chem. 2002;372:495–502.

27. Dos Santos Ferreira C, Silveira Martins P, Demicheli C, Brochu C, Ouellette M, Frézard F. Thiol-induced reduction of antimony(V) into antimony(III): A comparative study with trypanothione, cysteinyl-glycine, cysteine and glutathione. BioMetals. 2003;16:441–6.

28. Rees PH, Keating MI, Kager PA, Hockmeter WT. Renal clearance of pentavalent antimony (sodium stibogluconate). Lancet. 1980;2:226–9.

29. Pamplin CL, Desjardins R, Chulay J, Tramont E, Hendricks L, Canfield C. Pharmacokinetics of antimony during sodium stibogluconate therapy for cutaneous leishmaniasis. Clin. Pharmacol. Ther. 1981;29:270–1.

30. Al-Jaser M, El-Yazigi A, Croft SL. Pharmacokinetics of antimony in patients treated with sodium stibogluconate for cutaneous leishmaniasis. Pharm. Res. 1995;12:111–4.

31. Davidson RN, den Boer M, Ritmeijer K. Paromomycin. Trans. R. Soc. Trop. Med. Hyg. 2009;103:653–60.

32. Institute for One World Health. Application for inclusion of paromomycin in the WHO Model List of Essential Medicines. 2006. http://archives.who. int/eml/expcom/expcom15/applications/newmed/ paromomycin/paromomycin.pdf. Accessed 7 Feb 2017.

33. Sundar S, Jha TK, Thakur CP, Sinha PK, Bhattacharya SK. Injectable Paromomycin for Visceral Leishmaniasis in India. N. Engl. J. Med. 2007;356:2571–81.

34. Hens B, Brouwers J, Anneveld B, Corsetti M, Symillides M, Vertzoni M, et al. Gastrointestinal transfer: *In vivo* evaluation and implementation in *in vitro* and in silico predictive tools. Eur. J. Pharm. Sci. 2014;63:233–42.

35. Bissuel F, Cotte L, de Montclos M, Rabodonirina M, Trepo C. Absence of systemic absorption of oral paromomycin during long-term, high-dose treatment for cryptosporidiosis in AIDS. J. Infect. Dis. 1994;170:749–50.

36. Kanyok TP, Killian AD, Rodvold KA, Danziger LH. Pharmacokinetics of intramuscularly administered aminosidine in healthy subjects. Antimicrob. Agents Chemother. 1997;41:982–6.

37. Musa AM, Younis B, Fadlalla A, Royce C, Balasegaram M, Wasunna M, et al. Paromomycin for the treatment of visceral leishmaniasis in Sudan: A randomized, open-label, dose-finding study. PLoS Negl. Trop. Dis. 2010;4:4–10.

38. Kshirsagar S, Mordenti J, Blaschke T. Clinical pharmacokinetics of paromomycin sulfate in Indian visceral leishmaniasis patients. At: 46th Interscience Conference on Antimicrobial Agents and Chemotherapy (ICAAC); 27–30 September 2006; San Francisco, CA. Washington, DC: ASM Press. 2006. p. poster A – 1105.

39. Belloli C, Crescenzo G, Carli S, Villa R, Sonzogni O, Carelli G, et al. Pharmacokinetics and dosing regimen of aminosidine in the dog. Vet. Res. Commun. 1996;20:533–41.

40. Gordon RC, Regamey C, Kirby WMM. Serum protein binding of the aminoglycoside antibiotics. Antimicrob. Agents Chemother. 1972;2:214–6.

41. Seyffart G. Paromomycin. In: Seyffart, G, editor. Drug dosing in renal insufficiency. Netherlands: Spinger. 1991. p. 448.

42. Kirby WMM, Clarke JT, Libke RD, Regamey C. Clinical pharmacology of amikacin and kanamycin. J. Infect. Dis. 1976;134:S312–5.

43. Mudawi MME, Khalil EAG, Eltayeb IB, Musa AM, Shaddad SAI, Githiga IM, et al. The pharmacokinetics of paromomycin (aminosidine) in healthy volunteers and kala-azar patients. At: Annual Conference of Graduate Studies and Scientific Research, Medical and Health Studies - University of Khartoum. 2011.

44. Maarouf M, Adeline M, Solignac M, Vautrin D, Robert-Gero M. Development and characterization of paromomycin-resistant *Leishmania donovani* promastigotes. Parasite. 1998;5:167–73.

45. Coelho AC, Messier N, Ouellette M, Cotrim PC. Role of the ABC transporter PRP1 (ABCC7) in pentamidine resistance in *Leishmania* amastigotes. Antimicrob. Agents Chemother. 2007;51:3030–2.

46. Kotthaus J, Kotthaus J, Schade D, Schwering U. New prodrugs of the antiprotozoal drug pentamidine. ChemMedChem. 2011;6:2233–42.

47. Bronner U, Doua F, Ericsson Ö, Gustafsson LL, Miézan TW, Rais M, et al. Pentamidine concentrations in plasma, whole blood and cerebrospinal fluid during treatment of Trypanosoma gambiense infection in Côte d'Ivoire. Trans. R. Soc. Trop. Med. Hyg. 1991;85:608–11.

48. Donnelly H, Bernard EM, Rothkotter H, Gold JWM, Armstrong D. Distribution of pentamidine in patients with AIDS. J. Infect. Dis. 1988;157:985–9.

49. Thomas SHL, Page CJ, Blower PJ, Chowienczyk P, Ward A, Kamali F, et al. Disposition of intravenous 123-iodopentamidine in man. Nucl. Med. Biol. 1997;24:327–32.

50. Berger BJ, Naiman NA, Hall JE, Peggins J, Brewer TG, Tidwell RR. Primary and secondary metabolism of pentamidine by rats. Antimicrob. Agents Chemother. 1992;36:1825–31.

51. Bronner U, Gustafsson LL, Doua F, Ericsson Ö, Miézan T, Rais M, et al. Pharmacokinetics and adverse reactions after a single dose of pentamidine in patients with Trypanosoma gambiense sleeping sickness. Br. J. Clin. Pharmacol. 1995;39:289–95.

52. Li X, Björkman A, Andersson TB, Gustafsson LL, Masimirembwa CM. Identification of human cytochrome P450s that metabolise anti-parasitic drugs and predictions of *in vivo* drug hepatic clearance from in vitro data. Eur. J. Clin. Pharmacol. 2003;59:429–42.

53. Conte Jr JE, Upton RA, Phelps RT, Wofsy CB, Zurlinden E, Lin ET. Use of a specific and sensitive assay to determine pentamidine pharmacokinetics in patients with Aids. J. Infect. Dis. 1986;154:923–9.

54. Conte Jr JE. Pharmacokinetics of intravenous pentamidine in patients with normal renal function or receiving hemodialysis. J. Infect. Dis. 1991;163:169–75.

55. Waalkes TP, Denham C, DeVita VT. Pentamidine: Clinical pharmacologic correlations in man and mice. Clin. Pharmacol. Ther. 1970;11:505–12.

56. Vöhringer HF, Arasteh K, Link H, Ehninger G, Hardtmann I. [Determinants of serum pentamidine concentration in the human] (in german). Med Klin (Munich). 1992;87:24–9.

57. Conte Jr JE, Upton RA, Lin ET. Pentamidine pharmacokinetics in patients with AIDS with impaired renal function. J. Infect. Dis. 1987;156:885–90.

58. Comtois R, Pouliot J, Vinet B, Gervais A, Lemieux C. Higher pentamidine levels in AIDS patients with hypoglycemia and azotemia during treatment of pneumocystis carinii pneumonia. Am. Rev. Respir. Dis. 1992;146:740–4.

59. Samanta TB, Das N, Das M, Marik R. Mechanism of impairment of cytochrome P450-dependent metabolism in hamster liver during leishmaniasis. Biochem. Biophys. Res. Commun. 2003;312:75–9.

60. Barioni MB, Ramos AP, Zaniquelli MED, Acuña AU, Ito AS. Miltefosine and BODIPY-labeled alkylphosphocholine with leishmanicidal activity: Aggregation properties and interaction with model membranes. Biophys. Chem. 2015;196:92–9.

61. Berman J. Miltefosine to treat leishmaniasis. Expert Opin. Pharmacother. 2005;6:1381–8.

62. Kötting J, Marschner NW, Neumüller W, Unger C, Eibl H. Hexadecylphosphocholine and octadecyl-methyl-glycero-3-phosphocholine: a comparison of hemolytic activity, serum binding and tissue distribution. Prog. Exp. Tumor Res. 1992;34:131–42.

63. Moreira RA, Mendanha SA, Hansen D, Alonso A. Interaction of miltefosine with the lipid and protein components of the erythrocyte membrane. J. Pharm. Sci. 2013;102:1661–9.

64. Sindermann H, Engel J. Development of miltefosine as an oral treatment for leishmaniasis. Trans. R. Soc. Trop. Med. Hyg. 2006;100:2–5.

65. Marschner N, Kötting J, Eibl H, Unger C. Distribution of hexadecylphosphocholine and octadecyl-methyl-glycero-3-phosphocholine in rat tissues during steady-state treatment. Cancer Chemother. Pharmacol. 1992;31:18–22.

66. Breiser A, Kim DJ, Fleer EA, Damenz W, Drube A, Berger M, et al. Distribution and metabolism of hexadecylphosphocholine in mice. Lipids. 1987;22:925–6.

67. Kip AE, Rosing H, Hillebrand MJX, Castro MM, Gomez MA, Schellens JHM, et al. Quantification of miltefosine in peripheral blood mononuclear cells by high-performance liquid chromatography-tandem mass spectrometry. J. Chromatogr. B. Analyt. Technol. Biomed. Life Sci. 2015;6:356–72.

68. Roy SL, Atkins JT, Gennuso R, Kofos D, Sriram RR, Dorlo TPC, et al. Assessment of blood-brain barrier penetration of miltefosine used to treat a fatal case of granulomatous amebic encephalitis possibly caused by an unusual Balamuthia mandrillaris strain. Parasitol. Res. 2015;114:4431–9.

69. Bianciardi P, Brovida C, Valente M, Aresu L, Cavicchioli L, Vischer C, et al. Administration of miltefosine and meglumine antimoniate in healthy dogs: clinicopathological evaluation of the impact on the kidneys. Toxicol. Pathol. 2009;37:770–5.

70. Dorlo TPC, Van Thiel PPAM, Huitema ADR, Keizer RJ, De Vries HJC, Beijnen JH, et al. Pharmacokinetics of miltefosine in old world cutaneous leishmaniasis patients. Antimicrob. Agents Chemother. 2008;52:2855–60.

71. Dorlo TPC, Huitema ADR, Beijnen JH, De Vries PJ. Optimal dosing of miltefosine in children and adults with visceral leishmaniasis. Antimicrob. Agents Chemother. 2012;56:3864–72.

72. Dorlo TPC, Rijal S, Ostyn B, De Vries PJ, Singh R, Bhattarai N, et al. Failure of miltefosine in visceral leishmaniasis is associated with low drug exposure. J. Infect. Dis. 2014;210:146–53.

73. Welte R, Eschertzhuber S, Weiler S, Leitner-Rupprich S, Aigner M, Lass-Florl C, et al. Biliary amphotericin B pharmacokinetics and pharmacodynamics in critically

ill liver transplant recipients receiving treatment with amphotericin B lipid formulations. Int. J. Antimicrob. Agents. 2015;46:325–31.

74. Janknegt R, de Marie S, Bakker-Woudenberg IAJM, Crommelin DJA. Liposomal and lipid formulations of amphotericin B: clinical pharmacokinetics. Clin. Pharmacokinet. 1992;23:279–91.

75. Block ER, Bennett JE, Livoti LG, Klein WJJ, MacGregor RR, Henderson L. Flucytosine and amphotericin B: hemodialysis effects on the plasma concentration and clearance: studies in man. Ann. Intern. Med. 1974;80:613–7.

76. Bekersky I, Fielding RM, Dressler DE, Lee JW, Buell DN, Walsh TJ. Plasma protein binding of amphotericin B and pharmacokinetics of bound versus unbound amphotericin B after administration of intravenous liposomal amphotericin B (AmBisome) and amphotericin B deoxycholate. Antimicrob. Agents Chemother. 2002;46:834–40.

77. Kagan L, Gershkovich P, Wasan KM, Mager DE. Dual physiologically based pharmacokinetic model of liposomal and nonliposomal amphotericin B disposition. Pharm. Res. 2014;31:35–45.

78. Ringdén O, Meunier F, Tollemar J, Ricci P, Tura S, Kuse E, et al. Efficacy of amphotericin B encapsulated in liposomes (AmBisome) in the treatment of invasive fungal infections in immunocompromised patients. J. Antimicrob. Chemother. 1991;28:73–82.

79. Vogelsinger H, Weiler S, Djanani A, Kountchev J, Bellmann-Weiler R, Wiedermann CJ, et al. Amphotericin B tissue distribution in autopsy material after treatment with liposomal amphotericin B and amphotericin B colloidal dispersion. J. Antimicrob. Chemother. 2006;57:1153–60.

80. Strenger V, Meinitzer A, Donnerer J, Hofer N, Dornbusch HJ, Wanz U, et al. Amphotericin B transfer to CSF following intravenous administration of liposomal amphotericin B. J. Antimicrob. Chemother. 2014;69:2522–6.

81. Christiansen KJ, Bernard EM, Gold JWM, Armstrong D. Distribution and activity of amphotericin B in humans. J. Infect. Dis. 1985;152:1037–43.

82. Smith PJ, Olson JA, Constable D, Schwartz J, Proffitt RT, Adler-Moore JP. Effects of dosing regimen on accumulation, retention and prophylactic efficacy of liposomal amphotericin B. J. Antimicrob. Chemother. 2007;59:941–51.

83. Boswell GW, Buell D, Bekersky I. AmBisome (liposomal amphotericin B): a comparative review. J. Clin. 1998;38:583–92.

84. Gershkovich P, Wasan EK, Sivak O, Li R, Zhu X, Werbovetz KA, et al. Visceral leishmaniasis affects liver and spleen concentrations of amphotericin B following administration to mice. J. Antimicrob. Chemother. 2009;65:535–7.

85. Fielding RM, Smith PC, Wang LH, Porter J, Guo LSS. Comparative pharmacokinetics of amphotericin B after administration of a novel colloidal delivery system, ABCD, and a conventional formulation to rats. Antimicrob. Agents Chemother. 1991;35:1208–13.

86. Gubbins PO, Amsden JR, McConnell SA, Anaissie EJ. Pharmacokinetics and buccal mucosal concentrations of a 15 milligram per kilogram of body weight total dose of liposomal amphotericin B administered as a single dose (15 mg/kg), weekly dose (7.5 mg/kg), or daily dose (1 mg/kg) in peripheral stem cell tran. Antimicrob. Agents Chemother. 2009;53:3664–74.

87. Bekersky I, Fielding RM, Dressler DE, Lee W, Buell DN, Walsh TJ, et al. Pharmacokinetics, excretion, and mass balance of liposomal amphotericin B (AmBisome) and amphotericin B deoxycholate in humans. Antimicrob. Agents Chemother. 2002;46:828–33.

88. Walsh TJ, Goodman JL, Pappas P, Bekersky I, Buell DN, Roden M, et al. Safety, tolerance and pharmacokinetics of high-dose liposomal amphotericin B (AmBisome) in patients infected with *Aspergillus* species and other filamentous fungi: maximum tolerated dose study. Antimicrob. Agents Chemother. 2001;45:3487–96.

89. Walsh TJ, Yeldandi V, McEvoy M, Gonzalez C, Chanock S, Freifeld A, et al. Safety, tolerance, and pharmacokinetics of a small unilamellar liposomal formulation of amphotericin B (AmBisome) in neutropenic patients. Antimicrob. Agents Chemother. 1998;42:2391–8.

90. Hope WW, Goodwin J, Felton TW, Ellis M, Stevens DA. Population pharmacokinetics of conventional and intermittent dosing of liposomal amphotericin B in adults: A first critical step for rational design of innovative regimens. Antimicrob. Agents Chemother. 2012;56:5303–8.

91. Würthwein G, Young C, Lanvers-Kaminsky C, Hempel G, Trame MN, Schwerdtfeger R, et al. Population pharmacokinetics of liposomal amphotericin B and caspofungin in allogeneic hematopoietic stem cell recipients. Antimicrob. Agents Chemother. 2012;56:536–43.

92. Hong Y, Nath CE, Yadav SP, Stephen KR, Earl JW, Mclachlan AJ. Population pharmacokinetics of liposomal amphotericin B in pediatric patients with malignant diseases. Antimicrob. Agents Chemother. 2006;50:935–42.

93. Ohata Y, Tomita Y, Suzuki K, Maniwa T, Yano Y, Sunakawa K. Pharmacokinetic evaluation of liposomal amphotericin B (L-AMB) in patients with invasive fungal

infection: Population approach in Japanese pediatrics. Drug Metab. Pharmacokinet. 2015;30:400–9.

94. Lestner JM, Groll AH, Aljayyoussi G, Seibel NL, Shad A, Gonzalez C, et al. Population pharmacokinetics of Liposomal Amphotericin B in Immunocompromised Children. Antimicrob. Agents Chemother. 2016;60:7340–6.

95. Heinemann V, Bosse D, Jehn U, Kahny B, Wachholz K, Debus A, et al. Pharmacokinetics of liposomal amphotericin B (Ambisome) in critically ill patients. Antimicrob. Agents Chemother. 1997;41:1275–80.

96. Institute for Health Metrics and Evaluation (IHME). GBD Results Tool. Seattle, WA: IHME, University of Washington, 2016. http://ghdx.healthdata.org/gbd-results-tool. Accessed 7 Feb 2017.

97. Anderson BJ, Holford NHG. Mechanism-based concepts of size and maturity in pharmacokinetics. Annu. Rev. Pharmacol. Toxicol. 2008;48:303–32.

98. Ostyn B, Hasker E, Dorlo TPC, Rijal S, Sundar S, Dujardin J, et al. Failure of miltefosine treatment for visceral leishmaniasis in children and men in South-East Asia. PLoS One. 2014;9:e100220.

99. Rijal S, Ostyn B, Uranw S, Rai K, Bhattarai NR, Dorlo TPC, et al. Increasing failure of miltefosine in the treatment of kala-azar in nepal and the potential role of parasite drug resistance, reinfection, or noncompliance. Clin. Infect. Dis. 2013;56:1530–8.

100. Castro MM, Gomez MA, Kip AE, Cossio A, Ortiz E, Navas A, et al. Pharmacokinetics of miltefosine in children and adults with cutaneous leishmaniasis. Antimicrob Agents Chemother. 2017; 61(3): e02198-16.

101. Starke JR, Jr EOM, Kramer WG, Sheldon L, Starke JR, Mason EO, et al. Pharmacokinetics of amphotericin B in infants and children. J. Infect. Dis. 1987;155:766–74.

102. Koren G, Lau A, Klein J, Golas C, Bologa-Campeanu M, Soldin S, et al. Pharmacokinetics and adverse effects of amphotericin B in infants and children. J. Pediatr. 1988;113:559–63.

103. Alvar J, Aparicio P, Aseffa A, Den Boer M, Cañavate C, Dedet JP, et al. The relationship between leishmaniasis and AIDS: The second 10 years. Clin. Microbiol. Rev. 2008;21:334–59.

104. Tittle V, Bull L, Boffito M, Nwokolo N. Pharmacokinetic and pharmacodynamic drug interactions between antiretrovirals and oral contraceptives. Clin. Pharmacokinet. 2015;54:23–34.

105. Inselmann G, Volkmann A, Heidemann HT. Comparison of the effects of liposomal amphotericin B and conventional amphotericin B on propafenone metabolism and hepatic cytochrome P-450 in rats.

Antimicrob. Agents Chemother. 2000;44:131–3.

106. Brockmeyer NH, Gambichler T, Bader A, Kreuter A, Kurowski M, Sander P, et al. Impact of Amphotericin B on the cytochrome P450 system in HIV-infected patients. Eur. J. Med. Res. 2006;9:51–4.

107. Menez C, Buyse M, Chacun H, Farinotti R, Barratt G. Modulation of intestinal barrier properties by miltefosine. Biochem. Pharmacol. 2006;71:486–96.

108. Brustoloni YM, Cunha RV, Cônsolo LZ, Oliveira ALL, Dorval MEC, Oshiro ET. Treatment of visceral leishmaniasis in children in the Central-West Region of Brazil. Infection. 2010;38:261–7.

109. Libório AB, Rocha NA, Oliveira MJC, Franco LFLG, Aguiar GBR, Pimentel RS, et al. Acute kidney injury in children with visceral leishmaniasis. Pediatr. Infect. Dis. J. 2012;31:451–4.

110. Adedoyin A, Bernardo JF, Swenson CE, Bolsack LE, Horwith G, DeWit S, et al. Pharmacokinetic profile of ABELCET (amphotericin B lipid complex injection): Combined experience from phase I and phase II studies. Antimicrob. Agents Chemother. 1997;41:2201–8.

111. Silva JSF e, Galvao TF, Pereira MG, Silva MT. Treatment of American tegumentary leishmaniasis in special populations: A summary of evidence. Rev. Soc. Bras. Med. Trop. 2013;46:669–77.

112. Zheng G, Zhong H, Guo Z, Wu Z, Zhang H, Wang C, et al. Levels of heavy metals and trace elements in umbilical cord blood and the risk of adverse pregnancy outcomes: A population-based study. Biol. Trace Elem. Res. 2014;160:437–44.

113. Mueller M, Balasegaram M, Koummuki Y, Ritmeijer K, Santana MR, Davidson R. A comparison of liposomal amphotericin B with sodium stibogluconate for the treatment of visceral leishmaniasis in pregnancy in Sudan. J. Antimicrob. Chemother. 2006;58:811–5.

114. Morgan DJ, Guimaraes LH, Machado PR, D'Oliveira Jr. A, Almeida RP, Lago EL, et al. Cutaneous leishmaniasis during pregnancy: exuberant lesions and potential fetal complications. Clin. Infect. Dis. 2007;45:478–82.

115. Bossolasco S, Gaiera G, Olchini D, Gulletta M, Martello L, Bestetti A, et al. Real-Time PCR assay for clinical management of human immunodeficiency virus-infected patients with visceral leishmaniasis. J. Clin. Microbiol. 2003;41:5080–4.

116. Coelho DR, De-Carvalho RR, Rocha RCC, Saint'Pierre TD, Paumgartten FJR. Effects of in utero and lactational exposure to SbV on rat neurobehavioral development and fertility. Reprod. Toxicol. 2014;50:98–107.

117. Miranda ES, Miekeley N, De-Carvalho RR, Paumgartten FJR. Developmental toxicity of meglumine

antimoniate and transplacental transfer of antimony in the rat. Reprod. Toxicol. 2006;21:292–300.

118. Paumgartten FJR, Chahoud I. Embryotoxicity of meglumine antimoniate in the rat. Reprod. Toxicol. 2001;15:327–31.

119. Harstad TW, Little BB, Bawdon RE, Knoll K, Roe D, Gilstrap LC. Embryofetal effects of pentamidine isethionate administered to pregnant Sprague-Dawley rats. Am. J. Obstet. Gynecol. 1990;163:912–6.

120. Dorlo TPC, Balasegaram M, Lima MA, De Vries PJ, Beijnen JH, Huitema ADR. Translational pharmacokinetic modelling and simulation for the assessment of duration of contraceptive use after treatment with miltefosine. J. Antimicrob. Chemother. 2012;67:1996–2004.

121. Donald PR, Sellars SL. Streptomycin ototoxicity in the unborn child. South African Med. J. 1981;60:316–8.

122. Pilmis B, Jullien V, Sobel J, Lecuit M, Lortholary O, Charlier C. Antifungal drugs during pregnancy: an updated review. J. Antimicrob. Chemother. 2014;70:14–22.

123. Novarini A, Montanari A, Bruschi G, Rossi E, Borghetti A, Migone L. The kinetics of aminosidine in renal patients with different degrees of renal failure. Clin. Nephrol. 1975;4:23–4.

124. Hernández E, Oliet A, Gallar P, Llanos M, Guerra L, Vigil A. Amphotericin B for visceral leishmaniasis in hemodialysis. Nephron. 1991;59:666.

125. Muther RS, Bennett WM. Peritoneal clearance of amphotericin B and 5-fluorocytosine. West. J. Med. 1980;133:157–60.

126. Vogelsinger H, Joannidis M, Kountchev J, Bellmann-Weiler R, Wiedermann CJ, Bellmann R. Pharmacokinetics of liposomal amphotericin B during extracorporeal albumin dialysis. Artif. Organs. 2006;30:118–21.

127. Bellmann R, Egger P, Gritsch W, Bellmann-Weiler R, Joannidis M, Kaneider N, et al. Amphotericin B lipid formulations in critically ill patients on continuous veno-venous haemofiltration. J. Antimicrob. Chemother. 2003;51:671–81.

128. Wu JQ, Shao K, Wang X, Wang RY, Cao YH, Yu YQ, et al. *In vitro* and *in vivo* evidence for amphotericin B as a P-glycoprotein substrate on the blood-brain barrier. Antimicrob. Agents Chemother. 2014;58:4464–9.

129. Osei-Twum J, Wasan KM. Does P-glycoprotein contribute to amphotericin B epithelial transport in Caco-2 cells? Drug Dev. Ind. Pharm. 2015;41:1130–6.

130. Ménez C, Legrand P, Rosilio V, Lesieur S, Barratt G. Physicochemical characterization of molecular assemblies of miltefosine and amphotericin B. Mol. Pharm. 2006;4:281–8.

131. Kip AE, Rosing H, Hillebrand MJX, Blesson S, Mengesha B, Diro E, et al. Validation and clinical evaluation of a novel method to measure miltefosine in leishmaniasis patients using dried blood spot sample collection. Antimicrob. Agents Chemother. 2016;60:2081–9.

132. Ayestarán A, López RM, Montoro JB, Estíbalez A, Pou L, Julià A, et al. Pharmacokinetics of conventional formulation versus fat emulsion formulation of amphotericin B in a group of patients with neutropenia. Antimicrob. Agents Chemother. 1996;40:609–12.

133. Benson J, Nahata MC. Pharmacokinetics of amphotericin B in children. Antimicrob. Agents Chemother. 1989;33:1989–93.

134. Kan VL, Bennett JE, Amantea MA, Smolskis MC, McManus E, Grasela DM, et al. Comparative safety, tolerance, and pharmacokinetics of amphotericin B lipid complex and amphotericin B desoxycholate in healthy male volunteers. J. Infect. Dis. 1991;164:418–21.

135. Nath CE, McLachlan AJ, Shaw PJ, Gunning R, Earl JW. Population pharmacokinetics of amphotericin B in children with malignant diseases. Br. J. Clin. Pharmacol. 2001;52:671–80.

Supplementary table 1. General information on the pharmacokinetic studies included in the review.

Author	Patient population	Country	# patients	Age (years)	Weight (kg)	Gender (% male)	Formulation / Brand	IM/IV/ Oral	Analytical method	LLOQ (µg/mL plasma)	PK analysis	Model
Pentavalent antimonials												
Al-Jaser et al. [30]	Cutaneous leishmaniasis	Saudi Arabia	29	32.3±7.3	60-75	100%	Pentostam (SSG)	IM	ET AAS	N/A	Compartmental (individual)	1-CMT
Chulay et al. [18]	Visceral leishmaniasis	Kenya	5	31.4±20.3	47.4±8.05	N/A	Pentostam (SSG) (n=2) / Glucan-time (MA) (n=3)	IM	Anodic stripping voltametry	0.03	Compartmental (individual)	2-CMT with lag-time for 4/5 patients
Cruz et al. [11]	Cutaneous leishmaniasis											
	Adult: 20 mg/ kg/day, 20 days	Colombia	9	26 (20-36)	62 (56-120)	100%	Glucantime (MA)	IM	ET AAS	0.05	NCA	-
	Child: 20 mg/ kg/day, 20 days	Colombia	9	4 (3-6)	15 (13-18)	33%	Glucantime (MA)	IM	ET AAS	0.05	NCA	-
	Child: 20 mg/ kg/day, 19 days + 30 mg/kg/day day 20	Colombia	6	4.5 (3-6)	17.5 (13-21)	50%	Glucantime (MA)	IM	ET AAS	0.05	NCA	-
Pamplin et al. [29]	Cutaneous leishmaniasis	US	10	N/A	N/A	N/A	Pentostam (SSG)	IV	Aniotic voltametry	N/A	Compartmental (individual)	3-CMT
Zaghloul et al. [19]	Cutaneous leishmaniasis	Saudi Arabia	12	31.1±7.0	66.4±8.7	100%	Pentostam (SSG)	IM	ET AAS	0.008	Compartmental (individual) / NCA	2-CMT model, first-order input
Paromomycin												
Kanyok et al. [36]	Healthy volunteers						Aminosidine sulfate (Gabbromicina)	IM	HPLC-UV	0.5	Compartmental (individual)	1-CMT model, first-order input / output + lag-time
	12 mg/kg	US	8	26.4±2.5	68.2±14.0	50%						
	15 mg/kg	US	8	29.0±7.8	70.7±13.0	50%						
Kshirsagar et al. [38]	Visceral leish-maniasis	India	448	22.1± 12.3[a]	35.5±11.8[a]	65%	Paromomycin Sulfate (Pharmamed Parenterals)	IM	LC-MS/MS	0.5	Compartmental (population)	

Author	Patient population	Country	# patients	Age (years)	Weight (kg)	Gender (% male)	Formulation / Brand	IM/IV/ Oral	Analytical method	LLOQ (µg/mL plasma)	PK analysis	Model
Pentamidine												
Bronner et al. [47]	African trypanosomiasis	Cote d'Ivoire	11	38 (12-65)	54 (34-66)	55%	Pentamidine dimesylate (Lomidine)	IM	HPLC - Fluorescence	5.4 ng/mL	NCA	-
Bronner et al. [51]	African trypanosomiasis	Cote d'Ivoire	11	26 (19-42)	63 (50-84)	82%	Pentamidine isethionate (Pentacarinat)	IV 2h	HPLC - Fluorescence	1 ng/mL	NCA	-
Conte et al. [53]	AIDS / P. carinii pneumonia	US	12	37±9	62±17	100%	Pentamidine isethionate (Pentam 300)	IM (n=6) IV (n=6) 2h	HPLC - Fluorescence	2.3 ng/mL	Compartmental (individual)	2-CMT model, zero-order input
Conte et al. [57]	AIDS / P. carinii pneumonia	US	20	38±9 excl. 2 children	64±8 excl. 2 children	90%	Pentamidine isethionate (Pentam 300)	IM (n=5) IV(n=15) 0.5-2h	HPLC - Fluorescence	2.3 ng/mL	Compartmental (individual)	2-CMT model, zero-order input
Conte et al. [54]	AIDS / P. carinii pneumonia	US	10[b]	40±6	66±10	100%	Pentamidine isethionate (Pentam 300)	IV 2h	HPLC - Fluorescence	0.58 ng/mL	Compartmental (individual) / NCA	3-CMT model
	Volunteer hemodialysis		9	44±10	73±10	67%	Pentamidine isethionate (Pentam 300)	IV 2h	HPLC - Fluorescence	0.58 ng/mL	Compartmental (individual) / NCA	3-CMT model
	Acute P. carinii pneumonia - Last dose only		5	38±9	80±8	100%	Pentamidine isethionate (Pentam 300)	IV 2h	HPLC - Fluorescence	0.58 ng/mL	Compartmental (individual) / NCA	3-CMT model
Thomas et al. [49]	AIDS	UK	5	N/A	60.2 (58-65)	100%	Pentamidine isethionate (Pentam 300)	IV	HPLC-UV	10-20 ng/mL	Compartmental (individual)	2-CMT model, zero order input
Miltefosine												
Berman [61]	No general information available											

Author	Patient population	Country	# patients	Age (years)	Weight (kg)	Gender (% male)	Formulation / Brand	IM/IV/ Oral	Analytical method	LLOQ (µg/mL plasma)	PK analysis	Model
Castro et al. [100]	Cutaneous leishmaniasis						Impavido	Oral	LC-MS/MS	0.004	NCA	-
	Adults	Colombia	30	33.53 ±8.32	70.84 ±11.73	46.67%						
	Children (<12y)	Colombia	30	8.16 ±2.58	26.22 ±7.62	60%						
Dorlo et al. [70]	Cutaneous leishmaniasis	The Netherlands	31	24 (19-49)	85 (70-113)	97%	Impavido	Oral	LC-MS/MS	0.004	Compartmental (population)	2-CMT, first order absorption
Dorlo et al. [71]							Impavido	Oral	LC-MS/MS		Compartmental (population)	2-CMT, first order absorption
	Visceral leishmaniasis - Pediatric	India	39	7 (3-11)	15 (9-23)	59%				0.005		
	Visceral leishmaniasis - Adult	India	40	19 (12-50)	36 (16-58)	75%				0.005		
	Cutaneous leishmaniasis[c]	The Netherlands	31	24 (19-49)	85 (70-113)	97%				0.004		
Dorlo et al. [72]	Visceral leishmaniasis	Nepal	81[d]	20 (2-65)	40 (8-56)	62%	Impavido	Oral	LC-MS/MS	0.004	Compartmental (population)	2-CMT, first order absorption
Amphotericin B												
Ayestaran et al. [132]	Neutropenic	Spain	8	41.8±19.6	63.8±6.8	75%	D-AMB (Fungizone)	IV 1 h	HPLC-UV	0.05	Compartmental (individual) /NCA	2-CMT
Bekersky et al. [87]	Healthy volunteers							IV 2 h	LC-MS/MS / -UV	2.0 / 0.1	NCA	N/A
	L-AMB	US	5	30±5	79±11	80%	L-AMB (AmBisome)					
	D-AMB	US	5	49±16	77±9	80%	D-AMB (Fungizone)					
Benson et al. [133]	Pediatric (various infections)	US	12	0-14 (range)	21.6±13.3	42%	D-AMB (Fungizone)	IV 2-4.5 h	HPLC-UV	0.1	NCA	N/A

Author	Patient population	Country	# patients	Age (years)	Weight (kg)	Gender (% male)	Formulation / Brand	IM/IV/ Oral	Analytical method	LLOQ (µg/mL plasma)	PK analysis	Model
Gubbins et al. [86]	Peripheral Stem Cell Transplant	US					L-AMB (AmBisome)	IV 2 h	HPLC-UV	0.1	NCA	N/A
	1.0 mg/kg daily		6	57.5±12.9	71.7±13.3	50%						
	7.5 mg/kg weekly		4	61.0±7.7	83.9±26.1	75%						
	15 mg/kg, single dose		6	56.7±7.1	87.5±27.1	67%						
Heinemann et al. [95]	Critically ill	Germany						IV 1 h	HPLC-UV	0.05	Compartmental (individual)	2-CMT
	L-AMB		16^e	47 (20-67)	72 (57-85)	50%	L-AMB (AmBisome)					
	D-AMB		6	56 (49-76)	70 (50-120)	83%	D-AMB (Fungizone)					
Hong et al. [92]	Malignant disease - pediatric	Australia	39	7 (0.2-17)	28.8 kg (mean)	67%	L-AMB (AmBisome)	IV 1 h	HPLC-UV	0.1	Compartmental (population)	2-CMT, zero order input, first-order elimination
Hope et al. [90]^f	Invasive fungal infection	United Arab Emirates					L-AMB (AmBisome)	IV 2 h	HPLC-UV	0.05	Compartmental (population)	3-CMT
	Intermittent dosing		15	36 (17-55)	68 kg (mean)	7%						
	Conventional dosing		15	38 (18-55)	68 kg (mean)	60%						
Kan et al. [134]	Healthy volunteers	US	16	26.6 (20-38)	74.2 (55-87)	100%	D-AMB (Fungizone)	IV	HPLC-UV	0.025	NCA	N/A
Koren et al. [102]	Pediatric patients (various infections)	Canada	13	Range 0-18	N/A	N/A	D-AMB	N/A	HPLC-UV	0.1	Compartmental (individual)	1-CMT
Lestner et al. [94]	Immunocompromised children	US	35	8.7±4.6	26.9±14.0	63%	L-AMB (AmBisome)	IV 1 h	HPLC-UV	0.05	Compartmental (population)	2-CMT
Nath et al. [135]	Malignant disease - pediatric	Australia	83	6 (1-16)	23.3±1.3	59%	D-AMB (Fungizone)	IV 2 h	HPLC-UV	0.1	Compartmental (population)	2-CMT

1

Author	Patient population	Country	# patients	Age (years)	Weight (kg)	Gender (% male)	Formulation / Brand	IM/IV/ Oral	Analytical method	LLOQ (µg/mL plasma)	PK analysis	Model
Ohata et al. [93]	Invasive fungal infection	Japan	39	8.4±4.5	27.1±14.1	59%	L-AMB (AmBisome)	IV 1-1.25 h	HPLC-UV	0.1	Compartmental (population)	2-CMT, zero order input, first-order elimination
Walsh et al. [89]	Neutropenic	US					L-AMB (AmBisome)	IV 1h	HPLC-UV	0.05	NCA	N/A
	1.0 mg/kg	US	8	44.5±6.1	N/A	38%						
	2.5 mg/kg	US	8	41.3±4.0	N/A	38%						
	5.0 mg/kg	US	12	35.2±4.4	N/A	25%						
	7.5 mg/kg	US	8	36.5±6.2	N/A	63%						
Walsh et al. [88]	Immunocompromised/ invasive fungal infections						L-AMB (AmBisome)	IV 2 h	HPLC-UV	0.1	NCA	N/A
	7.5 mg/kg	US	8	40.4±9.5	N/A[g]	100%						
	10.0 mg/kg	US	10	39.8±10.9	N/A[g]	90%						
	12.5 mg/kg	US	7	47.6±12.6	N/A[g]	71%						
	15.0 mg/kg	US	19	44.6±12.7	N/A[g]	68%						
Würthe-wein et al. [91]	Hematopoietic stem cell recipients						L-AMB (AmBisome)	IV	HPLC-UV	0.1	Compartmental (population)	2-CMT
	L-AmpB monotherapy	Germany	17	39 (18-60)	72 (44-105)	65%						
	L-AmpB+ CAS[h]	Germany	17	48(20-61)	80 (54-99)	59%						

Data provided as either a) mean±standard deviation or median (range), unless indicated otherwise. N/A: Not Available. IM: intramuscular, IV: intravenous, LLOQ: lower limit of quantitation, NCA: non-compartmental analysis, CMT: compartmental, ET AAS: Electrothermal atomic absorption spectroscopy, HPLC: high-performance liquid chromatography, MS/MS: tandem mass spectrometry, L-AMB: liposomal amphotericin B, D-AMB: amphotericin B deoxycholate

[a]Not provided on poster [38], but provided for 501 patients included in clinical results of trial [33]; used as proxy for 448/501 patients included in population PK model
[b]For 4 patients only trough and peak levels were available, not included in the PK model
[c]Same patients as described in Dorlo et al. [70] included in this population PK model
[d]Included are 61 adults and 20 children, demographics not available separately
[e]PK analysis only performed on 10 patients that received 2.8-3.0 mg/kg dose
[f]Only 28 out of 30 patients included in population PK model
[g]Weight values not reported, but no significant difference in weight between the dosing regimens was reported
[h]These patients received combination of L-AMB with caspofungin (CAS)

Chapter **2**

| Bioanalysis

Chapter 2.1

Validation and clinical evaluation of a novel method to measure miltefosine in leishmaniasis patients using dried blood spot sample collection

A.E. Kip
H. Rosing
M.J.X. Hillebrand
S. Blesson
B. Mengesha
E. Diro
A. Hailu
J.H.M. Schellens
J.H. Beijnen
T.P.C. Dorlo

ABSTRACT

To facilitate future pharmacokinetic studies of combination treatments against leishmaniasis in remote regions in which the disease is endemic, a simple cheap sampling method is required for miltefosine quantification. The aims of this study were to validate a liquid chromatography-tandem mass spectrometry method to quantify miltefosine in dried blood spot (DBS) samples and to validate its use with Ethiopian patients with visceral leishmaniasis (VL). Since hematocrit (Ht) levels are typically severely decreased in VL patients, returning to normal during treatment, the method was evaluated over a range of clinically relevant Ht values.

Miltefosine was extracted from DBS samples using a simple method of pretreatment with methanol, resulting in >97% recovery. The method was validated over a calibration range of 10 to 2,000 ng/mL, and accuracy and precision were within ±11.2% and ≤7.0% (≤19.1% at the lower limit of quantification), respectively. The method was accurate and precise for blood spot volumes between 10 and 30 µL and for Ht levels of 20 to 35%, although a linear effect of Ht levels on miltefosine quantification was observed in the bioanalytical validation. DBS samples were stable for at least 162 days at 37°C.

Clinical validation of the method using paired DBS and plasma samples from 16 VL patients showed a median observed DBS/plasma miltefosine concentration ratio of 0.99, with good correlation (Pearson's r = 0.946). Correcting for patient-specific Ht levels did not further improve the concordance between the sampling methods. This successfully validated method to quantify miltefosine in DBS samples was demonstrated to be a valid and practical alternative to venous blood sampling that can be applied in future miltefosine pharmacokinetic studies with leishmaniasis patients, without Ht correction.

INTRODUCTION

Miltefosine is currently the only oral drug for both cutaneous leishmaniasis (CL) and visceral leishmaniasis (VL), and new studies to evaluate the use of miltefosine-based combination therapies in VL patients and in HIV-coinfected VL patients are under way [1]. Recently, it was discovered that miltefosine treatment failure was associated with lower levels of drug exposure; the time that miltefosine plasma concentrations were >10 times the 50% effective concentration (17.9 µg/mL) was correlated with final treatment failure or success [2]. This finding emphasizes the need for adequate pharmacokinetic (PK) monitoring in such clinical trials.

Both CL and VL are poverty-related diseases that mainly affect populations in resource-poor and remote regions of Africa, Asia, and South America. Classically, human blood plasma is collected by venous sampling for the measurement of drug concentrations, e.g., employing liquid chromatography-tandem mass spectrometry (LC-MS/MS). A bioanalytical method to quantify miltefosine levels in plasma was validated and reported previously [3]. However, technologies such as LC-MS/MS are not available in the regions in which VL is endemic; therefore, samples need to be transported to appropriate facilities for analysis. The required cold storage [3] and transport of these plasma samples are logistically highly challenging, as well as expensive. In addition, plasma sampling by venipuncture is an invasive and risky sampling method, particularly for severely weakened and anemic HIV-coinfected VL patients. A large proportion of VL patients in East Africa are pediatric [4], which limits both the total volume and the number of plasma PK samples that can be obtained through venous blood sampling. Dried blood spot (DBS) sampling is an attractive alternative to plasma sampling in such settings because it is minimally invasive and requires only a small volume of blood [5–9], which is particularly advantageous in pediatric studies [10,11]. In addition, storage and shipment at room temperature are possible and therefore would be simple and low cost, which is preferred in remote areas without proper laboratory facilities.

Major hurdles in the application of DBS sample collection are the effects of hematocrit (Ht) levels and blood spot volumes on miltefosine quantification [12–14]. Ethiopian VL patients had decreased median Ht levels of 25% (range, 23 to 30%) at the initiation of treatment [15], which slowly moved toward Ht levels of 33% (range, 27 to 37%) after 30 days of treatment with sodium antimony gluconate [15]. HIV-coinfected VL patients showed similar Ht values during active VL infections (mean hemoglobin concentration of 9 g/dl, corresponding to a Ht value of approximately 27% [16]). Since miltefosine has a long terminal half-life (30.9 days) [17] and accumulates during treatment, pharmacokinetic sampling is typically performed at various time points during treatment and up to several months after the end of treatment. Ht values show high within-subject variability within this period, which may influence the outcomes of drug measurements with DBS sample collection.

Additionally, blood spot volumes can vary widely between patients, due to variations in blood flow and the penetration of the lancet in the finger. The viscosity of the blood increases with increased Ht levels [18]; therefore, the blood flow and possibly blood spot volumes can be expected to be larger for patients with lower Ht levels.

Here we describe the development and validation of a rapid LC-MS/MS method to quantify miltefosine levels in DBS samples in a range from 10 to 2,000 ng/mL, according to the current Food and Drug Administration (FDA) and European Medicines Agency (EMA) guidelines [19,20] and the European Bioanalysis Forum (EBF) recommendations [21,22] for DBS assays. Furthermore, this study evaluates and validates the clinical applicability of this

method by comparing paired DBS and plasma samples from 16 Ethiopian HIV-coinfected VL patients who received miltefosine treatment.

METHODS

Chemicals and reagents

Miltefosine was purchased from Sigma-Aldrich (Zwijndrecht, the Netherlands). Deuterated miltefosine (miltefosine-D4, Figure 1) was purchased from Alsachim (Illkirch Graffenstaden, France). Methanol and water were obtained from Biosolve Ltd. (Valkenswaard, the Netherlands). Ammonia (25%) was purchased from Merck (Amsterdam, the Netherlands).
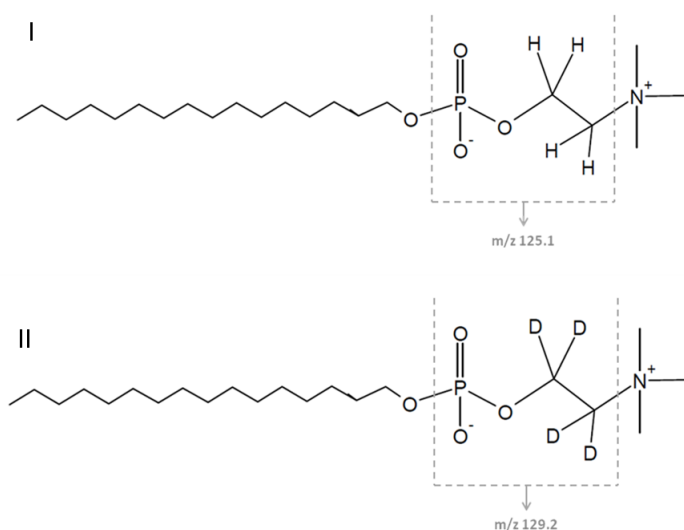
Figure 1. Structural formulas of miltefosine (I) and the internal standard miltefosine-D4 (II), indicating the m/z fragments.

Materials

For the collection of DBS samples, pure cellulose-based cards (Whatman 903 protein saver cards) were used. These cards, together with foil bags and desiccant packages for storage of DBS samples, were purchased from GE Healthcare Europe GmbH (Diegem, Belgium). A Harris 3.0-mm micropuncher was used to punch the DBS samples. Whole blood (WB) was collected in K_2-EDTA BD Vacutainers from healthy volunteers and stored at 2 to 8°C for a maximum of 2 days. WB was adjusted to a Ht level of 30% ± 1% (Ht30 WB), to mimic the Ht levels of VL patients, by dilution with plasma. Ht levels were determined with the Cell Dyn Hematology analyzer (Abbott Diagnostics, Lake Forest, IL, USA).

Preparation of calibration standards and QC samples

Stock solutions of 1 mg/mL miltefosine were prepared from independent weighings in methanol-water (1:1 [vol/vol]). Separate stocks were diluted to working solutions with methanol-water (1:1 [vol/vol]) for the preparation of calibration standards and quality control (QC) samples. A stock solution of 1 mg/mL deuterated miltefosine (miltefosine-D4)

was prepared and diluted to an internal standard (IS) working solution of 4,000 ng/mL miltefosine-D4 in methanol-water (1:1 [vol/vol]). This working solution was further diluted with methanol to an extraction solution of 20 ng/mL miltefosine-D4 in 100% methanol. The stock and working solutions were stored at nominally −20°C.

Calibration standards were diluted 1:20 (vol/vol) in Ht30 WB to final concentrations of 10, 20, 100, 500, 1,000, 1,400, 1,800, and 2,000 ng/mL. QC samples were diluted 1:20 (vol/vol) in Ht30 WB to final concentrations of nominally 10, 24, 300, and 1,600 ng/mL (lower limit of quantification [LLOQ], low-level QC [QCL], mid-level QC [QCM], and high-level QC [QCH], respectively). Additionally, a sample above the upper limit of quantification (>ULOQ), i.e., 40,000 ng/mL, was prepared and used to determine dilution integrity.

A volume of 20 µL of spiked whole blood was spotted on Whatman 903 cards and air dried for at least 3 h at room temperature. When samples that had been dried for 3 h were compared to samples that had been dried overnight (15 to 20 h), no effect was found for the additional drying time (bias within ±6.1%).

Sample pretreatment

After drying, a 3.0-mm punch was taken from the center of the DBS and transferred to a 1.5-mL Eppendorf tube. To prevent spot-to-spot puncher carryover, an unspotted filter punch was taken after each sample punch. A total of 150 µL of extraction solution (20 ng/mL miltefosine-D4 in methanol) was added to each sample with the exception of double blanks, to which 150 µL of methanol was added. The tubes were mixed for 10 s, sonicated for 30 min, and mixed for another 30 s. Subsequently, the final extract was transferred to an autosampler vial, and 10 µL was injected onto the high-performance liquid chromatography (HPLC) column. No additional recovery of miltefosine from the blood spots was found when longer sonication times were used.

Liquid chromatography-tandem mass spectrometry

Chromatographic separation was performed as described for the previously validated miltefosine plasma method [3], using a Gemini C18 precolumn (4.0 mm by 2.0-mm inside diameter [i.d.]; Phenomenex, Torrance, CA, USA) and Gemini C18 analytical column (150 mm by 2.0-mm i.d.; particle size, 5 µm; Phenomenex), with isocratic elution with 10 mM ammonia in 95% methanol (vol/vol) at 0.3 mL/min. The HPLC system (Agilent 1100 series; Agilent, Palo Alto, CA, USA) consisted of a binary pump, in-line degasser, autosampler (at 4°C), and column oven (at 25°C). The miltefosine concentrations were analyzed on an API-3000 triple-quadrupole mass spectrometer (MS) equipped with a turbo-ion-spray source (Sciex, Framingham, MA, USA), operating in positive ion mode. Table 1 summarizes the MS operating parameters.

Validation of assay for quantification of miltefosine in DBS samples

The validation of the assay was performed according to the most current EMA and FDA guidelines for the validation of bioanalytical assays [19,20], with respect to the following aspects: calibration model, accuracy and precision, LLOQ, selectivity (endogenous interferences and cross-analyte interferences), carryover (instrumentation and spot-to-spot carryover), dilution integrity, matrix effects, and recovery. Additional experiments were performed for the application of dried blood spots as a matrix according to EBF recommendations [21,22]; blood spot volume, blood spot homogeneity, and different WB Ht values were tested for their

Table 1. MS operating parameters for determination of miltefosine in dried blood spots.

Parameter		
Run duration	5.0 min	
Ionspray voltage	+4.5 kV	
Turbo gas temperature	400 °C	
Turbo gas flow	7 L/min	
Nebuliser gas	11 psi	
Curtain gas	9 psi	
Collision gas	6 psi	
	Miltefosine	**Miltefosine-D4**
Parent mass	408.5 m/z	412.6 m/z
Product mass	125.1 m/z	129.2 m/z
Dwell time	400 ms	400 ms
Collision energy	43 V	43 V
Collision exit potential	22 V	22 V
Declustering potential	71 V	71 V
Focussing potential	290 V	290 V
Entrance potential	12 V	12 V
Typical retention time	2.6 min	2.6 min

effects on accuracy and precision at two concentrations (QCL and QCH). Stability for up to 162 days was tested at four nominal temperatures, i.e., −70°C, −20°C, room temperature (20 to 25°C), and 37°C.

Clinical application
As part of a larger randomized clinical trial (ClinicalTrials registration no. NCT02011958) investigating the treatment of Ethiopian HIV-coinfected VL patients with high-dose liposomal amphotericin B alone (total dose of 40 mg/kg, given over 24 days) or liposomal amphotericin B (total dose of 30 mg/kg, given over 11 days) in combination with a 28-day miltefosine regimen (2.5 mg/kg daily), paired plasma and DBS samples were collected from 16 patients. Ethical approval was obtained from the Ethiopian National Research Ethics Review Committee, the institutional review board of the University of Gondar in Ethiopia, and ethics committees from Médecins Sans Frontières, the London School of Hygiene & Tropical Medicine, and the Institute of Tropical Medicine (Antwerp, Belgium). Regulatory approval was obtained from the Food, Medicine, and Health Administration and Control Authority in Ethiopia. All patients provided written informed consent before entering the study. DBS and plasma samples were collected simultaneously on day 29 of miltefosine treatment, 1 day after the last miltefosine dose, when patients are considered to have reached steady-state/maximal levels.

Plasma samples were collected using K_2EDTA BD Vacutainers; after centrifugation, plasma was isolated and was maintained at −20°C until analysis. DBS samples were collected from a finger-prick using a lancet (GST Corp., New Delhi, India). A drop of blood was applied to a Whatman 903 protein saver card without touching the filter paper with the finger tip. DBS samples were allowed to air dry for at least 3 h before being stored in an airtight and watertight zipper-lock bag containing at least three desiccant packages. DBS samples were stored and

transported by courier at room temperature. Ht levels of the patients were determined with a Beckman Coulter AcT Diff hematology analyzer (Beckman Coulter, Fullerton, CA, USA).

Observed DBS and plasma concentrations were compared using weighted Deming regression, and a Bland-Altman difference plot was used to depict the agreement between the two methods. All statistical analyses were performed with R (version 3.1.2). The acceptance criteria for the agreement between the observed and derived plasma concentrations were based on the guideline for incurred sample reanalysis of the EMA, i.e., the difference between the observed and derived miltefosine plasma concentrations should be within ±20% for at least 67% of the samples [20].

RESULTS

Calibration model
Calibration standards at eight concentrations in the range of 10 to 2,000 ng/mL were prepared and analyzed in duplicate on 3 separate days at the beginning and end of the analytical run. To obtain the lowest total bias across the range, the linear regression of the analyte/internal standard peak area ratio (AR) versus the concentration of miltefosine (x) was weighted, $1/x^2$. The calibration curve was accepted if 75% of the nonzero calibration standards were within ±15% of their nominal concentrations (±20% for the LLOQ). At least one calibration standard at the LLOQ and ULOQ should be accepted. All three calibration curves met these criteria and had correlation coefficients (R^2) of ≥0.9964.

Accuracy and precision
The accuracy and precision of the method were determined by analyzing the LLOQ, QCL, QCM, and QCH five times in three separate analytical runs. Intra-assay and interassay bias values were within ±15% of the nominal concentrations for all QC samples. As presented in Table 2, intra-assay and interassay precision values (expressed as coefficient of variation [CV] values) were ≤7.0% for QCL, QCM, and QCH and ≤19.1% for the LLOQ. Therefore, both the accuracy and precision of the method were found to be acceptable.

Lower limit of quantitation
The first blank and the five LLOQ quality control samples were used to determine the signal-to-noise ratio in three analytical runs. The signal-to-noise ratio of miltefosine at the LLOQ level was above 5 for all three runs (i.e., 9.6, 5.3, and 5.8). Figure 2 shows representative LC-MS/MS ion chromatograms for miltefosine and the internal standard in a double-blank sample and an LLOQ sample.

Specificity and selectivity
Six different batches of human WB were collected from six healthy donors and adjusted to Ht30 WB, and both a double-blank sample and an LLOQ sample were prepared from each batch. The samples were processed and analyzed as described above. The six LLOQ samples were all within ±20% of their nominal values. For the double-blank samples, five of the six batches showed no interference at the retention time of miltefosine over 20% of the peak area of the LLOQ sample and none showed a peak for miltefosine-D4 higher than 5% of the internal standard peak area. Therefore, the selectivity was considered to be sufficient.

To test the cross-analyte interference, an ULOQ sample was prepared as described

Table 2. Intra-assay and interassay accuracy (bias) and precision (CV) determined by analyzing quality control samples at four concentrations: i.e., LLOQ (10.1 ng/mL), QCL (24.2 ng/mL), QCM (302 ng/mL), and QCH (1,610 ng/mL).

Run	Nominal miltefosine concentration (ng/ml)	Bias (%)	CV (%)	# replicates
1	10.1	-9.0	9.1	5
2	10.1	8.1	7.1	5
3	10.1	4.8	19.1	5
Inter-assay	10.1	1.3	14.3	15
1	24.2	1.2	5.8	5
2	24.2	6.3	4.6	5
3	24.2	1.1	6.5	5
Inter-assay	24.2	2.8	5.8	15
1	302	2.0	1.3	5
2	302	-2.5	3.6	5
3	302	11.2	6.2	5
Inter-assay	302	3.6	7.0	15
1	1,610	-0.5	5.4	5
2	1,610	0.9	5.2	5
3	1,610	5.5	3.5	5
Inter-assay	1,610	1.9	5.1	15

above but subsequently processed with the addition of methanol as the extraction solvent (without the internal standard). Additionally, the internal standard was spiked separately in a double-blank sample at the nominal concentration. No internal standard interferences were observed for the analyte signal, and no interference from the analyte was measured for the specific mass transition of the internal standard.

Dilution integrity
The mean miltefosine concentration at the end of a 28-day treatment (150 mg/day) was found to be ~30,000 ng/mL in Dutch CL patients [17]. Therefore, an >ULOQ sample of 40,000 ng/mL was used in the dilution integrity experiment. The >ULOQ sample was prepared as described previously, and the final extract was subsequently diluted 100-fold with the final extract of a processed blank DBS (extracted with extraction solvent containing the internal standard). The dilution steps were as follows: first, 10 µL of >ULOQ final extract was diluted with 90 µL of blank final extract; subsequently, 10 µL of this dilution was further diluted with another 90 µL of blank final extract. The deviations of the diluted >ULOQ samples were within ±3.3% of the nominal concentration, and the precision was ≤2.0%; therefore, it was concluded that samples exceeding the ULOQ (up to 40,000 ng/mL) could be diluted as described, applying a dilution factor of 100.

Carryover
Two types of carryover are important to investigate in the validation of dried blood spot methods, namely, instrument carryover and spot-to-spot carryover caused by the punching device. These two sources of carryover were tested. Spot-to-spot carryover samples were

prepared by punching spots in the following sequence: an ULOQ sample, unspotted filter paper (to eliminate most of the carryover), a blank spot, unspotted filter paper, and a blank spot. The two blank spots were processed as described previously and injected after the ULOQ sample. The combined instrument and spot-to-spot carryover of the two samples was compared to the mean value of five LLOQ sample measurements and was found to be below 19.3% of the LLOQ.

However, in clinical practice, miltefosine concentrations are often expected to exceed the calibration range of 10 to 2,000 ng/mL. Samples with expected concentrations around the ULOQ or >ULOQ values should preferably be analyzed in one batch. After punching of a 40,000-ng/mL >ULOQ sample, carryover is acceptable (<20% of LLOQ) at the fourth blank spot punched subsequently.

Matrix factor and recovery

The matrix factor (MF) and recovery were tested in six different batches of Ht30 WB, spiked at QCL and QCH singularly. Ten-microliter spots were prepared from these solutions, so-called "processed DBS samples." For the analysis, the entire spot was cut out and processed as described previously, with 150 µL of extraction solvent. Additionally, "matrix-absent" and "matrix-present" samples were prepared, for which two neat solutions, namely, MF-low (MF-L) (24.4 ng/mL miltefosine) and MF-high (MF-H) (1,630 ng/mL miltefosine), were first prepared in extraction solvent (20 ng/mL miltefosine-D4 in methanol). The matrix-absent samples were prepared by diluting 10 µL of these neat solutions with 140 µL of extraction solvent. The matrix-present samples were prepared by cutting out the entire 10-µL blank spots of
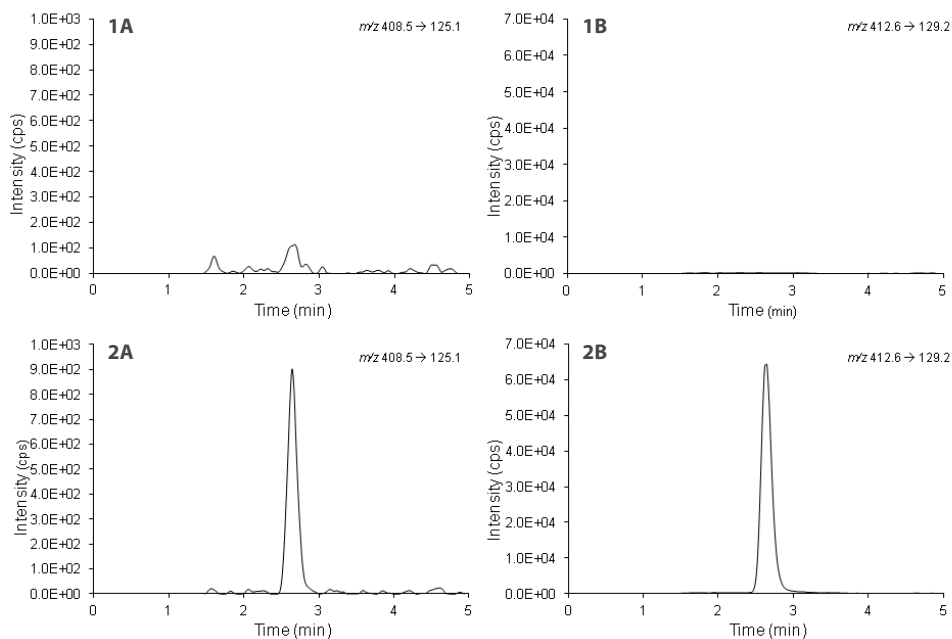
Figure 2. Representative LC-MS/MS ion chromatograms of miltefosine (1A) and internal standard miltefosine-D4 (1B) quantified in a double-blank DBS sample and of miltefosine (2A) and miltefosine-D4 (2B) in an LLOQ sample (10.1 ng/mL).

the six different Ht30 WB batches, after which 10 μL of MF-L or MF-H solution and 140 μL of extraction solvent were added.

The MF was calculated for each batch by calculating the ratio of the miltefosine peak area in the matrix-present sample to that in the matrix-absent sample. The MF at both tested concentrations was ~0.3 as a result of matrix effects (ion suppression). The IS-normalized MF was ~1.0, which indicated that the stable isotope-labeled internal standard was effectively compensating for any matrix effects. At both tested QC levels, the CVs of the absolute and IS-normalized MF values calculated from the six different Ht30 WB batches were below 11.5%.

Given that the internal standard is added as extraction solution, it is not part of the sample pretreatment; therefore, the IS-normalized values were used to determine recovery. The sample pretreatment recovery was calculated by comparing the area ratio (AR) of the processed DBS samples with the AR of the matrix-present samples. IS-normalized sample pretreatment recovery was ~100% (97.2% for QCL samples and 103% for QCH samples). At both tested QC levels, the CV of the IS-normalized recovery from the 6 batches was below 6.7%.

Both the matrix effect and recovery experiments were considered acceptable, because the CVs calculated for the six different Ht30 WB batches were consistent and below 15%.

Stability

DBS QC samples were prepared at two concentrations (QCL and QCH), as described previously, and were air dried at room temperature overnight. The following day, the samples were stored in sealed aluminum bags with three desiccant packages at four temperatures, i.e., −70°C, −20°C, room temperature (20 to 25°C), and 37°C. Stability was tested on days 34, 58, 107, and 162; the measured concentrations were within ±12.5% of the nominal concentrations and the precision was ≤10.7%. The stability of miltefosine in DBS samples was proven to be at least 5 months (162 days) at temperatures ranging from −70°C to 37°C, with storage in sealed aluminum bags with three desiccant packages.

Blood spot homogeneity

Blood spot homogeneity was investigated with 20-μL Ht30 WB DBS samples at QCL and QCH levels, in triplicate; 3.0-mm punches were taken at the perimeter instead of the center of the spots. The bias was 21.8% for the QCL level and 18.0% for the QCH level (CV, ≤7.4%), which points out the importance of punching the center of the spot.

Effect of blood spot volume

For all of the validation procedures described here, a standard fixed spot volume of 20 μL was used. QCL and QCH samples were spotted in blood spot volumes reflecting the procedure in clinical practice, i.e., 10, 15, 25, and 30 μL. Samples were analyzed in triplicate. Accuracy and precision were all within ±13.4%, indicating that variability in blood spot volumes between 10 and 30 μL had no effect on the accuracy and precision of the method (data not shown).

Effect of hematocrit levels

Human WB was adjusted to a range of Ht values that were expected in clinical practice with HIV-coinfected VL patients, i.e., 20, 23, 31, and 35%. For each Ht level, QCL and QCH samples were spiked and analyzed in triplicate. The accuracy and precision of DBS samples within this Ht range were all within ±14.1% and ≤7.2%, respectively, and therefore were

considered acceptable (within ±15%) (data not shown). However, a linear effect of Ht values on the miltefosine quantification was visible in these experiments; therefore, a wider range of Ht values was prepared, to investigate the relationship between Ht levels and the bias in miltefosine quantification. Human WB was adjusted to five different Ht levels (10, 21, 30, 40, and 51%), spiked at two concentrations (QCL and QCH), and spotted at a volume of 20 μL. Samples were analyzed in triplicate.

Figure 3 depicts the bias caused by Ht levels in the area ratio of quality control samples prepared in WB with different Ht levels, relative to standard quality control samples prepared in WB Ht30. The linear trend in the bias of the miltefosine concentrations with increasing Ht levels relative to Ht30 could be described by Equation 1 ($R^2 = 0.9761$):

Equation 1: $\text{Bias}_{Ht} = (0.013 \cdot Ht - 0.359) \cdot 100\%$

The same Ht range was spotted at 10, 30, 40 and 50 μL and the linear regression had approximately the same slope regardless of the blood spot volume (data not shown).

Clinical evaluation of DBS versus plasma concentrations in patient samples
A total of 16 paired DBS and plasma samples were available from miltefosine-treated Ethiopian HIV-coinfected VL patients. Samples originated from the last treatment day, at which miltefosine plasma concentrations exceed the ULOQ. Miltefosine concentrations ranged from 8,420 to 29,300 ng/mL and from 6,920 to 29,300 ng/mL for DBS and plasma samples, respectively. The median of the observed miltefosine DBS/plasma concentration ratio was
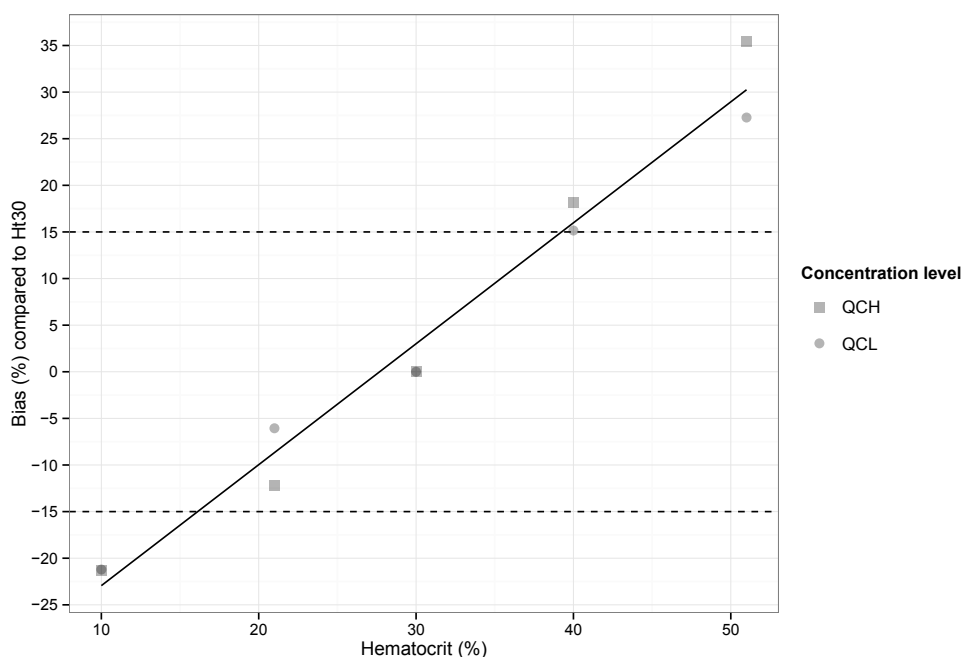
Figure 3. Effects of hematocrit levels on the accuracy of miltefosine quantification at two concentrations (i.e., QCL [24 ng/mL] and QCH [1,600 ng/mL]), depicted as bias (%) in the area ratio in comparison with Ht30 WB (used for calibration standards). The linear regression line is described as $\text{Bias}_{Ht} = (0.013 \times Ht - 0.359) \times 100\%$. Dashed lines, 15% bias.

0.99 (range, 0.83 to 1.22). The correlation between paired individual observed miltefosine plasma and DBS concentrations, using a weighted Deming regression, is depicted in Figure 4. The slope of the weighted regression line was 0.87 (95% confidence interval [CI], 0.70 to 1.04), with an intercept of 2,091 (95% CI, −1,132 to 5,313) (Pearson's r = 0.946). The line of true identity, with a regression slope of 1, lies within the 95% CI of the Deming regression line (Figure 4). This indicates an approximately equal distribution of miltefosine in blood plasma and erythrocytes.
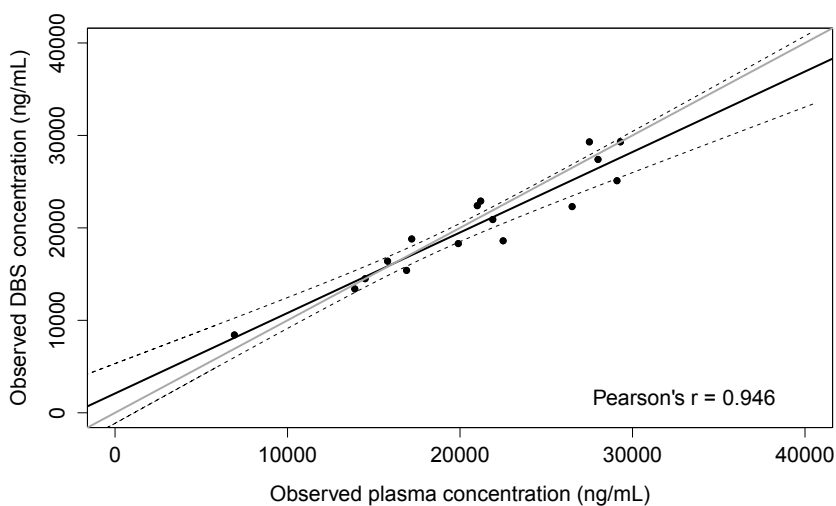
Figure 4. Observed miltefosine dried blood spot concentrations plotted against the corresponding observed plasma concentrations in paired patient samples (n=16). Solid black line, weighted Deming fit (2,091 0.87x; Pearson's r=0.946); dashed black lines, 95% confidence interval of the fit; solid gray line, line of true identity.

Miltefosine (MIL) plasma concentrations can thus be derived from the observed DBS concentrations by using the derived Deming regression equation, as follows:

Equation 2: $$[\text{MIL}]_{\text{plasma,derived}} = \frac{([\text{MIL}]_{\text{DBS}} - 2091)}{0.87}$$

All derived miltefosine plasma concentrations calculated from the observed DBS concentrations by using Equation 2 were within ±20% of the observed plasma concentrations, as shown in the Bland-Altman plot (Figure 5).

Large between-patient variability in baseline Ht levels is expected for VL patients, and Ht levels typically increase over time during the treatment period as patients recover from their infections. Given the effect of Ht levels on the miltefosine quantification with DBS samples established in the bioanalytical validation, the appropriateness of Ht correction of the clinical DBS concentrations was assessed using the patients' paired DBS and plasma samples. Individual patient Ht levels were available for all paired samples, ranging between 23.4% and 44.0%, with a median of 30.5%. We tested Ht correction of the observed DBS concentrations
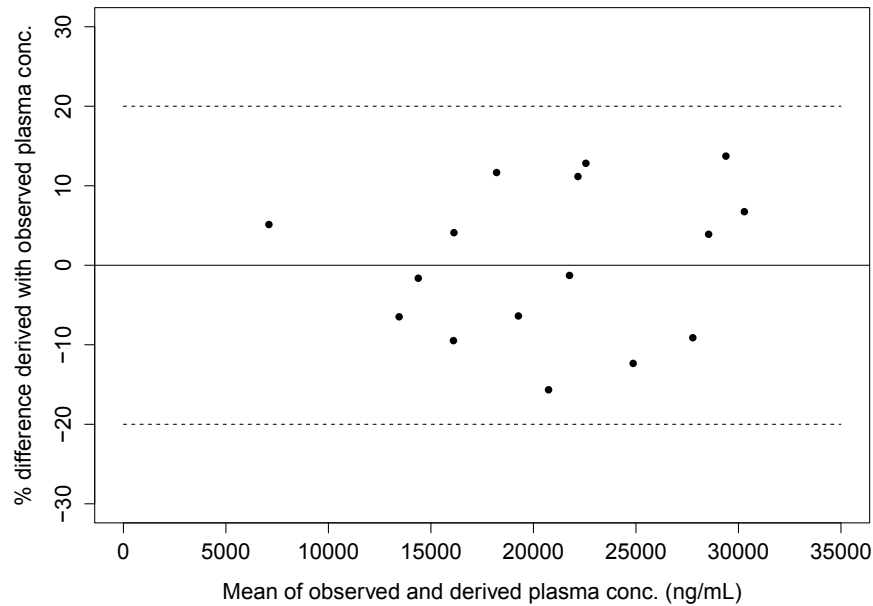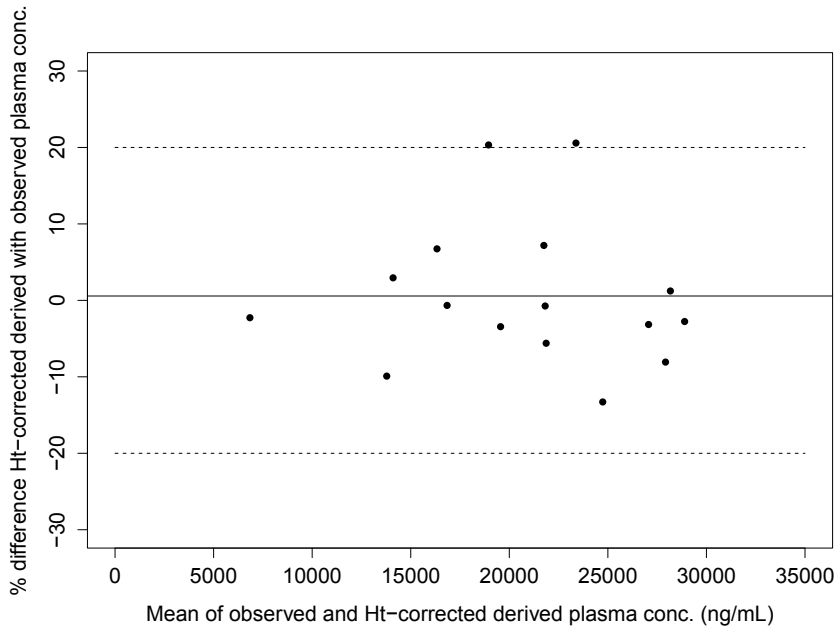
Figure 5. Bland-Altman difference plot depicting the differences between the plasma concentrations derived using the Deming regression equation, based on the observed DBS concentrations, and the observed plasma concentrations. Dashed lines, 20% bias, compared to the observed plasma concentrations.

for these clinical samples by using Equation 1, describing the effect of Ht levels on miltefosine quantification in the bioanalytical validation, which resulted in Equation 3:

Equation 3: $[\text{MIL}]_{\text{DBS,corrected}} = \dfrac{[\text{MIL}]_{\text{DBS,observed}}}{0.641 + 0.013 \cdot \text{Ht}}$

The correlation between the Ht-corrected DBS concentrations and the corresponding observed plasma concentrations using a weighted linear Deming regression resulted in a slope of 0.83 (95% CI, 0.73 to 0.94), with an intercept of 2,051 (95% CI, 238 to 3,863) (Pearson's r = 0.951) (graph not shown). The 95% CIs of both the slopes and intercepts of the Ht-corrected and non-Ht-corrected regression lines were overlapping, indicating that Ht correction does not provide a significantly better fit. While all derived plasma concentrations were within 20% of the observed plasma concentrations without Ht correction, 2 of the 16 paired samples were outside the ±20% bias, relative to the observed plasma concentrations, when the DBS concentrations were first corrected for Ht bias (Figure 6). Furthermore, no obvious or systematic trend in the bias of the derived plasma concentrations (no Ht correction) versus Ht levels was visible (Figure 7). Based on the clinical validation, correction of miltefosine DBS concentrations for Ht levels appeared not to be appropriate.

Figure 6. Bland-Altman difference plot depicting the differences between the Ht-corrected plasma concentrations derived using the Deming regression equation, based on the Ht-corrected DBS concentrations, and the observed plasma concentrations. Dashed lines, 20% bias, compared to the observed plasma concentrations.
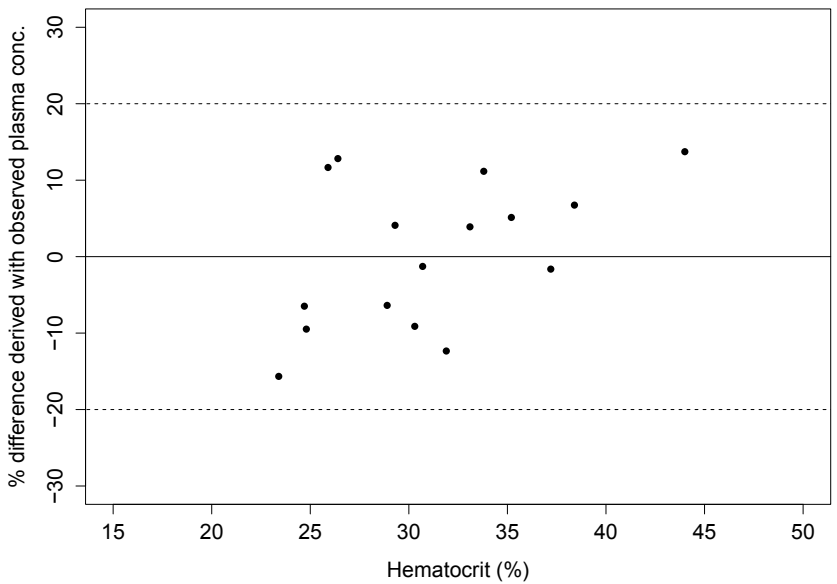
Figure 7. Differences between the plasma concentrations derived using the Deming regression equation, based on the observed DBS concentrations (without Ht correction), and the observed plasma concentrations versus hematocrit levels. Dashed lines, 20% bias, compared to the observed plasma concentrations.

DISCUSSION

The assay described here is the first assay to measure miltefosine concentrations in patients using less-invasive DBS sample collection, to facilitate future clinical trials investigating new antileishmanial treatment regimens including the drug miltefosine. The assay was successfully validated according to FDA/EMA guidelines and EBF recommendations. With this method, miltefosine can be accurately and precisely quantified with an LLOQ of 10 ng/mL, and concentrations as high as 40,000 ng/mL can be analyzed by 100-fold dilution. Paired miltefosine DBS and plasma samples were collected from 16 HIV-coinfected VL patients in Ethiopia. This clinical evaluation demonstrated good correlation between observed plasma and DBS concentrations. Miltefosine plasma concentrations derived from the observed DBS concentrations using a weighted Deming regression were within 20% of the observed plasma concentrations over a wide range of concentrations. We showed here that the observed miltefosine DBS concentrations were approximately equal to the paired observed plasma concentrations. This indicates an equal distribution of miltefosine between erythrocytes and plasma in blood of miltefosine-treated VL patients, an observation that has not been shown previously, to the best of our knowledge. DBS samples were found to be stable for at least 162 days at up to 37°C, using a simple storage procedure with desiccant packages, which enables storage of the miltefosine PK DBS samples at room temperature in tropical regions.

Influence of Ht levels on miltefosine DBS measurements
The patients included in our study showed variable Ht levels, as described previously [15], with a median of 30.5%, which is around the standardized Ht level of 30% used for the preparation of calibration standards and QC samples in this assay. Despite a linear correlation between Ht levels and the miltefosine DBS quantification bias observed during the laboratory bioanalytical validation, no such trend in bias due to Ht levels was found in the clinical application, with individual patients' Ht levels ranging from 23.4% to 44.0%. Ht correction did not significantly improve the calculation of the derived miltefosine plasma concentrations from the observed DBS concentrations in patient samples. Additionally, samples from 4 of 16 patients exceeded the validated Ht range (i.e., 35.2%, 37.2%, 38.4%, and 44.0%), but for those samples also the observed plasma concentrations were accurately described by the observed DBS concentrations, without the need for Ht correction.

These findings showed that the observed Ht effect on miltefosine quantification in the bioanalytical validation could not be confirmed in the clinical validation. Several factors can be hypothesized to have effects on miltefosine quantification in clinical practice, which together could potentially counteract the observed effect of Ht levels on miltefosine determinations. The most general explanation for the Ht effect on analyte quantification is that Ht levels affect the distribution of the applied blood over the filter paper [13]. Blood with high Ht levels spreads less, and therefore the fixed-diameter subpunches contain larger volumes of blood than do samples of blood with lower Ht levels. It could be argued that, when the bioanalytical validation samples are spotted with a pipette, more pressure is applied than during finger-prick spotting, in which the drop merely falls onto the paper. This difference in blood flow upon application of the blood spot to the filter paper might theoretically reduce the total blood volume contained in the 3.0-mm punch from the dried blood spot.

It could also be hypothesized that the blood spot volume is larger for patients with lower Ht levels, due to lower viscosity of the blood leading to higher blood flow. However,

when the blood spot diameters as indications of blood spot volumes [23] were compared for the blood spots in this clinical validation, no such trend between Ht levels and blood spot diameters was found for the patient samples ($R^2 = 0.002$) (data not shown). Therefore, this is not likely to explain the absence of Ht-related bias in the miltefosine quantification of clinical samples.

Additionally, the DBS samples used in the bioanalytical validation differed from the clinical DBS samples in terms of matrix. While the clinical samples were derived from capillary blood obtained by finger puncture, venous blood obtained by venipuncture was used for bioanalytical validation purposes, for practical reasons. It was reported previously that the analyte concentrations in these two matrices could differ, which was mostly explained by the slower distribution equilibrium toward the capillaries [24]. However, miltefosine accumulates during treatment and reaches steady-state levels during the last week of treatment for most patients. Because the clinical DBS samples were collected 1 day after the last dose of miltefosine, we did not expect the miltefosine concentration to differ between these two matrices.

Finally, during the bioanalytical validation, the effect of Ht was tested while other blood constituents, such as plasma proteins and other blood cells, were kept constant. In clinical samples, however, these blood constituents may be variable and potentially correlated with Ht levels, affecting the miltefosine quantification. For instance, serum albumin levels are significantly lower during active VL infections than those in healthy control subjects [25], as are Ht levels, and both anemia and low albumin levels were found to be risk factors for poor clinical outcomes in VL [26]. Therefore, low Ht levels and low albumin levels are expected to be correlated. Miltefosine is highly protein bound (96 to 98%), and the majority of the protein-bound fraction (97%) is bound to albumin [27]. This could imply that reduced serum albumin levels theoretically would lead to an increase in the unbound miltefosine fraction in plasma and correspondingly to increased distribution of miltefosine toward the erythrocytes [5]. The effects of blood protein changes, concurrent with low Ht levels, on the quantification of miltefosine cannot be accounted for in the bioanalytical validation.

In conclusion, various clinical factors potentially affect miltefosine quantification, cancelling out the systematic bias caused by Ht levels and making individual Ht correction redundant in clinical practice. The absence of bias due to Ht levels in the clinical samples makes the application of DBS sample collection easier in the field, without the explicit need for concurrent Ht measurements, and thus allows for DBS sample collection without expensive laboratory equipment.

Applicability of miltefosine DBS sampling method

For the clinical validation, we had only a limited number of paired samples available. While there is no strict consensus regarding the number of paired samples required for method comparisons, the evaluation of 40 samples has been proposed [28]. However, the collection of additional paired samples from the highly anemic HIV-coinfected patients in this study was unfortunately not feasible, due to practical limitations and ethical constraints. Paired patient samples were available over a wide but relatively high (>ULOQ) range of miltefosine plasma concentrations, between 6,920 and 29,300 ng/mL. However, as no trend could be observed concerning the effect of Ht levels on miltefosine quantification from DBS samples in clinical practice over this wide concentration range, we do not expect that Ht correction will be

needed for lower concentration ranges.

We have demonstrated that DBS sample collection is a valid alternative to plasma sampling for the quantification of miltefosine, which has many practical advantages. DBS sampling is minimally invasive and requires only a minute volume of blood. This is particularly beneficial for application of the method in a pediatric population (a large proportion of VL patients are <12 years of age), as well as, for example, highly anemic HIV-coinfected VL patients. Additionally, DBS collection constitutes a low biohazard, reducing the risk of needle stick incidents when sampling HIV-coinfected VL patients. Finally, expensive and logistically challenging cold-chain storage and transport are not required for the DBS samples, simplifying the conducting of PK studies in remote areas where leishmaniasis is endemic and only limited clinical and laboratory infrastructure is available.

TRANSPARENCY DECLARATIONS

None to declare.

ACKNOWLEDGEMENTS

2.1

REFERENCES

1. Omollo R, Alexander N, Edwards T, Khalil EAG, Younis BM, Abuzaid AA, et al. Safety and efficacy of miltefosine alone and in combination with sodium stibogluconate and liposomal amphotericin B for the treatment of primary visceral leishmaniasis in East Africa: study protocol for a randomized controlled trial. Trials. 2011;12:1–10.

2. Dorlo TPC, Rijal S, Ostyn B, de Vries PJ, Singh R, Bhattarai N, et al. Failure of miltefosine in visceral leishmaniasis is associated with low drug exposure. J. Infect. Dis. 2014;210:146–53.

3. Dorlo TPC, Hillebrand MJX, Rosing H, Eggelte TA, de Vries PJ, Beijnen JH. Development and validation of a quantitative assay for the measurement of miltefosine in human plasma by liquid chromatography-tandem mass spectrometry. J. Chromatogr. B. Analyt. Technol. Biomed. Life Sci. 2008;865:55–62.

4. Harhay MO, Olliaro PL, Vaillant M, Chappuis F, Lima MA, Ritmeijer K, et al. Who is a typical patient with visceral leishmaniasis? Characterizing the demographic and nutritional profile of patients in Brazil, East Africa, and South Asia. Am. J. Trop. Med. Hyg. 2011;84:543–50.

5. Emmons G, Rowland M. Pharmacokinetic considerations as to when to use dried blood spot sampling. Bioanalysis. 2010;2:1791–6.

6. Spooner N, Lad R, Barfield M. Dried blood spots as a sample collection technique for the determination of pharmacokinetics in clinical studies: considerations for the validation of a quantitative bioanalytical method. Anal. Chem. 2009;81:1557–63.

7. Wilhelm AJ, den Burger JCG, Swart EL. Therapeutic drug monitoring by dried blood spot: progress to date and future directions. Clin. Pharmacokinet. 2014;53:961–73.

8. Jager NGL, Rosing H, Schellens JHM, Beijnen JH. Procedures and practices for the validation of bioanalytical methods using dried blood spots: a review. Bioanalysis. 2014;6:2481–514.

9. Edelbroek PM, Heijden J van der, Stolk LML. Dried blood spot methods in therapeutic drug monitoring: methods, assays, and pitfalls. Ther. Drug Monit. 2009;31:327–36.

10. Patel P, Mulla H, Tanna S, Pandya H. Facilitating pharmacokinetic studies in children: a new use of dried blood spots. Arch. Dis. Child. 2010;95:484–7.

11. Pandya HC, Spooner N, Mulla H. Dried blood spots, pharmacokinetic studies and better medicines for children. Bioanalysis. 2011;3:779–86.

12. Denniff P, Spooner N. The effect of hematocrit on assay bias when using DBS samples for the quantitative bioanalysis of drugs. Bioanalysis. 2010;2:1385–95.

13. De Kesel PMM, Sadones N, Capiau S, Lambert WE, Stove CP. Hemato-critical issues in quantitative analysis of dried blood spots: challenges and solutions. Bioanalysis. 2013;5:2023–41.

14. O'Mara M, Hudson-Curtis B, Olson K, Yueh Y, Dunn J, Spooner N. The effect of hematocrit and punch location on assay bias during quantitative bioanalysis of dried blood spot samples. Bioanalysis. 2011;3:2335–47.

15. Hailu A, van der Poll T, Berhe N, Kager PA. Elevated plasma levels of interferon (IFN)-gamma, IFN-gamma inducing cytokines, and IFN-gamma inducible CXC chemokines in visceral leishmaniasis. Am. J. Trop. Med. Hyg. 2004;71:561–7.

16. Diro E, Ritmeijer K, Boelaert M, Alves F, Mohammed R, Abongomera C, et al. Use of pentamidine as secondary prophylaxis to prevent visceral leishmaniasis relapse in HIV infected patients, the first twelve months of a prospective cohort study. PLoS Negl. Trop. Dis. 2015;9:e0004087.

17. Dorlo TPC, van Thiel PPAM, Huitema ADR, Keizer RJ, de Vries HJC, Beijnen JH, et al. Pharmacokinetics of miltefosine in Old World cutaneous leishmaniasis patients. Antimicrob. Agents Chemother. 2008;52:2855–60.

18. Baskurt OK, Ph D, Meiselman HJ, Sc D. Blood rheology and hemodynamics. Semin. Thromb. Hemost. 2003;29:435–50.

19. US Food and Drug Administration FDA. Guidance for Industry: Bioanalytical Method Validation. 2001. http://www.fda.gov/downloads/Drugs/Guidances/ucm070107.pdf. Accessed 1 Dec 2015.

20. European Medicines Agency. Guideline on bioanalytical method validation. Committee for Medicinal Products for Human Use and European Medicines Agency. 2011. http://www.ema.europa.eu/docs/en_GB/document_library/Scientific_guideline/2011/08/WC500109686.pdf. Accessed 11 Nov 2015.

21. Timmerman P, White S, Globig S, Lüdtke S, Brunet L, Smith C, et al. EBF and dried blood spots: from recommendations to potential resolution. Bioanalysis. 2011;3:1787–9.

22. Timmerman P, White S, Cobb Z, De Vries R, Thomas E, Van Baar B. Update of the EBF recommendation for the use of DBS in regulated bioanalysis integrating the conclusions from the EBF DBS-microsampling consortium. Bioanalysis. 2013;5:2129–36.

23. Hall E, Flores S, De Jesús V. Influence of hematocrit and total-spot volume on performance characteristics of

dried blood spots for newborn screening. Int. J. Neonatal Screen. 2015;1:69–78.

24. Mohammed BS, Cameron G a, Cameron L, Hawksworth GH, Helms PJ, McLay JS. Can finger-prick sampling replace venous sampling to determine the pharmacokinetic profile of oral paracetamol? Br. J. Clin. Pharmacol. 2010;70:52–6.

25. Gomes CMC, Giannella-Neto D, Gama ME a, Pereira JCR, Campos MB, Corbett CEP. Correlation between the components of the insulin-like growth factor I system, nutritional status and visceral leishmaniasis. Trans. R. Soc. Trop. Med. Hyg. 2007;101:660–7.

26. Mourão MVA, Toledo Jr A, Gomes LI, Freire VV, Rabello A. Parasite load and risk factors for poor outcome among children with visceral leishmaniasis. A cohort study in Belo Horizonte, Brazil, 2010-2011. Mem. Inst. Oswaldo Cruz. 2014;109:147–53.

27. Kotting J, Marschner NW, Neumuller W, Unger C, Eibl H. Hexadecylphosphocholine and octadecyl-methyl-glycero-3-phosphocholine: a comparison of hemolytic activity, serum binding and tissue distribution. Prog. Exp. Tumor Res. 1992;34:131–42.

28. Clinical and Laboratory Standards Institute. Method comparison and bias estimation using patient samples; Approved Guideline -EP-09-A2. 2002. http://demo. nextlab.ir/getattachment/ea61dc31-19cc-492a-b0e1-e8ecc13a4a90/CLSI-EP09-A2.aspx. Accessed 20 Nov 2015.

2.1

Chapter 2.2

Volumetric absorptive microsampling (VAMS) as an alternative to conventional dried blood spots in the quantification of miltefosine in dried blood samples

A.E. Kip
K.C. Kiers
H. Rosing
J.H.M. Schellens
J.H. Beijnen
T.P.C. Dorlo

ABSTRACT

Miltefosine is an oral agent against the neglected tropical disease leishmaniasis, which is mostly endemic in resource-poor areas. Dried blood spot (DBS) sampling is an attractive alternative to plasma sampling for pharmacokinetic studies in these remote areas, but introduces additional variability in analyte quantification due to possible blood spot inhomogeneity and variability in blood spot volume and haematocrit values. Volumetric absorptive microsampling (VAMS) potentially overcomes a few of these issues as the VAMS device absorbs a fixed volume that is processed as a whole. We developed and validated an LC-MS/MS method for the quantification of miltefosine with this novel sampling technique with good performance in terms of linearity, selectivity, accuracy (bias within ±10.8%), precision (CV% ≤ 11.9%), recovery, carry-over and matrix effect. VAMS samples were stable for at least one month at room temperature and 37°C. The impact of haematocrit on assay accuracy was reduced compared to conventional DBS sampling, but indicated a declining recovery with increased haematocrit due to haematocrit dependency in recovery from the sampling device. A clinical validation will be required to investigate whether VAMS is an appropriate and cost-effective alternative sampling method to conventional DBS sampling.

INTRODUCTION

Miltefosine is currently the only oral drug in the treatment of the neglected tropical diseases cutaneous and visceral leishmaniasis (VL). The drug is now mainly being evaluated in combination therapies in special patient populations such as HIV co-infected VL patients. Since miltefosine exposure is a significant determinant of treatment outcome [1], pharmacokinetic analyses are important in the evaluation of new treatment regimens that include miltefosine.

Our group has recently published a novel bioanalytical assay for the quantification of miltefosine in dried blood spots (DBS) collected on Whatman 903 filter paper [2]. Despite the many advantages of DBS sample collection, this sampling method introduces new variables affecting the accuracy in the quantification of analytes [3–5] such as blood spot volume, blood spot homogeneity and individual time-varying haematocrit (Hct) levels. The most discussed hurdle in the application of this conventional DBS sampling, where a sub-punch of the blood spot is extracted from a DBS card, is the Hct effect on the viscosity of the blood leading to variability in the blood volume collected in the sub-punch taken from the sample for analysis [3]. Also in the bioanalytical validation of the aforementioned method quantifying miltefosine in DBS, there was a Hct effect on the accuracy of the method ranging between -21.3% to +35.4% in an Hct range from 10 to 51% [2]. Hct is a particularly important factor in VL patients, since their Hct levels are typically severely decreased during active disease (median 25%) and increase towards a median of 33% at the end of treatment [6]. Hct issues could be avoided in conventional DBS sampling by whole spot analysis of a volumetrically controlled blood spot applied by a capillary or pipette. However, this adds further complexity to the sampling method which is especially troublesome in the resource-poor endemic VL settings and/or would still require venous sampling.

A new sampling method in which a fixed volume of whole blood can be collected is volumetric absorptive microsampling (VAMS). The VAMS device (depicted in Figure 1) absorbs a small fixed volume of 10 μL whole blood by wicking onto a porous, hydrophilic tip [7]. At present, a total of six bioanalytical method validations applying VAMS have been published [8–13]. Across a 20-70% Hct range, the variation (CV%) in the median absorbed whole blood volume was only 3.6% [7], demonstrating that the VAMS device accurately and reproducibly absorbs a fixed volume of blood independent of Hct. Inter-laboratory variability in blood volume sampled by six different laboratories was only 8.7% [14]. Compared to venous sampling, the VAMS technique offers the same advantages as conventional DBS sampling: reduced blood sampling volumes, simplification of the sample collection (not requiring cannulae), simplification of pre-treatment methods, reduced costs of shipment and storage at room temperature. In addition, the VAMS device overcomes important issues related to conventional DBS sampling. A fixed volume is absorbed and processed as a whole, which means there is no additional variability of blood spot volume and blood spot homogeneity affecting the accuracy of the method. Moreover, VAMS sampling should in theory overcome the conventional DBS issue of variable blood volumes in sub-punches depending on the Hct level, since the volume collected with the VAMS device should be the same independent of Hct.

In this study, we describe the development and validation of an LC-MS/MS method for the quantification of miltefosine in dried blood collected with the VAMS device. An additional aim of this study was to evaluate the Hct effect on miltefosine quantification in comparison with the previously published conventional DBS method.

2.2

METHODS

Materials & chemicals

VAMS devices (brand name Mitra™) were purchased from Neoteryx, LLC (Torrance, CA, USA). Miltefosine (Figure 2) was supplied by Sigma-Aldrich (Zwijndrecht, the Netherlands) and deuterated miltefosine (miltefosine-D4, Figure 2) was purchased from Alsachim (Illkirch Graffenstaden, France). Methanol (HPLC grade) and water (HPLC grade) were purchased from Biosolve Ltd. (Valkenswaard, the Netherlands). Ammonia (25%) was purchased from Merck (Amsterdam, the Netherlands).

Whole blood was collected from healthy volunteers in K_2EDTA BD Vacutainers® and adjusted to mimic typical Hct values of VL patients (between 23 and 37% [6]) by addition of blood plasma of the same volunteer obtained after whole blood centrifugation. Hct levels were determined with either the Cell Dyn Hematology analyser (Abbot Diagnostics, Lake Forest, IL, USA) or the XN-3000 Hematology analyser (Sysmex, Kobe, Japan). Whole blood was stored at 2-8°C no longer than one week before the preparation of validation samples.

Figure 1. Picture of the VAMS device Mitra™ (www.neoteryx.com). The VAMS sampler consists of a hydrophilic polymeric tip attached to a plastic handle. The tip absorbs a fixed volume of approximately 10 μL.

LC-MS/MS system

Chromatographic separation and MS/MS analysis were performed with the same equipment and under the same settings as described previously in the validation of the conventional DBS method for the quantification of miltefosine [2]. Chromatographic separation was performed using a Gemini C18 analytical column on an HPLC system (Agilent 1100 series; Agilent, Palo Alto, CA, USA). The API-3000 triple-quadrupole mass spectrometer (MS) was used as a detector. LC-MS/MS details can be found in the supplementary information.

Preparation of calibration standards and quality control samples

Two stock solutions of 1 mg/mL miltefosine in methanol-water (1:1, v/v) were prepared from independent weightings. Separate stocks were used for the preparation of calibration standards and quality control (QC) samples. Working solutions were prepared in methanol-water (1:1, v/v). Calibration standards were subsequently prepared from these working solutions by a 1:20 (v/v) dilution in Hct-adjusted whole blood (Hct value of around 30%) to final nominal concentrations of 10, 20, 200, 750, 1500, 2250, 4000 and 5000 ng/mL. Similarly, QC samples were diluted from working solutions to final concentrations of nominally 10, 25, 450, and 3,750 ng/mL (lower limit of quantification [LLOQ], low-level QC [QCL], mid-level QC [QCM], and high-level QC [QCH], respectively). To test the dilution integrity, a sample above the upper limit of quantification (>ULOQ) of 50,000 ng/mL was prepared from a 1:20 (v/v) dilution in Hct-adjusted whole blood (Hct value of around 30%).

Samples were mixed carefully by inversion of the tube and applied to the VAMS device by touching the tip to the blood sample surface. After the tip was completely colored, the contact with the blood surface was extended for two seconds to ensure full absorption, as described previously [7]. Misuse of the VAMS device, such as double-dipping and immersing the tip past the shoulder, was attentively avoided [7]. The device was dried at ambient room temperature for at least three hours.

A stock solution of 1 mg/mL miltefosine-D4 was prepared in methanol-water (1:1, v/v) and diluted to an internal standard (IS) working solution of 400 ng/mL miltefosine-D4 in methanol (IS400).
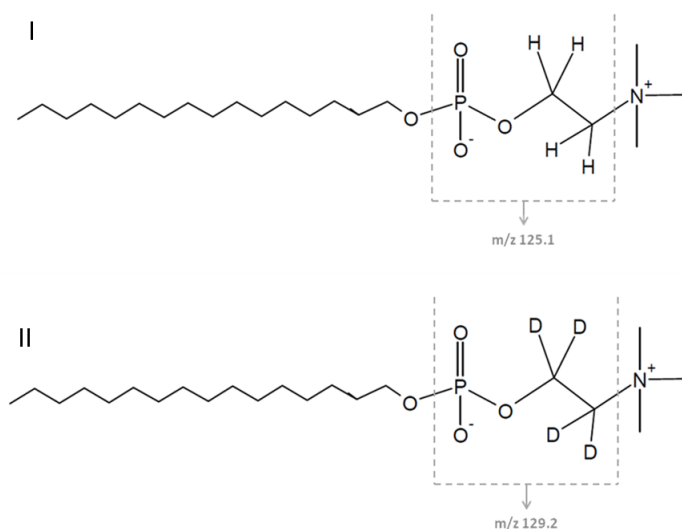
Figure 2. Chemical structures of (I) miltefosine and (II) miltefosine-D4.

Final pre-treatment method

The tip was separated from the holding device in a 2 mL Eppendorf tube to which 175 µL methanol was added. Samples were mixed for 15 min at 1,250 rpm. After vortex mixing the samples for an additional 30 s, 100 µL of extract was transferred to a clean 1.5 mL Eppendorf tube. For samples expected to be above the validated range, 10 µL of extract was transferred to a 1.5 mL Eppendorf tube containing 190 µL of methanol and subsequently vortex mixed for 30 s after which 100 µL was transferred to a clean Eppendorf tube. To all samples, 10 µL IS400 was added and samples were vortex mixed for 30 s. The final extract was transferred to vials and injected onto the column.

Validation

The method validation was based on the FDA and EMA guidelines for bioanalytical method validation [15,16]. The following validation tests were performed: calibration model, accuracy and precision, selectivity, dilution integrity, matrix factor, recovery, carry-over and stability. Additionally, the effect of Hct on analyte quantification was assessed as recommended by the European Bioanalysis Forum (EBF) for DBS methods [17].

Linearity

Fresh calibration standards were prepared in duplicate for all validation runs and injected at the beginning and end of each run. Analyte/IS peak area ratios were plotted against the corresponding nominal concentration and the linear regression was evaluated with both a 1/x and $1/x^2$ weighting factor, where x is the analyte concentration. Back-calculated concentrations should be within ±15% of the nominal concentration (or ±20% for the LLOQ). At least one calibration sample at LLOQ and ULOQ level should be within the requirements in each validation run.

Selectivity

Selectivity was evaluated by collecting whole blood from six different healthy volunteers and preparing a double blank and LLOQ sample for each batch. The chromatograms were evaluated for potential endogenous interferences. Selectivity was considered acceptable if observed interferences were ≤20% of the LLOQ for miltefosine and ≤5% of the IS signal for miltefosine-D4. According to the acceptance criteria, the accuracy and precision of the LLOQ samples should be within ±20% and ≤20%, respectively.

Accuracy, precision and dilution integrity

Intra- and inter-assay precision and accuracy were determined by analysing five processed replicates of the quality control samples (LLOQ, QCL, QCM and QCH) in three separate validation runs. Five replicates of the >ULOQ were prepared, diluted and analysed in one validation run to determine dilution integrity. The accuracy of the method is expressed as the bias from the measured analyte concentration and should be within ±15% of the nominal concentration (±20% for LLOQ). The intra-run bias (%) is calculated as the bias of the mean measured concentration per run, compared to the nominal concentration. The inter-run bias (%) is calculated as the bias of the overall mean measured concentration over all three runs, compared to the nominal concentration. The intra-run precision of the method was determined by calculating the percent coefficient of variation (%CV) for each set of replicates per run and was considered acceptable if ≤15% (≤20% for LLOQ). To calculate the inter-run variation, a one-way ANOVA was used.

Recovery and matrix factor

To evaluate recovery and the matrix factor, blank samples were prepared from six different whole blood batches in duplicate as described previously. From the same six batches of blood a QCL and QCH sample were prepared in singular. The recovery was calculated per separate whole blood batch from the ratio of the processed QC sample response to the response of the blank extract spiked with the required level of analyte to obtain the same miltefosine final extract concentration as the QC sample. The required analyte amount to be added was determined with the calculated average blood wicking volume as described in the Mitra™ certificate of conformance.

The matrix factor was calculated for each whole blood batch as the ratio of the spiked blank extract response versus the mean of the matrix free neat solution response (n=3).

Carry-over

The carry-over of the LC-MS/MS was tested by injection of two double blank processed samples directly after the injection of a processed ULOQ sample. The peak areas of the blanks

were compared to the mean area of the five LLOQ replicates. Carry-over was considered acceptable if ≤20% of the LLOQ for miltefosine and ≤5% of the IS signal for miltefosine-D4.

Stability
Short-term stability was tested for five days at room temperature (22±3°C) at the QCL and QCH concentration level. Long-term stability was tested for one month storage at room temperature (22±3°C) and at 37±3°C at the QCL and QCH concentration level. The VAMS devices were stored in the supplied clamshell storage containers in the dark (Neoteryx, LLC, Torrance, CA, USA).

Final extract stability was tested up to 5 days at 2-8°C at the QCL and QCH concentration level. Stock solutions of 1 mg/mL in methanol-water (1:1, v/v) were stored at -20°C for 28 months. Working solutions were stored at -20°C for 40 months at miltefosine concentrations of 80 and 40,000 ng/mL in methanol-water (1:1, v/v).

Hct effect on method accuracy
To determine the assay bias over a range of Hct, VAMS samples were prepared from K_2-EDTA whole blood adjusted to 10, 20, 41 and 50% Hct and spiked at QCL (25 ng/mL) and QCH (3,750 ng/mL) level in three-fold for each Hct level. Calibration standards were prepared as described above in whole blood adjusted to a Hct value of 30%. Accuracy (bias %) and precision (CV%) were considered acceptable across the Hct range if within ±15% and ≤15%, respectively.

Conventional DBS samples were prepared as described previously [2] in whole blood adjusted to Hct 14, 25, 29, 38 and 50%. DBS samples were prepared at the QCL (24 ng/mL) and QCH (1610 ng/mL) concentration level in three-fold for each Hct level. Concentrations were quantified using calibration standards spiked with miltefosine to whole blood adjusted to a Hct value of 29%. For both VAMS and DBS samples the bias was calculated as the difference between the mean calculated concentration and the nominal concentration.

RESULTS & DISCUSSION

Linearity
Calibration curves of analyte/IS peak area ratio versus nominal analyte concentration were evaluated and when a weighting factor of $1/x^2$ weighting was applied, the bias across the range was improved considerably. Linear regression correlation coefficients (R^2) were ≥0.9955 in all cases. All back-calculated calibration standard concentrations were within ±15% of their nominal value and coefficients of variation were below 15%. The linear range of 10-5,000 ng/mL for this method is therefore wider than for the previously published plasma (4-1,000 ng/mL [18]) and conventional DBS method (10-2,000 ng/mL [2]). Given the wide range of miltefosine concentrations encountered in patients [19], this wider bioanalytical range will reduce the number of samples requiring dilution.

Selectivity
The results for the selectivity of the validated method are shown in Table 1. There were no unexpected endogenous interferences >20% of LLOQ for miltefosine, nor >5% of the IS signal. The method was therefore considered to be selective. Additionally, the LLOQ could be analyzed precisely and accurately for all six batches (bias within ±19.1%, %CV 9.0%).

Table 1. Selectivity results for determination of miltefosine in dried blood samples collected with VAMS device prepared in six batches of blank whole blood — accuracy of the LLOQ (nominal concentration 9.99 ng/mL) per batch and relative interference as percentage of LLOQ in double blank per batch.

Batch whole blood	Hct (%)	Measured miltefosine concentration (ng/mL)	Accuracy LLOQ (bias, %)	Relative interference double blank (% of LLOQ)
#1	37	11.2	12.1	9.9
#2	43	11.4	14.1	5.4
#3	49	9.87	-1.2	7.3
#4	48	9.95	-0.4	4.5
#5	42	11.9	19.1	7.5
#6	48	9.61	-3.8	7.0

Accuracy, precision and dilution integrity

The intra- and inter-run mean biases, shown in Table 2, were within ±10.8% (within ±7.9% for the LLOQ), and thus meets the criteria for assay validation. Representative chromatograms are depicted in Figure 3. Intra- and inter-run precision were below 9.9% for all validation runs (≤11.9% for LLOQ), and therefore also meet the established criteria. The intra-run bias and precision for the 20-fold dilution of the <ULOQ sample (50,000 ng/mL) were 0.1% and 4.8%, respectively. The here validated method was therefore considered accurate and precise in a concentration-range between 10-50,000 ng/mL.

The expected miltefosine concentration-range in patients covers a wide range from 10 to 50,000 ng/mL [19]. This emphasizes the importance of dilution integrity for this method,

Table 2. Accuracy and precision of determination of miltefosine in dried blood samples collected with VAMS device.

QC level	Nominal miltefosine concentration (ng/mL)	Run	Intra-run mean bias (%)	Intra-run precision (%CV)	Inter-run mean bias (%)	Inter-run precision (%CV)
LLOQ	10	1	4.2	11.9		
		2	7.9	8.9	4.4	-[a]
		3	1.2	5.6		
QCL	25	1	2.2	9.9		
		2	1.7	4.8	-0.4	3.9
		3	-5.2	4.9		
QCM	450	1	10.8	7.5		
		2	0.1	7.4	4.5	4.8
		3	2.7	4.9		
QCH	3,750	1	3.4	5.5		
		2	-0.4	6.4	2.4	-[a]
		3	4.3	2.3		
>ULOQ	50,000	1	0.1	4.8		

[a]Inter-run precision could not be calculated (mean square between the groups is less than the mean square within the groups), meaning that there is no additional significant variation in performing the assay in different runs.

as samples above 5,000 ng/mL have to be diluted up to 10 times. As dried blood samples cannot be diluted before the sample pre-treatment, samples above the quantitation limit were diluted prior to addition of the internal standard. As described in the pre-treatment method, this required volume transfer of all samples – including calibration standards and QC samples – before the internal standard was added, which could potentially introduce additional variability. This validation revealed however no negative impact of this dilution method on the precision of the method.

Matrix factor and recovery

The absolute mean matrix factor was 0.637 (range 0.606-0.674) and 0.691 (range 0.532-0.802) at QCL and QCH, respectively. The mean normalized matrix factor (matrix factor analyte/ matrix factor IS) was 0.992 (range 0.941-1.033) and 0.996 (range 0.963-1.017) at QCL and QCH,

2.2
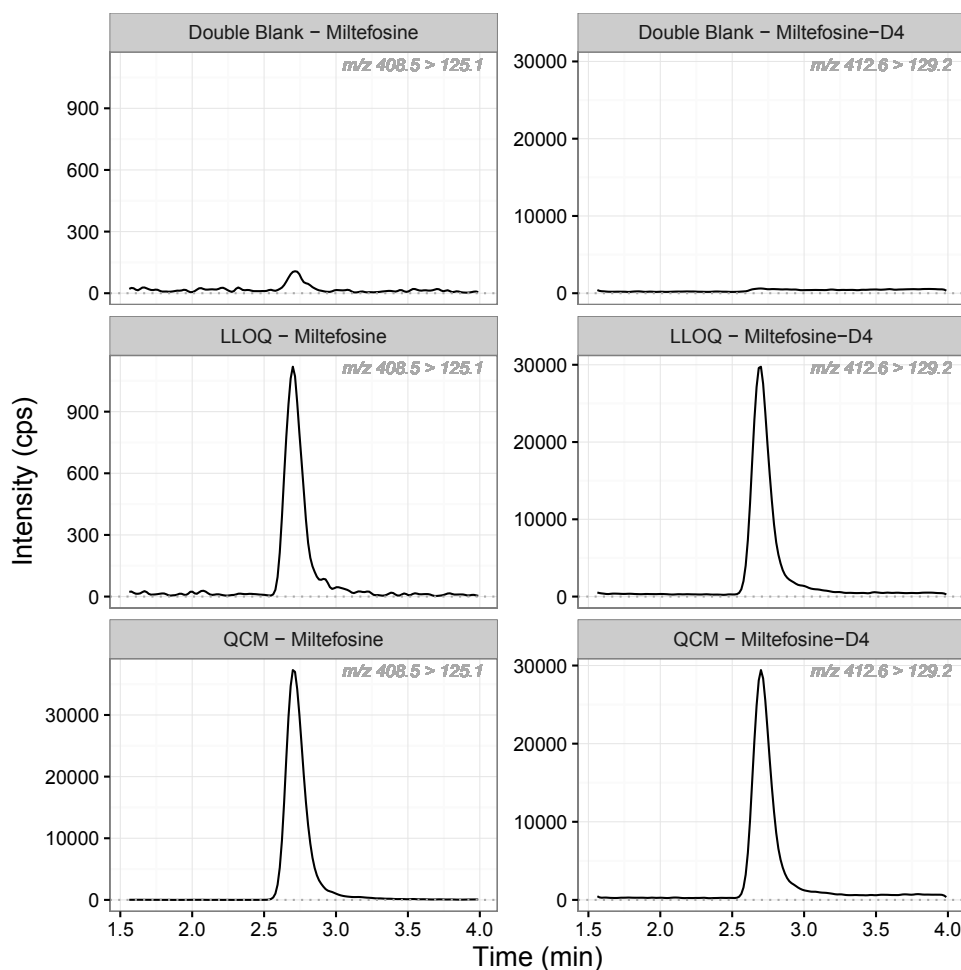
Figure 3. LC–MS/MS chromatograms obtained from double blank, LLOQ (10 ng/mL) and QCM (450 ng/mL) samples. Left is miltefosine, right is the deuterated internal standard miltefosine-D4.

respectively, indicating that the deuterated IS miltefosine-D4 effectively compensates for matrix effects. Mean normalized sample pre-treatment recovery was 69.7% (range 60.5-79.2%) and 70.6% (range 66.9-78.4%) as QCL and QCH, respectively. The matrix factor and recovery were reproducible for the six different batches of whole blood (%CV ≤10.8). Hct values of the six different batches ranged between 30 and 42%.

During the development phase of the pre-treatment method, extraction recovery with 5% $ZnSO_4 \cdot 7H_2O$ in water, as advised by the VAMS manufacturer for small molecule extraction, was compared to extraction with methanol using VAMS samples prepared at 1,600 ng/mL miltefosine in whole blood of 33 and 48% Hct. The variation in extraction recovery between Hct levels was lower for methanol (68.7% versus 60.3%, for 33 and 48% Hct respectively) than for extraction with 5% $ZnSO_4 \cdot 7H_2O$ in water (103% versus 78.5%). Furthermore the extraction with methanol resulted in an approximately three times higher absolute MS response compared to 5% $ZnSO_4 \cdot 7H_2O$ in water, due to the ion suppressive effects of the sulphate ions in the latter.

Carry-over
The response in the blank samples after injection of the ULOQ was ≤19.8% (0% for the IS) of the mean response at the LLOQ. Therefore, the carry-over is considered acceptable.

Stability
Miltefosine was stable in dried VAMS samples for at least one month at QCL and QCH levels at a room temperature of 22±3°C (bias -8.0 and -6.6%, respectively) and at 37°C (bias -9.7 and -13.0%, respectively). Since a declining trend in accuracy of the analysed miltefosine concentrations was observed, it could be considered to store samples in the freezer for longer storage periods (stability under these conditions was not evaluated). Final extract stability was acceptable for at least 5 days at 2-8°C (bias -2.0 and -3.6% for QCL and QCH, respectively). At -20°C, stock solutions (1 mg/mL) were stable for at least 28 months with a bias of 1.9%. Working solutions were stable for at least 40 months at -20°C (bias within ±4.4%).

Hematocrit effect on accuracy
As previously observed during the bioanalytical validation of the conventional DBS method [2], there was a trend visible in the impact of Hct on miltefosine quantification bias for conventional DBS (Figure 4). The bias in the measured miltefosine concentration was positively correlated with the Hct value of the whole blood: at low Hct values (14%) the bias was around -20% and at high Hct values (50%) the bias was around +25% (Figure 4), compared to whole blood calibration standards with an Hct value of 29%. This is in accordance with the published validation, in which the miltefosine DBS method could only be validated between 20-35% (biases within ±15%) [2]. In addition to the effect of Hct, the accuracy of the method was influenced by variability in blood spot volume and inhomogeneity of the spot [2].

The Hct effect on accuracy for the VAMS sampling methodology is also depicted in Figure 4. For both concentration levels (QCL and QCH) the accuracy (depicted as bias %), was inversely correlated with the Hct value with a positive bias for low Hct levels and a negative bias at higher Hct levels. While the bias was less pronounced than for conventional DBS sampling (in a range from Hct 10-50%, only the Hct 10% QCL values were outside the acceptable ±15% bias), an opposite trend was observed for this sampling method.

The Hct impact on accuracy was most probably attributable to the effect of Hct on

the analyte recovery described previously (at 1,600 ng/mL, the recovery was 69% for Hct 33% and 60% for Hct 48%). A total of six method validations have been described using the VAMS sample collection method for analyte quantification in whole blood [8–13], where four of these tested the effect of Hct on analyte recovery. All four studies found a lower recovery for higher Hct levels [8,11–13], which has been explained by the larger amount of erythrocytes entrapping the analyte in the pores of the VAMS device tip, obstructing analyte extraction [12]. The higher positive bias in lower Hct levels was also observed in our study.

In this VAMS method, accuracy and precision were acceptable in an extended Hct range of Hct 20-50%, compared to Hct 20-35% for conventional DBS sampling. The acceptable 15% bias in quantification was only just exceeded for the QCL level at Hct 10%, which even in the case of VL is an extreme that is rarely observed in clinical practice. Recently it was found that adding a sonication step to the sample pre-treatment could possibly improve the Hct-dependent recovery bias [13]. If a wider range of Hct values is expected in clinical practice than 20-50%, the addition of a sonication step in the pre-treatment method could be evaluated for its effect on recovery from the VAMS device.

2.2
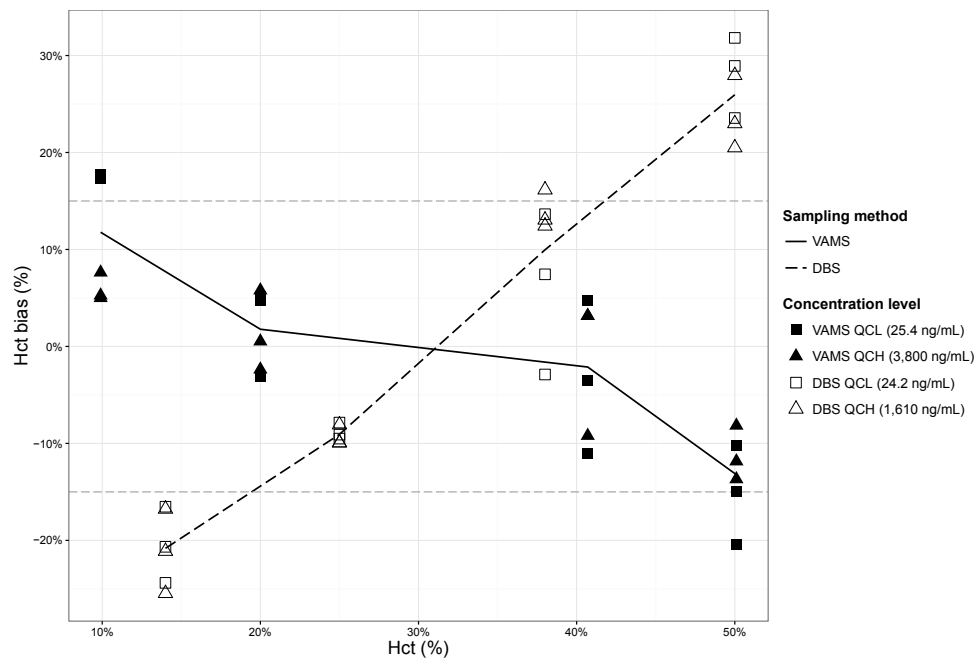
Figure 4. Hct effect on accuracies of the VAMS sampling method versus conventional DBS (on Whatman 903 filter paper) sampling, depicted as bias of analyzed compared to nominal miltefosine concentration. Dotted line depicts the DBS sampling method, solid line depicts the VAMS sampling method. Open symbols depict the DBS sampling method, closed symbols depict the VAMS sampling method. Squared symbols depict the QCL concentration level, triangle symbols depict the QCH concentration level (though at different concentrations between sampling methods).

Practical considerations

The advantage of the VAMS sampling method over other controlled volumetric methods - such as the use of capillaries to apply blood to DBS cards - is its ease of use in the clinic. This is

of special importance in the remote VL endemic areas without appropriate laboratory set-up. The trend towards a decrease in stability within one month storage at room temperature and 37°C is an issue of concern. There were no long-term stability issues with miltefosine in conventional DBS up to five months [2]. Long-term stability of the dried VAMS sample (>7 days) was only assessed in three studies, of which two encountered problems with long-term stability [8,10], but one did not [12]. For the applicability of this method in clinical practice in VL endemic areas, longer stability times are required and these should therefore be evaluated before application in the clinic.

A clinical evaluation of this method is scheduled to evaluate the VAMS sampling method as an appropriate alternative for conventional DBS sampling. While a correlation of the Hct value on miltefosine quantification could be observed in the bioanalytical validation of the conventional DBS method, no obvious or systematic effect of Hct could be observed in its clinical validation. This indicates that many other factors (also including blood spot volume and blood spot homogeneity in the case of DBS sampling) influence miltefosine quantification in DBS in clinical practice. Additionally, while this new sampling method is easy to use in a clinical setting, the method is more prone to misuse such as double-dipping or insufficient absorption. Clinical evaluation of the VAMS method will thus be required to investigate whether the variability in miltefosine quantification in dried blood is improved in clinical practice in comparison to DBS sampling.

One disadvantage of the VAMS sampling method is the relatively high costs in comparison to DBS Whatman-903 cards. As a Whatman-903 protein saver card fits five samples, one VAMS sample is approximately five times more expensive than a conventional DBS sample. Especially in resource-poor settings, this is an important consideration for the applicability of this sampling method and cost-effectiveness should be evaluated.

CONCLUSION

The novel and simple volumetric absorptive micro-sampling (VAMS) device, was evaluated for its applicability in quantitative miltefosine bioanalysis. Though the preparation of calibration standards and quality control samples is more time-consuming than for conventional DBS, the pre-treatment method is fast and simple with reproducible recovery. The analytical method showed a good performance in terms of linearity ($R^2 > 0.9955$), accuracy (bias within ±10.8%) and precision (CV% ≤11.9%).

In this bioanalytical validation, the VAMS collection process effectively diminished the effect of Hct on miltefosine quantification compared to conventional DBS sampling, however, a reversed Hct bias was introduced with this sampling method. In addition to the decreased Hct impact, this method eliminated additional variabilities due to blood spot volume and blood spot homogeneity. In conclusion, the bioanalytical method validation with the VAMS sampling technique showed a better performance compared to conventional DBS sampling.

REFERENCES

1. Dorlo TPC, Rijal S, Ostyn B, de Vries PJ, Singh R, Bhattarai N, et al. Failure of miltefosine in visceral leishmaniasis is associated with low drug exposure. J. Infect. Dis. 2014;210:146–53.

2. Kip AE, Rosing H, Hillebrand MJX, Blesson S, Mengesha B, Diro E, et al. Validation and clinical evaluation of a novel method to measure miltefosine in leishmaniasis patients using dried blood spot sample collection. Antimicrob. Agents Chemother. 2016;60:2081–9.

3. De Kesel PMM, Sadones N, Capiau S, Lambert WE, Stove CP. Hemato-critical issues in quantitative analysis of dried blood spots: challenges and solutions. Bioanalysis. 2013;5:2023–41.

4. O'Mara M, Hudson-Curtis B, Olson K, Yueh Y, Dunn J, Spooner N. The effect of hematocrit and punch location on assay bias during quantitative bioanalysis of dried blood spot samples. Bioanalysis. 2011;3:2335–47.

5. Denniff P, Spooner N. The effect of hematocrit on assay bias when using DBS samples for the quantitative bioanalysis of drugs. Bioanalysis. 2010;2:1385–95.

6. Hailu A, van der Poll T, Berhe N, Kager PA. Elevated plasma levels of interferon (IFN)-γ, IFN-γ inducing cytokines and IFN-γ inducible CXC chemokines in visceral leishmaniasis. Am. J. Trop. Med. Hyg. 2004;71:561–7.

7. Denniff P, Spooner N. Volumetric Absorbtive Micro Sampling (VAMS): a novel dried sample collection technique for quantitative bioanalysis. Anal. Chem. 2014;86:8489–95.

8. Parker SL, Roberts JA, Lipman J, Wallis SC. Quantitative bioanalytical validation of fosfomycin in human whole blood with volumetric absorptive microsampling. Bioanalysis. 2015;7:2585–95.

9. Houbart V, Cobraiville G, Servais A-C, Napp A, Merville M-P, Fillet M. Hepcidin determination in dried blood by microfluidic LC-MS/MS: comparison of DBS and volumetric absorptive microsampling for matrix effect and recovery. Bioanalysis. 2015;7:2789–99.

10. Miao Z, Farnham JG, Hanson G, Podoll T, Reid MJ. Bioanalysis of emixustat (ACU-4429) in whole blood collected with volumetric absorptive microsampling by LC – MS / MS. Bioanalysis. 2015;7:2071–83.

11. Denniff P, Parry S, Dopson W, Spooner N. Quantitative bioanalysis of paracetamol in rats using volumetric absorptive microsampling (VAMS). J. Pharm. Biomed. Anal. 2015;108:61–9.

12. De Kesel PMM, Lambert WE, Stove CP. Does volumetric absorptive microsampling eliminate the hematocrit bias for caffeine and paraxanthine in dried blood samples? A comparative study. Anal. Chim. Acta. 2015;881:65–73.

13. Mano Y, Kita K, Kusano K. Hematocrit-independent recovery is a key for bioanalysis using volumetric absorptive microsampling devices, Mitra™. Bioanalysis. 2015;7:1821–9.

14. Spooner N, Deniff P, Michielsen L, De Vries R, Ji QC, Arnold ME, et al. A device for dried blood microsampling in quantitative bioanalysis: overcoming the issues associated with blood hematocrit. Bioanalysis. 2015;7:653–9.

15. European Medicines Agency. Guideline on bioanalytical method validation. Committee for Medicinal Products for Human Use and European Medicines Agency. 2011. http://www.ema.europa.eu/docs/en_GB/document_library/Scientific_guideline/2011/08/WC500109686.pdf. Accessed 11 Nov 2015.

16. US Food and Drug Administration FDA. Guidance for Industry: Bioanalytical Method Validation. 2001. http://www.fda.gov/downloads/Drugs/Guidances/ucm070107.pdf. Accessed 1 Dec 2015.

17. Timmerman P, White S, Cobb Z, De Vries R, Thomas E, Van Baar B. Update of the EBF recommendation for the use of DBS in regulated bioanalysis integrating the conclusions from the EBF DBS-microsampling consortium. Bioanalysis. 2013;5:2129–36.

18. Dorlo TPC, Hillebrand MJX, Rosing H, Eggelte TA, de Vries PJ, Beijnen JH. Development and validation of a quantitative assay for the measurement of miltefosine in human plasma by liquid chromatography-tandem mass spectrometry. J. Chromatogr. B. Analyt. Technol. Biomed. Life Sci. 2008;865:55–62.

19. Dorlo TPC, van Thiel PPAM, Huitema ADR, Keizer RJ, de Vries HJC, Beijnen JH, et al. Pharmacokinetics of miltefosine in Old World cutaneous leishmaniasis patients. Antimicrob. Agents Chemother. 2008;52:2855–60.

2.2

SUPPLEMENTARY MATERIAL

LC-MS/MS SETTINGS

Data acquisition system

Software: Analyst
Supplier: AB Sciex

Supplementary table 1. HPLC parameters	
Autosampler tray temperature	4°C
Typical injection volume	5 µL
Syringe size	100 µL
Draw / Eject Speed	200 µL/min
Needle level	0.0 mm
Flush Solvent	100% methanol
Pre-Inject Wash Time	5 sec in flush port
Column Temperature	25±5°C
Min. Pressure	50 psi
Max. Pressure	3,500 psi

Supplementary table 2. LC gradient			
Mobile Phase B	10 mM ammoniumhydroxide in 95% methanol		
Type of elution	Isocratic		
Table	Time (min)	B%	Flow Rate (µL/min)
	0.0	100	300
Run time	4.5	100	300

Supplementary table 3. Valco diverter settings	
Time (min)	Position
0.0	A
1.5	B
4.0	A

Supplementary table 4. API3000 operating parameters		
Acquisition time (min)	4.5	
Source position	Ion spray vertical adjustment: +7	
	Ion spray horizontal adjustment: -5	
Scan Type	MRM	
Polarity	Positive	
Ion Source	Turbo Spray	
Resolution Q1	Unit	
Resolution Q3	Unit	
Source / Gas Parameters:		
Nebulizer gas pressure	11 (arbitrary units)	
Turbo gas flow	7 L/min	
Curtain gas pressure	9 (arbitrary units)	
Collision gas pressure	6 (arbitrary units)	
Ion spray voltage (ISV):	4,500 V	
Temperature (TEM)	400°C	
Dwell time	450 msec	
Miltefosine monitored ions (amu)	408.4 → 124.9	
Miltefosine-D4 monitored ions (amu)	412.61 → 129.2	
Compound Dependent Parameters	**Miltefosine 408.4 → 124.9**	**Miltefosine-D4 412.61 → 129.2**
Declustering Potential (DP)	71 V	71 V
Focusing Potential (FP)	290 V	290 V
Collision Energy (CE)	43 V	43 V
Collision Cell Exit Potential (CXP)	22 V	22 V
Entrance Potential (EP)	12 V	12 V

2.2

Chapter 2.3

Quantification of miltefosine in peripheral blood mononuclear cells by high-performance liquid chromatography-tandem mass spectrometry

A.E. Kip
H. Rosing
M.J.X. Hillebrand
M.M. Castro
M.A. Gomez
J.H.M. Schellens
J.H. Beijnen
T.P.C. Dorlo

ABSTRACT

Phagocytes, the physiological compartment in which *Leishmania* parasites reside, are the main site of action of the drug miltefosine, but the intracellular pharmacokinetics of miltefosine remain unexplored. We developed a bioanalytical method to quantify miltefosine in human peripheral blood mononuclear cells (PBMCs), expanding from an existing high performance liquid chromatography-tandem mass spectrometry method for the quantification of miltefosine in plasma. The method introduced deuterated miltefosine as an internal standard. Miltefosine was extracted from PBMC pellets by addition of 62.5% methanol. Supernatant was collected, evaporated and reconstituted in plasma. Chromatographic separation was performed on a reversed phase C18 column and detection with a triple-quadrupole mass spectrometer. Miltefosine was quantified using plasma calibration standards ranging from 4 to 1,000 ng/mL. This method was validated with respect to its PBMC matrix effect, selectivity, recovery and stability. No matrix effect could be observed from the PBMC content (ranging from 0.17 to 26.3×10^6 PBMCs) reconstituted in plasma, as quality control samples were within 3.0% of the nominal concentration (precision less than 7.7%). At the lower limit of quantitation of 4 ng/mL plasma, corresponding to 0.12 ng/10^6 PBMCs in a typical clinical sample, measured concentrations were within 8.6% of the nominal value. Recovery showed to be reproducible as adding additional pre-treatment steps did not increase the recovery with more than 9%. This method was successfully applied to measure intracellular miltefosine concentrations in PBMC samples from six cutaneous leishmaniasis patients up to one month post-treatment.

INTRODUCTION

The *Leishmania* parasite, causative agent of the neglected infectious disease leishmaniasis, resides and replicates within human phagocytes. These cells are therefore the main site of action of the antileishmanial drug miltefosine [1], however, the intracellular pharmacokinetics of the drug are currently unknown. Miltefosine is transported into cells both by passive incorporation in the cellular membranes (non-saturable from 20 to 200 µM/8.2 to 82 µg/mL) and by active carrier-mediated cellular transport (saturable at 50 µM/20.4 µg/mL) [2,3]. In Dutch cutaneous leishmaniasis (CL) patients, the average steady-state plasma concentration reached only in the last week of treatment during a standard 28-day miltefosine regimen, was 30.8 µg/mL [4]. Within the treatment period, the contribution of the active (saturable) transport is thus substantial and the relative contribution of both transport mechanisms on the intracellular miltefosine accumulation *in vivo* is expected to vary during treatment. The saturability of the active transport could result in substantial between-subject variability in intracellular miltefosine concentrations.

Resident tissue macrophages are the host cells for intracellular *Leishmania* survival and replication. Thus, intracellular drug quantification is pivotal to provide a better understanding of the drug disposition within the physiological compartment in which the parasites reside. Intracellular miltefosine concentrations better represent the drug concentrations to which the parasites are exposed and will probably relate more accurately to *Leishmania* drug susceptibility and pharmacokinetic/pharmacodynamic relationships than plasma drug concentrations.

We have previously validated an LC/MS-MS assay to measure miltefosine in plasma [5]. Here we expand this method to intracellular measurements. In this assay peripheral blood mononuclear cells (PBMCs) were used as a model to assess intracellular miltefosine accumulation within human leukocytes. The sample pre-treatment was modified and a partial validation was executed. This assay was evaluated using PBMC samples from six Colombian CL patients treated with a miltefosine monotherapy.

METHODS

Chemicals and reagents

Miltefosine and phosphate buffered saline (PBS) were purchased from Sigma-Aldrich (Zwijndrecht, the Netherlands), and deuterated miltefosine (miltefosine-D4, Figure 1) from Alsachim (Illkirch Graffenstaden, France). Acetonitrile, methanol and H_2O were obtained from Biosolve Ltd. (Valkenswaard, the Netherlands), ammonia 25%, triethylamine and acetic acid 99.8% from Merck (Amsterdam, the Netherlands) and Ficoll from GE Healthcare (Hoevelaken, the Netherlands). Blank Na-EDTA plasma was obtained from Bioreclamations (Baltimore, US).

Clinical sample collection, PBMC isolation and partial pre-treatment

Heparin-treated blood samples (10 mL for adults, 3 mL for children) were taken from CL patients ("Clinical application", p. 96 and centrifuged 10 min at 800 x g at room temperature. All plasma was transferred and stored at −80°C, while the remaining blood sample was diluted 1:4 in PBS and placed over a Ficoll gradient at a 1:5 Ficoll-to-blood ratio. Samples were centrifuged 15 min at 400 x g at room temperature and the mononuclear leukocyte layer was isolated. Subsequently the cells were washed two times with 10 mL PBS, resuspended

2.3

in 1 mL PBS and counted on a haemocytometer. Samples were centrifuged at 800 x g, the supernatant was removed, and the PBMC pellet stored at −80°C. Plasma and PBMC pellets were transported on dry ice to the bioanalytical laboratory and stored at −20°C until analysis.

The cell pellet was resuspended in 120 µL PBS, after which the cells were lysed by adding 200 µL methanol yielding a total volume of 320 µL 62.5% methanol-PBS (v/v). The sample was vortexed and centrifuged for 5 min at 20,000 x g. The supernatant, referred to as the "PBMC lysate" was transferred to a 1.5 mL tube. Depending on the expected concentration, the PBMC lysate volume transferred varied between 50 µL (expected concentration above upper limit of quantitation, ULOQ) and 280 µL (expected concentration close to lower limit of quantitation, LLOQ). Finally, the PBMC lysate was evaporated under a gentle stream of nitrogen and reconstituted in 250 µL of blank Na-EDTA human plasma. These so-called "reconstituted PBMC samples" were handled as normal plasma samples ("Plasma sample preparation and LC-MS/MS analysis", p. 95).

Preparation of plasma calibration standards and internal standard solution

Calibration standards were prepared in plasma. A stock solution of 1 mg/mL miltefosine was prepared in methanol-water (1:1, v/v). Calibration standard working solutions were further diluted from this stock solution with methanol−water (1:1, v/v) to final concentrations of 0.08, 0.2, 0.4, 1, 2, 4, 8, 16 and 20 µg/mL.

Calibration standards were freshly prepared before each run by spiking 570 µL of blank Na-EDTA human plasma with 30 µL of working solution, yielding calibration standards of 4, 10, 20, 50, 100, 200, 400, 800 and 1,000 ng/mL. Two 250 µL aliquots were prepared per calibration standard and processed for each analytical run.

An internal standard working solution was prepared by dilution of a stock solution of 1 mg/mL deuterated miltefosine (miltefosine-D4) in methanol-water (1:1, v/v) to 4,000 ng/mL with methanol-water (1:1, v/v).
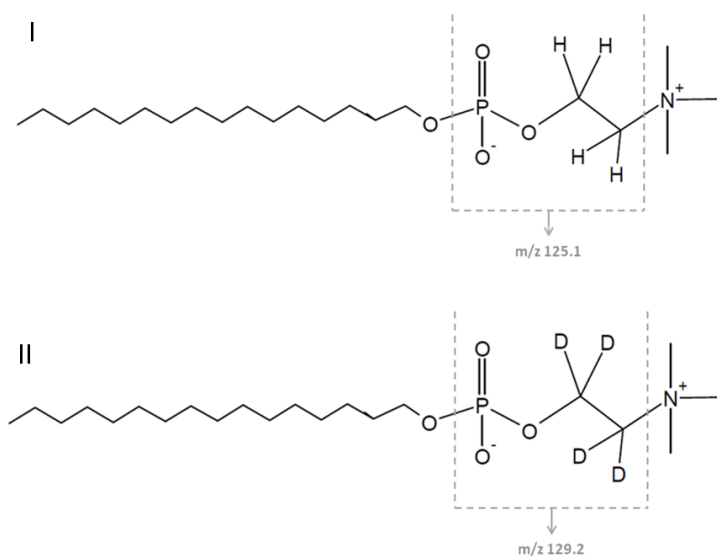

Figure 1. Structural formulas of miltefosine (I) and the internal standard miltefosine-D4 (II), indicating the m/z fragments.

Preparation of PBMC quality control samples

A separate stock solution of 1 mg/mL miltefosine in methanol-water (1:1, v/v) was prepared from an independent weighing for the preparation of quality control (QC) samples. PBMC QC working solutions were diluted from this stock solution with methanol-water (1:1, v/v) to concentrations of 0.6, 15 and 37.5 µg/mL and an LLOQ working solution of 0.2 µg/mL.

To mimic the study samples, QC samples were prepared freshly by spiking 5 µL of working solution to 95 µL of blank PBMC lysate. To prepare blank PBMC lysate, blank PBMCs were isolated from human leukocyte buffy coat (~50 mL, freshly derived from 500 mL whole blood) purchased from Sanquin (Amsterdam, the Netherlands). 200 mL PBS was added to the buffy coat, and 25 mL aliquots of this suspension were each carefully added to 12.5 mL of high density centrifugation medium Ficoll. After a 20 min 550 x g centrifugation at 4°C (without brake), the interface containing the PBMCs was transferred to a clean tube. Subsequently, the PBMCs of each aliquot were washed with 35 mL PBS and centrifuged at 1500 x g for 5 min at 4°C (without brake). The supernatant was discarded and the pellet was resuspended in 300 µL PBS. All aliquots were pooled and a cell count was performed with a Cell Dyn Hematology analyzer (Abbott Diagnostics, Lake Forest, IL, USA). After a 3000 x g centrifugation, PBS was removed to adjust the PBMC concentration to approximately 200×10^6 cells per mL PBS, to obtain reconstituted PBMC QC samples containing 7.1×10^6 cells, close to the mean found in patient samples ("Clinical application", p. 96). Depending on the final volume of blank PBMCs in PBS, a volume of methanol was subsequently added to obtain PBMC lysate of 62.5% methanol-PBS (v/v).

After spiking, the QCs were evaporated under a gentle stream of nitrogen and reconstituted in 250 µL of blank Na-EDTA human plasma. The final miltefosine concentrations of the reconstituted PBMC QCs were 12, 300 and 750 ng/mL (low; QCL, mid; QCM and high; QCH respectively). Considering an average of 7.1×10^6 PBMCs in the reconstituted PBMC samples, this would correspond to concentrations of 0.42, 11 and 26 ng/10^6 cells.

Plasma sample preparation and LC-MS/MS analysis

Reconstituted PBMC samples and plasma calibration standards were further prepared as previously described [5] with slight modifications. First, 25 µL of miltefosine-D4 (4,000 ng/mL) was added to each 250 µL aliquot, except for double blanks to which 25 µL methanol-water (1:1, v/v) was added. All samples were briefly vortexed and subsequently 700 µL of acetic acid buffer (1 M, pH 4.5) was added. Samples were vortexed and centrifuged 5 min at 23,100 x g at room temperature. The extraction of miltefosine was performed on Bond Elut PH SPE cartridges (Agilent Technologies, Amstelveen, the Netherlands), which were first conditioned with 1 mL acetonitrile and subsequently 1 mL acetic acid buffer (1 M, pH 4.5). Afterwards, samples were loaded on the SPE cartridges and the cartridges were washed with 1 mL methanol-water (1:1, v/v). The analyte was eluted with two times 750 µL of 0.1% (v/v) triethylamine in methanol. The eluate was transferred to a glass autosampler vial and 10 µL was injected on the analytical column.

The chromatographic separation and LC-MS/MS analysis was performed as described previously [5], but the more sensitive API3000 triple-quadrupole mass spectrometer was used, which was equipped with a turbo-ionspray source (AB Sciex, Framingham, MA, USA). Mass spectrometer settings were optimized on the API3000. Miltefosine was monitored at a mass transition of m/z 408.5 to 125.1 and miltefosine-D4 at m/z 412.6 to 129.2.

2.3

Partial validation procedure for PBMC samples

Due to the fact that this method is an extension of an existing previously validated method [5], a partial validation [6] was performed in which the following aspects were investigated.

Matrix effect of PBMC content

The amount of cells in PBMC pellets may vary from sample to sample due to physiological variability in the number of circulating PBMCs and the volume of blood collected. Additionally, PBMC lysate volumes transferred differ depending on the expected miltefosine concentration. To investigate the potential effect of PBMC content in the plasma matrix on the miltefosine quantification, blank PBMC samples in PBS were prepared containing different PBMC concentrations to yield reconstituted PBMC samples with final PBMC counts of 0.17, 4.0, 6.8, 16 and 26 x 10^6 cells (a range covering the clinical samples received, "Clinical application", p. 96). The cells were lysed with methanol to obtain PBMC lysate of 62.5% methanol-PBS (v/v). The blank PBMC lysate was spiked at the QCL and QCH level in triplicate to yield concentrations of 12.2 and 761 ng/mL miltefosine in the reconstituted PBMC samples. A matrix effect was considered when the measured analyte concentration was outside 85–115% of the nominal concentration.

Selectivity

Double blanks and LLOQ samples (5 µL working solution + 95 µL blank PBMC lysate) were prepared from blank PBMC lysate originating from six different individuals (six batches), to check the specificity and selectivity of this method. For four out of six batches, the signal-to-noise ratio of the LLOQ should be above 5 and the LLOQ samples should be within ±20% of the nominal concentration.

Recovery

One of the challenges in the determination of intracellular drug concentrations is that it is not possible to truly mimic the uptake of the analyte by PBMCs, and therefore it is not possible to quantitatively assess the absolute pre-treatment recovery of miltefosine from PBMCs. Therefore we have investigated whether the relative recovery could be improved by applying different methods to lyse PBMCs. Three patient samples were pre-treated with three different methods: (a) the method described previously; (b) same as (a), plus 1 hour freeze at -20°C; (c) same as (b), plus 30 min sonication. Additionally, microbead homogenization was evaluated on eight other patient samples in which the PBMC pellets appeared to not be homogeneously suspended.

If the additional yield due to an extra pre-treatment step was less than 15% for at least two thirds of the samples, it was not included in the final pre-treatment method.

Stability in 62.5% methanol-PBS (v/v)

PBMC lysate stability was tested by spiking blank PBMC lysate at QCL and QCH level in triplicate. The samples were stored at –20°C for 15 days. Stability was considered acceptable when the measured analyte concentration was within 85–115% of the nominal concentration.

Clinical application

PBMC and plasma samples were collected from January 2012 to October 2013 in an open label non-randomized pharmacokinetic clinical trial of miltefosine in children and adults

with CL. This study was approved and monitored by the institutional review board for ethical conduct of research involving human subjects of the Centro Internacional de Entrenamiento e Investigaciones Médicas (CIDEIM), in accordance with national (resolution 008430, República de Colombia, Ministry of Health, 1993) and international (Declaration of Helsinki and amendments, World Medical Association, Fortaleza, Brasil, October 2013) guidelines. Samples were collected nominally on day 1, 15 and 28 of a 1.8-2.5 mg/kg/day 28-day miltefosine regimen, and one, two, three and five months after treatment. Eleven patient samples were used for the bioanalytical validation of the recovery within this method. Subsequently, samples obtained from six patients in this study were included as a clinical validation to show the robustness and applicability of the developed method.

As described previously, PBMC samples were reconstituted in 250 μL plasma and quantified using plasma calibration standards, therefore the measured concentrations are in ng/mL plasma. These concentrations were corrected for the dilution factor (DF, Equation 1) and multiplied by 320/1,000 μL to calculate the total amount of miltefosine in the pellet (Equation 2). Subsequently, this value was converted to amount of miltefosine per 10^6 cells, based on the sample cell counts (Equation 3). The mean number of PBMCs in the reconstituted PBMC sample for the six patients (total samples, n = 25) was 6.8 x 10^6 PBMCs, with a range from 0.72 to 23 x 10^6 PBMCs.

The intracellular miltefosine concentration was calculated by using an average volume of 283 fl for a single peripheral blood mononuclear cell [7], equal to 0.000283 mL per 10^6 cells (Equation 4, in which "IC" stands for intracellular).

Equation 1: $\quad DF = \dfrac{PBMC\ lysate\ transferred\,(\mu L)}{250\ \mu L}$

Equation 2: $\quad MILT\left(\dfrac{ng}{pellet}\right) = \dfrac{[MILT]_{measured}\left(\frac{ng}{mL}\right)}{DF} \cdot \dfrac{320\ \mu L}{1000\ \mu L}$

Equation 3: $\quad MILT\left(\dfrac{ng}{10^6\,cells}\right) = \dfrac{MILT\left(\dfrac{ng}{pellet}\right)}{cell\ count\left(\dfrac{\#cells}{pellet}\right)} \cdot 10^6\,cells$

Equation 4: $\quad [MILT]_{IC}\left(\dfrac{\mu g}{mL}\right) = \dfrac{MILT\left(\dfrac{ng}{10^6\ cells}\right)}{10^3\left(\dfrac{ng}{\mu g}\right) \cdot 0.000283\left(\dfrac{mL}{10^6\ cells}\right)}$

RESULTS & DISCUSSION

Matrix effect of PBMC content
Table 1 shows the matrix effect of the different PBMC amounts in the reconstituted PBMC samples. The bias was within 3.0% of the nominal concentration and the coefficient of

Table 1. Matrix effect of different amounts of PBMCs in reconstituted PBMC sample (n=3).

Amount of PBMCs in reconstituted PBMC sample (x10^6)	Nominal concentration 12.2 ng/mL			Nominal concentration 761 ng/mL		
	Mean calculated concentration (ng/mL)	Precision (%CV)	Bias (%)	Mean calculated concentration (ng/mL)	Precision (%CV)	Bias (%)
0.17	12.1	3.0	-0.8	738	1.2	-3.0
4.0	12.1	2.4	-1.1	756	4.3	-0.6
6.8	12.6	6.8	3.0	749	3.5	-1.6
16	12.1	4.5	-0.5	763	3.2	0.2
26	12.5	7.7	2.7	755	0.6	-0.7

variation (CV%) within 7.7%. It can be concluded that the PBMC counts expected in clinical practice do not influence the accuracy of the method and that there was no additional matrix effect due to the PBMC content.

Selectivity

A peak with the same retention time and mass transition as miltefosine was observed both in plasma and reconstituted PBMC double blanks (reconstituted in the same plasma), possibly due to a memory effect. The memory effect was constant over the run and did not decrease in intensity as for the 20 plasma double blanks injected within one run, the memory peak remained at an average signal of 22% of the LLOQ. This memory effect was not observed in the previously validated method [5], but this could possibly be explained by the increased sensitivity as a result of a change in the mass spectrometer. The memory effect was independent of the injected sample and no additional effect was measured after injecting the ULOQ. Reconstitution solvents were tested and found not to be contaminated. For 5 out of the 6 tested batches of PBMCs, the interference in the blanks was an average of 23% of the LLOQ and was thus comparable to the interference found in the plasma of the reconstituted PBMC sample. The interference was constant over the run and therefore the calibration standards corrected for this. The accuracies of the LLOQ samples were within 94.1% and 108.6% of the nominal concentration and were therefore found to be acceptable. Because the six PBMC batches each contained different cell amounts, the highest of the six (8.5 x 10^6 cells in the reconstituted PBMC sample) was taken as a reference to calculate an LLOQ of 0.12 ng per million cells. It should be mentioned that the LLOQ is dependent on the amount of PBMCs in the reconstituted PBMC sample, as the LLOQ (expressed per million cells) decreases with an increase of the amount of cells isolated. Figure 2 shows representative chromatograms of a double blank, LLOQ and QCL sample.

It could be argued that because the memory peak in double blanks is higher than 20% of the LLOQ the selectivity is not sufficient, as the signal to noise ratio is below 5. However, because the miltefosine signal in double blanks is stable between different batches of plasma and PBMC matrices, and because the LLOQ is still measured precisely and accurately, the selectivity of the assay was considered acceptable.

Recovery

The addition of a freezing or sonication step did not yield an increase in intracellular miltefosine recovery of more than 5%. The increase in miltefosine recovery due to microbead
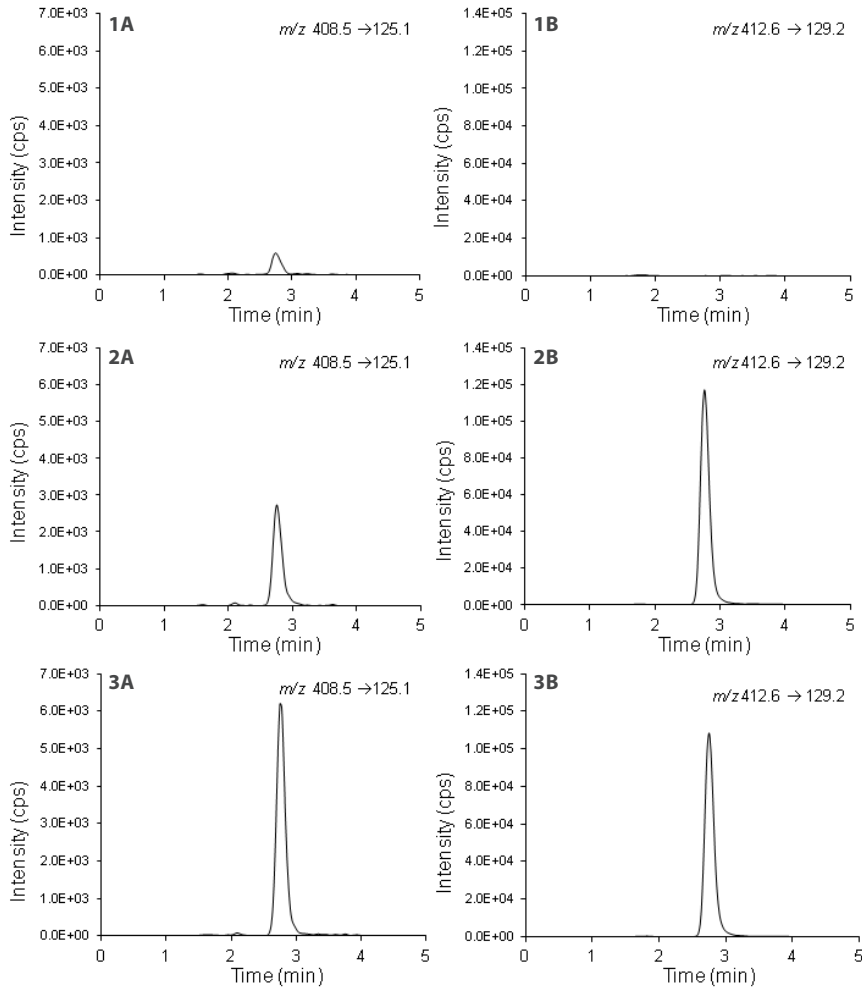
Figure 2. Representative ion chromatograms of the 1) double blank; 2) LLOQ (4 ng/mL) and 3) QCL (12.2 ng/mL). The left panel (A) shows the miltefosine ion chromatogram and the right panel (B) the internal standard miltefosine-D4 ion chromatograms.

homogenization was less than 9% for seven out of eight patient samples. It was concluded that the method had an acceptable reproducibility regarding the release of miltefosine from PBMCs and therefore these extra steps were not added to the pre-treatment method.

Stability in 62.5% methanol-PBS (v/v)
QCs spiked in PBMC blank lysate were stable for at least 15 days at −20°C. The mean measured concentrations were 99.2% and 98.6% of the nominal concentration for QCL and QCH respectively, with acceptable variation (<3.2%).

Clinical application
Plasma concentration-time curves and corresponding intracellular concentration-time curves for six CL patients are presented in Figure 3. The intracellular miltefosine kinetic profile is similar
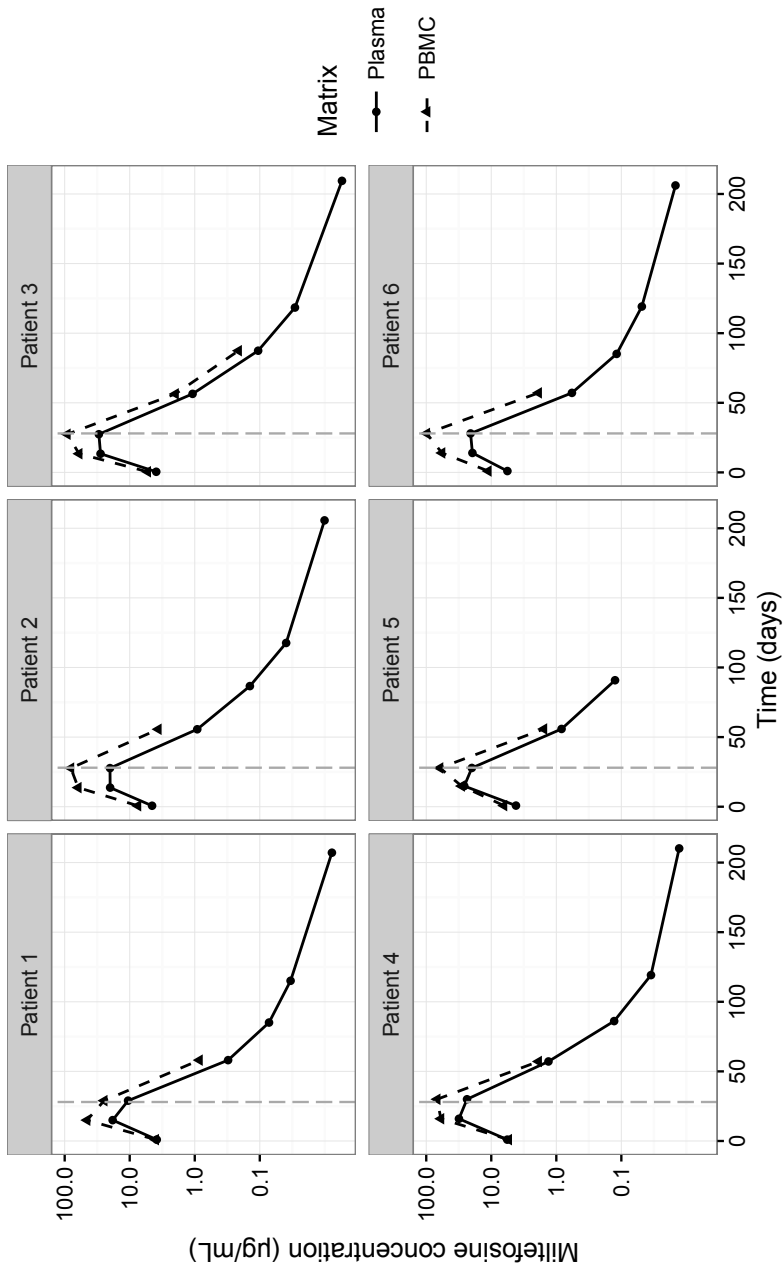
Figure 3. Representative concentration-time curves of miltefosine plasma concentrations (solid line) and intracellular miltefosine concentrations (dashed line) for six cutaneous leishmaniasis patients. The vertical grey dashed line indicates the end of treatment.

to the kinetic profile of miltefosine plasma concentrations. This is particularly clear for patient 1, who showed a decline in miltefosine concentration between day 14 and day 28 of treatment which is apparent for both plasma and intracellular concentrations. Intracellular miltefosine concentrations were measurable up to one month post-treatment, and for patient 3 even up to two months post-treatment due to the high number of PBMCs isolated. Interestingly, end-of-treatment intracellular miltefosine concentrations were higher than the plasma miltefosine concentrations, indicating that an accumulation of miltefosine takes place in PBMCs.

CONCLUSION & FUTURE PERSPECTIVE

A pre-treatment method, additional to a previously validated method for quantitation of miltefosine in plasma, was successfully developed and validated to measure miltefosine concentrations in isolated PBMCs. The method showed to be reproducible and selective, and the LLOQ was sufficient to quantify intracellular miltefosine concentrations in patient samples up to one month post-treatment. The LLOQ of this assay was 0.12 ng miltefosine per million cells, based on 8.5×10^6 cells in the reconstituted PBMC sample. To allow for quantification of miltefosine for a longer period after treatment, the LLOQ could be further decreased by augmenting the number of isolated PBMCs per sample or by using more sensitive mass spectrometry equipment.

An initial exploration of intracellular miltefosine concentrations in samples from CL patients showed similar kinetic profiles in intracellular and plasma concentrations, and suggests drug accumulation in PBMCs. Since miltefosine is used in the treatment of infection with the intracellular *Leishmania* parasite, intracellular pharmacokinetic data can enrich our understanding of the exposure-response relationship of this drug. The here presented bioanalytical method can be applied to further establish this relationship.

TRANSPARENCY DECLARATIONS

None.

ACKNOWLEDGEMENTS

2.3

REFERENCES

1. Dorlo TPC, Balasegaram M, Beijnen JH, de Vries PJ. Miltefosine: a review of its pharmacology and therapeutic efficacy in the treatment of leishmaniasis. J. Antimicrob. Chemother. 2012;67:2576–97.

2. Ménez C, Buyse M, Farinotti R, Barratt G. Inward translocation of the phospholipid analogue miltefosine across Caco-2 cell membranes exhibits characteristics of a carrier-mediated process. Lipids. 2007;42:229–40.

3. Ménez C, Buyse M, Dugave C, Farinotti R, Barratt G. Intestinal absorption of miltefosine: contribution of passive paracellular transport. Pharm. Res. 2007;24:546–54.

4. Dorlo TPC, van Thiel PPAM, Huitema ADR, Keizer RJ, de Vries HJC, Beijnen JH, et al. Pharmacokinetics of miltefosine in Old World cutaneous leishmaniasis patients. Antimicrob. Agents Chemother. 2008;52:2855–60.

5. Dorlo TPC, Hillebrand MJX, Rosing H, Eggelte TA, de Vries PJ, Beijnen JH. Development and validation of a quantitative assay for the measurement of miltefosine in human plasma by liquid chromatography-tandem mass spectrometry. J. Chromatogr. B. Analyt. Technol. Biomed. Life Sci. 2008;865:55–62.

6. US Food and Drug Administration FDA. Guidance for Industry: Bioanalytical Method Validation. 2001. http://www.fda.gov/downloads/Drugs/Guidances/ucm070107.pdf. Accessed 13 Jan 2015.

7. Simiele M, D'Avolio A, Baietto L, Siccardi M, Sciandra M, Agati S, et al. Evaluation of the mean corpuscular volume of peripheral blood mononuclear cells of HIV patients by a coulter counter to determine intracellular drug concentrations. Antimicrob. Agents Chemother. 2011;55:2976–8.

2.3

Chapter **3**

| Clinical
pharmacokinetics

Chapter 3.1

Simultaneous population pharmacokinetic modelling of plasma and intracellular miltefosine concentrations in Colombian cutaneous leishmaniasis patients and exploration of exposure-response relationships

A.E. Kip
M.M. Castro
M.A. Gomez
A. Cossio
J.H.M. Schellens
J.H. Beijnen
N.G. Saravia
T.P.C. Dorlo

SYNOPSIS

OBJECTIVES: *Leishmania* parasites reside within macrophages and the direct target of antileishmanial drugs is therefore inside these cells. We aimed to characterize intracellular miltefosine kinetics by developing a population pharmacokinetic (PK) model simultaneously describing plasma and intracellular pharmacokinetics in cutaneous leishmaniasis patients. Furthermore, we explored exposure-response relationships and simulated an allometric dosing regimen.

PATIENTS AND METHODS: The population PK model was developed with NONMEM, using a dataset including 338 plasma and 194 peripheral blood mononuclear cell (PBMC) observations from Colombian cutaneous leishmaniasis patients - 29 children aged 2-12y and 22 adults - receiving 1.8-2.5 mg/kg/day miltefosine for 28 days. Exposure-response relationships were explored with a logistic regression in R.

RESULTS: A three-compartment model with intracellular miltefosine accumulation within the central compartment best fitted the data. Intracellular miltefosine distribution was described with an intracellular to plasma concentration ratio of 2.17 (relative standard error, RSE 4.9%) and intracellular distribution rate constant of 1.23 day^{-1} (RSE 14%). In exploring exposure-response relationships, both plasma and intracellular model-based exposure estimates significantly influenced probability of cure. A proposed PK target for the plasma area under the concentration-time curve from day 0-28 of >535 µg·day/mL corresponded to >95% probability of cure. In linear dosing simulations, 18.3% of children compared to 2.8% of adults failed to reach 535 µg·day/mL. In children, this percentage decreased to 1.8% after an allometric dosing regimen simulation.

CONCLUSIONS: A miltefosine population PK model was developed describing a delayed intracellular accumulation from plasma into PBMCs. Miltefosine exposure was significantly related to probability of cure in these cutaneous leishmaniasis patients. The proposed exploratory PK target should be validated in a larger cohort study.

INTRODUCTION

Leishmania are protozoan parasites that cause the tropical disease leishmaniasis, which can result in diverse clinical manifestations, such as systemic infection (visceral leishmaniasis) or the skin lesions of cutaneous leishmaniasis. The parasites primarily reside and replicate in macrophages during infection of humans or other mammalian hosts. Although the direct target of antileishmanial drugs is inside macrophages, the intracellular pharmacokinetics of these drugs was never characterized until it was recently described for miltefosine [1].

Miltefosine is currently the only registered oral drug for treatment of leishmaniasis. Several hypotheses exist for the mechanisms of action of miltefosine, including disturbance of lipid-dependent cell signaling and induction of mitochondrial dysfunction and apoptosis, which require macrophage membrane sequestering or cell entry of miltefosine [2].

A large portion (57%) of total miltefosine has been found to be sequestered in the Caco-2 cell membrane after *in vitro* incubation, while a small portion was transported across the membrane (7%) [3]. Sequestered miltefosine in the outer membrane leaflet was transported towards the inner leaflet by both passive and active transport mechanisms in the clinically observed range of miltefosine plasma concentrations [3,4]. Inter-individual variability in saturation of the active inward translocation of miltefosine could potentially result in between-subject variability in the intracellular exposure of parasites to this drug.

Miltefosine pharmacokinetics has until recently only been described in plasma, in both cutaneous and visceral leishmaniasis patients [5–7]. Children with visceral leishmaniasis were found to be underexposed to miltefosine in comparison to adults when treated with the conventional linear 28-day 2.5 mg/kg daily dosing regimen. Furthermore, a relationship between miltefosine exposure and probability of final treatment cure was established in visceral leishmaniasis [7]. An allometric dosing regimen based on fat free mass (FFM) was proposed to increase miltefosine exposure in children to adult levels, in order to increase the probability of cure [6].

A pharmacokinetic (PK) clinical trial was conducted to compare the pharmacokinetics of miltefosine in pediatric and adult cutaneous leishmaniasis patients in Colombia, the results of which have recently been published [1]. The non-compartmental PK analysis (NCA) in this report contains the first description of intracellular miltefosine exposure in peripheral blood mononuclear cells (PBMCs). Intracellular miltefosine steady-state concentrations were found to be around two-fold higher than plasma concentrations, which could be clinically relevant with regard to miltefosine's intracellular mode of action. Lower miltefosine exposure in pediatric compared to adult patients was confirmed, both in plasma and intracellularly, but no exposure-response relation could be discerned [1].

The objective of the present study was to develop a population PK model with the data of the aforementioned study [1], describing the kinetics of intracellular accumulation of miltefosine in PBMCs by simultaneous modelling of plasma and intracellular miltefosine concentrations. Using a non-linear mixed effects modelling approach, miltefosine exposure can be more accurately described than with NCA, particularly with the sparse sampling scheme achievable in young children as was employed in this study [8]. Additionally, we explored the exposure-response relationship between plasma and intracellular exposure and treatment outcome, and we simulated an allometric dosing regimen in both children and adults using the developed population PK model.

3.1

METHODS

Study population, PK sampling and bioanalysis

Data for this model based analysis originated from an open-label clinical trial investigating the pharmacokinetics of a 28-day 1.8-2.5 mg/kg daily miltefosine monotherapy for the treatment of cutaneous leishmaniasis patients (registered as NCT01462500). The non-compartmental PK data, toxicity and treatment outcome have been published previously [1]. Ethical approval was obtained from the institutional ethical review board of the Centro Internacional de Entrenamiento e Investigaciones Médicas (CIDEIM) and the Colombian National Institute for Food and Drug Safety (INVIMA). Written informed consent, and ascent in the case of children >7 years of age, was obtained from each patient. Sixty patients (thirty adults and thirty children) were treated in two outpatient clinical facilities in CIDEIM Cali and Tumaco, Colombia [1]. Cure was defined as complete re-epithelization and absence of inflammatory signs for all lesions at the end of a six month follow-up period.

Plasma and mononuclear cell samples were obtained from heparin anticoagulated peripheral blood collected pre-dose after 1, 14 and 28 days of treatment, and during the six month follow-up period on day 60, 90, 120 and 210 after start of treatment. Samples were transported and stored at -20°C until analysis. Analysis was performed with liquid chromatography-tandem mass spectrometry (LC-MS/MS) [1,9,10]. Intracellular concentrations were calculated as described previously using the PBMC cell count and average cell volume [9,11].

PK samples were only available for 59 patients. Seven patients were excluded from the population PK analysis due to potential non-adherence based on their PK profiles (>40% decrease in miltefosine concentration during treatment) [1]. One additional patient was excluded due to missing dosing data, bringing the total of patients included in the population PK model to 51. Of these, two patients were lost to follow-up. As treatment outcome could not be evaluated for these patients, data from 49 patients were included in the exposure-response exploratory analysis.

Population PK analysis

Data management was performed in R (version 3.1.2) and Excel (Office 2007). Non-linear mixed effects modeling was performed with NONMEM (version 7.3) using a first-order conditional estimation procedure with interaction between inter-individual variability and residual error components. Piraña (version 2.8.1) was used in model building as an interface between NONMEM, Perl-speaks-NONMEM (PsN, version 3.4.2), R, and the R-package Xpose (version 4.5.3) to evaluate model performance.

Minimization of the objective function value (OFV, minus twice the log likelihood) was used as a basic evaluation method to guide the selection of a structural, stochastic and covariate model (selection criteria ΔOFV ≥3.84, p<0.05). Goodness of fit and predictive performance of the models were evaluated by graphical methods and visual predictive check (VPC) based on 1,000 simulated replicates, respectively. A bootstrap (1,000 samples) was performed to assess precision and reliability of the final parameter estimates. Shrinkage of empirical Bayes estimates and residual error components were evaluated in all models.

<u>Structural model</u>
Population PK models were first evaluated using miltefosine plasma data only to identify the

best structural model. A previously developed open two-compartment model with first-order absorption and linear elimination from the central compartment was taken as reference model from which further structural models were developed [5,6]. Subsequently, PBMC PK data were added to the dataset and various parameterizations were evaluated to link intracellular to plasma data.

The primary PK parameters estimated were clearances (elimination clearance or inter-compartmental clearance) and volumes of distribution (V). Both clearance and V were expressed relative to bioavailability, since the absolute bioavailability of miltefosine is unknown. Due to limited sampling per dosing interval, the absorption rate (k_a) was fixed at 9.6 day^{-1}, based on previously reported values [7].

Stochastic model
Between-subject variability (BSV) in PK parameters was estimated with an exponential model. Residual variability was modeled with separate proportional errors for plasma and intracellular data, since more variability and error is expected in PBMC compared to plasma separation.

Covariate model
Covariate selection was done using forward inclusion and backward elimination with the final structural PK model, with selection criteria of ΔOFV $\geq$3.84 (p<0.05) and $\geq$6.64 (p<0.01), respectively. Body weight and FFM were evaluated as covariates on V and clearance. Clearance and V were scaled to a standard weight of 70 kg or FFM of 53 kg to make results comparable to previously published studies [6,7]. An allometric power function was used with a power of 0.75 for clearance and 1 for V (representing linear scaling), based on a previously published population PK model [6].

FFM was initially calculated as described in Equation 1 where HT is height (in meters), WT is weight (in kg), WHS_{max} is 42.92 or 37.99 kg/m^2 and WHS_{50} is 30.93 or 35.98 kg/m^2 for males and females, respectively [12].

Equation 1: $\quad \text{FFM} = \text{WHS}_{max} \cdot \text{HT}^2 \cdot \left(\dfrac{\text{WT}}{\text{WHS}_{50} \cdot \text{HT}^2 + \text{WT}} \right)$

Due to the large proportion of pediatric patients in this study, the previously described age maturation component in FFM calculation was used (Equations 2 and 3) [13], estimating FFM with a sigmoid hyperbolic function asymptoting towards the predicted adult FFM described in Equation 1, with age and gender as additional covariates.

Equation 2: $\quad \text{FFM (males)} = \left[0.88 + \left(\dfrac{1 - 0.88}{\left[1 + \left(\frac{\text{AGE}}{13.4} \right)^{-12.7} \right]} \right) \right] + \left[\dfrac{9,270 \cdot \text{WT}}{6,680 + \left(216 \cdot \frac{\text{WT}}{\text{HT}^2} \right)} \right]$

Equation 3: $\quad \text{FFM (females)} = \left[1.11 + \left(\dfrac{1 - 1.11}{\left[1 + \left(\frac{\text{AGE}}{7.1} \right)^{-1.1} \right]} \right) \right] + \left[\dfrac{9,270 \cdot \text{WT}}{8,780 + \left(244 \cdot \frac{\text{WT}}{\text{HT}^2} \right)} \right]$

3.1

Model-based estimates of exposure and exploring exposure-response relationships

Model based estimates of the area under the concentration-time curve (AUC) were calculated for each individual included in the population PK model by integrating the area under the individual model-based predicted miltefosine concentrations over time until end of day 28 of treatment (AUC_{0-D28}) and infinity ($AUC_{0-\infty}$), both in plasma (AUC_{PL}) and intracellularly in PBMCs (AUC_{IC}). Of the 51 patients included, *Leishmania* strains were isolated for 37 patients, of which 89% corresponded to *L.V. panamensis*. Therefore, a previously reported typical *in vitro* IC_{50} of 10.6 µM (equivalent to 4.3 µg/mL) [14] for *L.V. panamensis* was used to calculate time>IC_{50} (total time the individual model-based predicted miltefosine concentration was above IC_{50}, in days) and the AUC>IC_{50} (integration of area under individual model-based predicted concentration above IC_{50}, in µg·day/mL), for both plasma and intracellular concentrations.

The exposure-response relationships based on model-based estimates were explored with a logistic regression analysis in R. The logistic regression analysis was performed on a binary outcome (0=failure, 1=cure) as described in Equation 4 for $AUC_{PL,0-D28}$ (in µg·day/mL) as an example exposure variable. λ_i is the log odds of cure for the ith individual, λ_b represents the baseline log odds of cure and θ_1 describes the drug effect on the log odds.

Equation 4: $\lambda_i = \lambda_b + \theta_1 \cdot (AUC_{PL,0\text{-}D28,i})$

Subsequently, λ_i was converted to probability of cure for the ith individual (p_i) with Equation 5.

Equation 5: $p_i = \dfrac{e^{\lambda_i}}{1 + e^{\lambda_i}}$

Additional independent covariates available (baseline lesion size, lesion duration before treatment, number of lesions, sex, ethnicity and age) were evaluated as additional predictor variable next to the exposure variable, as described in Equation 6 with θ_2 describing the effect of the covariate (COV) on the log odds of cure for the ith individual.

Equation 6: $\lambda_i = \lambda_b + \theta_1 \cdot (AUC_{PL,0\text{-}D28,i}) + \theta_2 \cdot (COV_i)$

Previously determined individual susceptibility data of the isolated strains [1] were also evaluated as a covariate in addition to drug effect as described in Equation 6. For 13/49 patients included in the exposure-response exploratory analysis, susceptibility data were unavailable and thus the median value was imputed.

Simulations of allometric dosing regimen

Drug exposure after allometric dosing [6] was compared to conventional linear 2.5 mg/kg/day dosing. PK curves were simulated (n=1,000) for patients with similar anthropometric characteristics as the subjects in the original data set. The allometric dose was based on

FFM as calculated with Equation 2 and 3 [13]. As an example, using these study participants' anthropometric characteristics, the allometric dose of subjects between 4 and 7 years old would lie between 2.8-3.2 mg/kg/day, as opposed to the standard 2.5 mg/kg dose. The linear 2.5 mg/kg/day dosing regimen and allometric dosing regimen were both rounded to the nearest 10 mg capsule, based on available formulations (10 or 50 mg).

RESULTS

Patient and sample inclusion in population PK model

Demographic characteristics of the 51 study participants included in the population PK analysis are described in Table 1. All intracellular miltefosine concentrations on day 90 and afterwards were excluded from PK analysis because for >80% of these samples miltefosine concentrations were below the lower limit of quantitation (<LLOQ). One plasma concentration was <LLOQ, and was therefore excluded. Two PBMC and two plasma samples were excluded due to the high absolute conditionally weighted residuals (CWRES>4). Finally, concentration data from 339 plasma and 194 PBMC samples were included in the population PK model.

Table 1. Demographics of patient population included in population PK model.

Parameter	Adults	Children	All
Total no. of patients	22	29	51
Female patients [no. (%)]	12 (54.5)	12 (41.4)	24 (47.1)
Ethnicity			
Afro-Colombian [no. (%)]	17 (77.3)	21 (72.4)	38 (74.5)
Mestizo [no. (%)]	5 (22.7)	8 (27.6)	13 (25.5)
Daily dose of miltefosine (mg/kg/day)	2.1 (1.4-2.8)	2.3 (2.0-2.5)	2.2 (1.4-2.8)
Age (yr)	34 (21-51)	8 (2-12)	19 (2-51)
Body weight (kg)	71.1 (50.4-102)	26.5 (12.6-45.9)	45.7 (12.6-102)
Height (cm)	165 (152-182)	126 (92-153)	143 (92-182)
Fat-free mass (kg)[a]	48.3 (33.7-70.9)	20.6 (10.5-30.1)	32.6 (10.5-70.9)
Patients with treatment failure [no. (%)]	0 (0)	5 (17.2)	5 (9.8)
Treatment centers			
Cali [no. (%)]	8 (36.4)	8 (27.6)	16 (31.4)
Tumaco [no. (%)]	14 (63.6)	21 (72.4)	35 (68.6)

All values are mean (range), unless indicated otherwise.
[a]As calculated in the final population PK model, with the maturation function

Population pharmacokinetics of plasma and intracellular miltefosine

Intracellular accumulation appeared not to be direct but delayed, since the median intracellular:plasma concentration ratio increased from 1.2 after 1 day of treatment, to 2.9 after 28 days of treatment. The variability in observed intracellular concentrations was larger compared to plasma: the relative standard deviation for day 28 intracellular concentrations was 91%, compared to 33% for plasma. This can partially be explained by higher variability in PBMC bioanalysis, but might also be indicative of larger variability in miltefosine uptake between patients.
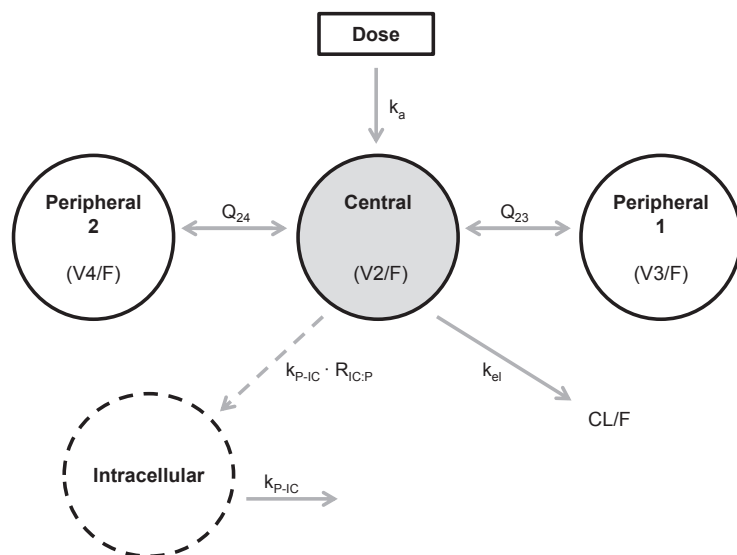
Figure 1. Schematic representation of structural population pharmacokinetic model of miltefosine in cutaneous leishmaniasis patients. V_2 represents the central volume of distribution. V_3 and V_4 represent the two peripheral compartments and Q_{23} and Q_{24} their respective intercompartmental clearances. k_a, absorption rate; F, bioavailability; CL, clearance; k_{el}, elimination rate constant; $k_{P:IC}$, intracellular distribution rate constant; $R_{IC:P}$, steady-state intracellular to plasma ratio.

A three-compartment model significantly improved the fit (ΔOFV -232) compared to the previously developed two-compartment model [6,7], as the latter over predicted concentrations on day 28 and 120. The model that described the intracellular data best, was found to be an intracellular accumulation within the central compartment without mass transfer to the intracellular compartment. This distribution was described by a steady-state intracellular to plasma ratio ($R_{IC:P}$) plus intracellular distribution rate constant between plasma and intracellular compartment (k_{P-IC}) (Figure 1, Equation 7, where A_{IC} represents the amount of drug in the intracellular compartment, A_C the amount of drug in the central compartment and V_c the volume of distribution of the central compartment).

Equation 7: $\quad \dfrac{dA_{IC}}{dt} = k_{P-IC} \cdot \left(\left(R_{IC:P} \cdot \dfrac{A_c}{V_c} \right) - A_{IC} \right)$

Final parameter estimates are presented in Table 2. The $R_{IC:P}$ was found to be 2.17 (95% CI: 1.98-2.39), indicating an approximately two-fold higher intracellular miltefosine concentration compared to plasma. The delayed distribution was described with the k_{P-IC} of 1.23 (95% CI: 0.94-1.58) day^{-1}. The mean of the individual estimates of $R_{IC:P}$ and k_{P-IC} were comparable between adults and children ($R_{IC:P}$ was 2.3 and 2.2; and k_{P-IC} was 1.2 and 1.3, respectively).

Allometric scaling of V_c and clearance by FFM significantly improved the fit compared to scaling by total body weight (ΔOFV -12). Inclusion of the maturation component in FFM calculation also improved the model significantly (ΔOFV -7.5). Other evaluated covariates did not improve the model significantly.

The VPC of the final population PK model showed good predictive performance of the model compared to the observations (Figure 2). Standard goodness-of-fit plots

Table 2. Parameter estimates of final population pharmacokinetic model.

Parameter	Unit	Population estimate (%RSE[b])	[95% CI][c]	BSV (%RSE[b])	[95% CI][c]	Shrinkage (%)
Absorption rate constant (k_a)	day^{-1}	9.6[d]	-	N.E.		
Clearance (CL/F)[a]	L/day	4.62 (2.8)	4.38-4.88	15.2 (11.4)	11.7-18.5	2.1
Volume of central compartment (V_2/F)[a]	L	28.5 (3.3)	26.7-30.3	11.0 (19.4)	6.1-14.7	32.5
Intercompartmental clearance central volume – peripheral compartment 1 (Q_{24}/F)	L/day	0.42 (17.8)	0.29-0.59	N.E.		
Volume peripheral compartment 1 (V_4/F)	L	3.85 (12.9)	2.97-4.93	N.E.		
Intercompartmental clearance central volume – peripheral compartment 2 (Q_{25}/F)	L/day	0.0274 (6.4)	0.0241-0.0311	N.E.		
Volume peripheral compartment 2 (V_5/F)	L	2.02 (4.9)	1.85-2.23	N.E.		
Intracellular distribution rate constant (k_{P-IC})	day^{-1}	1.23(13.5)	0.94-1.58	45.0 (31.6)	1.7-65.3	27.3
Steady-state intracellular to plasma ratio ($R_{IC:P}$)	-	2.17 (4.9)	1.98-2.39	28.6 (15.1)	19.8-36.6	11.2
Proportional residual error plasma	%	16.3 (6.3)	14.4-18.4			9.8
Proportional residual error intracellular	%	29.3 (6.2)	25.8-32.9			17.7

BSV=between-subject-variability. N.E. = not estimated.
[a]Estimates are provided for patient with a fat-free mass of 53 kg
[b]RSE% was calculated as the standard error
[c]95% confidence intervals were calculated by the percentile method from bootstrap (n=1,000)
[d]Due to absence of sampling in absorption phase, fixed to previously established value of 9.6
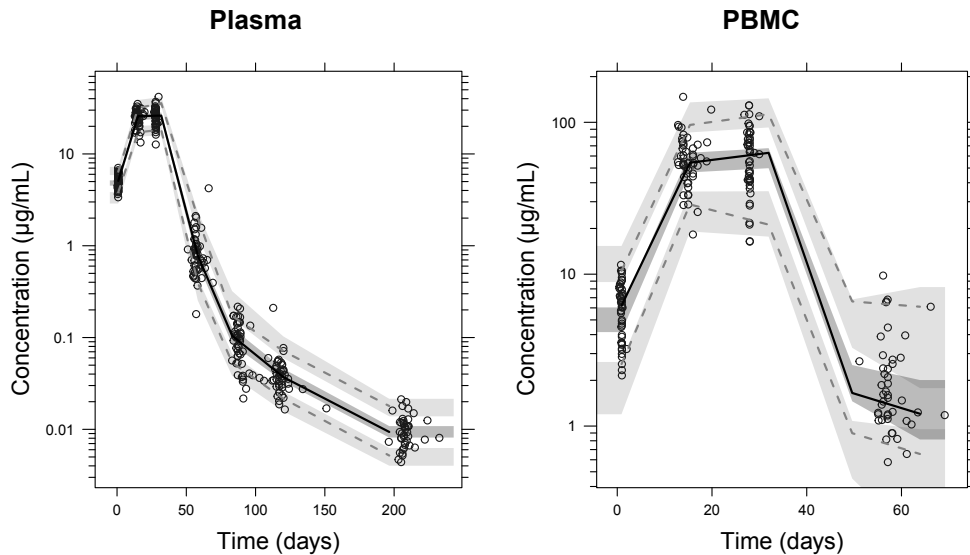

Figure 2. Visual predictive check of the final population pharmacokinetic model for plasma miltefosine concentrations (left) and miltefosine concentrations intracellular in peripheral blood mononuclear cells (right). Open circles represent individual observations and solid/dashed lines show the median and 5th/95th percentile of the observed data. Dark/light-grey shading indicate 95% confidence intervals of predicted data median and 5th/95th percentile.

(Supplementary Figure 1 and 2) indicated no obvious deviations, except for a slight over prediction of the highest plasma concentrations after inclusion of intracellular data in the final PK model.

Using the final population parameter estimates, the plasma elimination half-lives were calculated to be 3.5 days, 7.6 days and a terminal elimination half-life of 51 days. Secondary PK parameters related to exposure were calculated from individual exposure estimates of the 51 patients in the final model and are described in Table 3. Plasma and intracellular exposure variables were significantly higher for adults compared to children.

Table 3. Secondary pharmacokinetic parameters calculated from individual exposure estimates of 51 patients included in the final population pharmacokinetic model.

Exposure parameter	Adults (mean±SD)	Children (mean±SD)	p-value
$C_{max,PL}$ (μg/mL)	34.1±6.8	22.5±3.8	4.16e-08[a],**
$C_{max,IC}$ (μg/mL)	79.9±22.2	47.8±17.3	1.56e-07[b],**
$AUC_{PL,0-D28}$ (μg·day/mL)	789±102	545±64	2.11e-11[a],**
$AUC_{IC,0-D28}$ (μg·day/mL)	1,707±374	1,169±379	4.82e-06[b],**
$AUC_{PL,0-\infty}$ (μg·day/mL)	1,056±164	688±94	1.21e-10[a],**
$AUC_{IC,0-\infty}$ (μg·day/mL)	2,405±635	1,533±517	4.10e-07[b],**
$AUC{>}IC_{50,PL,0-\infty}$ (μg·day/mL)	822±146	481±85	4.75e-11[a],**
$AUC{>}IC_{50,IC,0-\infty}$ (μg·day/mL)	2,126±608	1,282±496	4.68e-07[b],**
$Time{>}IC_{50,PL,0-\infty}$ (day)	43±4	37±2	5.07e-08[b],**
$Time{>}IC_{50,IC,0-\infty}$ (day)	52±6	44±4	6.35e-06[c],**

C_{max} = miltefosine concentration on the last treatment day, AUC=area under the concentration-time curve, PL=plasma, IC=intracellular, IC_{50}=half maximal inhibitory concentration. **p<0.001
[a]Welch two-sample t-test
[b]Wilcoxon rank sum test
[c]Two-sample t-test

Exploration of exposure-response relationship

Of the 49 patients included in the exposure-response analysis, five pediatric patients presented with treatment failure. Exploration of the contribution of individual exposure variables to treatment outcome, indicated a significant influence of all exposure values on probability of cure (Table 4). As an example, each 10 μg·day/mL increase in $AUC_{PL,0-D28}$ resulted in an increased odds ratio for cure of 1.64 (95%CI 1.18-3.09, λ_B = -23.6). Probability of failure (calculated with Equation 4 and 5) increased from 0.06% to 22.6% for a decrease in $AUC_{PL,0-D28}$ from the median value of 623 μg·day/mL to 500 μg·day/mL. Based on this analysis, the $AUC_{PL,0-D28}$ should exceed 535 μg·day/mL to reach a >95% probability of cure. The $AUC_{PL,0-D28}$ of all adults in our analysis exceeded this potential PK target, but 12/28 children (43%) did not attain this value. Probability of clinical cure as a function of the $AUC_{PL,0-D28}$ is depicted in Figure 3. The wide confidence intervals reflect the small number of patients that failed treatment.

Drug susceptibility of the clinical isolate, baseline lesion size, number of lesions, time of lesion duration prior to treatment, age and gender were not significantly associated with log odds of cure in addition to miltefosine exposure.

Table 4. Logistic regression analysis of exposure variables affecting the probability of clinical cure after miltefosine monotherapy in cutaneous leishmaniasis patients.

Exposure variable	Odds ratio	95%CI	Likelihood ratio significance
$C_{max,PL}$ (per µg/mL)	1.46	1.12 – 2.18	p<0.01
$C_{max,IC}$ (per µg/mL)	1.06	1.00 – 1.14	p<0.05
$AUC_{PL,0-D28}$ (per 10 µg·day/mL)	1.64	1.18 – 3.09	p<0.001
$AUC_{IC,0-D28}$ (per 10 µg·day/mL)	1.04	1.01 – 1.09	p<0.05
$AUC_{PL,0-\infty}$ (per 10 µg·day/mL)	1.32	1.09 – 1.93	p<0.001
$AUC_{IC,0-\infty}$ (per 10 µg·day/mL)	1.03	1.01 – 1.08	p<0.01
$AUC{>}IC_{50,PL,0-\infty}$ (per 10 µg·day/mL)	1.46	1.13 – 2.36	p<0.001
$AUC{>}IC_{50,IC,0-\infty}$ (per 10 µg·day/mL)	1.04	1.01 – 1.08	p<0.01
$Time{>}IC_{50,PL,0-\infty}$ (per day)	2.05	1.23 – 4.91	p<0.01
$Time{>}IC_{50,IC,0-\infty}$ (per day)	1.26	1.01 – 1.70	p<0.05

AUC=area under the concentration-time curve, PL=plasma, IC=intracellular, IC_{50}=half maximal inhibitory concentration.
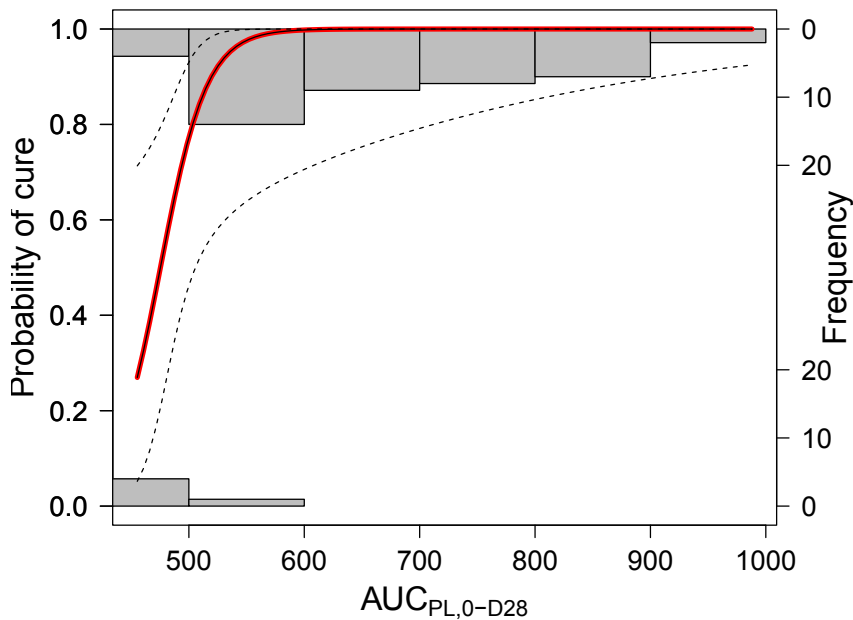
Figure 3. Probability of clinical cure by miltefosine monotherapy as a function of the plasma area under the concentration-time curve up to the end of treatment ($AUC_{PL,0-D28}$). The solid line represents the predicted probability of cure for the patients in this trial with the logistic model, and the dotted lines indicate the 95% confidence interval. The histograms represent the observations and are indicating the number of patients (frequency) in the corresponding $AUC_{PL,0-D28}$ intervals that either cure (top of graph) or fail (bottom of graph) after miltefosine monotherapy.

Simulation of allometric dosing

$AUC_{PL,0-D28}$ values following simulations of the linear and allometric dosing regimens are provided in Table 5. Allometric dosing of miltefosine resulted in similar exposure levels between children and adults in this patient cohort. Simulating allometric dosing, the fraction of children not attaining the proposed $AUC_{PL,0-D28}$ threshold of 535 µg·day/mL corresponding to a >95% probability of cure, was only 1.8%, compared to 18.3% after simulating a linear 2.5 mg/kg dose.

Table 5. Comparison of miltefosine exposure levels following simulation of different dosing regimens.

Dosing regimen	Age category	$AUC_{PL,0-D28}$ (mean (95%CI)	% under the 95% probability of cure exposure treshold[a]
Linear dosing	Child (≤12y)	629 (437-858)	18.3%
	Adults (≥18y)	751 (529-1,013)	2.8%
Allometric dosing	Child (≤12y)	708 (545-903)	1.8%
	Adults (≥18y)	693 (521-883)	3.5%

Exposure to miltefosine as AUC (area under the concentration curve) in plasma (PL) from zero to day 28 ($AUC_{PL,0-D28}$) simulated for Colombian cutaneous leishmaniasis patients with the final population PK model after linear and allometric dosing, for both adults and children.
[a]535 µg·day/mL $AUC_{PL,0-D28}$

DISCUSSION

We report a population PK model characterizing the pharmacokinetics of miltefosine in plasma and PBMCs and describe the population pharmacokinetics of miltefosine in adults and children with cutaneous leishmaniasis.

The observed plasma and intracellular miltefosine concentrations were well described and predicted by the final model. The V_c was smaller than previously documented (28.5 L versus 38.5-40.1 L), due to the inclusion of a second peripheral compartment [5–7]. The two peripheral compartments were required to accurately describe the observed multi-phasic elimination phase. Tri-phasic elimination has never been observed previously for miltefosine [5], but was most probably an artefact of denser sampling in the first three months after treatment in the current study.

Implementation of the intracellular distribution rate constant (k_{P-IC}) was required to characterize the delay in intracellular accumulation of miltefosine. In Caco-2 cells, only 6.8% of miltefosine was transported across cells after a 3 h incubation, while 57% accumulated in the membranes, from which intracellular release was slow (5% in 24 h) [3]. Inward translocation of miltefosine within the cellular membrane was found *in vitro* to be partially dependent on active saturable transport [3,4]. These sequential processes could hypothetically explain the delay in intracellular miltefosine accumulation, potentially leading to variability in intracellular accumulation between patients.

Compared to the previously reported model-based $AUC_{PL,0-D28}$ estimate of approximately 500 µg·day/mL for Indian pediatric visceral leishmaniasis patients [6], the $AUC_{PL,0-D28}$ estimate for pediatric patients in this study was 9% higher (545 µg·day/mL). Large differences between these two patient populations in miltefosine PK characteristics such as metabolism and distribution are therefore not expected, though these could theoretically have been anticipated because of differences in clinical presentation (amongst others:

altered liver physiology, low albumin levels and malnutrition in visceral but not cutaneous leishmaniasis).

Although the clinical trial from which the current data originated was not powered to evaluate efficacy, our results might provide a potential miltefosine exposure target in the treatment of cutaneous leishmaniasis. In contrast to a previous multivariate analysis using NCA PK estimates [1], population PK model-based estimates of plasma and intracellular miltefosine exposure were significantly associated with probability of cure, of which $AUC_{PL,0-D28}$ was further evaluated. Differences in results between these methodologies could be caused by the sparse sampling scheme of the trial, implemented to decrease invasiveness for the pediatric study participants. The NCA PK estimates from the previous analysis were therefore substantially underestimating the $AUC_{PL,0-D28}$ (e.g. for children 456±100 µg·day/mL compared to the 545±64 µg·day/mL model based estimate).

In this study, both plasma and intracellular miltefosine exposure were significantly related to probability of cure, which would be expected given their high correlation. In future clinical studies, intracellular exposure could potentially be predicted from plasma PK using the here developed population PK model. It might be valuable to relate intracellular PK to individual IC_{50} (or IC_{90}) values from clinical parasite isolates to calculate individual time>IC_{50} and AUC>IC_{50} exposure variables. Exploration of these intracellular PK-PD variables could aid in understanding the contribution of *Leishmania* drug susceptibility to individual therapeutic outcome.

As IC_{50} values were not available for the study participants, the *in vitro* IC_{50} for *L.V. panamensis* (4.3 µg/mL) was used [14]. Miltefosine susceptibility of the isolated strains from study participants varied widely, with individual miltefosine susceptibility scores (% reduction in parasite load after *in vitro* exposure to 16 µM miltefosine) between 12 and 98% [1]. Using the median IC_{50} to calculate time>IC_{50} and AUC>IC_{50} could therefore be arguable. We performed a sensitivity analysis of the exposure-response analysis with IC_{50} values up to 10 µg/mL (25 µM). This miltefosine concentration was achieved in all study participants and no profound differences in significance of the exposure-response relationship were found [data not shown]. Furthermore, we aimed to capture the variability in susceptibility of strains by including the individual miltefosine susceptibility scores (% reduction in parasite load after *in vitro* exposure to 16 µM miltefosine [15]) as a covariate effect on probability of cure in addition to drug exposure. No additional effect on probability of cure was identified, possibly due to the small sample size and missing susceptibility data for two out of the five patients who failed treatment.

Lastly, model-based simulations showed that an allometric dose regimen would result in a higher probability of reaching the proposed $AUC_{PL,0-D28}$ threshold of 535 µg·day/mL for children. The safety of this allometric regimen is currently being evaluated in East Africa (NCT02431143) and Bangladesh (NCT02193022). Differences in simulated (82%, Table 4) versus observed target attainment (57%) in children after conventional dosing could be explained by the lower administered daily dose of 2.3 mg/kg (Table 1, range 2.0-2.5 mg/kg) compared to simulated 2.5 mg/kg [1]. Furthermore, the 90-100% range adherence to treatment for patients in this study [1] could also have contributed to lower target attainment compared to the full 100% compliance simulated.

3.1

CONCLUSION

We developed a population PK model, which in addition to plasma miltefosine pharmacokinetics also describes the intracellular kinetics in PBMCs, characterizing miltefosine exposure in a compartment that can be regarded a closer approximation of miltefosine's *in vivo* target site of action. In the future, the model can be used for the prediction of individual intracellular concentration data, which can subsequently be related to individual *Leishmania* drug susceptibility to identify the impact of susceptibility and exposure on therapeutic outcome. In the here presented exploratory exposure-response analysis, both plasma and intracellular miltefosine exposure parameters were significantly associated with probability of cure. A 535 µg/mL $AUC_{PL,0-D28}$ threshold could be proposed from our analysis as a potential PK target, but its validity should be evaluated in a larger cohort of patients.

## ACKNOWLEDGEMENTS

FUNDING

TRANSPARENCY DECLARATIONS

Authors declare no conflict of interest.

REFERENCES

1. Castro MM, Gomez MA, Kip AE, Cossio A, Ortiz E, Navas A, et al. Pharmacokinetics of miltefosine in children and adults with cutaneous leishmaniasis. Antimicrob Agents Chemother. 2017; 61(3): e02198-16.

2. Dorlo TPC, Balasegaram M, Beijnen JH, de Vries PJ. Miltefosine: a review of its pharmacology and therapeutic efficacy in the treatment of leishmaniasis. J. Antimicrob. Chemother. 2012;67:2576–97.

3. Ménez C, Buyse M, Dugave C, Farinotti R, Barratt G. Intestinal absorption of miltefosine: contribution of passive paracellular transport. Pharm. Res. 2007;24:546–54.

4. Ménez C, Buyse M, Farinotti R, Barratt G. Inward translocation of the phospholipid analogue miltefosine across Caco-2 cell membranes exhibits characteristics of a carrier-mediated process. Lipids. 2007;42:229–40.

5. Dorlo TPC, van Thiel PPAM, Huitema ADR, Keizer RJ, de Vries HJC, Beijnen JH, et al. Pharmacokinetics of miltefosine in Old World cutaneous leishmaniasis patients. Antimicrob. Agents Chemother. 2008;52:2855–60.

6. Dorlo TPC, Huitema ADR, Beijnen JH, De Vries PJ. Optimal dosing of miltefosine in children and adults with visceral leishmaniasis. Antimicrob. Agents Chemother. 2012;56:3864–72.

7. Dorlo TPC, Rijal S, Ostyn B, de Vries PJ, Singh R, Bhattarai N, et al. Failure of miltefosine in visceral leishmaniasis is associated with low drug exposure. J. Infect. Dis. 2014;210:146–53.

8. Charles B. Population pharmacokinetics: an overview. Aust Prescr. 2014;37:210–3.

9. Kip AE, Rosing H, Hillebrand MJX, Castro MM, Gomez MA, Schellens JHM, et al. Quantification of miltefosine in peripheral blood mononuclear cells by high-performance liquid chromatography-tandem mass spectrometry. J. Chromatogr. B. Analyt. Technol. Biomed. Life Sci. 2015;998-999:57–62.

10. Dorlo TPC, Hillebrand MJX, Rosing H, Eggelte TA, de Vries PJ, Beijnen JH. Development and validation of a quantitative assay for the measurement of miltefosine in human plasma by liquid chromatography-tandem mass spectrometry. J. Chromatogr. B. Analyt. Technol. Biomed. Life Sci. 2008;865:55–62.

11. Simiele M, D'Avolio A, Baietto L, Siccardi M, Sciandra M, Agati S, et al. Evaluation of the mean corpuscular volume of peripheral blood mononuclear cells of HIV patients by a coulter counter to determine intracellular drug concentrations. Antimicrob. Agents Chemother. 2011;55:2976–8.

12. Janmahasatian S, Duffull SB, Ash S, Ward LC, Byrne NM, Green B. Quantification of lean bodyweight. Clin. Pharmacokinet. 2005;44:1051–65.

13. Al-Sallami HS, Goulding A, Grant A, Taylor R, Holford N, Duffull SB. Prediction of Fat-Free Mass in children. Clin. Pharmacokinet. 2015;54:1169–78.

14. Escobar P, Matu S, Marques C, Croft SL. Sensitivities of *Leishmania* species to hexadecylphosphocholine (miltefosine), ET-18-OCH3 (edelfosine) and amphotericin B. Acta Trop. 2002;81:151–7.

15. Fernandez O, Diaz-Toro Y, Valderrama L, Ovalle C, Valderrama M, Castillo H, et al. Novel approach to *in vitro* drug susceptibility assessment of clinical strains of *Leishmania* spp. J. Clin. Microbiol. United States; 2012;50:2207–11.

3.1
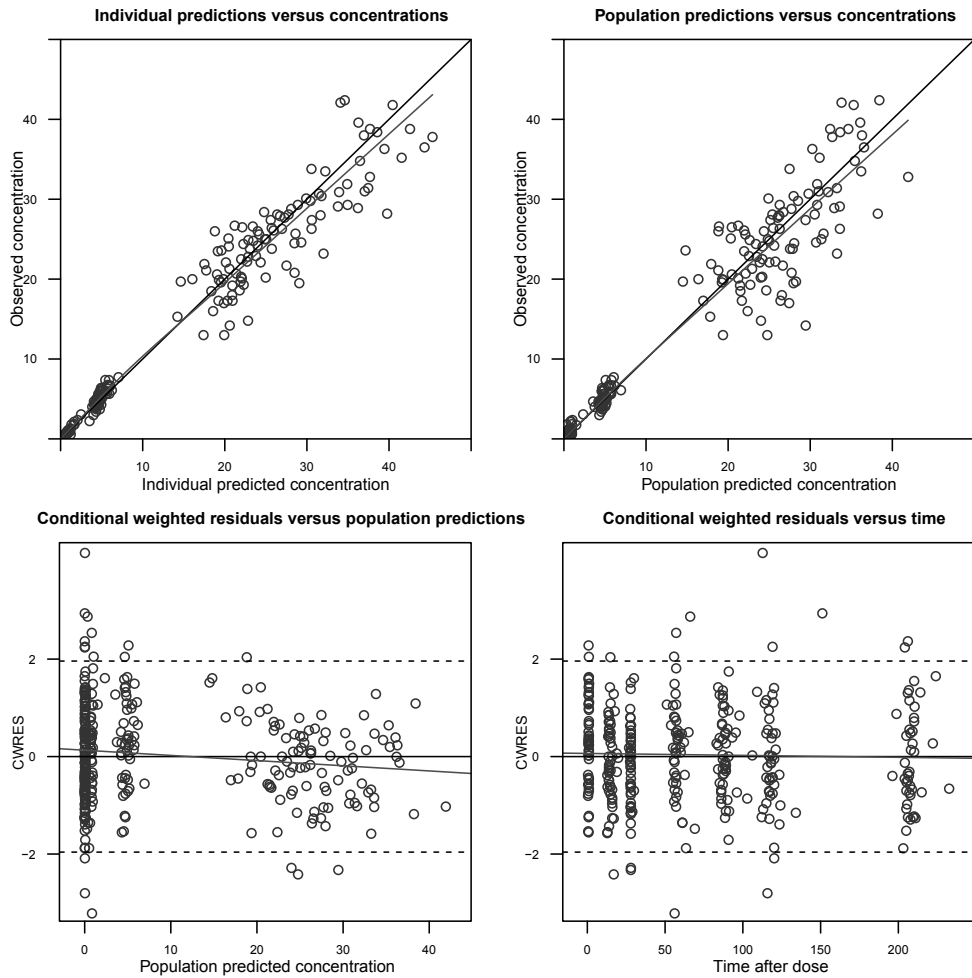
Supplementary figure 1. Basic goodness of fit plot for <u>plasma</u> miltefosine concentrations. Observed concentrations versus population predicted concentrations, observed concentrations versus individual predicted concentrations, conditional weighted residuals versus population predicted concentrations and conditional weighted residuals versus time. The solid black line represents the line of identity or unity and the grey line is the locally weighted least square regression line to indicate trends. CWRES: conditionally weighted residuals.
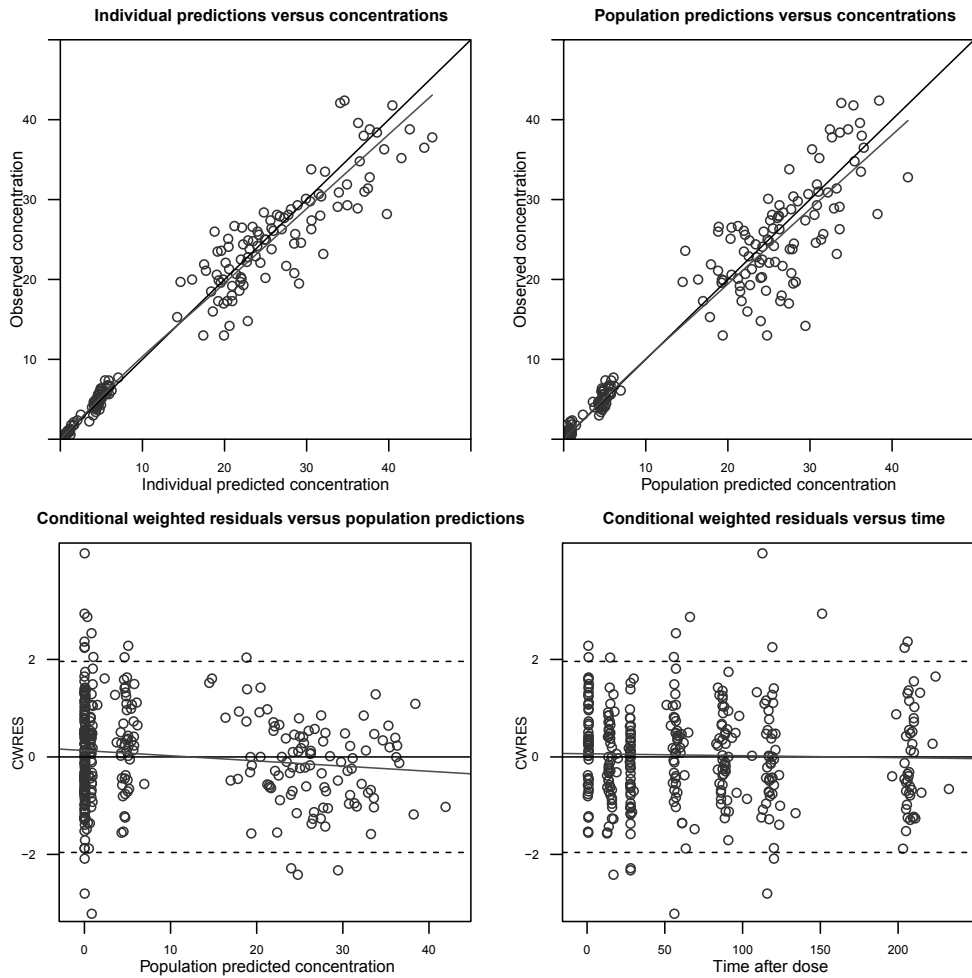
Supplementary figure 2. Basic goodness of fit plot for <u>intracellular</u> miltefosine concentrations. Observed concentrations versus population predicted concentrations, observed concentrations versus individual predicted concentrations, conditional weighted residuals versus population predicted concentrations and conditional weighted residuals versus time. The solid black line represents the line of identity or unity and the grey line is the locally weighted least square regression line to indicate trends. CWRES: conditionally weighted residuals.

3.1

Chapter 3.2

Miltefosine exposure after a novel allometric dosing regimen in paediatric visceral leishmaniasis patients in Kenya and Uganda

A.E. Kip
L. Were
A. Solomos
F. Alves
R. Kimutai
J.H.M. Schellens
J.H. Beijnen
M. Wasunna
R. Juma
J. Mbui
J. Olobo
T.P.C. Dorlo

Interim analysis

ABSTRACT

Conventional 2.5 mg/kg daily dosing of the oral drug miltefosine has demonstrated lower efficacy in paediatric compared to adult visceral leishmaniasis (VL) patients, most probably due to significantly lower drug exposure in children. To assess whether drug exposure in children could be increased, an open-label clinical trial was conducted in Kenya and Uganda evaluating the pharmacokinetics (PK) of allometric miltefosine dosing.

Thirty paediatric VL patients between 4 and 12 years old received a miltefosine dose between 2.7 and 3.9 mg/kg daily for 28 days, depending on their estimated fat-free mass. Miltefosine plasma concentrations were analyzed by liquid chromatography-tandem mass spectrometry. A population PK model was developed using non-linear mixed effects modelling. Observed miltefosine exposure after allometric dosing was compared to historic observations after conventional 2.5 mg/kg daily dosing in paediatric patients and simulations based on these data.

More rapid accumulation was observed after allometric dosing compared to observations after conventional dosing in paediatric patients (C_{day7} 5.88 versus 2.67 μg/mL, p=0.07, Mann Whitney U-test). End of treatment concentrations, however, were comparable between the two dosing regimens (20.9 versus 19.5 μg/mL), most probably due to a plateau in miltefosine accumulation in the third treatment week of allometric dosing, observed in 37% of patients. Miltefosine PK was best described by a two-compartmental model with a 62% decreased relative bioavailability at start of treatment. Variability (CV%) in end of treatment concentrations was lower after allometric (16.3%) compared to conventional dosing (35.5%), resulting in a four-fold decrease in the proportion of patients failing to attain the 17.9 μg/mL threshold previously associated with probability of cure (7% versus 29%).

Higher target attainment in combination with a 12% higher area under the concentration-time curve ($AUC_{0-\infty}$) might have contributed to the observed higher efficacy of allometric compared to conventional dosing. For future dose optimization, the initial decrease in relative bioavailability and the observed plateau in miltefosine accumulation in a subset of patients should be investigated, as these PK non-linearities negatively affect miltefosine exposure.

INTRODUCTION

Visceral leishmaniasis (VL) is a devastating tropical disease, especially affecting the paediatric population: more than half of the global burden of VL is amongst children under the age of 15 [1,2]. Several studies have shown a lower efficacy of miltefosine in the treatment of paediatric VL patients. In a phase IV trial in India and Nepal, 6.4% of children versus 3.4% of adults showed therapeutic failure when treated with a standard mg/kg miltefosine treatment [3]. Children under the age of 12 had a significantly higher risk of relapse in Nepal, with an incidence risk ratio of 2.43 [4]. Similarly, in India and Nepal, relapses were two to three times more common in VL patients under the age of 15, compared to patients over 25 years old [5]. The disparity between adult and paediatric cure rates was even more profound in East Africa: in Kenya and Sudan the VL cure rate of miltefosine monotherapy was only 59% (95% confidence interval, CI: 36% - 79%) in children under the age of 12, compared to 86% (95% CI: 68% - 96%) in patients of 12 years or older [6].

Miltefosine exposure has been shown to be significantly associated with treatment outcome in VL [7,8]. In Nepal, the length of time the miltefosine plasma concentration was above 10 times the half maximal effective concentration of miltefosine ($10xEC_{50}$) was significantly associated with treatment success [7]. In East Africa, the length of time above EC_{90} was found to affect the time to relapse of disease [8].

Conventionally, children and adults are treated with the same linear 2.5 mg/kg daily dose. After administration of this conventional mg/kg dose, children were found to be under exposed compared to adults [7,9,10]. A recent study confirmed significant underexposure in children in an East African VL patient population, with a 33% lower area under the concentration-time curve (AUC) compared to adults after receiving the conventional dosing regimen [6,8]. A previously developed population PK model, based on conventional dosing data, showed that fat-free mass (FFM) was a significant covariate allometrically scaled on clearance (CL) and volume of distribution (V) [9]. Simulations with an allometric dosing schedule, administering a relatively higher mg/kg dose to patients with lower FFM, predicted that children would reach adult exposure levels [9].

An open-label clinical trial has been conducted to evaluate the pharmacokinetics (PK), as well as the safety, of the proposed allometric miltefosine dosing regimen for the treatment of paediatric VL patients in Uganda and Kenya. This report contains the population PK analysis of the PK data collected in this clinical trial, with the specific aim of characterizing and describing the observed PK and to compare it to results from the conventional dosing study [6,8]. Finally, we aimed to assess possible explanations for the differences observed and explore the link to treatment outcomes.

METHODS

Study population
Thirty paediatric VL patients aged 4 to 12 years were included in this clinical trial at two clinical sites in areas endemic for VL: Kacheliba in Kenya and Amudat in Uganda. Ethical approval was obtained from national and local ethics committees in Kenya (Kenya Medical Research Institute, Nairobi) and Uganda (Makerere University, Kampala) prior to the start of the trial. Parents/guardians of the patients were informed of the study in their own language and provided written informed consent before any enrolment procedures were initiated. The

3.2

study was registered with ClinicalTrials.gov with the identifier NCT02431143.

Patients received a daily allometric miltefosine dose of between 2.7-3.9 mg/kg for 28 days. The dosing schedule is displayed in Table 1 and is based on FFM estimation based on weight and height, as described previously [11]. FFM was calculated as described in Equation 1, where HT is height (in meters), WT is weight (in kg), WHS_{max} is 42.92 or 37.99 kg/m^2 and WHS_{50} is 30.93 or 35.98 kg/m^2 for males and females, respectively [11].

Equation 1: $$FFM = WHS_{max} \cdot HT^2 \cdot \left(\frac{WT}{WHS_{50} \cdot HT^2 + WT} \right)$$

The allometric dose is subsequently calculated as described in Equation 2, with the estimated FFM of the individual (FFM_i), based on the standard dose ($Dose_{std}$) of 150 mg and the standard fat-free mass (FFM_{std}) of 53 kg. An allometric power component (PWR) of 0.75 is used. The allometric dose was rounded to the nearest 10 mg capsule, as smaller quantities are not available.

Equation 2: $$Dose_{allometric} = Dose_{std} \cdot \left(\frac{FFM_i}{FFM_{std}} \right)^{PWR}$$

Patients were hospitalized in the health centres for the entire treatment and miltefosine intake was monitored. Patients returned to the clinical sites for follow-up at one and six months after the end of treatment. The clinical outcomes of this study will be reported elsewhere.

Sample collection and analysis
Plasma samples were collected pre-treatment, 8 hours after the first dose, pre-dose on days 7, 14, 21 and 28 of treatment and during the follow-up visits at one and six months after treatment. Samples were stored at -20°C and transported, frozen, to the bioanalytical laboratory in Amsterdam, where they were stored at -20°C until further analysis. The samples were analysed for their miltefosine concentration using liquid chromatography coupled to tandem mass spectrometry (LC-MS/MS), as validated previously, with a lower limit of quantitation (LLOQ) of 4 ng/mL [12].

Observed miltefosine exposure after allometric dosing versus conventional dosing
PK data from the paediatric population (age ≤12 years old) from the aforementioned conventional dosing study in East Africa [6,8] were used to compare exposure in conventional and allometric miltefosine dosing regimens.

Comparing observed with predicted miltefosine exposure after allometric dosing
The observed PK profiles in this clinical trial after administration of the allometric miltefosine dose, were compared to simulations using a population PK model previously developed based on data from both adult and paediatric East African VL patients receiving the conventional 2.5 mg/kg linear dose [6,8]. The parameter estimates of this population PK model were fixed while a visual predictive check (VPC) was run with NONMEM using dosing and covariate records from the paediatric patients of the allometric dosing clinical trial described here. The VPC (n=1,000) was visualized in R (version 3.1.2) with the "xpose4" R-package (version 4.5.3).

Table 1. Daily allometric miltefosine dose (mg) for males (left) and females (right) based on fat-free mass.

HT (cm) → / ↓WT (kg)	Male									Female								
	80-89	90-99	100-109	110-119	120-129	130-139	140-149	150-159	160	80-89	90-99	100-109	110-119	120-129	130-139	140-149	150-159	160
7																		
8	40									30								
9	40									30								
10	40	40								30	40							
11	40	40								40	40	40						
12	40	50								40	40	40						
13	50	50	50							40	40	40						
14	50	50	50							40	40	40	50					
15	50	50	60							40	40	50	50					
16	50	50	60	60						40	50	50	50					
17	50	60	60	60						40	50	50	50	50				
18	50	60	60	60	70					50	50	50	50	60				
19	50	60	60	70	70					50	50	50	60	60				
20	50	60	60	70	70					50	50	50	60	60	60			
21	60	60	60	70	70	70				50	50	60	60	60	60			
22	60	60	70	70	80	80				50	50	60	60	60	60			
23	60	60	70	70	80	80				50	50	60	60	60	70	70		
24	60	60	70	70	80	80	80			50	50	60	60	60	70	70		
25	60	60	70	80	80	80	80			50	60	60	60	70	70	70		
26	60	70	70	80	80	80	100			50	60	60	60	70	70	70	70	
27	60	70	70	80	80	80	100			50	60	60	70	70	70	70	80	
28	60	70	70	80	80	100	100	100		50	60	60	70	70	70	80	80	
29	60	70	70	80	80	100	100	100		50	60	60	70	70	70	80	80	
30	60	70	80	80	100	100	100	100		50	60	60	70	70	80	80	80	80

Row headers indicate the patients' weight (kg) and column headers indicate the patients' height (cm). Areas indicated in grey shading indicate patients that are at risk of severe malnutrition and these patients were not included in the trial.

3.2

Population PK model development

Plasma PK data were analysed in a population approach using non-linear mixed effects modelling in NONMEM with first-order conditional estimation with interaction. The starting point was a structural two-compartmental model with first-order absorption and elimination to and from the central compartment as previously described for miltefosine [7–9,13]. As the bioavailability of miltefosine is unknown, all disposition parameters are expressed relative to bioavailability (e.g. CL/F, V/F). Both weight and FFM were evaluated as body size descriptors, scaled linearly and allometrically to the power 0.75 and 1 for CL and V respectively, as previously described [9]. FFM was calculated as described previously in Equation 1 [11].

Between-subject variability (BSV) was evaluated for all PK parameters and inclusion was evaluated based on a drop in objective function value (OFV), clinical relevance and a drop in residual error. BSV was described with an exponential model. The residual error was described by a proportional error model, and inclusion of an additive error did not further improve the fit.

Individual miltefosine exposure estimates were calculated by integrating the AUC of the model-predicted individual concentration-time curves, from day 0 to end of treatment (AUC_{0-EOT}) and from day 0 to day 365 ($AUC_{0-\infty}$).

Model evaluation

Model evaluation was performed in multiple ways. For hierarchical models, model development was driven by the drop in OFV, in which a significant decrease in OFV (dOFV) was defined as -3.84 for $p<0.05$ and -6.63 for $p<0.01$, for one degree of freedom (χ^2 distribution). Basic goodness-of-fit plots were evaluated to assess the model fit as a population and for each individual separately. A visual predictive check (1,000 simulated replicates) was performed to assess the predictive performance of the final model. Model robustness was evaluated using a bootstrap (1,000 samples).

Statistics

Data are represented as mean ± SD, unless indicated otherwise. All statistical tests were performed in R (version 3.1.2) with a Mann-Whitney U-test, unless indicated otherwise.

Software

Model estimation, evaluation and simulation was performed in NONMEM (version 7.3, ICON Development Solutions, Ellicott City, MD, USA) with Pearl speaks NONMEM (PsN, version 4.2.0). Pre-processing of data was performed in R (version 3.1.2), as was graphical representation with the R package 'ggplot2'. Visual predictive checks were plotted with the R package 'Xpose' (version 4.5.3). Piraña (version 2.8.1) was used as an interface between NONMEM, PsN and R.

RESULTS

Demographics

The demographics of the patient population in this trial are described in Table 2. The patients were between 4 and 12 years old and were all below 30 kg. The median daily allometric miltefosine dose received was 3.2 mg/kg (range 2.7 to 3.9 mg/kg), and no doses were missed. One patient experienced treatment failure at day 25 of treatment and received rescue

Table 2. Demographics and treatment information for the study population.

Parameter	
Total no. of patients	30
Female patients [no. (%)]	8 (26.7)
Daily dose of miltefosine (mg/kg/day)	3.2 (2.7-3.9)
Patients with unfinished regimen [no. (%)][a]	1 (3.3)
Age (yr)	7 (4-12)
Body weight (kg)	21.8 (13.0-29.5)
Height (cm)	125 (99.0-145)
Fat-free mass (kg)[b]	18.2 (10.8-24.3)
Patients with initial failure [no. (%)]	1 (3.3)
Patients with relapse [no. (%)]	2 (6.7)
Treatment centers	
Kacheliba, Kenya [no. (%)]	21 (70.0)
Amudat, Uganda [no. (%)]	9 (30.0)

All values are given as median (range), unless stated otherwise.
[a]One patient received rescue treatment at day 25 and therefore did not finish the regimen.
[b]Calculated as previously described [11].

medication. Two patients relapsed during the follow-up period, on day 168 and day 206 after start of treatment.

Observed miltefosine concentration-time profiles after allometric dosing
Excluding pre-treatment samples, which were all below the LLOQ, a total of 206 samples were collected from 30 patients. Three samples were excluded from data interpretation, as the analyzed miltefosine concentration indicated a steep (>70%) decrease during treatment, which is physiologically improbable due to the accumulation of miltefosine during treatment and its long terminal half-life [14]. Observed miltefosine plasma concentration-versus-time profiles after allometric dosing are depicted in Figure 1, split per treatment center. It was observed that levels of miltefosine in both patients experiencing treatment failure in the Amudat treatment center were below that of patients that were cured.

Day 28 miltefosine concentrations, available for 27 patients, were slightly, but significantly, lower in the Amudat treatment center (Amudat 19.1±1.31 vs Kacheliba 22.4±3.50 µg/mL, p=0.01816). There were no significant differences in end of treatment concentrations between gender or age categories (4-6 years old versus 7-12 years old). Unexpectedly, for 37% of patients, the miltefosine concentration plateaued or even decreased between day 14 and day 21 (change in concentration between -19% and 10%), after which concentrations increased >18% (range 18-58%) towards day 28. Representative concentration-time curves of a patient with decreasing (patient 1) and with plateauing (patient 2) miltefosine concentrations in the third week of treatment are depicted in Figure 2. Patients 3 and 4 in the same figure show a concentration-time profile in line with previously reported miltefosine concentration-time profiles [8,13].

Out of 203 observations, only two were <LLOQ (4 ng/mL). Both were incorporated into the subsequent population PK analysis, one with a concentration of 2.8 ng/mL (above detection limit) and one (below detection limit) with a concentration of LLOQ/2 (2 ng/mL).
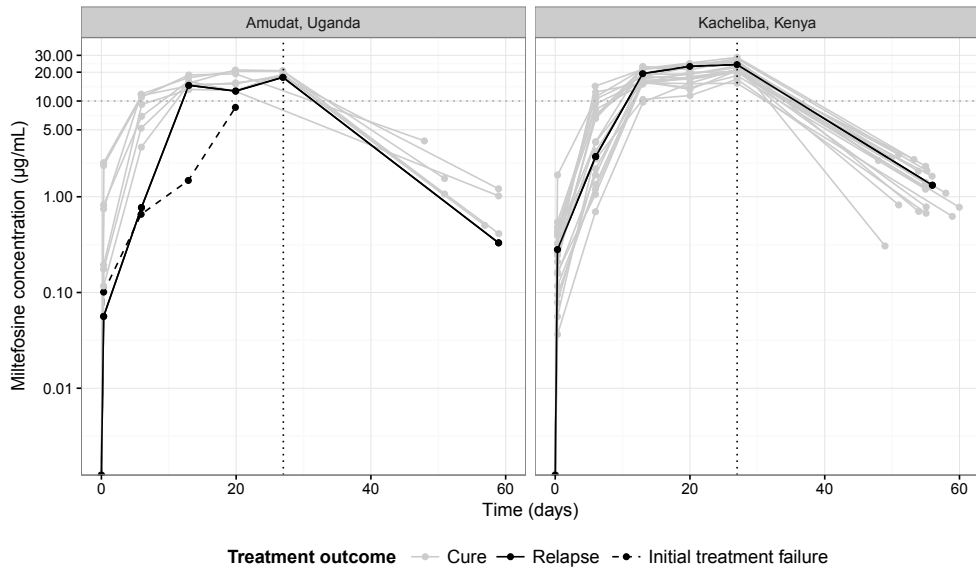
3.2

Figure 1. Observed miltefosine concentration-time curves up to one month post treatment per patient, split per treatment center. Light grey lines represent patients that were cured, black lines represent the patient that experienced initial treatment failure (dashed line) and the patients that relapsed (solid line). The vertical black dotted line indicates end of treatment.
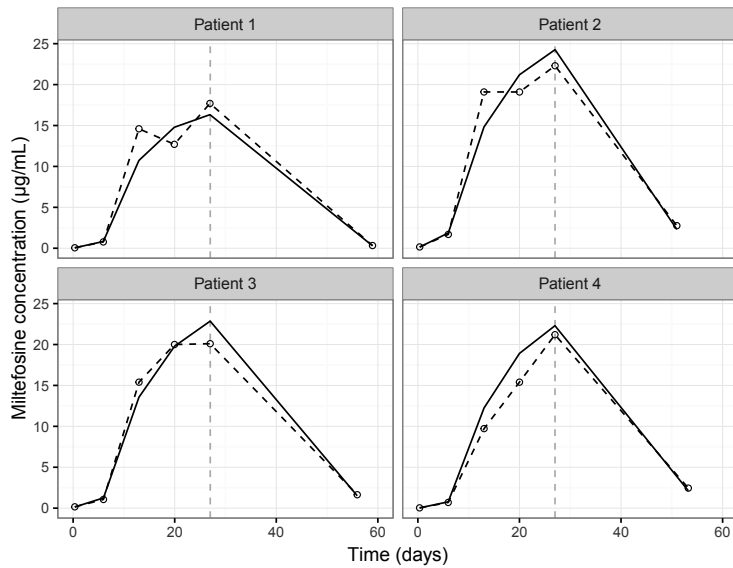

Figure 2. Representative observed concentration-time curves of miltefosine in four patients (dashed line) and the associated final model fit (solid line). Open circles represent the individual observations. The vertical dashed line is the end of treatment (day 28). Patients 1 and 2 show a decline and plateau respectively in their miltefosine concentration in the third week of treatment, patients 3 and 4 do not.

Descriptive pharmacokinetics comparison between allometric dosing and historic conventional dosing data

Miltefosine concentrations from the current allometric study and historical concentration data after conventional miltefosine dosing in paediatric patients [8] were compared. There are other differences between these patient groups, since patients included in the conventional dosing trial (n=21) were older at 10 (7-12) years, and heavier at 24 (16-34) kg. Furthermore, the majority of patients in this trial were from Sudan [8].

A trend towards accumulation to a higher miltefosine concentration level in the first week of treatment was observed for paediatric patients receiving allometric dosing with a median day 7 concentration of 5.88 µg/mL (range 0.66-14.3 µg/mL) compared to 2.67 µg/mL (range 0.70-12.8) for paediatric patients receiving conventional dosing (p=0.07). However, end of treatment concentrations were similar at 20.9±3.41 µg/mL for children receiving allometric dosing compared to 19.5±6.93 µg/mL previously found after conventional dosing in children. Variability (CV%) in the miltefosine end of treatment concentration was substantially lower after allometric dosing (16.3%) compared to conventional dosing (35.5%).

Differences in age and weight in the paediatric population treated with either allometric or conventional dosing were evaluated in relation to exposure, but no significant differences or trends could be observed. For example, in the age category 7-9 years, end of treatment concentrations were 22.5±7.0 µg/mL (n=8) after conventional dosing and 22.1±3.6 µg/mL (n=12) after allometric dosing.

Observed versus predicted miltefosine exposure after allometric dosing

Figure 3 shows a comparison of the observed and predicted miltefosine concentrations after allometric dosing in this paediatric East African patient population. Up to day 14, observations
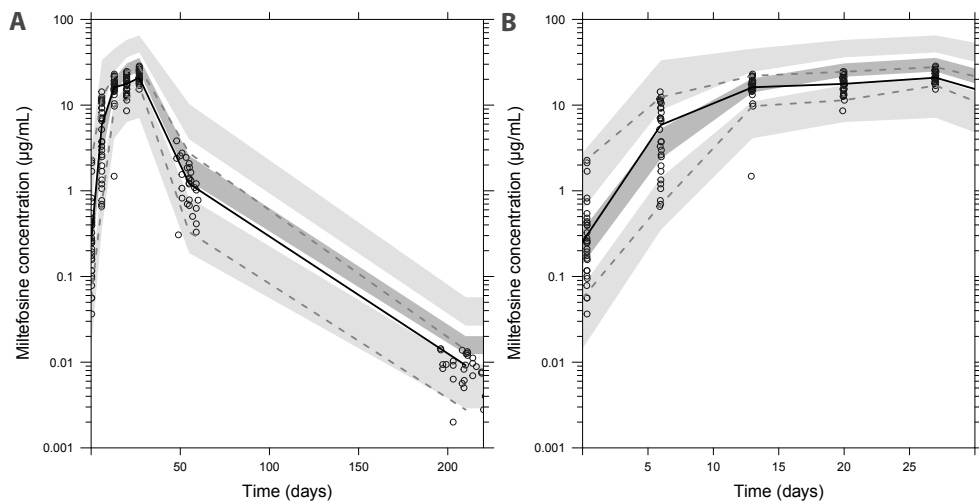
3.2

Figure 3. Visual predictive check (n=1,000) of predicted miltefosine concentrations using fixed parameter estimates from a previously developed PK model [8], using the dosing and covariate records from the patients in the allometric miltefosine dosing trial. Open circles represent the observations, with the solid line as the median and striped lines as the 5th and 95th percentile of observations. The dark grey area represents the 95% confidence interval (CI) of the predicted median concentrations; the light grey areas represent the 95% CI of the 5th and 95th percentile of the predicted concentrations. Figure 3A shows observations and predictions up to six months post treatment. Figure 3B only shows the observations and predictions during treatment, up to day 28.

were in line with the simulated miltefosine concentrations, with a slight under-prediction of the day 7 median concentration. From day 21 onwards, the observed median miltefosine concentration of 17.7 µg/mL was 34% lower than the predicted 26.9 µg/mL. The median observed end of treatment concentration was 20.9 µg/mL compared to the predicted 29.7 µg/mL. The observed 95% inter-percentile range of 16.9-27.8 µg/mL was smaller than the predicted 10.6-58.7 µg/mL, indicating a decrease in variability of exposure.

Population PK modeling

A two-compartmental model was finally selected as structural model. Adding FFM as a covariate on the central volume of distribution (V_2) and CL significantly improved the fit (ΔOFV -9.7). The allometric power components were fixed at 0.75 for CL and 1 for V_2, based on biological principles [15]. Estimating the allometric power component of CL and V_2 did not result in a significant drop in OFV, nor did the estimated values differ substantially (0.768 and 0.936, respectively). The implementation of allometric scaling by FFM on the volume of the peripheral compartment (V_3) further improved the model (ΔOFV -15.9).

The estimation of k_a was impeded by the very sparse sampling in the absorption phase. With this structural base model, a physiologically improbable k_a of only 0.11 day^{-1} was estimated corresponding to an absorption half-life of 6.3 days, resulting in a structurally overestimated day 7 concentration and underestimated day 14 concentration. A step-wise decrease in bioavailability was introduced, as was previously observed [8], from 0 until the day 7 sampling point, recovering to 100% relative bioavailability. This temporary difference in bioavailability (ΔF) was estimated to be -61.9% (RSE 11.6%) and improved the model significantly (ΔOFV -20.1). A linear piece-wise change in bioavailability was tested, but did not improve the model significantly. Furthermore, time until recovery of bioavailability was included as a parameter estimate, but led to over-parameterization.

Implementation of BSV on ΔF significantly improved the model (ΔOFV -65.5) and

Table 3. Parameter estimates of final population PK model.

Parameters	Population estimate [%RSE^b]	95% CI^c	Unit	% BSV [%RSE^b]	Shrinkage (%)	Population estimates scaled to 53 kg FFM^d
Absorption rate constant (k_a)	1.60 [25.6]	1.02-2.70	day^{-1}	99.4 [31.9]	17	
Clearance (CL/F)^a	2.92 [3.46]	2.71-3.11	L/day	10.3 [33.6]	11	6.56
Volume of central compartment (V_2/F)^a	26.1 [3.51]	24.3-27.9	L	N/E	-	76.9
Intercompartmental clearance (Q/F)	0.0284 [17.2]	0.0234-0.0449	L/day	N/E	-	
Volume peripheral compartment (V_3/F)^a	2.45 [5.78]	2.22-2.79	L	N/E	-	7.21
Change in bioavailability (ΔF)	-61.9 [11.6]	-72.7 - -44.3	%	93.3[19.7]	2	
Proportional residual error	5.64	3.40-8.4	%	N/E	17	

N.E. = not estimated. BSV = between subject variability.
^{a}Estimates provided for patient with a fat-free mass of 18 kg.
^{b}Calculated as: 100 x (standard deviation/mean value), based on 1,000 bootstrap samples.
^{c}95% confidence intervals were calculated by the percentile method from bootstrap (n=1,000)
^{d}Scaled allometrically by FFM with allometric power components of 0.75 for CL and 1 for V
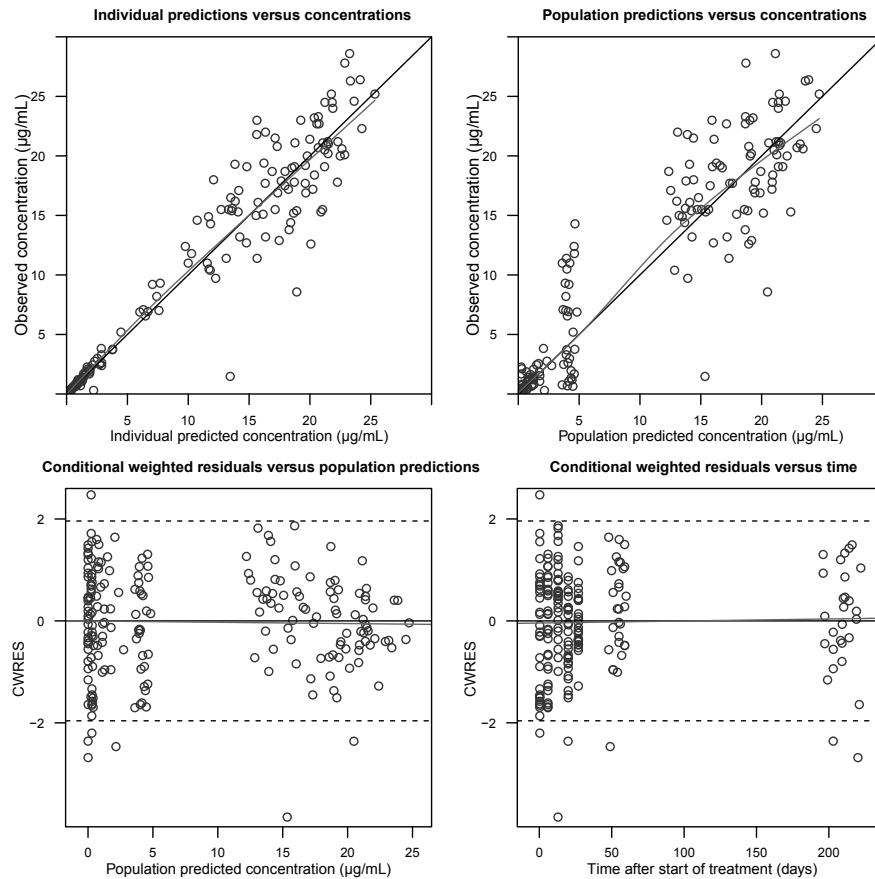
Figure 4. Basic goodness-of-fit plots of the final population model. The plots include observed versus individual model predicted concentrations, observed versus population predicted concentrations, conditional weighted residuals (CWRES) versus population predicted concentration, and CWRES versus time.

increased the k_a estimate to a more physiologically plausible level (1.6 day^{-1}). To better capture the variability observed in the absorption phase, BSV was implemented on k_a, significantly improving the model fit in the first week of treatment (ΔOFV -32.3). BSV could not be estimated for V_2 after the implementation of BSV on ΔF and k_a.

Basic goodness-of-fit plots are displayed in Figure 4 and final model parameter estimates are provided in Table 3. The visual predictive check of the final model (Figure 5) showed an acceptable prediction of the observed miltefosine concentrations after allometric dosing, though variability was over-predicted for the last two weeks of treatment. Due to the high BSV on ΔF, the predictive interval in the first week of treatment was relatively large in comparison to later time points. The plateau or decline during the third week of treatment was not well predicted by the model (patient 1 and 2 in Figure 2) and indicates unexpected non-linearity.

The median AUC$_{0-EOT}$ and AUC$_{0-\infty}$ based on individual model-based estimates were 367 µg·day/mL (range 268-503 µg·day/mL) and 610 µg·day/mL (range 396-782 µg·day/mL), respectively. The median model-based C$_{max}$ was 21.8 µg/mL (range 16.4 - 25.4 µg/mL).

DISCUSSION

This study is the first to describe the PK of an allometric miltefosine dosing regimen in a paediatric patient population suffering from visceral leishmaniasis. Miltefosine plasma concentrations accumulated faster after allometric dosing compared to historical data on conventional dosing in paediatric patients, with an 120% higher median day 7 concentration of 5.88 versus 2.67 μg/mL. Miltefosine also accumulated faster than predicted after administration of an allometric dose, shown by the higher than predicted median day 7 concentration in Figure 3. The median $AUC_{0-\infty}$ of 610 μg·day/mL in patients treated with an allometric dose was 12% higher than the 545 μg·day/mL previously observed in paediatric patients treated with a conventional miltefosine dose [8], which could be attributed to the more rapid miltefosine accumulation due to the higher dosing.

Considering the median 28% dose increase (median dose of 3.2 mg/kg compared to the conventional dose of 2.5 mg/kg), exposure increase was not dose-proportional. The lower than previously predicted miltefosine end of treatment concentration after allometric dosing is probably due to the observed plateau or even decrease in miltefosine concentration during the third week of treatment, present in 11/30 patients (37%). This is particularly visible in Figure 3, as observations were still in line with predictions up to day 14, but deviated from the third week of treatment onwards. This non-linearity was not observed in a previous miltefosine PK study in East Africa, although the day 21 sample was only available for adults [8].

No physiological explanation was found for this (temporary) halt in miltefosine accumulation. There were no demographic differences between patients with and without a plateau in miltefosine accumulation, nor were there any indications of sample stability issues. One hypothesis evaluated concerned the influence of albumin, which is severely lowered in VL patients, and could result in a higher fraction of unbound miltefosine in plasma, leading to increased clearance of the drug. Rising albumin levels during clinical improvement could cause increased protein-binding and subsequent increasing miltefosine plasma concentrations. Albumin concentrations have been assessed in a subset of patients but did not differ between patients with and without plateauing miltefosine accumulation. Other possible explanations or correlations were evaluated – co-infections or co-medication during treatment, haematological changes – but also could not explain the observed plateau in miltefosine accumulation in a subset of patients. The patients' CRFs recorded full compliance; non-compliance could therefore not be an explanation either. Changing patterns in type and amount of food intake during the treatment and subsequent changes in bioavailability could be an alternative hypothetical explanation, but data were not available to support this hypothesis.

Interestingly, in addition to an overall increase in exposure, variability in exposure and PK parameters between patients was low after the allometric dose regimen. The variability in observed $AUC_{0-\infty}$ was much higher for patients treated with a conventional dose, with a median (range) of 545 (314-1080) μg·day/mL, compared to the currently evaluated allometric dose at 610 (396-782) μg·day/mL. Reducing the variability in exposure is particularly important for those patients on the lower boundary of exposure, probably contributing to the overall increase in efficacy. A saturable absorption process has previously been described for miltefosine *in vitro* [16], potentially affecting bioavailability at higher gastrointestinal miltefosine concentrations, which could lead to a decrease in variability of exposure. On the other hand, saturable bioavailability could also lead to an increased variability as a result of inter-patient differences.
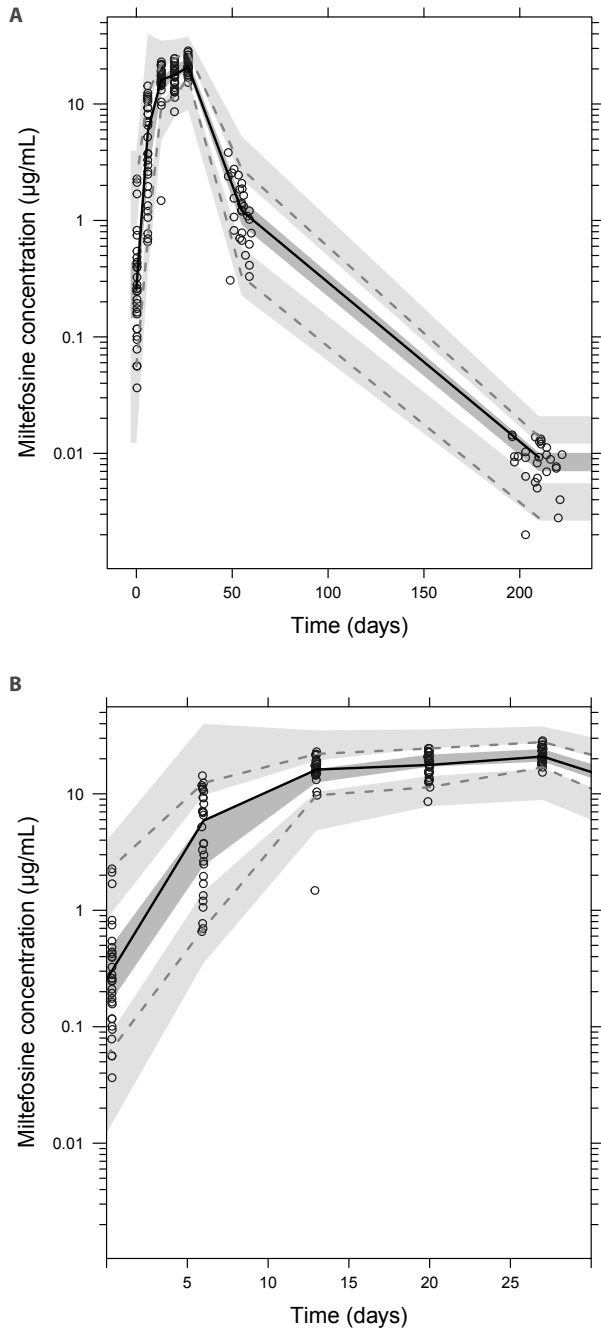
Figure 5. Visual predictive check (VPC) of the final population pharmacokinetic model. Open circles represent individual observations and solid/dashed lines show the median and 5th/95th percentile of the observed data. Dark/light-grey shading indicates 95% CI of predicted data median and 5th/95th percentile. Figure 5A shows observations and predictions up to six months post treatment. Figure 5B only shows the observations and predictions during treatment, up to day 28.

3.2

A two-compartment population PK model with decreased bioavailability up to the day 7 sampling point best fitted the observed miltefosine concentrations. Due to the relatively small range in weight and FFM of the included patients, different weight descriptions for scaling did not greatly affect the fit. Comparing the PK parameters of the developed population PK model with previously published values, CL was around 1.5- to 2-fold higher for the patients in this trial (6.4 L/day, normalized to a patient with a FFM of 53 kg) compared to previously published values of between 3.69 and 4.48 L/day [7–9,13]. Furthermore, the V_2 of 76 L was larger than previously described (38.5 L - 53.7 L [7–9,13]). These differences could be an artefact of the extrapolation of parameters from this paediatric population (FFM 18 kg) to a normalized 53 kg FFM.

The reduction in bioavailability of 61.9% was in line with a previous model-based observation for conventional miltefosine dosing in East African VL patients, describing a reduced bioavailability of 71% during the first seven days of treatment with miltefosine monotherapy [8]. Malnutrition could potentially have an effect on bioavailability, as described in more depth previously [8]. In this trial, an increase in food intake was observed after the first week, coinciding with clinical improvement, possibly improving bioavailability. Furthermore, it could be hypothesized that absorption of miltefosine from the gut is decreased due to a disease effect, for example due to affected blood circulation in the gastrointestinal tract. The most profound haematological improvements could be observed after the first week of treatment - with a 55% increase in mean WBC count and 31% increase in mean haemoglobin levels – indicating clinical improvement, which could potentially lead to recovered miltefosine absorption. It is still unknown why the decreased relative bioavailability in the first treatment week was only observed in East Africa, and not in other countries e.g. India or Nepal.

The step-wise change in bioavailability included in the model is a rather empirical measure to describe this phenomenon, but due to limited sampling in the absorption phase it was not possible to describe this non-linearity in a more physiologically plausible manner. The estimated k_a of 1.60 day^{-1} is most likely an artefact of the extremely sparse sampling in the absorption phase (one sample on the first day of treatment), and the corresponding absorption half-life is improbably high. Most studies report a k_a of around 9.6 day^{-1} [7], but estimating k_a gave a better fit than fixing the k_a to 9.6. More importantly, large differences were observed between patients in the absorption and accumulation of miltefosine during the absorption phase. This has been illustrated by the large improvements in model fit after introducing BSV on the bioavailability decrease and k_a parameters. Various absorption models – such as transit compartments and two parallel absorption processes with distinct absorption rates [17] – were evaluated to better describe the accumulation to steady-state concentrations, but either did not improve the model or were quickly over-parameterized due to the sparse sampling schedule. Using prior information from the population PK model based on conventional dosing [8] trough the prior subroutine in NONMEM, led to over-prediction of miltefosine concentrations in the last week of treatment, as expected based on the simulations (Figure 3).

The model developed did not account for the unexpected non-linearity in the PK of miltefosine, resulting in a halt in accumulation or even decline in miltefosine concentrations in the third week of treatment, causing day 14 concentrations to be generally under- and day 21 concentrations to be slightly over-predicted. There is no solid hypothesis to explain the cessation in accumulation and this, in combination with the sparse sampling schedule, prevented us from capturing this trend in the population PK model.

Efficacy improved to 90%, with a good safety profile, when treating paediatric VL

patients with an allometric dose (manuscript in preparation), compared to an efficacy of 59% in paediatric East African VL patients receiving a conventional 2.5 mg/kg miltefosine dose [6]. It could be proposed that the increased $AUC_{0-\infty}$ contributed to the observed increase in efficacy. This increase in $AUC_{0-\infty}$ was mainly attributed to the higher accumulation within the first two weeks of treatment (120% higher median day 7 concentration) at a time when parasite biomass in patients is the highest, which may be critical to the eventual treatment response. This is in line with observations in two out of three patients failing treatment. Both patients displayed a lower miltefosine concentration in the first two weeks of treatment compared to other patients (Figure 1).

The higher efficacy after allometric dosing could also potentially be the result of the lower variability in exposure (CV% 16.3 vs 35.5% in end of treatment concentration) after allometric miltefosine dosing, compared to observations after conventional dosing. Only 2 out of 30 patients (7%) failed to reach the 17.9 µg/mL PK target previously used in assessing the probability of cure in Nepalese VL patients [9]. Conversely, in the paediatric population of the conventional miltefosine dosing trial, 29% of patients failed to reach this 17.9 µg/mL threshold (analysis with data from [8]).

CONCLUSION

In conclusion, allometric miltefosine dosing can be considered an improvement over the conventional dosing regimen in paediatric VL patients, as shown by the higher total miltefosine exposure and lower variability in exposure after allometric dosing. Both these aspects could have potentially contributed to the higher efficacy of allometric compared to conventional dosing in paediatric VL patients.

The decreased bioavailability in the first week of treatment, which was also previously observed after conventional dosing, and the plateauing of miltefosine accumulation in the third week of treatment, had a substantial and detrimental effect on miltefosine exposure. Future research should focus on unraveling the causes of these observed non-linearities.

3.2

ACKNOWLEDGEMENTS

FUNDING

REFERENCES

1. Mueller YK, Kolaczinski JH, Koech T, Lokwang P, Riongoita M, Velilla E, et al. Clinical epidemiology, diagnosis and treatment of visceral leishmaniasis in the Pokot endemic area of Uganda and Kenya. Am. J. Trop. Med. Hyg. 2014;90:33–9.

2. Harhay MO, Olliaro PL, Vaillant M, Chappuis F, Lima MA, Ritmeijer K, et al. Who is a typical patient with visceral leishmaniasis? Characterizing the demographic and nutritional profile of patients in Brazil, East Africa, and South Asia. Am. J. Trop. Med. Hyg. 2011;84:543–50.

3. Bhattacharya SK, Sinha PK, Sundar S, Thakur CP, Jha TK, Pandey K, et al. Phase 4 trial of miltefosine for the treatment of Indian visceral leishmaniasis. J. Infect. Dis. 2007;196:591–8.

4. Rijal S, Ostyn B, Uranw S, Rai K, Bhattarai NR, Dorlo TPC, et al. Increasing failure of miltefosine in the treatment of kala-azar in nepal and the potential role of parasite drug resistance, reinfection, or noncompliance. Clin. Infect. Dis. 2013;56:1530–8.

5. Ostyn B, Hasker E, Dorlo TPC, Rijal S, Sundar S, Dujardin J, et al. Failure of miltefosine treatment for visceral leishmaniasis in children and men in South-East Asia. PLoS One. 2014;9:e100220.

6. Wasunna M, Njenga S, Balasegaram M, Alexander N, Omollo R, Edwards T, et al. Efficacy and safety of AmBisome in combination with sodium stibogluconate or miltefosine and miltefosine monotherapy for African visceral leishmaniasis: phase II randomized trial. PLoS Negl. Trop. Dis. 2016;10:e0004880.

7. Dorlo TPC, Rijal S, Ostyn B, De Vries PJ, Singh R, Bhattarai N, et al. Failure of miltefosine in visceral leishmaniasis is associated with low drug exposure. J. Infect. Dis. 2014;210:146–53.

8. Dorlo TPC, Kip AE, Younis BM, Ellis SE, Alves F, Beijnen JH, et al. Reduced miltefosine exposure in East African visceral leishmaniasis patients affects the time to relapse of infection. 2017; Submitted for publication.

9. Dorlo TPC, Huitema ADR, Beijnen JH, De Vries PJ. Optimal dosing of miltefosine in children and adults with visceral leishmaniasis. Antimicrob. Agents Chemother. 2012;56:3864–72.

10. Castro MM, Gomez MA, Kip AE, Cossio A, Ortiz E, Navas A, et al. Pharmacokinetics of miltefosine in children and adults with cutaneous leishmaniasis. Antimicrob Agents Chemother. 2017; 61(3): e02198-16.

11. Janmahasatian S, Duffull SB, Ash S, Ward LC, Byrne NM, Green B. Quantification of lean body weight. Clin. Pharmacokinet. 2005;44:1051–65.

12. Dorlo TPC, Hillebrand MJX, Rosing H, Eggelte TA, de Vries PJ, Beijnen JH. Development and validation of a quantitative assay for the measurement of miltefosine in human plasma by liquid chromatography-tandem mass spectrometry. J. Chromatogr. B. Analyt. Technol. Biomed. Life Sci. 2008;865:55–62.

13. Dorlo TPC, Van Thiel PPAM, Huitema ADR, Keizer RJ, De Vries HJC, Beijnen JH, et al. Pharmacokinetics of miltefosine in old world cutaneous leishmaniasis patients. Antimicrob. Agents Chemother. 2008;52:2855–60.

14. Dorlo TPC, Balasegaram M, Beijnen JH, de vries PJ. Miltefosine: A review of its pharmacology and therapeutic efficacy in the treatment of leishmaniasis. J. Antimicrob. Chemother. 2012;67:2576–97.

15. Anderson BJ, Holford NHG. Mechanism-based concepts of size and maturity in pharmacokinetics. Annu. Rev. Pharmacol. Toxicol. 2008;48:303–32.

16. Menez C, Buyse M, Farinotti R, Barratt G. Inward translocation of the phospholipid analogue miltefosine across Caco-2 cell membranes exhibits characteristics of a carrier-mediated process. Lipids. 2007;42:229–40.

17. Yu H, van Erp N, Bins S, Mathijssen RHJ, Schellens JHM, Beijnen JH, et al. Development of a pharmacokinetic model to describe the complex pharmacokinetics of pazopanib in cancer patients. Clin. Pharmacokinet. 2017; 56(3):293-303

3.2

Chapter 3.3

Pharmacokinetics and pharmacodynamics of 12-week allometric miltefosine dosing in paediatric post-kala-azar dermal leishmaniasis patients in Bangladesh

A.E. Kip
M.G. Hasnain
M. A. Mural
J. Baker
J.H.M. Schellens
J.H. Beijnen
D. Mondal*
T.P.C. Dorlo*

*Shared senior authors

To be submitted

ABSTRACT

Background. A lower miltefosine exposure in pediatric compared to adult visceral leishmaniasis (VL) patients has previously been established after conventional 2.5 mg/kg dosing. A 12 week allometric miltefosine dosing regimen has now been evaluated in pediatric post-kala-azar dermal leishmaniasis (PKDL) patients in Bangladesh, in which children with a lower fat-free mass (FFM) received a relatively higher mg/kg dose.

Methods. Eighty pediatric PKDL patients aged 4 to 17 years were treated 12 weeks with a median daily miltefosine dose of 2.8 mg/kg (range 1.8-3.9 mg/kg). Dried blood spot samples were collected pre-treatment, during treatment on day 14, 28 and 84 (last treatment day), and 1, 3, 6 and 9 months after the last treatment day. Miltefosine concentrations were determined using a validated liquid-chromatography tandem-mass spectrometry method. The non-compartmental pharmacokinetic analysis was performed in R. Regressions were performed in R correlating exposure variables C_{max}, AUC_{0-D28} and AUC_{0-D365} with treatment outcome parameters: incomplete lesion resolution at the end of the one-year follow-up period (logistic) and lesion score decrease over time (linear). All results are reported as mean±SD.

Results. Miltefosine day 28 concentrations were 29.5±6.6 µg/mL and remained steady until day 84 (28.2±8.4 µg/mL). Male patients, however, reached significantly higher day 84 concentrations than female patients (30.9±8.6 versus 26.0±7.7 µg/mL, p=0.0081, Welch two sample t-test). The AUC_{0-D28} of 573±115 µg·day/mL was higher than previously reported after conventional dosing in pediatric VL patients (~500 µg·day/mL). Baseline lesion score was a significant predictor of incomplete lesion resolution at the end of follow-up (p= 0.00129), but exposure variables such as AUC_{0-D28} were not. In an explorative analysis only selecting patients with an above median lesion score, C_{max} was significantly correlated to lesion score decrease between day 0 and 175 (decrease % = 8.88-2.18·C_{max}, p=0.00589).

Conclusions. Miltefosine exposure was increased towards adult levels after allometric dosing in paediatric PKDL patients. Significantly higher exposure levels in male compared to female patients warrants further research in identifying the most appropriate body size descriptor in determining the allometric miltefosine dose.

INTRODUCTION

Post-kala-azar dermal leishmaniasis (PKDL) is a skin manifestation that can develop after primary treatment of visceral leishmaniasis (VL). In Asia, 10-20% of patients develop PKDL within three years after VL treatment [1]. The skin rash may be macular, papular, nodular or mixed, but is macular in 90% of cases in Bangladesh [2].

A three-month treatment with oral miltefosine (<25 kg 50 mg daily, >25 kg 100 mg daily) in Indian PKDL patients showed an acceptable cure rate >90% [3,4] at 12 month follow-up. In a larger patient cohort of 57 Indian PKDL patients treated with a flat dose of 50 mg miltefosine twice-daily for three months, efficacy was 89.5% with a follow-up of 18 months [5]. The pharmacokinetics (PK) of miltefosine has not been described previously in PKDL patients, only in VL and CL (cutaneous leishmaniasis) patients. Disparities in miltefosine PK could occur between PKDL and VL patients, as the altered liver physiology in VL could possibly affect the metabolism or distribution of the drug. Miltefosine PK in PKDL patients compared to CL patients could potentially differ due to factors related to malnutrition in PKDL patients, as a decreased bioavailability during the first week of treatment in underweight East African VL patients has been hypothesized to be attributable to malnutrition [6].

In previous pharmacokinetic studies, a lower miltefosine exposure in pediatric compared to adult VL and CL patients has been established after conventional 2.5 mg/kg dosing [7–9]. In VL, lower drug exposure has been associated with a lower probability of cure and shorter time to relapse [6,8]. No exposure-response relationship has until now been evaluated in PKDL treatment with miltefosine.

To increase miltefosine exposure in pediatric leishmaniasis patients, an allometric dosing schedule has previously been proposed [7], in which patients with a lower fat-free mass (FFM) receive a relatively higher daily mg/kg miltefosine dose. The safety and efficacy of this dosing regimen was evaluated in a 12-week treatment period of pediatric PKDL patients younger than 18 years old in Bangladesh. As part of this clinical trial, the PK of this allometric dosing regimen was studied with the objectives to characterize miltefosine PK after allometric dosing and to evaluate whether miltefosine exposure in children could be increased to adult levels. Furthermore, the link between drug exposure and treatment response in PKDL was explored.

METHODS

Study population and study set-up

Eighty paediatric PKDL patients in the age of 4 to 17 years old from the district of Mymensingh in Bangladesh were included in this non-randomized single group study. The study protocol was approved by the Research Review Committee and Ethical Review Committee (ERC) of the International Centre for Diarrhoeal Disease Research, Bangladesh (ICDDR,B). Written informed consent was obtained from all participants or their parents. The study was registered as NCT02193022.

Children were treated with a daily allometric dose of miltefosine (Impavido, Paladin Labs, Montréal, Canada) as reported previously (Supplementary table 1) [7] for a total of 12 weeks. Dosing schedules were distinct for male and female patients, caused by differences in fat-free mass estimation [7,10]. The dose was based on weight and height on the first day of treatment and was kept constant during the 12-week treatment, regardless of potential weight

gain during this period. To ensure full treatment compliance, direct observed treatment (DOT) was conducted through study health workers, as described in the protocol [11].

Response to treatment was monitored at the end of treatment (day 84), and every three months during the one year follow-up period after treatment by evaluating the skin lesion score. The skin lesion score is a composite metric describing both the number of lesions and the spread of lesions over the skin surface. Its calculation has been described elsewhere [11]. The baseline lesion score describes the skin lesion score at start of treatment. Efficacy and safety data will be reported elsewhere [11].

Sample collection and analysis

Miltefosine dried blood spot (DBS) samples were collected pre-treatment, on day 14, 28 and 84 of treatment, and one (day 114), three (day 175), six (day 267) and nine (day 365) months after the end of treatment. Samples were collected approximately three hours post-dose (range 1.5-4.5 h). Due to the extent of miltefosine accumulation at the first sampling time point on day 14, this is expected to only marginally affect the between-patient comparison of analysed concentrations. Samples were air-dried for at least three hours at room temperature before storage in a zip-lock bag at room temperature. Transportation to and storage at the bioanalytical laboratory in Amsterdam was at the same conditions.

The miltefosine concentrations were determined using liquid chromatography coupled to tandem mass spectrometry (LC-MS/MS), as validated previously [12], with a lower limit of quantitation (LLOQ) of 10 ng/mL. Miltefosine distributes approximately equally between plasma and erythrocytes, and a median paired miltefosine DBS/plasma concentration ratio of 0.99 was reported [12]. Therefore miltefosine DBS concentrations were considered identical to miltefosine plasma concentrations. Clinical validation of the DBS method (haematocrit range 23-44%) showed that haematocrit correction was not required to calculate plasma concentrations from analysed DBS concentrations [12]. As the average haematocrit in this study (38%) was within this range, no haematocrit correction was applied.

Pharmacokinetic analysis

Data analysis was performed in R (version 3.3.1), using R package "ggplot2" for the graphical presentation. A two-stage non-compartmental analysis was performed with the R package "ncappc". The area under the concentration-time curve (AUC) was calculated from day 0 to 365 (AUC_{0-D365}). To compare the AUC values with previously reported one month miltefosine treatments, the AUC was also calculated from day 0 to 28 (AUC_{0-D28}). C_{max} equals the highest analysed concentration, and can be regarded as the steady-state concentration.

Continuous data are represented as mean±standard deviation (SD), unless indicated otherwise. In figures, data are presented using the nominal sampling time point.

Exposure-response relation

A logistic regression analysis was performed in R with the binary outcome "1" for patients with unresolved lesions and "0" for patients with complete resolution of skin lesions, at the one year follow-up time point. Baseline lesion score and exposure variables C_{max}, AUC_{0-D28} and AUC_{0-D365} were evaluated in a univariate analysis. Furthermore, exposure variables were evaluated in combination with baseline lesion score in a multivariate analysis.

Correlations between exposure variables and lesion score decrease over time were evaluated with a linear regression in R. Baseline lesion score was also correlated with lesion

score decrease over time in univariate analysis and in multivariate analysis combined with exposure variables. Lesion score decrease over time was evaluated from baseline to day 175, 267 and 365 after the start of treatment.

RESULTS

Demographics and sample collection
Demographics of the study population are presented in Table 1. One patient dropped out of the trial due to compliance issues. A total of 632 samples were collected from 79 patients. Age and weight distributions were comparable between male and female patients. Female patients received a lower daily dose of 2.6 mg/kg daily compared to males (3.2 mg/kg), as proposed in the allometric dosing schedule in Supplementary table 1.

The baseline lesion score was 81 (range 2-545), without significant differences between male and female patients. Response at end of treatment, expressed as median (interquartile-range, IQR) percentage decrease in lesion score compared to baseline, was -29.0% (-54.2 to -2.8%). Response to treatment at day 175 and day 267 was -69.2% (-81.0 to -50.0%) respectively -84.6% (-98.5 to -74.6%). At the one year follow-up time point, 22 out of 79 patients had unresolved lesions, as indicated by a positive lesion score. Interestingly, 7/37 male patients (18.9%) still had unresolved lesions at one year follow-up, versus 15/42 (35.7%) female patients.

Table 1. Demographics and treatment information of study population in pharmacokinetic analysis.

Parameter	Total	Male	Female
Total no. of patients	79	37	43
Daily dose of miltefosine (mg/kg/day)	2.8 (1.8-3.9)	3.2 (2.4-3.9)	2.6 (1.8-3.9)
Age (yr)	10 (4-17)	10 (4-17)	10 (5-16)
Body weight (kg)	27.6 (14.0-62.2)	25.3 (14.0-55.2)	29.2 (14.8-62.2
Height (cm)	134 (95-168)	133 (95-168)	140 (95-158)
Fat-free mass (kg)[a]	23.1 (10.8-46.8)	24.0 (12.9-46.8)	22.4 (10.8-38.8)
Lesion score baseline (day 0)	81 (2-545)	90 (3-483)	74 (2-545)
Lesion score end of treatment (day 84)	54 (0-530)	65 (2-355)	51 (0-530)
Lesion score at six month follow-up (day 267)	6 (0-400)	5 (0-132)	8 (0-400)

All values are given as median (range), unless stated otherwise.
[a]Calculated as described previously [10].

Concentration-time profiles of miltefosine after allometric dose
The majority of patients reached steady state concentrations within one month of treatment, at a mean day 28 concentration of 29.6±6.7 µg/mL. Concentrations remained steady until end of treatment at day 84 (29.3±7.4 µg/mL), though a concentration decrease was observed in patients aged 13 to 17 years (31.1 to 28.8 µg/mL, p=0.195, paired t-test). Miltefosine concentrations decreased 30-58% between day 28 and 84 for ten out of 79 patients. There were no differences in day 84 concentration between age categories 4-9 years (30.0±8.5 µg/mL, n=27), 10-12 years (29.0±6.7 µg/mL, n=31) and 13-17 years (28.8±6.9 µg/mL, n=21).

Figure 1 depicts the median miltefosine concentration time profiles for male and
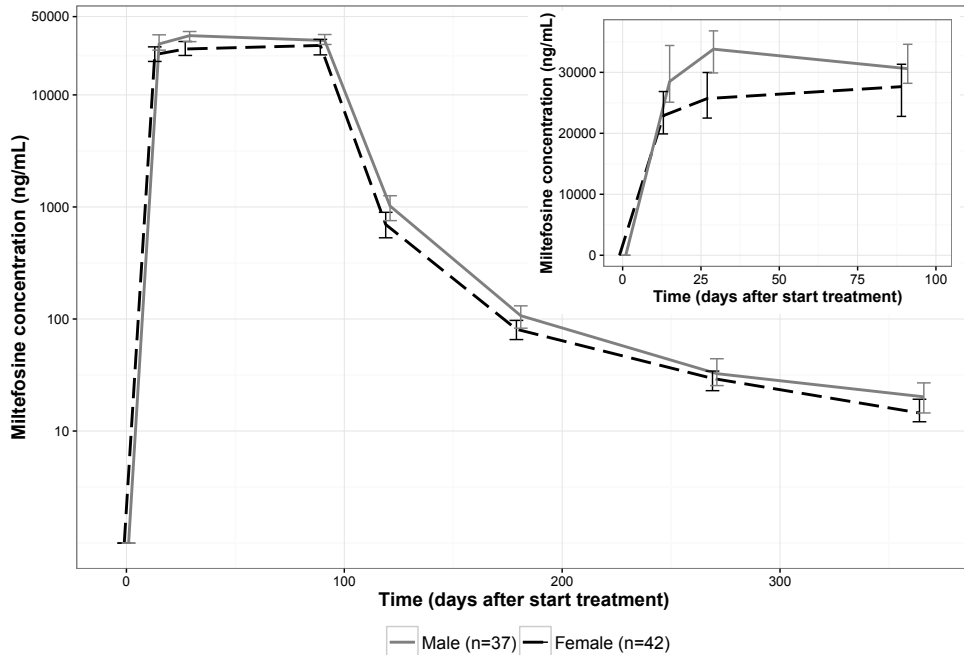
Figure 1. Concentration-time profile for male (n=37) and female (n=42) pediatric PKDL patients treated with 12 weeks allometric miltefosine dose. Grey solid line represents the median observed miltefosine concentrations for male patients, the black striped line the median observed miltefosine concentrations for female patients. Error bars represent the inter-quartile range (IQR). The window in the right top corner represents the observations during treatment represented on an absolute y-axis as opposed to the logarithmic y-axis of the overall plot.

female PKDL patients. Day 84 steady state concentrations were significantly higher for male patients (32.0±7.1 μg/mL) than female patients (26.9±6.8, p=0.00519, Mann Whitney U-test).

Non-compartmental analysis
The mean AUC_{0-D360} and AUC_{0-D28} in this study were 2,662±520 and 571±113 μg·day/mL, respectively. AUC_{0-D360} and AUC_{0-D28} were significantly higher for male (2,959±433 and 638±95 μg·day/mL) compared to female patients (2,400±446 and 513±94 μg·day/mL, p=5.4·10^{-7}/ p=2.7·10^{-7}, Mann Whitney U-test/two sample t-test). There were no profound differences in exposure between age categories, as depicted in Figure 2 for AUC_{0-D28}. C_{max} was 32.8±6.4 μg/mL and the miltefosine plasma elimination half-life was particularly long at 75.5±17.7 days.

Miltefosine exposure versus response
The C_{max} of 30.6±5.6 μg/mL was lower for patients with a positive lesion score at the one year follow-up (n=22), than for patients with complete resolution of skin lesions (33.6±6.6 μg/mL, n=57), though this difference was not significant (p=0.06552, two-sample t-test). No significant differences in AUC_{0-D360} or AUC_{0-D28} were observed.

Only baseline lesion score was significantly related to incomplete resolution of lesions at the one year follow-up time point (likelihood ratio test p= 0.00129). The baseline probability of incomplete resolution of lesions at the end of follow-up was 14%, with a 1.0051 odds ratio increase for each unit increase in baseline lesion score. This translates into a 20%
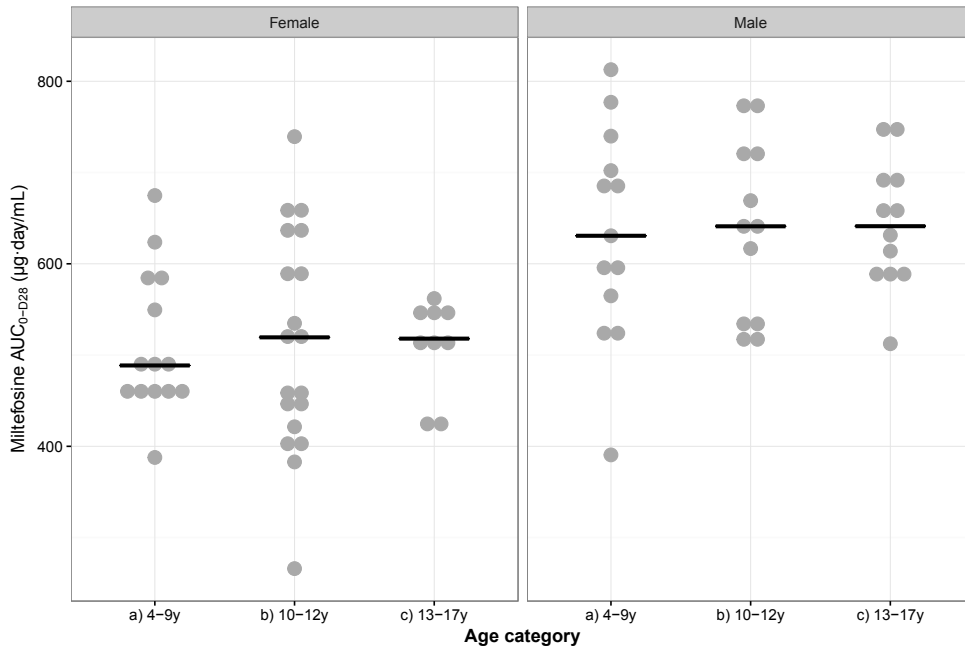
Figure 2. The area under the concentration-time curve from day 0 to day 28 (AUC$_{0-D28}$) per age category and gender. Dots indicate the individual calculated AUC$_{0-D28}$, the horizontal line indicates the median per age category for female versus male.

probability of incomplete lesion resolution at the end of follow-up at a median lesion score of 81, but an >55% probability for patients with a lesion score >400 (10% of patients). When adding exposure variables to baseline lesion score in a multivariate analysis, none of the exposure variables was statistically significant.

In univariate linear regression analysis, exposure variables C$_{max}$, AUC$_{0-D28}$ and AUC$_{0-D365}$ were not significantly correlated with lesion score decrease, regardless of the time point that lesion score decrease was determined (day 175, 267 or 365 after start of treatment). Baseline lesion score, however, was significantly correlated with the lesion score decrease from baseline to day 267 (-86.7+0.0422·baseline lesion score, p=0.0075, R^2=0.09) and to day 365 (-95.6+0.0407·baseline lesion score, p=0.0004, R^2=0.15). In multivariate analysis, exposure variables were not statistically significant in addition to baseline lesion score.

Low lesion scores could have a deterministic effect in identifying a possible exposure-response relation, as patients with less severity of the disease have a higher chance of curing faster regardless of exposure reached. In a more explorative analysis, only patients with an above median lesion score (>81) were selected and the linear regression was repeated. Significant correlations were observed between C$_{max}$ and the lesion score decrease at day 175 (8.88-2.18·C$_{max}$, p=0.00589, R^2=0.19, Figure 3), day 267 (-16.1-1.83·C$_{max}$, p=0.00941, R^2=0.17) and day 365 (-40.9-1.34·C$_{max}$, p=0.0225, R^2=0.13) compared to baseline, though with high variability as indicated by the low R^2. AUC$_{0-D28}$ and AUC$_{0-D365}$ were less significant predictors [data not shown].
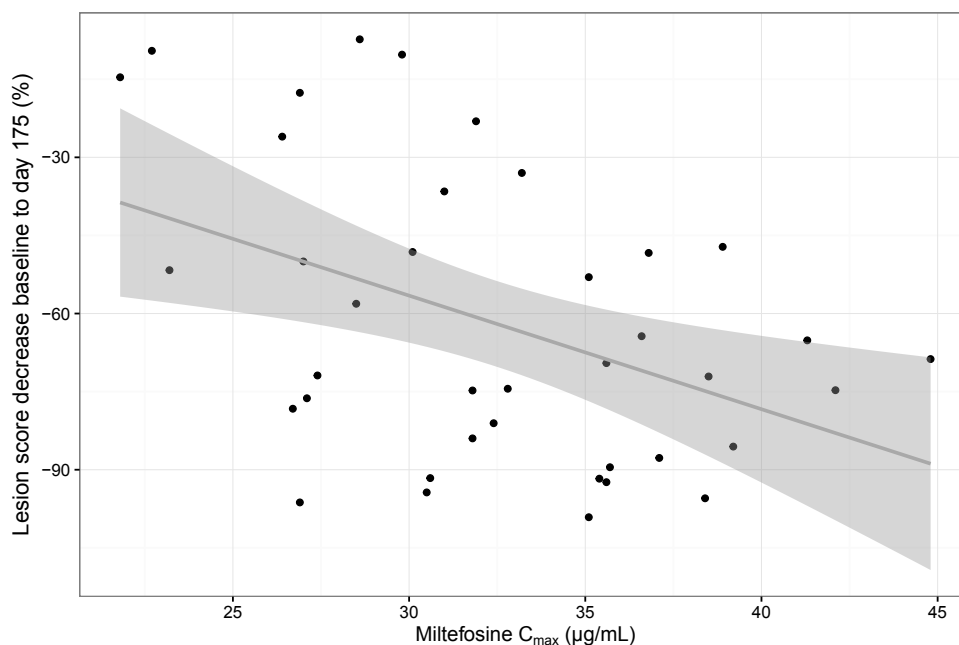
3.3

Figure 3. Miltefosine C_{max} as derived by non-compartmental analysis (NCA) versus lesion score decrease between start of treatment and day 175 after start of treatment (%) in the subset of patients with baseline lesion scores above the median of 81. Black dots indicate individual observations, the grey line represents the linear regression line (lesion score decrease (%) = 8.88-2.18·C_{max}) and the grey area the 95% confidence interval of the regression line.

DISCUSSION

This is the first description of miltefosine PK in PKDL patients after allometric dosing. As this is the first study reporting the PK of a 12-week miltefosine therapy as opposed to one month regimens, the AUC_{0-D28} was used to compare results to previous miltefosine pharmacokinetic studies. The mean AUC_{0-D28} of 573±115 μg·day/mL was ~15% higher compared to the approximately 500 μg·day/mL model based estimate after linear dosing in pediatric VL patients [7]. This indicates that miltefosine exposure in pediatric patients was successfully increased towards adult exposure levels, as previously predicted by simulations with a population pharmacokinetic model based on linear dosing data [7]. The AUC_{0-D28} in this study is calculated with an NCA analysis, probably underestimating the AUC during accumulation due to the sparse sampling schedule. This implies that actual miltefosine exposure after allometric dosing is probably even over 15% higher than after conventional dosing, for which AUC values were calculated with model-based estimates.

After conventional 2.5 mg/kg dosing for 28 days, 90% of adult VL patients reached an AUC_{0-D28} of 412 μg·day/mL, while this threshold was only reached by 71.4% of children in that study [7]. In this allometric dosing study, 92% of children reached an AUC_{0-D28} of 412 μg·day/mL, which is in line with the previously predicted 97% [7]. Similarly, the C_{max} in 100% of children treated with an allometric miltefosine dose (in 96% of children on day 28) exceeded 18.8 μg/mL, opposed to 66.7% of children treated with linear miltefosine dosing [7].

Ten of 79 included patients showed a 30-58% decline in miltefosine concentrations

between day 28 and 84. Non-compliance might have contributed to this decline, as achieving compliance in a self-administered oral treatment over such extended periods of time is challenging [13]. This hypothesis is strengthened by the observation that the decline was mostly visible in the 13-17 adolescent age category, generally known to be less compliant [13]. As the allometric dose administered remained constant during the 12-week treatment despite possible weight gain, increase in body weight within the treatment period could be hypothesized to contribute to a decrease in steady-state concentrations as a result of a higher clearance. However, as the median weight gain (range) of these patients was only 5% (-1 to 14%), this probably did not substantially contribute to the observed concentration decrease.

Female patients receiving an allometric dose were significantly lower exposed to miltefosine than male patients. Due to this disparity, 97.2% of male patients and 88.1% of female patients in the here-described study reached the 412 µg·day/mL AUC_{0-D28} threshold. The difference in miltefosine exposure between male and female patients could potentially be attributed to the FFM estimation method. The allometric dosing algorithm is based on achieving similar steady-state concentrations between adults and children by scaling the dose with the patient's estimated FFM, as clearance was found to be allometrically scaled by FFM [7]. FFM was calculated from weight and height as described previously, with different formulas for male and female patients due to differences in body composition [10]. These formulas are based on a semi-mechanistic equation to predict FFM in a population of 373 Australians in an age range of 18-82 years and weight range of 41-217 kg [10]. Possibly these findings in this Australian population cannot be extrapolated to the Bangladeshi population. Furthermore, PKDL patients are often malnourished, which could largely influence the calculation of FFM in this patient population. Potentially, differences in FFM calculations from weight and height are not so profound between male and female patients in this specific population.

Furthermore, the age range of the population that the FFM calculation equations are based on [10] was much higher than observed in this paediatric study (10 (4-17) years). Body composition alters with increasing age and consequently FFM as calculated from weight and height could alter. A maturation function for FFM estimation for children has recently been described [14]. Based on this maturation function, which differs between males and females, the FFM of boys in the here described allometric study would be overestimated using the adult male formula, resulting in a higher than proposed dose in boys. However, the existence of the maturation function – based on over a thousand males and females from New Zealand aged 3-30 - has not yet been validated in other patient populations.

FFM as previously estimated is potentially not the most reliable approximation of FFM in this population and possibly other body size parameters should be used in the allometric scaling of clearance and in the calculation of appropriate dosing regimens. The allometric scaling of dose by FFM in this study, was based on a population pharmacokinetic model developed based on data of both adult and paediatric visceral and cutaneous leishmaniasis patients [7]. Due to high variances in body composition between these populations, miltefosine PK was best described by including FFM instead of weight allometrically scaled on clearance and volume of distribution. In the future, weight might be considered as body mass descriptor to calculate the allometric dosing regimen, to address the observed differences between male and female patients, at least in this population. However, it is unclear whether this result can be extrapolated to other patient populations, as no differences in miltefosine exposure were observed between East African male and female pediatric VL patients after

3.3

allometric dosing (Chapter 3.2).

A much higher proportion of female patients (35.7%) compared to male patients (18.9%) still had unresolved lesions at the one year follow-up time point, though baseline lesion scores did not differ significantly. Lower miltefosine exposure for female patients might have contributed to this. However, no significant exposure-response relation could be identified with this descriptive non-compartmental analysis, relating miltefosine exposure to lesion score decrease during treatment. Nonetheless, these results might be influenced by the statistically significant effect of baseline lesion score on treatment outcome, as could be deducted from the significant correlation of C_{max} with lesion score decrease when only selecting patients with an above median baseline lesion score. Probably, patients with a less severe PKDL infection, have a higher probability of healing naturally without pharmaco-therapeutic intervention. These exposure-outcome relations could be further investigated in a more mechanistic approach using population pharmacokinetic modelling. An additional advantage of this approach is that AUC_{0-D28} or AUC_{0-D365} can more accurately be described, and could possibly be better correlated with outcome.

CONCLUSION

In line with predictions, miltefosine exposure was increased towards adult levels after allometric dosing in paediatric PKDL patients, without significant differences between age categories. However, exposure was significantly higher in male compared to female pediatric patients. This warrants further study in establishing the most appropriate body size descriptor in the allometric scaling of clearance and hence the scaling of the allometric dose to achieve similar steady state concentrations in male and female patients.

Using the exposure variables from the descriptive NCA analysis, no significant correlations with treatment outcome could be established, most probably due to the deterministic effect of baseline lesion score on outcome. Only selecting patients with an above median baseline lesion score, C_{max} was significantly correlated with lesion score decrease over time. A more mechanistic approach to this analysis could potentially be more powered to clarify the exposure-response relation of miltefosine in PKDL patients.

ACKNOWLEDGEMENTS

FUNDING

REFERENCES

1. Zijlstra EE. The immunology of post-kala-azar dermal leishmaniasis (PKDL). Parasit. Vectors. 2016;9:464.

2. Mondal D, Khan MGM. Recent advances in post-kala-azar dermal leishmaniasis. Curr. Opin. Infect. Dis. 2011;24:418–22.

3. Sundar S, Sinha P, Jha TK, Chakravarty J, Rai M, Kumar N, et al. Oral miltefosine for Indian post-kala-azar dermal leishmaniasis: A randomised trial. Trop. Med. Int. Heal. 2013;18:96–100.

4. Sundar S, Singh A, Tiwari A, Shukla S, Chakravarty J, Rai M. Efficacy and safety of miltefosine in treatment of Post-Kala-Azar Dermal Leishmaniasis. ScientificWorldJournal. 2015;doi: 10.1155/2014/548010.

5. Ramesh V, Singh R, Avishek K, Verma A, Deep DK, Verma S, et al. Decline in clinical efficacy of oral miltefosine in treatment of post kala-azar dermal leishmaniasis (PKDL) in India. PLoS Negl. Trop. Dis. 2015;9:e0004093.

6. Dorlo TPC, Kip AE, Younis BM, Ellis SE, Alves F, Beijnen JH, et al. Reduced miltefosine exposure in East African visceral leishmaniasis patients affects the time to relapse of infection. 2017; Submitted for publication.

7. Dorlo TPC, Huitema ADR, Beijnen JH, De Vries PJ. Optimal dosing of miltefosine in children and adults with visceral leishmaniasis. Antimicrob. Agents Chemother. 2012;56:3864–72.

8. Dorlo TPC, Rijal S, Ostyn B, De Vries PJ, Singh R, Bhattarai N, et al. Failure of miltefosine in visceral leishmaniasis is associated with low drug exposure. J. Infect. Dis. 2014;210:146–53.

9. Castro MM, Gomez MA, Kip AE, Cossio A, Ortiz E, Navas A, et al. Pharmacokinetics of miltefosine in children and adults with cutaneous leishmaniasis. Antimicrob Agents Chemother. 2017; 61(3): e02198-16.

10. Janmahasatian S, Duffull SB, Ash S, Ward LC, Byrne NM GB. Quantification of lean body weight. Clin Pharmacokinet. 2005;44:1051–65.

11. Mondal D, Hasnain MG, Hossain MS, Ghosh D, Ghosh P, Hossain H, et al. Study on the safety and efficacy of miltefosine for the treatment of children and adolescents with post-kala-azar dermal leishmaniasis in Bangladesh, and an association of serum vitamin E and exposure to arsenic with post-kala-azar dermal leishmaniasis. BMJ Open. 2016;6:e010050.

12. Kip AE, Rosing H, Hillebrand MJX, Blesson S, Mengesha B, Diro E, et al. Validation and clinical evaluation of a novel method to measure miltefosine in leishmaniasis patients using dried blood spot sample collection. Antimicrob. Agents Chemother. 2016;60:2081–9.

13. Osterberg L, Blaschke T. Adherence to medication. N. Engl. J. Med. 2005;353:487–97.

14. Al-Sallami HS, Goulding A, Grant A, Taylor R, Holford N, Duffull SB. Prediction of Fat-Free Mass in Children. Clin. Pharmacokinet. 2015;54:1169–78.

3.3

Supplementary table 1. Daily allometric miltefosine dose (mg) for males (left) and females (right) based on fat-free mass.

Male

HT (cm) → / ↓WT (kg)	80-89	90-99	100-109	110-119	120-129	130-139	140-149	150-159	160
7									
8	40								
9	40								
10	40	40							
11	40	40							
12	40	50							
13	50	50	50						
14	50	50	50						
15	50	50	60	60					
16	50	50	60	60					
17	50	60	60	60					
18	50	60	60	60	70				
19	50	60	60	70	70				
20	50	60	60	70	70				
21	60	60	60	70	70	70			
22	60	60	70	70	70	80			
23	60	60	70	70	80	80			
24	60	60	70	70	80	80	80		
25	60	60	70	70	80	80	80		
26	60	70	70	80	80	80	100		
27	60	70	70	80	80	80	100		
28	60	70	80	80	80	100	100	100	
29	60	70	80	80	80	100	100	100	
30	60	70	80	80	100	100	100	100	

Female

HT (cm) → / ↓WT (kg)	80-89	90-99	100-109	110-119	120-129	130-139	140-149	150-159	160
7									
8	30								
9	30								
10	30	40							
11	40	40	40						
12	40	40	40						
13	40	40	40						
14	40	40	40	50					
15	40	40	50	50					
16	40	50	50	50					
17	40	50	50	50	50				
18	50	50	50	50	60				
19	50	50	50	60	60				
20	50	50	50	60	60	60			
21	50	50	60	60	60	60			
22	50	50	60	60	60	60			
23	50	50	60	60	60	70			
24	50	50	60	60	60	70	70		
25	50	60	60	60	70	70	70		
26	50	60	60	60	70	70	70		
27	50	60	60	70	70	70	70	70	
28	50	60	60	70	70	70	80	80	
29	50	60	60	70	70	70	80	80	
30	50	60	60	70	70	80	80	80	80

Row headers indicate the patients' weight (kg) and column headers indicate the patients' height (cm). Areas indicated in grey shading indicate patients that are at risk of severe malnutrition and these patients were not included in the trial.

3.3

Chapter 3.4

Pharmacokinetics of concomitantly administered antileishmanial and antiretroviral drugs in Ethiopian visceral leishmaniasis patients co-infected with HIV

A.E. Kip
S. Blesson
F. Alves
R. Kimutai
P. Menza
B. Mengesha
J.H.M. Schellens
J.H. Beijnen
A. Hailu
E. Diro
T.P.C. Dorlo

Interim analysis

ABSTRACT

Background. Despite the high prevalence of HIV co-infection in Ethiopian visceral leishmaniasis (VL) patients, the effect of HIV-VL co-morbidity on the pharmacokinetics (PK) of antileishmanial and antiretroviral (ARV) drugs is still unknown. Furthermore, interactions between antileishmanial and ARV drugs in simultaneous administration have not been studied.

Methods. Ten HIV co-infected VL patients were treated with 5 mg/kg liposomal amphotericin B (L-AMB) monotherapy on days 1, 2, 3, 4, 5, 10, 17 and 24 of treatment and 20 patients with 5 mg/kg L-AMB on days 1, 3, 5, 7, 9 and 11 of treatment combined with 28 days 50 mg oral miltefosine twice daily from day 1. Miltefosine, efavirenz, nevirapine, lopinavir and ritonavir concentrations were determined in dried blood spots and total AMB in plasma using liquid chromatography-tandem mass spectrometry.

Results. The day 1 median AMB C_{max} was 24.6 µg/mL (range 12.4-66.1 µg/mL) and increased after repeated dosing to 40.9 and 33.2 µg/mL on the last day of combination and monotherapy, respectively. The median day 28 miltefosine concentration was 18,700 ng/mL (interquartile range: 15,400-22,500 ng/mL). No significant relationship between (combined) antileishmanial exposure and treatment outcome could be established in this descriptive analysis. Concentrations of efavirenz and nevirapine were generally stable during antileishmanial treatment, though two patients showed profound alterations to values outside the therapeutic window.

Conclusion/discussion. This is the first description of antileishmanial and antiretroviral drug PK in concomitant administration and the first report of AMB PK in VL patients. The day 1 AMB C_{max} of 24.6 µg/mL was two-fold lower than previously observed in non-VL patients (57.6 µg/mL). An approximately 35% lower miltefosine exposure was observed compared to a previous study in adult VL patients in Eastern Africa, only partially explained by the 19% lower administered dose (2.1 versus 2.6 mg/kg/day). The lower exposure in this population possibly indicates that a higher dose could be considered in this patient population, as a significant miltefosine exposure-effect relationship has previously been established for VL. Adequate drug exposure in these HIV co-infected patients is especially important to avoid drug resistance, as relapse frequencies are especially high in this population with limited treatment options.

INTRODUCTION

Human immunodeficiency virus (HIV) co-infection is reported in 2-9% of all visceral leishmaniasis (VL) patients in endemic regions, with rates up to 40% in some regions of Ethiopia [1]. Treatment outcome in this patient population is of particular concern, with high rates of treatment failure and relapse [1]. In addition, conventional antimony treatment leads to unacceptable rates of severe toxicity (pancreatitis, cardiotoxicity and severe vomiting) and a ten-fold higher mortality rate than in non-co-infected patients [1,2], stressing the need for the development and evaluation of new, more efficacious and safer treatment regimens for HIV co-infected VL patients. A recent randomized open-label clinical trial (registered as NCT02011958) in Northern Ethiopia evaluated the efficacy and safety of a liposomal amphotericin B (L-AMB) monotherapy and a combination therapy of L-AMB with miltefosine in treatment of HIV co-infected VL patients, of whom the majority concomitantly received antiretroviral treatment (ART).

Defining pharmacokinetic-pharmacodynamic relationships has been shown to be pivotal in clinical decision-making regarding dosing regimens against various infectious diseases [3–6]. In the case of antileishmanial treatment, lower miltefosine exposure has been associated with lower probability of cure [7] and shorter time to relapse [8] in VL. Also in ART, exposure-response relationships have been established, such as lower treatment efficacy in patients with efavirenz trough levels below 1 μg/mL or nevirapine trough levels below 3.4 μg/mL [9,10].

In VL patients co-infected with HIV, both diseases could potentially have an effect on the PK of both antileishmanial and antiretroviral (ARV) drugs. Non-nucleoside reverse transcriptase inhibitors (NNRTIs) and protease inhibitors (PIs) are both metabolized by a multitude of liver enzymes (CYP3A4, CYP2B6, CYP2C9, CYP2D6 etc. [11]). As liver physiology is profoundly altered in VL due to parasite infection and increased macrophage loads, this could potentially affect NNRTI and PI metabolism and thus ARV drug exposure. Nonetheless, neither the PK of ARV drugs in VL patients nor the PK of antileishmanial drugs miltefosine and L-AMB in HIV patients has been evaluated previously. Of even more relevance, the PK of the pivotal antileishmanial drug L-AMB has never been studied in VL patients, while altered liver physiology could potentially affect liposome clearance of L-AMB.

Besides possible disease-specific effects on PK, drug-drug interactions could affect exposure and thereby the efficacy of the concomitantly administered drugs. Amphotericin B deoxycholate has been associated with the modulation of cytochrome P450 (CYP) enzyme activity [12], which could affect the metabolism of and thus exposure to NNRTIs and PIs. No information is available on this mechanism for the liposomal formulation, although it can be expected that the effect is less profound due to the lower free fraction present [13]. Furthermore, both L-AMB and miltefosine are known to accumulate in the liver, which could potentially influence NNRTI and PI metabolism. Both L-AMB (>96%) [14] and miltefosine (96-98%) [15] are highly protein-bound, as are the ARV drugs nevirapine (60%) and efavirenz, ritonavir and lopinavir (>95%) [16]. VL patients have severely decreased protein levels, which could potentially result in competition in protein binding in VL patients [17–19].

The PK of miltefosine has been studied in combination with L-AMB, but a potential effect of miltefosine co-administration on L-AMB PK has not been evaluated. *In vitro* no PK interactions could be observed, except for the incorporation of the free fraction of AMB in miltefosine micelles that form above a critical micelle concentration of 11 μM (4.5 μg/mL) [20].

As part of the aforementioned clinical trial investigating L-AMB as monotherapy

3.4

and in combination with miltefosine in HIV co-infected VL patients, the PK of concomitantly administered antileishmanial and ARV drugs was assessed. Our objective was to provide the first description of L-AMB PK in VL patients. Furthermore, our aim was to describe the PK of both L-AMB and miltefosine in this particularly vulnerable patient population and to monitor any potential drug-drug interactions. Finally, the PK of ARV drugs was evaluated to characterize ARV drug exposure and compare it to established therapeutic windows.

METHODS

Study population
PK samples were collected in a clinical trial in Ethiopia investigating the safety and efficacy of L-AMB in monotherapy or in combination with miltefosine in treatment of HIV co-infected VL patients (registered as NCT02011958). The clinical trial was approved by the University of Gondar Institutional Research Board, Ethiopia, National Health Research Ethics Committee, Ethiopia, Médecins Sans Frontières (MSF) Ethics Review Board, Switzerland, Institute of Tropical Medicine (ITM) Institutional Review Board, Belgium, London School of Hygiene & Tropical Medicine (LSHTM) Ethics Committee, United Kingdom and the Food, Medicine and Health Care Administration and Control Authority (FMHACA), Addis Ababa, Ethiopia. Before enrolment, written informed consent was obtained from each patient. Patients received one of the two treatments: (1) L-AMB (AmBisome®, Gilead, Foster City, CA, USA) monotherapy at a total dose of 40 mg/kg (5 mg/kg on days 1 to 5, 10, 17 and 24) or (2) combination therapy of 30 mg/kg L-AMB (5 mg/kg on days 1, 3, 5, 7, 9, 11) combined with 28 days of 50 mg miltefosine bi-daily (Impavido®, Paladin Labs Inc., Canada).

Primary clinical outcome was evaluated after one treatment cycle at day 24 for patients in monotherapy and day 28 for patients in combination therapy. Patients that were still parasite positive by microscopy on the last treatment day but clinically well, received another cycle of the same treatment regimen ("extended treatment"). Patients that were parasite positive and unwell, received rescue treatment (any other antileishmanial treatment available). After extended treatment, patients that were still parasite positive received rescue treatment. Relapse-free survival was evaluated at 12 months after end of treatment (nominally day 390).

Patients already on ART continued their regimen. Patients not yet on ART started with a once-daily regimen of tenofovir (300 mg), lamivudine (300 mg) and efavirenz (600 mg) (TDF/3TC/EFV), during or at the end of antileishmanial treatment.

Sample collection, storage and transport
Miltefosine and ARV drug concentrations were determined in dried blood spots (DBS). Miltefosine samples were collected pre-treatment, pre-dose on day 11, day 28 (~12h after final dose), day 56 (~12h after final extended treatment dose, if applicable), and one and six months after treatment. ARV samples were collected pre-dose (trough level) and 4-5 hours post-dose (peak level) on the first and last day of antileishmanial treatment. If patients were not yet on ART at the start of antileishmanial treatment, the first ARV PK samples were collected on the first day of ART, on which pre-dose concentrations were logically zero.

DBS samples were air-dried for at least 3 hours after collection. Samples were stored on site at room temperature in the dark in zip lock bags with at least three desiccant packages.

Under the same conditions, samples were transported to and subsequently stored at the bioanalytical laboratory in Amsterdam, the Netherlands.

K_2-EDTA plasma samples were collected for AMB quantification on the first and the last day of AMB treatment, corresponding to day 24 and day 11 for the monotherapy and combination therapy, respectively. Samples were collected at 2, 6 and 24 (trough level) hours after the start of infusion. As L-AMB was theoretically administered by a two-hour IV infusion, the sample collected 2 hours after start of infusion should represent the maximum observed concentration (C_{max}).

In addition, miltefosine K_2-EDTA plasma samples were collected on day 28 simultaneously with the miltefosine DBS sample to correlate DBS with plasma concentrations. AMB and miltefosine plasma samples were stored and transported at nominally -20°C.

Bioanalysis

Miltefosine DBS and plasma concentrations were quantified as described previously [21,22]. The lower limit of quantitation (LLOQ) was 10 ng/mL for the DBS assay and 4 ng/mL for the plasma assay. For the 20 paired plasma and DBS samples, the median difference between the analysed concentrations in DBS and plasma was -1.1%, ranging between -17.3% and +21.7%. Only one DBS concentration was outside the ±20% bias, indicating that >2/3 of samples were within the ±20% bias usually accepted for incurred sample re-analysis [23], when considering DBS concentrations to be identical to plasma concentrations.

ARV drug concentrations were quantified in DBS as previously described [24], with slight alterations. Only NNRTI (efavirenz and nevirapine) and PI (lopinavir and ritonavir) concentrations were analysed. Calibration standards and quality control samples were prepared in whole blood, adjusted to a haematocrit (Hct) of 30%±1% to mimic the typical Hct values in VL patients (as described previously for the miltefosine DBS method [21]). The effect of Hct on accuracy and precision of the method was evaluated and was acceptable from Hct 21-40% for efavirenz, nevirapine, and ritonavir, and 21-35% for lopinavir. The LLOQ was 0.1 μg/mL for efavirenz, nevirapine, and lopinavir and 0.05 μg/mL for ritonavir. Plasma concentrations of efavirenz and nevirapine were calculated from analysed DBS concentrations, as described in the clinical method validation, using analysed individual Hct values [25]. Lopinavir/ritonavir plasma concentrations were calculated with previously reported equations [26].

Total AMB plasma concentrations were analysed in a range from 0.5-100 μg/mL with liquid chromatography tandem mass spectrometry (LC-MS/MS). Sample pre-treatment involved protein precipitation by adding 1,000 μL methanol to 50 μL of plasma. After centrifugation, the supernatant was injected onto the LC-MS/MS system and chromatographic separation was performed on a Gemini C18 column (50 mm x 2.0 mm; Phenomenex, Torrance, CA, USA). Gradient elution was applied using mobile phase A 0.1% formic acid in water and mobile phase B 100% methanol in the following gradient: 30% B (0.2 mL/min, 0-0.45 min), 95% B (0.2 mL/min, 0.50-4.45 min), 30% B (0.4 mL/min, 4.50-6.0 min). Detection was performed on a triple quadruple mass spectrometer with turbo ion spray interface (API3000, Sciex, Framingham, MA, USA) in positive-ion mode with a total run time of 6.0 min. The measured transition was from 924.5 to 743.5. AMB peak areas were plotted against the corresponding nominal concentration and the linear regression was optimal with a $1/x^2$ weighting factor, where x is the analyte concentration. The analytical method was validated with good performance in terms of linearity, selectivity, accuracy (bias within ±8.9%), precision (CV% ≤8.9%), recovery, carry-over and matrix effect. AMB was found to be

3.4

stable for at least 15 months in plasma.

In addition, we evaluated whether the developed bioanalytical method accurately analysed the total AMB concentration, including the liposome encapsulated proportion. Water was added to 50 mg of AmBisome® (Gilead, Foster City, CA, USA) in the original vial, to a final concentration of 5 mg/mL AMB. Subsequently, control human K_2-EDTA plasma was spiked to concentrations of 1.5 and 75 µg/mL AMB and these samples were pre-treated as described previously. As bias was within ±15% and the coefficients of variation were below 15%, it could be concluded that the liposomal formulation had no effect on the accuracy and precision of this method.

Data analysis

Data analysis was performed in R (version 3.3.1), and R package "ggplot2" was used for the graphical presentation. Non-compartmental analysis (NCA) was performed with the R package "ncappc", and the C_{max} and area under the concentration-time curve (AUC) were reported. The AUC was calculated over different time spans for miltefosine and AMB.

For AMB, the first available time point is directly after infusion, therefore the AMB concentration at t=0 is set to zero, to integrate the AUC during infusion. The AUC is integrated between t=0 and t=24h (AUC_{0-24h}) on day 1 ($AUC_{D1,0-24h}$) and the last day of treatment ($AUC_{D24,0-24h}$/$AUC_{D11,0-24h}$). The accumulation of AMB was expressed as the D24/D1 (monotherapy) or D11/D1 (combination therapy) AUC_{0-24h} ratio, calculated by dividing the individual AUC_{0-24h} on the last treatment day by the individual AUC_{0-24h} on day 1.

For miltefosine, the AUC was calculated from day 0-28 (AUC_{0-D28}) and from day 0-210 ($AUC_{0-\infty}$). If day 210 concentrations were below the LLOQ, these concentrations were assumed to be zero for $AUC_{0-\infty}$ calculations.

To evaluate the effect of antileishmanial treatment on ARV drug exposure, the concentration change was calculated as the ratio of ARV drug concentration at the end of one antileishmanial treatment cycle divided by the ART concentration at the start of treatment. Therefore, patients not yet on ART on day 1 of antileishmanial treatment were excluded from this analysis.

Data are represented as median (interquartile range), unless indicated otherwise. For normally distributed variables, the two sample t-test was used when comparing groups with equal variances, and the Welsh two-sample t-test when comparing groups with unequal variances. In case of non-normal distribution, the Mann Whitney U-test was applied. In evaluating correlations, a linear regression was performed in R.

RESULTS

Demographics

Patient characteristics are depicted in Table 1. A total of 30 male HIV co-infected VL patients were included in the PK sub-study of this trial, of whom 10 patients were included in the monotherapy arm and 20 patients in the combination therapy arm.

At the start of antileishmanial treatment, 8 patients in the monotherapy arm and 15 patients in the combination therapy arm were already on ART (Supplementary table 1). At the end of antileishmanial treatment, all patients were on ART, the most common combination of which was TDF/3TC/EFV, administered to 23 of the 30 patients. Of the other seven patients, treatments included efavirenz (n=2), nevirapine (n=4) and lopinavir/ritonavir (n=1). For the

majority of patients already on ART before antileishmanial treatment, the total length of ART so far was available and ranged widely between 2 and 1937 days (median 346 days for patients receiving L-AMB and miltefosine combination therapy, median 244 days for patients receiving L-AMB monotherapy). During VL treatment (including extended treatment), ART was directly observed and no doses were missed during this period. No information is available on ART compliance after VL treatment.

In the monotherapy arm, three out of ten patients were cured at the end of one treatment cycle, two received rescue treatment and five received extended treatment. In

Table 1. Demographics and treatment information of study population.

Parameter	Total	Monotherapy L-AMB	Combination therapy L-AMB + MIL
Total no. of patients	30	10	20
Male patients [no. (%)]	30 (100)	10 (100)	20 (100)
Age (yr)	33 (27-45)	36 (27-45)	33 (28-44)
Body weight day 0 (kg)	47.0 (36.0-73.0)	48.5 (41.5-67.0)	46.5 (36.0-73.0)
Body weight day 28 (kg)	50.0 (35.0-75.0)	52.5 (37.0-70.5)	49.5 (35.0-75.0)
Height (cm)	170 (158-180)	170 (158-180)	170 (159-180)
Treatment outcome after one treatment cycle			
Cure [no. (%)]	13 (43)	3 (30)	10 (50)
Receive rescue treatment [no. (%)]	3 (10)	2 (20)	1 (5)
Receive extended treatment [no. (%)]	14 (47)	5 (50)	9 (45)
Treatment outcome after two treatment cycles			
Cure [no. (%)]	9 (30)	1 (10)	8 (40)
Rescue treatment [no. (%)]	5 (17)	4 (40)	1 (5)
Primary infection [no. (%)]	14 (47)	5 (50)	9 (45)
Secondary infection [no. (%)]	16 (53)	5 (50)	11 (55)
Previously treated with L-AMB	9	3	6
Previously treated with MIL	4	2	2
ART at start antileishmanial treatment [no. (%)]			
TDF-3TC-EFV (300/300/600mg)	15 (50)	7 (70)	8 (40)
Other treatments including EFV	3 (10)		3 (15)
Other treatments including NVP	4 (13)	1 (10)	3 (15)
Other treatments including LPV/r	1 (3)		1 (5)
No treatment	7 (23)	2 (20)	5 (25)
ART at end antileishmanial treatment [no. (%)]			
TDF-3TC-EFV (300/300/600 mg)	23 (77)	9 (90)	14 (70)
Other treatments including EFV	2 (7)		2 (10)
Other treatments including NVP	4 (13)	1 (10)	3 (15)
Other treatments including LPV/r	1 (3)		1 (5)

All values are given as median (range), unless stated otherwise. L-AMB: liposomal amphotericin B; MIL: miltefosine; EFV: efavirenz; NVP: nevirapine; LPV: lopinavir; RTV: ritonavir. TDF-EFV-3TC: tenofovir-efavirenz-lamuvidine

3.4.

combination therapy, ten out of 20 patients were cured at the end of one treatment cycle, one received rescue treatment and nine received extended treatment.

Amphotericin B pharmacokinetics

AMB concentrations on the first and last day of treatment were available for all 30 patients. One sample was above the upper limit of quantitation, but was included assuming linear extrapolation of the calibration curve. For three patients, day 1 samples were collected at 4, 8 and 26 hours after start of infusion and these samples were therefore excluded from the analysis.

Day 1 C_{max} was 24.6 µg/mL in a range from 12.4-66.1 µg/mL. Further exposure variables on both the first and last treatment day are described in Table 2. Median trough levels increased during treatment from 5.37 (2.45-9.05) to 10.1 (5.94-11.3) µg/mL for monotherapy, and from 2.20 (1.23-3.58) to 6.82 (3.79-14.2) µg/mL for the combination therapy. The D24/D1 AUC_{0-24h} ratio was 1.3 (1.1-1.6) for the monotherapy and the D11/D1 AUC_{0-24h} ratio 2.4 (1.5-3.8) for the combination therapy, though these cannot be directly compared due to differences in intermittent dosing time spans. There was no significant effect of weight on the accumulation (monotherapy p=0.48, combination therapy p=0.28). There was no significant difference in observed C_{max} on the first treatment day between patients already on ART at 24.1 (17.1-34.4) µg/mL compared to the seven patients not yet on ART at 28.3 (16.5-50.9) µg/mL. In addition,
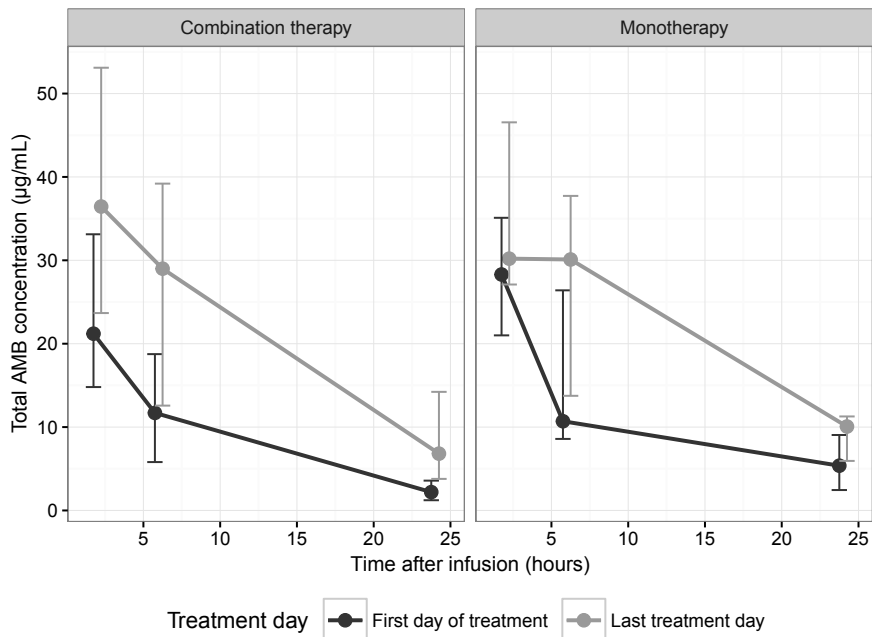

Figure 1. Median total amphotericin B (AMB) concentration on the first treatment day (black lines) for monotherapy (n=9) and combination therapy (n=18) and the last treatment day (light grey lines) for monotherapy (day 24, n=10) and combination therapy (day 11, n=20). Error bars indicate the interquartile-range (IQR).

Table 2. AMB median C$_{max}$ and AUC$_{0-24h}$ as output from NCA analysis.

	First treatment day		Last treatment day	
	Monotherapy	Combination therapy	Monotherapy	Combination therapy
C$_{max}$	28.3 (21.0-40.8)	21.2 (14.8-33.1)	33.2 (29.0-46.6)	40.9 (25.4-53.1)
AUC$_{0-24h}$	209 (173-570)	195 (114-305)	492 (271-587)	436 (240-696)
N=	9	18	10	20

Values expressed as median (interquartile range). There were no significant differences between treatment arms.

there were no significant differences in the C$_{max}$ nor AUC$_{0-24h}$ on the last treatment day for ART regimens including either efavirenz, nevirapine or lopinavir/ritonavir. No correlation between C$_{max}$ or AUC$_{0-24h}$ and weight could be observed.

Miltefosine pharmacokinetics

The average miltefosine dose received was 2.1 mg/kg (range 1.4-2.8 mg/kg). All pre-treatment miltefosine concentrations were below the LLOQ. All samples were correctly collected before the next miltefosine dose and can be considered pre-dose samples. Three samples with physiologically improbable values on day 210 (concentrations above 2,000 ng/mL) were excluded from the results. Day 210 concentrations were mostly below the LLOQ. For seven patients, day 210 concentrations were not available, and set to zero for AUC$_{0-\infty}$ calculations.

Figure 2 depicts the miltefosine concentration-time curves per patient, split for patients that were cured at the end of one treatment cycle and patients that were not (parasite
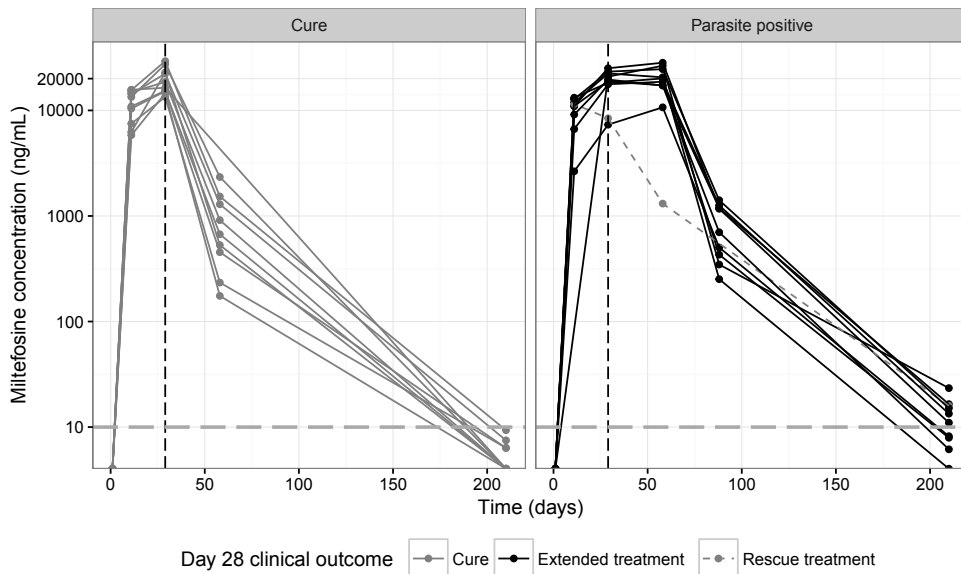

Figure 2. Miltefosine concentration-time curves for patients who were cured (left, n=10) and patients that were still parasitologically positive (right, n=10) at the end of one treatment cycle. The dashed vertical black line indicates the end of one treatment cycle (day 28) and the horizontal grey dashed line indicates the lower limit of quantitation of 10 ng/mL. Note that for the 10 patients who were parasitologically positive at day 28, one patient received rescue treatment (grey dashed line) and the others received an additional treatment cycle of the same regimen.

3.4

positive). Day 28 concentrations were 18,700 (15,400-22,500) ng/mL, without significant difference between patients that were cured (17,500 (15,300-22,800) ng/mL) and patients still parasitologically positive (19,200 (17,900-22,000) ng/mL) at the end of one treatment cycle, while receiving similar mg/kg dosages (2.2 (2.1-2.3) mg/kg versus 2.1 (2.0-2.4) mg/kg). Two patients showed particularly low miltefosine exposure with day 28 concentrations of 9,900 ng/mL and 7,270 ng/mL respectively, and both were still parasite positive at the end of one treatment cycle. During the second treatment cycle, miltefosine concentrations remained stable with a 20,100 (17,300-24,600) ng/mL concentration at the end of extended treatment. The AUC_{0-D28} was 314 (275-377) µg·day/mL and showed to be similar (p=0.36) between patients who were cured on day 28 at 330 (285-395) µg·day/mL and patients who were still parasitologically positive at 314 (263-364) µg·day/mL. $AUC_{0-\infty}$ was 524 (428-685) µg·day/mL for patients receiving one treatment cycle, and 1,066 (1,016-1,317) µg·day/mL for patients receiving two treatment cycles.

Figure 3 depicts the difference in day 28 miltefosine concentrations for patients treated with different ARV regimens. Median day 28 miltefosine concentrations were significantly higher for patients treated with nevirapine (25,100 ng/mL) compared to patients treated with efavirenz (18,000 ng/mL, p=0.04, two-sample t-test), but only three patients received nevirapine in the combination therapy arm. There was no difference in miltefosine day 28 concentration for the five patients who were not yet on ART at start of antileishmanial treatment, compared to the patients that were. No correlations were detected between dose/weight and C_{max}/AUC_{0-D28}.
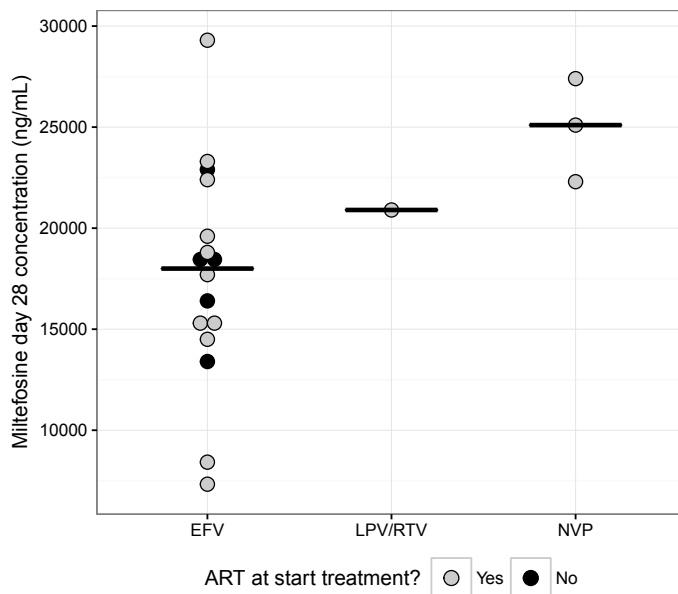
Figure 3. Day 28 miltefosine concentrations for patients treated with ART including either efavirenz (EFV, n=16), lopinavir/ritonavir (LPV/RTV, n=1) or nevirapine (NVP, n=3). Dots indicate the individual observations, in grey for patients already on ART at start of antileishmanial treatment and in black for patients who start ART during antileishmanial treatment (on day 11, 14, 16, 27 or 28). Horizontal blacklines indicate the median day 28 miltefosine concentrations per ARV drug.

Antileishmanial exposure in relation to treatment outcome

Only evaluating AMB exposure, considering either $AUC_{D1,0-24h}$, $AUC_{D11, 0-24h}$, $AUC_{D24, 0-24h}$, D24/D1 or D11/D1 AUC_{0-24h} ratio, there was no significant difference between patients cured at the end of the first antileishmanial treatment cycle and patients still parasite positive, for both the mono- and combination therapy group. As mentioned previously, there was no significant difference in miltefosine exposure between these groups either.

Figure 4 depicts the relationship between combined antileishmanial drug exposure and treatment outcome at the end of one combination therapy cycle (day 28). No correlation was detected between combined miltefosine and AMB exposure and treatment outcome.

While evaluating the D11/D1 AMB AUC_{0-24h} ratio as a measure of drug accumulation versus the miltefosine AUC_{0-D28}, a significant correlation between them was detected, though with high variability (p=0.0313, R^2=0.26, Figure 5). Since miltefosine slowly accumulates during treatment towards a steady-state concentration, miltefosine AUC_{0-D28} can be considered a measure of total miltefosine accumulation, indicating that patients with above median AMB accumulation also showed above median miltefosine accumulation.
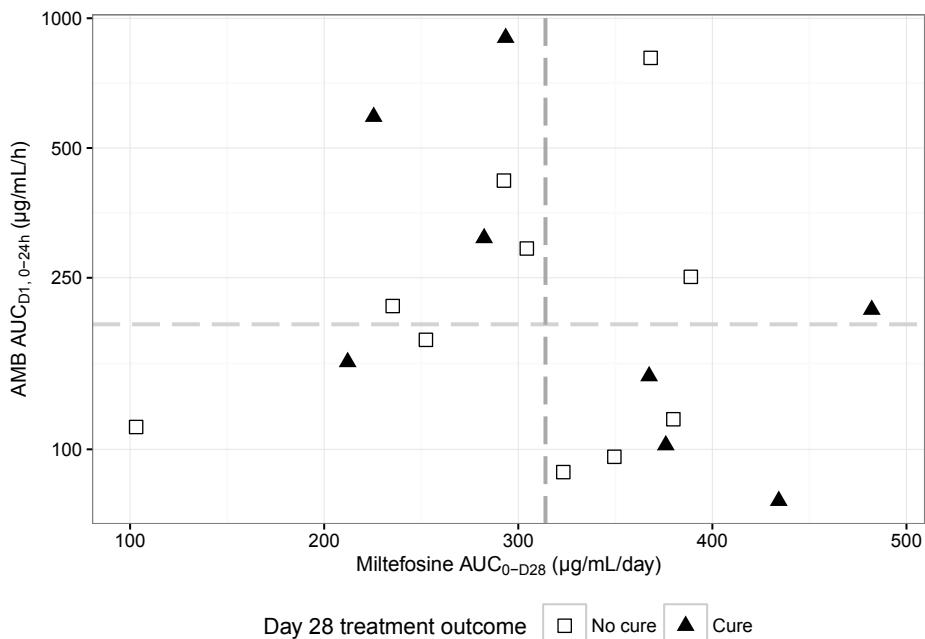
Figure 4. Individual observations of the area under the concentration-time curve (AUC) for miltefosine from day 0 to day 28 (AUC_{0-D28}) on the x-axis and the AUC of amphotericin B (AMB) from time 0 to 24 h on the first day of treatment ($AUC_{D1, 0-24 h}$) on the y-axis. Solid triangles indicate patients that were cured on day 28 and open squares indicate patients that were still parasitologically positive on day 28. The horizontal dashed line indicates the median AMB $AUC_{D1,0-24h}$ exposure at 195 µg/mL/h, while the vertical dashed line indicates the median miltefosine exposure AUC_{0-D28} at 314 µg/mL/day. Only 18 patients were included in this analysis, as two patients had distinct sampling schedules on day 1 and could therefore not be compared.
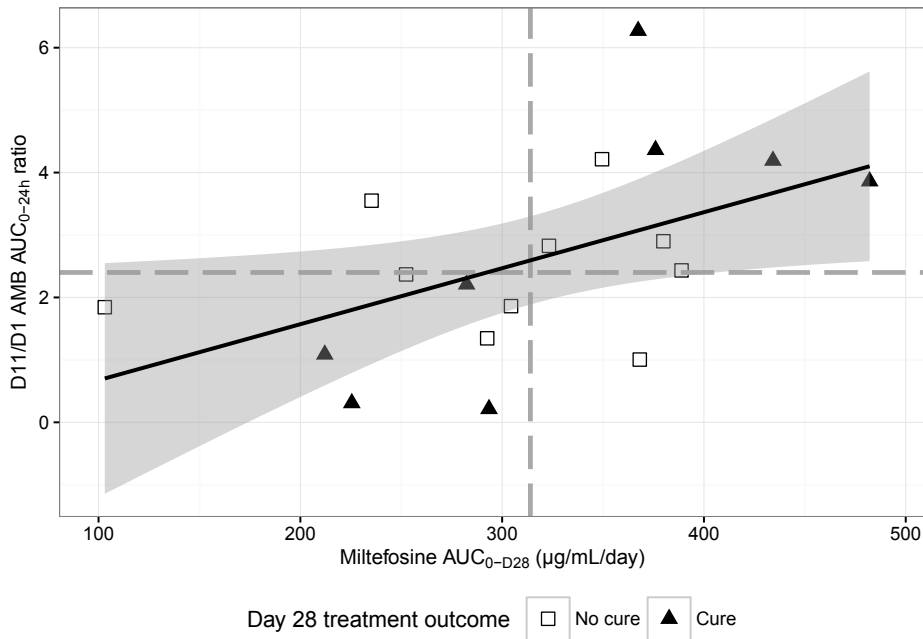
Figure 5. AMB accumulation is displayed on the y-axis as the D11/D1 AMB AUC$_{0-24h}$ ratio, and miltefosine exposure (miltefosine AUC$_{0-D28}$) on the x-axis. The black line indicates the linear regression line between the two (p=0.0313, R^2 = 0.26), and the grey shaded area the 95% confidence interval. Solid triangles indicate patients that were cured on day 28 of treatment, open squares indicate patients that were still parasitologically positive on day 28. The horizontal dashed line indicates the median D11/D1 AMB AUC$_{0-24h}$ ratio of 2.4, while the vertical dashed line depicts the median miltefosine exposure AUC$_{0-D28}$ at 314 µg/mL/day. Only 18 patients were included in this analysis, as two patient had distinct sampling schedules on day 1 and could therefore not be compared.

ARV drug concentrations during antileishmanial treatment

Peak samples were collected at 4.2 (range 3.2-4.7) h after dose, and all trough levels were collected at 0.1 (range 0.2-0) h before dosing.

Trough and peak plasma concentrations of efavirenz on the first and last antileishmanial treatment day of the first treatment regimen are depicted in Table 3 and Figure 6. Excluding the seven patients not yet on ART, the efavirenz concentration change during antileishmanial treatment was 0.81 (0.49-1.26) for peak and 1.10 (0.71-1.67) for trough levels, without significant differences between treatment arms. However, efavirenz trough levels in one monotherapy patient increased around two-fold from 3.4 to 6.7 µg/mL (and there was a similar increase in peak levels). For one combination therapy patient efavirenz trough levels decreased from 9.2 to 3.4 µg/mL.

Figure 7 shows the peak and trough levels of nevirapine. One combination therapy patient started ART on the first day of antileishmanial treatment (trough level of zero) and therefore both trough and peak levels increased during treatment. In general, nevirapine concentrations remained relatively stable, except for the L-AMB monotherapy patient, with a nevirapine trough concentration decreasing from 4.1 to 2.5 µg/mL (below the 3.4 µg/mL therapeutic target level [10]).

Table 3. Efavirenz peak and trough concentrations in combination and monotherapy, for those patients already treated with ART on the first day of antileishmanial treatment and those who started ART during treatment.

	Day	ART on first antileishmanial treatment day?	Total patients (no.)	Efavirenz trough level (µg/mL)	Efavirenz peak level (µg/mL)	Trough <1 µg/mL (no.)	Trough >4 µg/mL (no.)
Combination therapy	1	Yes	11	1.28 (0.65-2.66)	4.91 (2.97-5.32)	5	1
		No[c]	4	-	3.36 (2.69-3.97)	-	-
	28	Yes	10[b]	1.32 (0.98-1.97)	3.24 (2.50-4.56)	3	0
		No[c]	5	1.06 (0.58-1.76)	4.00 (3.16-4.62)	1	2
Monotherapy[a]	1	Yes	7	1.35 (1.08-1.86)	3.85 (2.73-4.22)	2	0
	24	Yes	7	1.83 (1.22-1.97)	4.60 (2.23-4.76)	2	1

Values are median (inter-quartile range), unless indicated otherwise.
[a]Two patients in monotherapy started ART on last day of antileishmanial treatment and were therefore not sampled during treatment
[b]One patient excluded as below LLOQ for both peak and trough level on day 28, possibly due to non-compliance
[c]Day 1 in these patients is the first day of ART, varying between patients between day 11 and 28 of antileishmanial treatment. For patient that started on day 28, the day 1 sample was not collected as day 1 and 28 coincide.
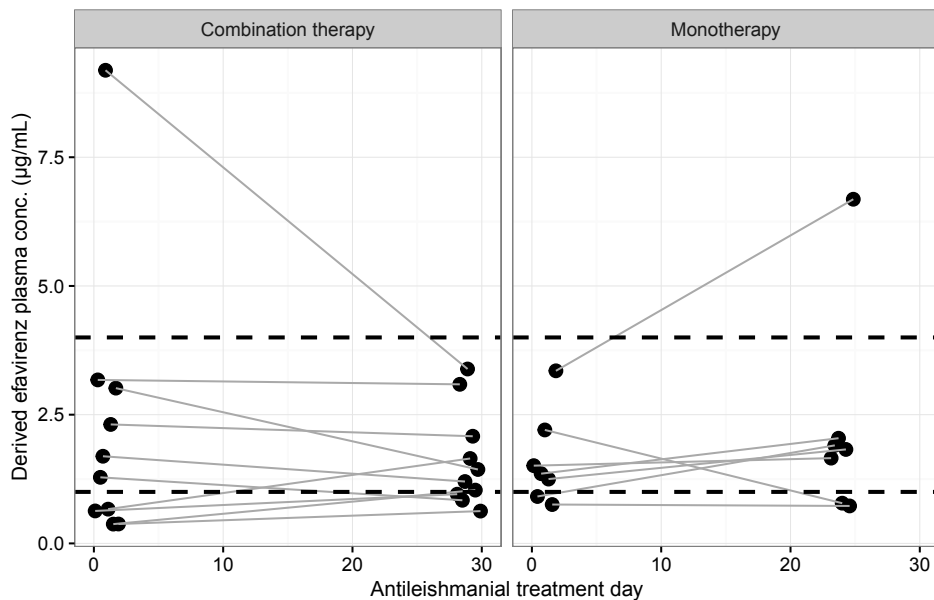
Figure 6. Efavirenz trough levels per patient at start and end of treatment for combination therapy (n=10) and monotherapy (n=7). Patients not yet on ART on the first antileishmanial treatment day were excluded, as was one combination therapy patient with undetectable efavirenz levels at end of treatment. The horizontal dashed black lines depict the 1-4 µg/mL therapeutic window previously described for efavirenz.

For the patient receiving lopinavir/ritonavir, the lopinavir trough concentration at start and end of treatment (7.7 and 4.3 µg/mL, respectively) were above the previously reported 4 µg/mL target [27]. Ritonavir trough levels also decreased during treatment from 0.33 µg/mL to 0.21 µg/mL.

3.4

Figure 7. Nevirapine peak and trough concentrations. Indicated with the black dashed line is the lower limit of the therapeutic window at 3.4 µg/mL. One patient in the combination therapy group started ART on the first day of antileishmanial treatment (trough level of zero).

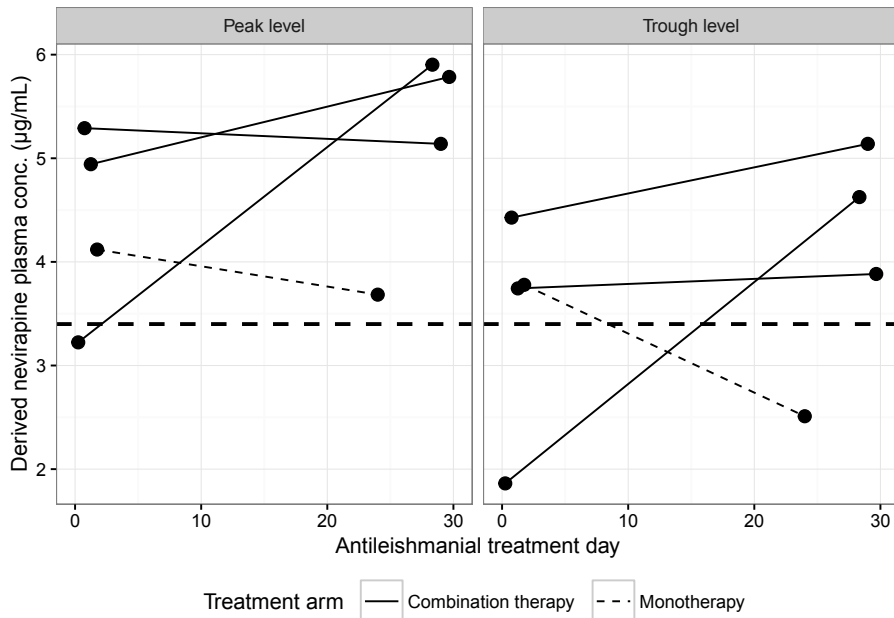## DISCUSSION

To our knowledge, this is the first study to characterize L-AMB PK in VL patients. Previous studies on L-AMB PK were performed either in healthy volunteers or patients with invasive fungal infections (described in Chapter 1). Total AMB exposure was lower than previously described. In the AmBisome® manufacturer's product monograph a C_{max} of 57.6±21.0 µg/mL (mean±SD) was reported after a single 5 mg/kg dose in 12 patients [28], compared to 24.6 (17.0-34.9) µg/mL in this trial. The value in the product monograph is in line with the reported 18.0-22.9 µg/mL after 2-3 mg/kg [13,29,30] and 75.9-95.5 µg/mL after 7.5 mg/kg [31,32], when dose-proportionality is assumed. The lower observed AMB exposure might be related to VL disease pathogenesis. Liposomes are cleared from the circulation by macrophages of the reticuloendothelial system (RES), mainly in the liver and spleen [33]. It could be hypothesized that clearance of AMB is affected by the increased liver macrophageal load leading to changes in drug distribution and possibly also an increased drug elimination. A potential (additional) HIV effect on L-AMB exposure also cannot be excluded. As there was no difference in day 1 AMB exposure between patients already on ART versus patients that were not, no drug-drug interaction between ARV drugs administered in this trial and AMB is expected.

For two patients on day 1 and three patients on the last treatment day, the AMB C_{max} was observed at six hours after start of infusion instead of the expected two hours after start of infusion. For one of these patients this could be explained by sample collection before the end of infusion (infusion time longer than two hours), but no justification could be found in

sampling or infusion time data for the other patients.

No significant relationship could be identified between L-AMB exposure and treatment outcome. As this is the first description of L-AMB PK in treatment of VL patients, it is still unknown what is the best approximation of AMB exposure at its target site. On the one hand, the active moiety of L-AMB in VL is unknown and can either be the free or liposomal encapsulated fraction. In addition, it is not yet established if and how plasma exposure correlates to target site exposure. It could be hypothesized that increased clearance by the RES organs liver and spleen could actually increase AMB exposure at its target site of action, while plasma levels are decreased. Furthermore, next to antileishmanial drug exposure, a multitude of other host- and parasitic factors could have influenced outcome, such as immunological disturbances caused by HIV.

While exposure was lower than previously described, the wide inter-individual variability in observed concentrations is in line with previous L-AMB PK studies, and has been previously explained by inter-individual variability in liposomal uptake into tissue compartments or differences in AMB release from the liposome carrier [29,30,34]. As has been documented previously, accumulation was observed upon multiple dosing [29]. No significant differences were observed in the C_{max} or AUC_{0-24h} on the last treatment day between monotherapy and combination therapy, although the interpretation is hampered by between-treatment differences in dosing intervals and high inter-patient variability.

Multiple AMB population PK models described body weight as a covariate on clearance and volume of distribution [29,34–36]. No correlation, however, could be observed between C_{max}, AUC_{0-24h} nor D24/D1 or D11/D1 AUC_{0-24h} ratio and weight in our descriptive analysis, possibly due to the narrow range of patients' body weights in this trial.

The median miltefosine day 28 concentration of 18,700 (15,400-22,500) ng/mL was approximately 35% lower than the reported concentrations of around 30,000 ng/mL [37,38], and the miltefosine AUC_{0-D28} of 314 (275-377) µg·day/mL was 37% lower compared to the previously observed 497 (191-767) µg·day/mL in other adult Eastern African VL patients [8]. Though it should be noted that in previous studies miltefosine exposure was determined in plasma matrix instead of DBS, clinical validation of the bioanalytical method showed that analyzed miltefosine concentrations in DBS were only 1.1% lower than analyzed plasma concentrations, indicating that this effect is negligible.

The lowered miltefosine exposure could partially be attributed to the flat dosing of 50 mg miltefosine twice daily, which corresponded to a 2.1 mg/kg/day dose (range 1.4-2.8 mg/kg), 19% lower than the 2.6 mg/kg/day administered in the previously reported PK study in adult VL patients in Eastern Africa [8,39]. Body weight (or fat-free mass) has previously been reported to be a scaled covariate on clearance and volume of distribution [7,38]. However, as patients received a flat 100 mg/day dose, patients with a lower body weight consequently received a higher mg/kg/day dose, possibly obscuring the effect of body weight on exposure in this descriptive analysis.

The observed 24,900 ng/mL day 28 miltefosine concentration for patients receiving ART including nevirapine is in line with reported values, considering the 19% lower dose. The significantly lower 17,600 ng/mL day 28 miltefosine concentration for patients treated with ART including efavirenz, could imply a potential effect of efavirenz on miltefosine accumulation. However, given the small sample size, only cautious hypotheses can be formulated regarding this possible interaction.

It is possible that the highly protein-bound (99.5%) efavirenz competes with

3.4

miltefosine for binding the already lowered VL patient albumin levels, while this competition could be less marked for nevirapine (60% protein-bound). Additionally, there could be differences between ARV drugs in P-glycoprotein (P-gp) transporter induction, potentially influencing miltefosine exposure, as intracellular miltefosine concentrations were found to be significantly and reversely correlated with MDR1 gene expression [40]. Similar levels of upregulation of P-gp expression have been observed *in vitro* with much lower levels of efavirenz compared to nevirapine [41].

While lower miltefosine exposure has previously been related to a lower probability of cure in VL [7], no such effect was observed in this study, possibly due to a combination of the small number of patients in the study and the multitude of factors besides drug exposure determining treatment response, especially in immunosuppressed HIV/VL co-infected patients. However, one patient whose miltefosine concentration declined 27% between day 11 and day 28 (8,420 ng/mL on day 28, 55% lower than the population median, see Figure 2), received rescue treatment after one treatment cycle. This patient showed a weight decrease from 48 to 39 kg during treatment, indicating a worsened clinical condition, possibly resulting in lower absorption and bioavailability.

Though no correlation could be found between treatment outcome and combined exposure to AMB and miltefosine, a significant correlation between AMB and miltefosine accumulation was observed which has not been described previously. This correlation might be caused by similar distribution patterns and mechanisms for both L-AMB and miltefosine. Furthermore, an additional effect could be hypothesized to result from free AMB accumulation within miltefosine micelles when concentrations are above the critical micelle concentration of 11.1 μM (4.5 μg/mL), as reported previously *in vitro* [20]. However, as both the free fraction of miltefosine and AMB are small [14,15], this effect is probably negligible. Additionally, it could be envisaged that miltefosine micelles and AMB liposomal carriers fuse, altering their composition and possibly influencing their clearance. Liposome clearance in the liver has been found to be largely dependent on liposome composition such as size, charge and headgroup composition [42].

Efavirenz concentrations on the first day of antileishmanial treatment were similar to the previously reported trough concentration of 1.21 (0.83-1.86) in a large Ethiopian population (n=215) [43]. The therapeutic window of efavirenz between 1-4 μg/mL is well defined, with higher risk of treatment failure when efavirenz trough concentrations are below 1 μg/mL and increased risk of neuropsychiatric adverse reactions with peak concentrations above 4 μg/mL [9,10]. A large proportion of patients showed efavirenz concentrations below 1 μg/mL, which was observed previously as well for non-VL patients [43], but this proportion did not change upon antileishmanial treatment. In general, no profound effect of antileishmanial treatment could be observed on efavirenz or nevirapine concentrations, but exceptions were observed at an individual patient level.

CONCLUSION

To our knowledge, this study is the first describing the PK of concomitantly administered miltefosine, L-AMB and ARV drugs in HIV co-infected VL patients. Both AMB and miltefosine exposure were lower than previously observed. The lowered AMB exposure could potentially be caused by a change in clearance due to altered liver physiology in VL, as its PK has never been studied in VL patients. The lower miltefosine exposure can partially, but not exclusively,

be attributed to the 19% lower dosing and possibly indicate that a higher dose should be considered to achieve equivalent exposure as previously found in Eastern African adult VL patients, since miltefosine exposure has previously been found to be significantly associated to treatment outcome. The lower than expected antileishmanial drug exposure of both L-AMB and miltefosine emphasizes the importance of investigating the PK of co-administered antileishmanial and ART drugs in these specifically vulnerable patients. Adequate drug exposure in these HIV co-infected patients is of utmost importance to avoid drug resistance, as relapse frequencies are especially high in this population with limited treatment options.

3.4

REFERENCES

1. Alvar J, Aparicio P, Aseffa A, Den Boer M, Cañavate C, Dedet JP, et al. The relationship between leishmaniasis and AIDS: The second 10 years. Clin. Microbiol. Rev. 2008;21:334–59.

2. Ritmeijer K, Veeken H, Melaku Y, Leal G, Amsalu R, Seaman J, et al. Ethiopian visceral leishmaniasis: Generic and proprietary sodium stibogluconate are equivalent; HIV co-infected patients have a poor outcome. Trans. R. Soc. Trop. Med. Hyg. 2001;95:668–72.

3. Simpson JA, Zaloumis S, DeLivera AM, Price RN, McCaw JM. Making the most of clinical data: reviewing the role of pharmacokinetic-pharmacodynamic models of anti-malarial drugs. AAPS J. 2014;16:962–74.

4. Mouton JW, Brown DFJ, Apfalter P, Cantón R, Giske CG, Ivanova M, et al. The role of pharmacokinetics/pharmacodynamics in setting clinical MIC breakpoints: The EUCAST approach. Clin. Microbiol. Infect. 2012;18:E37–45.

5. Pagkalis S, Mantadakis E, Mavros MN, Ammari C, Falagas ME. Pharmacological considerations for the proper clinical use of aminoglycosides. Drugs. 2011;71:2277–94.

6. Alsultan A, Peloquin CA. Therapeutic drug monitoring in the treatment of tuberculosis: An update. Drugs. 2014;74:839–54.

7. Dorlo TPC, Rijal S, Ostyn B, De Vries PJ, Singh R, Bhattarai N, et al. Failure of miltefosine in visceral leishmaniasis is associated with low drug exposure. J. Infect. Dis. 2014;210:146–53.

8. Dorlo TPC, Kip AE, Younis BM, Ellis SE, Alves F, Beijnen JH, et al. Reduced miltefosine exposure in East African visceral leishmaniasis patients affects the time to relapse of infection. 2017; Submitted for publication.

9. Marzolini C, Telenti A, Decosterd LA, Greub G, Biollaz J, Buclin T. Efavirenz plasma levels can predict treatment failure and central nervous system side effects in HIV-1-infected patients. AIDS. 2001;15:71–5.

10. Dahri K, Ensom MHH. Efavirenz and nevirapine in HIV-1 infection: is there a role for clinical pharmacokinetic monitoring? Clin. Pharmacokinet. 2007;46:109–32.

11. Tittle V, Bull L, Boffito M, Nwokolo N. Pharmacokinetic and pharmacodynamic drug interactions between antiretrovirals and oral contraceptives. Clin. Pharmacokinet. 2015;54:23–34.

12. Inselmann G, Inselmann U, Heidemann HT. Amphotericin B and liver function. Eur. J. Intern. Med. 2002;13:288–92.

13. Bekersky I, Fielding RM, Dressler DE, Lee W, Buell DN, Walsh TJ, et al. Pharmacokinetics, excretion, and mass balance of liposomal amphotericin B (AmBisome) and amphotericin B deoxycholate in humans. Antimicrob. Agents Chemother. 2002;46:828–33.

14. Bekersky I, Fielding RM, Dressler DE, Lee JW, Buell DN, Walsh TJ. Plasma protein binding of amphotericin B and pharmacokinetics of bound versus unbound amphotericin B after administration of intravenous liposomal amphotericin B (AmBisome) and amphotericin B deoxycholate. Antimicrob. Agents Chemother. 2002;46:834–40.

15. Dorlo TPC, Balasegaram M, Beijnen JH, de vries PJ. Miltefosine: A review of its pharmacology and therapeutic efficacy in the treatment of leishmaniasis. J. Antimicrob. Chemother. 2012;67:2576–97.

16. Boffito M, Back DJ, Blaschke TF, Rowland M, Bertz RJ, Gerber JG, et al. Protein binding in antiretroviral therapies. AIDS Res. Hum. Retroviruses. 2003;19:825–35.

17. Lima Maciel BL, Lacerda HG, Queiroz JW, Galvão J, Pontes NN, Dimenstein R, et al. Association of nutritional status with the response to infection with *Leishmania chagasi*. Am. J. Trop. Med. Hyg. 2008;79:591–8.

18. Gomes CMC, Giannella-Neto D, Gama MEA, Pereira JCR, Campos MB, Corbett CEP. Correlation between the components of the insulin-like growth factor I system, nutritional status and visceral leishmaniasis. Trans. R. Soc. Trop. Med. Hyg. 2007;101:660–7.

19. Libório AB, Rocha NA, Oliveira MJC, Franco LFLG, Aguiar GBR, Pimentel RS, et al. Acute kidney injury in children with visceral leishmaniasis. Pediatr. Infect. Dis. J. 2012;31:451–4.

20. Ménez C, Legrand P, Rosilio V, Lesieur S, Barratt G. Physicochemical characterization of molecular assemblies of miltefosine and amphotericin B. Mol. Pharm. 2006;4:281–8.

21. Kip AE, Rosing H, Hillebrand MJX, Blesson S, Mengesha B, Diro E, et al. Validation and clinical evaluation of a novel method to measure miltefosine in leishmaniasis patients using dried blood spot sample collection. Antimicrob. Agents Chemother. 2016;60:2081–9.

22. Dorlo TPC, Hillebrand MJX, Rosing H, Eggelte TA, de Vries PJ, Beijnen JH. Development and validation of a quantitative assay for the measurement of miltefosine in human plasma by liquid chromatography-tandem mass spectrometry. J. Chromatogr. B. Analyt. Technol. Biomed. Life Sci. 2008;865:55–62.

23. European Medicines Agency. Guideline on bioanalytical method validation. Committee for Medicinal Products for Human Use and European Medicines Agency. 2011. http://www.ema.europa.eu/docs/en_GB/document_library/Scientific_guideline/2011/08/WC500109686.pdf. Accessed 17 Feb 2017.

24. ter Heine R, Rosing H, van Gorp ECM, Mulder JW, van der Steeg WA, Beijnen JH, et al. Quantification of protease inhibitors and non-nucleoside reverse transcriptase inhibitors in dried blood spots by liquid chromatography-triple quadrupole mass spectrometry. J. Chromatogr. B Anal. Technol. Biomed. Life Sci. 2008;867:205–12.

25. Kromdijk W, Mulder JW, Rosing H, Smit PM, Beijnen JH, Huitema ADR. Use of dried blood spots for the determination of plasma concentrations of nevirapine and efavirenz. J. Antimicrob. Chemother. 2012;67:1211–6.

26. Meesters RJW, Van Kampen JJA, Reedijk ML, Scheuer RD, Dekker LJM, Burger DM, et al. Ultrafast and high-throughput mass spectrometric assay for therapeutic drug monitoring of antiretroviral drugs in pediatric HIV-1 infection applying dried blood spots. Anal. Bioanal. Chem. 2010;398:319–28.

27. Breilh D, Pellegrin I, Rouzes A, Berthoin K, Xuereb F, Budzinski H, et al. Virological, intracellular and plasma pharmacological parameters predicting response to lopinavir/ritonavir (KALEPHAR Study). Aids. 2004;18:1305–10.

28. Astellas Pharma Canada Inc. Product Monograph. 2009. http://www.astellas.ca/pdf/en/monograph/2009-03-07. Accessed 20 Dec 2016.

29. Ohata Y, Tomita Y, Suzuki K, Maniwa T, Yano Y, Sunakawa K. Pharmacokinetic evaluation of liposomal amphotericin B (L-AMB) in patients with invasive fungal infection: Population approach in Japanese pediatrics. Drug Metab. Pharmacokinet. 2015;30:400–9.

30. Würthwein G, Young C, Lanvers-Kaminsky C, Hempel G, Trame MN, Schwerdtfeger R, et al. Population pharmacokinetics of liposomal amphotericin B and caspofungin in allogeneic hematopoietic stem cell recipients. Antimicrob. Agents Chemother. 2012;56:536–43.

31. Walsh TJ, Goodman JL, Pappas P, Bekersky I, Buell DN, Roden M, et al. Safety, tolerance and pharmacokinetics of high-dose liposomal amphotericin B (AmBisome) in patients infected with Aspergillus species and other filamentous fungi: maximum tolerated dose study. Antimicrob. Agents Chemother. 2001;45:3487–96.

32. Gubbins PO, Amsden JR, McConnell SA, Anaissie EJ. Pharmacokinetics and buccal mucosal concentrations of a 15 milligram per kilogram of body weight total dose of liposomal amphotericin B administered as a single dose (15 mg/kg), weekly dose (7.5 mg/kg), or daily dose (1 mg/kg) in peripheral stem cell tran. Antimicrob. Agents Chemother. 2009;53:3664–74.

33. Gregoriadis G. Overview of liposomes. J. Antimicrob. Chemother. 1991;28:39–48.

34. Hong Y, Nath CE, Yadav SP, Stephen KR, Earl JW, Mclachlan AJ. Population pharmacokinetics of liposomal amphotericin B in pediatric patients with malignant diseases. Antimicrob. Agents Chemother. 2006;50:935–42.

35. Hope WW, Goodwin J, Felton TW, Ellis M, Stevens DA. Population pharmacokinetics of conventional and intermittent dosing of liposomal amphotericin B in adults: A first critical step for rational design of innovative regimens. Antimicrob. Agents Chemother. 2012;56:5303–8.

36. Lestner JM, Groll AH, Aljayyoussi G, Seibel NL, Shad A, Gonzalez C, et al. Population pharmacokinetics of liposomal amphotericin B in immunocompromised children. Antimicrob. Agents Chemother. 2016;60:7340–6.

37. Dorlo TPC, van Thiel PPAM, Huitema ADR, Keizer RJ, de Vries HJC, Beijnen JH, et al. Pharmacokinetics of miltefosine in Old World cutaneous leishmaniasis patients. Antimicrob. Agents Chemother. 2008;52:2855–60.

38. Dorlo TPC, Huitema ADR, Beijnen JH, De Vries PJ. Optimal dosing of miltefosine in children and adults with visceral leishmaniasis. Antimicrob. Agents Chemother. 2012;56:3864–72.

39. Wasunna M, Njenga S, Balasegaram M, Alexander N, Omollo R, Edwards T, et al. Efficacy and safety of AmBisome in combination with sodium stibogluconate or miltefosine and miltefosine monotherapy for African visceral leishmaniasis: phase II randomized trial. PLoS Negl. Trop. Dis. 2016;10:e0004880.

40. Dohmen LCT, Navas A, Vargas DA, Gregory DJ, Kip AE, Dorlo TPC, et al. Functional validation of ABCA3 as a miltefosine transporter in human macrophages: impact on intracellular survival of leishmania (viannia) panamensis. J. Biol. Chem. 2016;291:9638–47.

41. Weiss J, Weis N, Ketabi-Kiyanvash N, Storch CH, Haefeli WE. Comparison of the induction of P-glycoprotein activity by nucleotide, nucleoside, and non-nucleoside reverse transcriptase inhibitors. Eur. J. Pharmacol. 2008;579:104–9.

42. Scherphof GL, Kamps JAAM. The role of hepatocytes in the clearance of liposomes from the blood circulation. Prog. Lipid Res. 2001;40:149–66.

43. Ngaimisi E, Habtewold A, Minzi O, Makonnen E, Mugusi S, Amogne W, et al. Importance of Ethnicity, CYP2B6 and ABCB1 Genotype for efavirenz pharmacokinetics and treatment outcomes: a parallel-group prospective cohort study in two Sub-saharan Africa populations. PLoS One. 2013;8: e67946.

3.4

Supplementary table 1. Specific ART regimens administered to patients at start and at end of antileishmanial treatment.

ART regimen	Dose	Patients on ART regimen at start antileishmanial treatment		Patients on ART regimen at end antileishmanial treatment	
		Monotherapy	Combination therapy	Monotherapy	Combination therapy
Total number of patients (no.)		10	20	10	20
Total number of patients on ART (no.)		8	15	10	20
TDF- 3TC-EFV	300/300/600 mg	7	8	9[b]	14
TDF- 3TC-NVP	300 mg OD/300 mg OD/200 mg BID		1		1
AZT- 3TC-EFV	300 mg BID/300 mg OD /600 mg OD		2[a]		1
AZT- 3TC-NVP	150/150/280 mg BID	1		1	
	300/150/200vmg BID		1		1
	600 mg OD/300 mg OD/200 mg BID		1		1
ABC-3TC-EFV	600/300/600 mg		1		1
ABC/3TC/LPV/r	600/300/400/100 mg		1		1
Not on ART (no.)		2[b]	5[c]		

BID = bi-daily, OD = once-daily, TDF = tenofovir, EFV = efavirenz, 3TC = lamivudine, NVP = nevirapine, AZT = zidovudine, ABC = abacavir, LPV/r = lopinavir+ritonavir
[a]One patients switched to TDF -3TC-EFV (300/300/600 mg) on day 18 of antileishmanial treatment
[b]Both patients not on ART at start of antileishmanial treatment started with TDF -3TC-EFV (300/300/600 mg) on day 23 of antileishmanial treatment
[c]All five patients not on ART at start of antileishmanial treatment started with TDF -3TC-EFV (300/300/600 mg) between day 11 and day 28 of antileishmanial treatment

3.4.

Chapter **4**

| Clinical
pharmacodynamics

Chapter 4.1

Systematic review of biomarkers
to monitor therapeutic response
in leishmaniasis

A.E. Kip
M. Balasegaram
J.H. Beijnen
J.H.M. Schellens
P.J. de Vries
T.P.C. Dorlo

ABSTRACT

Recently, there has been a renewed interest in the development of new drugs for the treatment of leishmaniasis. This has spurred the need for pharmacodynamic markers to monitor and compare therapies specifically for visceral leishmaniasis, in which the primary recrudescence of parasites is a particularly long-term event that remains difficult to predict. We performed a systematic review of studies evaluating biomarkers in human patients with visceral, cutaneous, and post-kala-azar dermal leishmaniasis, which yielded a total of 170 studies in which 53 potential pharmacodynamic biomarkers were identified. In conclusion, the large majority of these biomarkers constituted universal indirect markers of activation and subsequent waning of cellular immunity and therefore lacked specificity. Macrophage-related markers demonstrate favorable sensitivity and times to normalcy, but more evidence is required to establish a link between these markers and clinical outcome. Most promising are the markers directly related to the parasite burden, but future effort should be focused on optimization of molecular or antigenic targets to increase the sensitivity of these markers. In general, future research should focus on the longitudinal evaluation of the pharmacodynamic biomarkers during treatment, with an emphasis on the correlation of studied biomarkers and clinical parameters.

INTRODUCTION

Significant progress has been made the past few decades in our understanding of the pathophysiology and immunological mechanisms involved in the fatal parasitic infection visceral leishmaniasis (VL) and its dermal counterpart, cutaneous leishmaniasis (CL). Despite this progress, these scientific efforts have not directly led to new and better treatment options for patients suffering from these neglected tropical diseases. Fortunately, public interest and momentum in drug discovery and development for the leishmaniases have been renewed, which is substantiated, for instance, by the Drugs for Neglected Diseases *initiative* (DND*i*) in the last decade [1,2]. This renewed interest stipulates the need for more modalities to compare and monitor therapeutic interventions.

Classical clinical features used to evaluate individual treatment responses of patients with VL include the normalization of spleen/liver size, defervescence, and the normalization of blood cell counts (as an indicator of recovering bone marrow). Likewise, for CL, the sizes of the inner and outer borders of cutaneous lesions are used as proxy determinants of parasite biomass, although reepithelialization, crustation, and a multiplicity of skin lesions complicate interpretation. These individual clinical features are, however, rarely used in the quantitative comparison of antileishmanial therapies in the context of a clinical trial. Within such trials, the current standard confirmation of initial cure for VL is a Leishmania-negative spleen or bone marrow aspirate confirmed by microscopy, a very invasive semiquantitative technique which cannot be regularly repeated [3–7]. For CL, the confirmation of initial cure is much less clear: most clinical trials have defined "cure" as the absence of all inflammatory signs (skin edema and/or hardening) and complete scarring or reepithelialization of ulcerative lesions at the 3-month follow-up [8–10].

For both VL and CL, confirmation of a final cure as a primary endpoint is even more complicated by the long time periods between initial cure and recrudescence of parasites, requiring long follow-up periods (up to 6 or 12 months) to establish final cure [11]. Parasite recrudescence is a rare and slow-developing event which is difficult to predict, mainly because little is known about the causes or risk factors. To compare the efficacies of treatment regimens, sensitive and specific markers that correlate with treatment effect and can predict long-term clinical outcome, by noninvasive sampling methods, are urgently needed.

The general definition of biomarkers, a neologism for "biological markers," was previously established by the working group on biomarkers of the U.S. National Institutes of Health (NIH) as "a characteristic that is objectively measured and evaluated as an indicator of normal biological processes, pathogenic processes, or pharmacological responses to a therapeutic intervention" [12]. The use of biomarkers as surrogate endpoints in trials for leishmaniasis may have several possible advantages. First, they can be used for additional (earlier) analyses because primary clinical endpoints are both sparse and available only after a very long period of follow-up. Second, biomarker measurements are faster and less invasive than conventional clinical evaluations. Third, the use of biomarkers may allow the design of smaller, more efficient clinical studies, thereby speeding up the regulatory evaluation and approval of drugs [13]. This systematic review focuses on the identification and evaluation of biomarkers to monitor treatment response in cases of VL, CL, and post-kala-azar dermal leishmaniasis (PKDL), with a focus on the pharmacodynamic potential of these biomarkers to be used in comparative clinical trials. To our knowledge, this is the first systematic review of biomarkers in leishmaniasis.

4.1

METHODS

Literature search strategy

Potential biomarkers for VL, CL, and PKDL were identified by a primary-literature search performed using PRISMA (Preferred Reporting Items for Systematic Reviews and Meta-Analyses) guidelines, querying the PubMed database, restricted to the English language, as follows: "(((Leishmaniasis[title]) or Kala-azar[title]) or PKDL[title]) and (((((((((biomarker) or biomarkers) or marker) or markers) or level) or levels) or concentration) or activity) or profile)." This electronic search was performed from November 2013 to August 2014, and the date last searched was 19 August 2014. Results were screened manually to identify relevant publications based on title and/or abstract. Publications that did not focus on the identification or evaluation of biomarkers were excluded. Selected publications were then evaluated according to the exclusion criteria as described in Table 1. If the abstract did not clearly indicate whether a study met the initial inclusion criteria, the entire publication was assessed. Secondary literature was subsequently identified using references from the identified primary literature and related publications on PubMed and by specifically querying PubMed using the term of the identified biomarker in combination with "Leishmaniasis" and/or "Kala-azar".

Table 1. Exclusion criteria.

Exclusion criteria	Rationale
Method uses *ex vivo* assays	*Ex vivo* growth of cells is not feasible in practice, and the link with clinical relevance is unclear
Assay is nonquantitative	Quantitation necessary for pharmacodynamic applicability
Sampling methods are invasive (e.g., splenic aspirate, high blood volumes)	Not feasible/cannot be done repetitively
Genetic markers are associated with drug resistance	Cannot be used to monitor treatment response during treatment
Genetic markers are associated with susceptibility to leishmaniasis	Not in scope of this article
No comparison with healthy controls	No information on " healthy levels"
Other	Not relevant to the topic for various reasons

Evaluation criteria

The biological and clinical pharmacodynamic potential of biomarkers was evaluated based on five criteria: (i) time to normalcy, i.e., the time needed for the biomarker level to regress to healthy/control levels; (ii) specificity, in relation to concomitant (infectious) diseases, such as malaria and HIV; (iii) sensitivity, the marker's quantitation in (treated) patients compared to that in healthy controls and its association with treatment cure or failure; (iv) additional sensitivity, i.e., further assessment of sensitivity by more in-depth association of the marker's quantitation to standard clinical markers of disease, such as spleen and lesion size; and (v) geographical applicability. Biomarkers were given a score (−/+/++/?) for each criterion as further explained in Table 2.

Table 2. Criteria to evaluate the pharmacodynamic potential of biomarkers.

Criterium	Reason for score of:			
	-	+	++	?
Regression to normalcy	Occurs >1 mo after treatment	Occurs within 1 mo after treatment	Occurs within treatment period	Unknown
Specificity	The biomarker lacks specificity when coinfections are present	The biomarker is specific for leishmaniasis with at least 1 coinfection (e.g., HIV)	The biomarker is specific for leishmaniasis with >1 coinfection	The biomarker is not tested in coinfected patients
Sensitivity (quantitative comparison of marker levels)	Marker levels are not significantly different from those of healthy controls	Marker levels are significantly different from those of healthy controls	Marker levels are shown to reflect treatment outcome (e.g., there are significant differences between levels in refractory and recovered patients)	Marker levels are not compared to those of healthy controls
Additional sensitivity (correlation with clinical markers)	Marker levels show no correlation with clinical parameters	Markers show correlation with other biomarkers (e.g., IL-10 levels or comparable)	Markers show correlation with clinical parameters (e.g., spleen size)	Clinical correlation is not tested
Geographical applicability	There is contradicting evidence from different countries/regions	There is confirmed evidence from >1 country	There is confirmed evidence from >1 continent	Not tested in multiple countries

RESULTS

Literature search
The primary-literature search identified 1,875 studies for which the titles were screened and assessed for eligibility. 1,547 records were found to be nonrelevant and excluded. Thereafter, abstracts and, subsequently, the full text of the remaining studies were assessed for their eligibility; 133 articles were eventually included in this systematic review. Thirty-seven studies were additionally identified through a secondary-literature search (Figure 1).

Identified biomarkers
Fifty-three potential biomarkers were identified for VL, CL, and PKDL and are summarized in Supplementary table 1. The identified biomarkers were grouped into (a) direct markers of parasite biomass, such as parasite DNA/RNA detection and antigen-based detection, and (b) indirect markers, such as macrophage-related markers, cytokines, receptors, acute-phase proteins, and other biomarkers. Biomarkers are further discussed in this section only if they demonstrate promising potential based on the evaluation criteria (>4+). Antibodies were excluded from Supplementary table 1 because of their long elimination half-lives ("Antibody detection", p. 190).

4.1
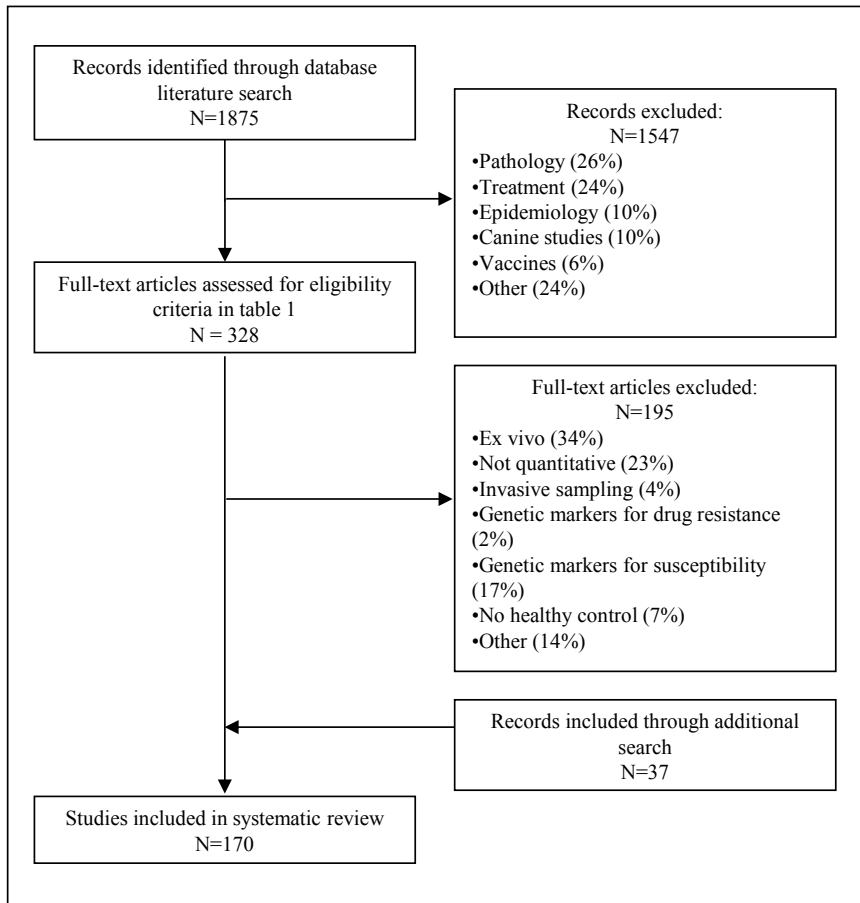
Figure 1. Study flow diagram.

<u>Direct markers</u>

Parasite detection
Assessing the viable parasite load within a patient is probably the most direct marker of disease status for leishmaniasis, and assessing the reduction of the viable parasite biomass would allow for exact monitoring of the therapeutic response. Several target genes have been identified and used for the molecular identification and quantification of *Leishmania* in clinical samples, including kinetoplast DNA (kDNA, both mini- and maxicircles), small-subunit (SSU) RNA, such as 18S rRNA, and 7SL RNA. For VL patients, the measurement of the *Leishmania* parasite load in blood using quantitative PCR (qPCR) has been evaluated mainly for diagnosis but also as a proxy value of the overall parasite load and clinical response during and after treatment [14–26]. The parasite load in blood rapidly decreases upon initiation of treatment, in parallel with clinical improvement [14–17]. qPCR of blood of East African VL patients reflected differences in treatment responses to different AmBisome dosages [27], however, the sensitivity of the assay was lower than for Indian VL patients [28].

For CL, the parasite burden is localized and confined to the upper layer of the dermis, in which it is probably homogenously spread in the inflammatory zone that surrounds the necrotic ulcer [29]. Confirmation of parasites by microscopy or, if available, PCR-based techniques from lesion biopsy specimens or scrapings is currently the diagnostic practice for CL [30–36]. Quantitation of parasite RNA in repeated lesion biopsy specimens has been demonstrated as a technique to assess the parasite burden in CL lesions [35,37]. Treatment response was quantified in CL patients, demonstrating declines in *Leishmania major* parasite loads of ~1 log/week after initiation of miltefosine treatment, which paralleled clinical improvement [29]. Swabbing of lesions, which is less invasive than biopsy, was performed to determine whether parasite DNA/RNA loads were diagnostic for CL, and the sensitivity was around 90% [38–40]. The pharmacodynamic use of repeated swabbing has not yet been reported. Interestingly, the presence of parasites in CL has also been shown at (unaffected) extralesional sites [38,40], opening up other possibilities for less invasive sampling procedures. For PKDL, *Leishmania* DNA was also detected in lesion material before treatment; a significantly higher parasite burden was found in chronic lesions than in transient lesions, with burdens reduced to nondetectable levels posttreatment [17]. The pharmacodynamic use of newer molecular tools (e.g., loop-mediated isothermal amplification [LAMP]) [41,42] has not yet been investigated.

Antigen-detection
Disease-specific antigen detection is regularly used as a predictive biomarker, e.g., for various cancer types [43], and is potentially useful for infectious diseases as well. For leishmaniasis, however, the application of antigen tests has been limited mainly to diagnostics making use of a urine-based latex agglutination assay (KAtex), which detects a heat-stable low-molecular-weight carbohydrate antigen found in the urine of VL patients [26,44–46]. The method has been successfully evaluated and compared to other methods for diagnosis of VL patients in various geographical areas, ranging from East Africa to South Asia [3,26,47–55]. Even though specificity was consistently high (98% to 100%) in these studies, sensitivity appeared to be very low to moderate (48% to 95.2%), with a high discrepancy between studies. Studies from India and Sudan indicated that the urine antigen detection test became negative in cured VL patients at least 30 days after the end of treatment [48,49], indicating a possible pharmacodynamic use of this assay.

<u>Indirect markers</u>

Macrophage-related markers
Leishmania parasites reside and replicate inside the phagocytic cells of the reticuloendothelial system, mainly macrophages, increasing the overall macrophage biomass in the host. Since the macrophage load also decreases again with waning parasitic infection, soluble macrophage-related markers—specifically when produced by infected macrophages—are potential semidirect biomarkers. Neopterin is a heterocyclic pteridine compound which is synthesized by macrophages after gamma interferon (IFN-γ) stimulation [56]. It is considered an indicator of activation of cellular immunity. Increased neopterin production is found in a broad range of diseases, e.g., in viral infections (HIV, hepatitis B and C) and infections due to intracellular bacteria (tuberculosis, malaria). Serum neopterin concentrations were elevated in VL patients compared to levels in controls and decreased to normal concentrations at the

4.1

end of treatment in cured patients, whereas they were still significantly increased in refractory patients [57]. Serum neopterin concentrations were not found to be elevated in CL patients [58].

Adenosine deaminase (ADA), found particularly in macrophages and lymphocytes, is a key enzyme in the breakdown of adenosine, a purine nucleoside that suppresses the inflammatory responses. For VL, serum ADA activity was increased at diagnosis and returned to almost normal concentrations at the end of therapy (day 30) in Nepalese and Indian patients [59–62]. At diagnosis, activity appeared higher in VL patients than in malaria, leprosy, or tuberculosis patients [60]. Also, in Turkish CL patients, adenosine deaminase was increased at the time of diagnosis [63].

Cytokines
Recovery from VL is linked mainly to the CD4^{+} T-cell-mediated cellular immune response. More specifically, the Th1-mediated response is generally associated with macrophage activation, host resistance, and protection against *Leishmania* parasites, leading to control of disease. Conversely, the Th2-mediated response is associated with downregulation of macrophage activation and eventually progression of disease. Unfortunately, this distinction between Th1 and Th2 activation is a simplified model, and many patients demonstrate a nonspecific immune response profile.

The most studied cytokines are the proinflammatory cytokines IFN-γ and tumor necrosis factor alpha (TNF-α) and the regulatory cytokine interleukin-10 (IL-10). Plasma IL-10 was found to be increased in Indian patients with active VL and could be detected in the keratinocytes and sweat glands of patients who eventually developed PKDL [64]. The increase of IL-10 concentrations in VL patients was later confirmed in a range of countries, including, among others, India, Brazil, and Ethiopia [65–77]. IL-10 levels were found to drop significantly after successful treatment [66,70,73,78], to near-control levels 5 to 7 days posttreatment [74]. Ansari et al. found no difference in pretreatment IL-10 levels between responsive and unresponsive patients [74]. For CL, IL-10 might be a possible pharmacodynamic marker indicating treatment failure, as IL-10 mRNA levels in lesion biopsy specimens were found to be positively associated with unresponsiveness to treatment [79,80]. Cured mucocutaneous leishmaniasis (MCL) patients demonstrated a higher percentage of IL-10-expressing cells pretreatment than relapsing patients [81]. Interestingly, IL-10 was found to be positively correlated with the parasite load in the blood of VL patients [17,70] and lesional tissue of PKDL patients [82].

TNF-α is a cytokine produced mainly by activated macrophages. TNF-α levels were found to be significantly increased in patients with active VL [77,83–85]; they declined during treatment [85–89], and returned to healthy-control levels at the end of treatment [84]. Unresponsive patients retained elevated levels of TNF-α [85]. In contrast, other studies found minimal levels of this cytokine in Indian VL patients [74,90,91]. Moreover, TNF-α was also present in asymptomatic VL patients [83], complicating the interpretation of TNF-α in cases of VL. For CL patients, studies of TNF-α serum levels are contradictory; some studies found elevated levels of TNF-α in the plasma of CL patients that decreased posttreatment compared to healthy controls [92–95], but others could confirm this only for MCL patients [85,96]. TNF-α mRNA levels in lesion biopsy specimens were found to be positively correlated with lesion size [80].

IFN-γ is a critical soluble cytokine for innate and adaptive immunity against

intracellular infections and is involved in the activation of macrophages. IFN-γ levels were found to be significantly elevated in patients with active VL, which was confirmed in a wide range of countries: India [74,75], Bangladesh [70], Brazil [70,72,73,77], Ethiopia [67,68], Sicily [66], and Iran [65]. During and after successful treatment, IFN-γ levels were found to drop significantly but remained elevated compared to levels in healthy controls [66,70,73,75,78]. In contrast, Cenini et al. [84] showed that IFN-γ levels returned to healthy-control levels at the end of treatment. Moreover, IFN-γ plasma concentrations appeared to be significantly higher after the end of treatment in patients unresponsive to therapy than in responsive patients treated with sodium stibogluconate (SSG) [74,75]. Discrepant results in asymptomatic VL patients indicated that IFN-γ was elevated in 48% of asymptomatic Brazilian patients but that it was undetectable in the vast majority of asymptomatic Ethiopian patients [67,83]. Additionally, a recent study of Brazilian pediatric VL patients showed that low levels of IFN-γ were associated with signs of severity, such as jaundice or hemorrhage [97]. In CL lesion biopsy specimens, no significant difference in IFN-γ levels could be found between patients with favorable and unfavorable lesion evolutions [79].

For PKDL patients, the expression of the mRNA of the three cytokines IL-10, IFN-γ, and TNF-α in lesions was found to be significantly elevated compared to that in control tissues [74,82]. After treatment, these levels were restored to near-control levels [74]. Ganguly et al. found that IL-10 and IFN-γ levels were significantly higher in patients with polymorphic PKDL than in patients with macular PKDL [98].

Concerning patients with HIV-VL coinfection, only TNF-α and IFN-γ serum levels were still significantly elevated in HIV patients when they developed VL coinfection, while IL-10 levels tended to decrease [99]. Also, compared to Chagas disease, dengue fever, and tuberculosis patients, leishmaniasis patients showed high levels of TNF-α [70]. TNF-α and IFN-γ levels increased significantly when malaria patients developed a VL coinfection [100].

The interleukins IL-6 [74,75,77,84,101] and IL-12 [65,67,69,70] (often measured as the concentration of the subunit IL-12p40) were also found to be significantly increased in the sera of VL patients. In Sudanese and Ethiopian VL patients, IL-6 returned to normal concentrations within the treatment period [84,101] and seemed indicative of relapse events [101]. However, IL-6 was not correlated with spleen/liver size [73]. Also IL-12 levels were found to drop significantly within 30 days of treatment [73] and was largely absent in cured and asymptomatic cases [67,69]. In contrast, in Bangladesh and Brazil, IL-12 was shown to be elevated in asymptomatic VL cases [83,90]. Both interleukins also showed pharmacodynamic potential in CL patients. IL-12 was correlated with unfavorable lesion evolution and lesion duration [80,102]. IL-6 mRNA from biopsy specimens was correlated with lesion size, and also IL-6 serum concentrations were found to be elevated in CL patients [80,94].

IL-18 was also increased in patients with active VL compared to levels in healthy controls [67]. Interestingly, a significant decrease in urinary IL-18 levels was detected during treatment [103]. Urinary detection of biomarkers would be ideal due to its noninvasive collection method.

Soluble CD40 ligand (sCD40L) (also called sCD154) was significantly decreased in VL patients at diagnosis compared to levels in controls in areas of endemicity [70, 87]. During treatment, sCD40L levels increased toward healthy control levels. However, similar CD40L levels were found for Chagas disease and VL patients, which might cause specificity issues [87].

4.1

Cell-surface molecules and circulating receptors
Levels of circulating soluble cytokine receptors for IL-2 and IL-4 (sIL-2R and sIL-4R, respectively) were elevated in patients with active VL, with higher concentrations of sIL4R than in patients with other local and systemic parasitic infections [57,104–106]. Serum sIL-2R concentrations correlated with *Leishmania* DNA serum levels [70] and significantly decreased during treatment [57,70], but returned to normal only after several months [105]. At the start of treatment, sIL-2R levels were also significantly higher in patients developing PKDL than in patients not developing PKDL [64]. Additionally, mRNA levels of the IL-2R α-chain were significantly elevated in lesions of PKDL patients before treatment and returned to control levels posttreatment [82].

Circulating sCD4 and sCD8 were increased at the start of treatment and returned to levels comparable to those in healthy controls within several months after treatment [57,105]. sCD8 was significantly decreased posttreatment in responders to therapy compared to levels in nonresponders, making it a possible suitable pharmacodynamic marker [57].

Serum levels of the soluble receptors for TNF (sTNFRs) were significantly elevated in patients with active VL compared to levels in controls in areas of endemicity and nonendemicity [91]. Responding patients showed a steep decrease in sTNFR levels already at day 15 during treatment, in contrast to nonresponders [86,91].

Acute-phase proteins
Acute-phase proteins widely used as clinical markers of inflammation and infection, which increase during many (non)infective inflammatory diseases and malignancies, also increase during VL. C-reactive protein (CRP), serum amyloid A protein (SAA), and alpha-1-acid glycoprotein (AGP) were increased in Kenyan VL patients upon diagnosis and reached normal levels before or at the end of treatment (SAA and AGP) or at 60 days posttreatment (CRP) [107]. Elevation of CRP levels was confirmed for Indian patients with active VL [75]. Interestingly, pretreatment CRP levels were lower in patients responding fast to treatment than in slow-responders, with lower splenic parasite counts [107], which was confirmed in a large Indian pediatric VL cohort [108]. An increased pretreatment CRP concentration in VL patients was associated with the development of PKDL [109], while CRP levels were not significantly elevated in PKDL patients. However, the specificity of acute-phase proteins in the monitoring of VL treatments is probably low, as they are increased in a myriad of other infectious and noninfectious inflammatory illnesses.

Other markers
Arginase catalyzes the metabolism of l-arginine into l-ornithine and urea. The resulting diminishing bioavailability of l-arginine is regarded as a potent mechanism of immune suppression and impairment of T-cell responses. In patients with active VL and CL, arginase activity in plasma was found to be significantly increased, and levels returned to control levels for VL patients during SSG treatment [110,111]. VL-HIV coinfection patients appeared to have increased arginase activity compared to VL patients, both in plasma and peripheral blood mononuclear cells (PBMCs) [112]. In PKDL patients, arginase activity declined after miltefosine treatment but not after SSG treatment [113].

Antibody-detection
All of the current first-line diagnostic serological tests for VL are antibody detection tests

[114,115]. Two serological tests are currently being used in the field: the direct agglutination test (DAT), based on numbers of killed whole L. *donovani* promastigotes, and the recombinant K39 (rK39)-based immunochromatographic antibody detection test. Other antigen-based assays have been developed for *Leishmania* antibody detection, using (recombinant) proteins rK9, rK26, rK28, *Leishmania infantum* cytosolic tryparedoxin peroxidase (LicTXNPx), rgp63, rLepp12, recombinant open reading frame F (rORFF), BHUP2, rKLO8, rHSP70, guanylate binding protein (GBP), galactosyl-α(1-3)galactose, 9-O-acetylated sialic acids, recombinant peroxidoxin, and amastin [116–130]. Unfortunately, antibodies against *Leishmania* parasites exhibit a long half-life and stay detectable for several months up to several years after an infection [tested by the DAT and for galactosyl-α(1-3)galactose, LicTXNPx, rK26, rK39, and BHUP2] [49,120,121,131–141], which compromises the diagnosis of a relapse case and also the pharmacodynamic application of these markers. However, it was found that for some antibodies (against the recombinant *Leishmania* antigens rH2A, KMP11, the "Q" protein, and 9-O-acetylated sialic acids), the levels do decrease significantly 30 to 60 days after treatment [129,142]. Furthermore, 1 week posttreatment, only ~40 to 50% of patients gave a positive signal for rLepp12, compared to 100% for rK39 and for direct agglutination [125]. Though not very sensitive (44%), *Leishmania*-specific immunoglobulin E (L-IgE) has been suggested to be a specific (98.3%) marker of active VL disease (*L. chagasi*), although it is undetectable at subclinical levels in VL patients, Chagas disease patients, and healthy controls [143–145]. Moreover, increased L-IgE concentrations were demonstrated to regress to normal values during the time span of treatment [143,145,146]. In cases of atypical cutaneous leishmaniasis, IgE levels were not significantly different from those of asymptomatic or healthy controls [147]. Anam et al. [144] also hinted at a possible (diagnostic) role for *L. donovani*-specific IgG3 antibody isotype detection. While the IgG3 antibody level decreases significantly posttreatment [148,149], the pharmacodynamic value of this marker is probably very low, as the time to normalcy for IgGs is longer than 3 months for both CL and VL patients [150–154].

Besides the drawback of the long half-lives of antibodies, antibody detection tests tend to be positive in a significant proportion of noninfected or otherwise asymptomatic individuals living in areas where VL is endemic [135,155,156]. Due to these crucial limitations in the use of antibodies to monitor therapies, these markers are excluded from Supplementary table 1.

DISCUSSION

General issues pertaining to the pharmacodynamic potential of biomarkers
Our systematic literature review identified 53 biomarkers for VL, CL, and/or PKDL. Several general issues might limit their pharmacodynamic potential. First, the large majority of biomarkers were evaluated only for their diagnostic use. Leishmaniasis patients were generally compared to healthy controls before the start of their treatment. Only a few VL studies have focused on differentiating active, clinical disease from subclinical or asymptomatic disease, although this might potentially be an interesting approach to demonstrate the Th1/Th2 paradigm. When a biomarker was evaluated for its ability to monitor a treatment effect, it was almost always done by comparison of pre- and posttreatment concentrations, without repeated longitudinal measurements. Therefore, the pharmacodynamic potential of most biomarkers remains difficult to assess based on the available literature.

Second, most identified biomarkers for leishmaniasis are indirect markers, i.e.,

4.1

universal markers of activation and the subsequent waning of cellular immunity. As a result, specificity may be low compared to that for patients suffering from common concomitant infections. Interestingly, a few biomarkers (TNF-α, CCL3, and CCL4) have been shown to be specific for HIV-VL coinfection patients rather than HIV patients. Other biomarkers (ADA and sIL4R) were elevated in patients with VL, but not malaria, indicating a possible value in malaria-VL coinfection. Despite these exploratory results, the majority of markers have not been tested against the most common VL coinfections, and further research is needed to establish their specificity as biomarkers.

Thirdly, multiple studies focused on correlating biomarker levels to clinical features of CL (e.g., lesion size), while this correlation was generally ignored for VL. In general, more emphasis should be put in future clinical trials on establishing a correlation between the studied biomarkers and clinical parameters.

Fourth, the time needed to regress to normalcy for the biomarkers (characterized by their elimination half-lives) remains a concern. For instance, almost all of the antibody-related markers have a very long elimination half-life of up to several months and stay present in the body long after the actual parasitic infection has been resolved. Their potential for pharmacodynamic monitoring of antileishmanial treatment is therefore probably negligible. *Leishmania* antigen detection might be more promising in that respect; however, this has been investigated mainly in the context of a diagnosis of VL, with only limited attention paid to repeated quantitative measurement during and after treatment. The less specific indirect markers, for example, AGP and TNF-α, often show preferable time-to-normalcy values.

Lastly, the practical feasibility, in terms of cost, invasiveness, and laboratory requirements, is an additional concern. The preferred sample matrix for a biomarker should be noninvasive (e.g., urine or saliva). All identified biomarkers were measured in blood or biopsy specimens, except for IL-18 and KAtex, both of which can be measured in urine. Though this review focused on biomarkers within the context of a clinical trial setting, it is important to note that equipment-free procedures not requiring a cold chain are required for the application of pharmacodynamic biomarkers in routine settings.

Selection of potential pharmacodynamic biomarkers
In this section, we will highlight and critically appraise the application of a selection of potential pharmacodynamic biomarkers, with some recommendations for research priorities.

Direct biomarkers
Recently, the quantitative application of molecular parasite detection methods as a pharmacodynamic measure was demonstrated, both in VL and CL. While this method measures the parasite directly and therefore is theoretically the most promising biomarker, there are some issues. First, the sensitivity of this marker for VL is relatively low (~80%) and seems to vary between geographical regions [27,28]. The parasite loads appear to decrease with clinical cure but are undetectable before clinical cure can be established. The parasites reside within the spleen, bone marrow, and liver, and plasma is therefore only a proxy reservoir of the parasite. Additionally, it remains unknown what the predictive value is of blood parasite loads in relapsing patients and controls in areas of endemicity. Last, it is unsuitable for routine monitoring due to its high costs (considering the ~€30/sample material costs and the required state-of-the-art laboratory equipment and trained technicians, this tool can be used only in a clinical trial setting).

Another direct biomarker with potential is the *Leishmania* carbohydrate antigen, which forms the basis for the diagnostic KAtex test. One of the biggest advantages of this biomarker is that it can be detected in urine. Its specificity is consistently high, but its sensitivity appears variable, which may make it suitable only in controlled settings. The *Leishmania*-specific antigen can be assessed quantitatively by enzyme-linked immunosorbent assay (ELISA), which makes it easier to adopt at primary health care facilities than the molecular detection methods.

Indirect biomarkers

Of the indirect biomarkers, the most promising are the macrophage-related markers, as these are directly related to parasitic infection of macrophages. ADA activity is increased in patients with VL and CL, returns to normal during treatment, and shows promising results in patients with HIV-VL coinfection. Unfortunately, this marker has no proven geographical applicability, and there are no data on the relation between ADA activity levels and clinical outcome.

Though most cytokines demonstrated a lack of specificity, a range of them showed promising results with regard to the other evaluation criteria. IL-10 correlated with the parasite load at the time of diagnosis, decreased during treatment, and was even associated with the occurrence of PKDL. However, IL-10 was increased as well in subclinical cases, which complicates its interpretation, certainly in the context of parasite recrudescence. Although studies from different regions contradict each other on its sensitivity, TNF-α shows the highest specificity in comparison to other cytokines, indicating that it might be applicable as a biomarker in certain regions of endemicity. Levels of other indirect markers (e.g., sTNFR, IL-6) appeared predictive for clinical outcome but require further evaluation with regard to the other criteria for us to be able to draw conclusions on their potential. A practical advantage of cytokines is that their ELISA kits are relatively low in cost and may be implemented on a large scale, even though a basic laboratory is still required.

CONCLUSIONS & FUTURE PERSPECTIVE

The biomarkers identified in this systematic review have been evaluated mainly for diagnostic purposes and do not (yet) meet the requirements for monitoring of clinical outcome as surrogate endpoints in clinical trials. Most promising for the application in pharmacodynamic evaluations are the highly specific direct biomarkers (DNA/RNA or antigenic markers), which appear to have a good correlation with clinical outcome. However, future research should specifically focus on the identification of optimal molecular and antigenic targets to increase the sensitivity of these tools. Macrophage-related markers are theoretically the most promising of the indirect markers, as they are directly linked to macrophage (and possibly parasite) load. Though neopterin and ADA have shown high sensitivity and geographical applicability as biomarkers, more evidence is needed to confirm their potential in predicting clinical outcome. Indirect markers, such as IL-10 and TNF-α, have demonstrated high sensitivity and seem to indicate clinical outcome. Nevertheless, given the lack of specificity and the complexity of the immunological response associated with VL infection, it is unlikely that a single immunological biomarker will be suitable to accurately monitor treatment response. These markers can still be of use in well-controlled trials with sufficient exclusion of concomitant diseases. However, they are not suitable for application in routine clinical care, as in that case, the biomarker should be able to discriminate clinical outcome at the level of an individual patient. Additional

4.1

efforts are needed to investigate the applicability of combinations of cytokines as biomarker profiles to monitor treatment outcome at the patient level.

In general, future biomarker research should extend its focus to biomarkers' pharmacodynamic potential by correlating longitudinal quantitative assessments of the marker (i.e., the marker concentration-time profile in response to therapy) to multiple clinical parameters.

The coming of age of new treatment options for leishmaniasis was long and eagerly awaited, but now that this moment approaches, we urgently need better and more accurate tools to evaluate their potential superiority over existing regimens and rationalize their dosing schedule. Evaluation of pharmacodynamic biomarkers is therefore of crucial importance to optimize and accelerate drug development for this neglected tropical disease.

TRANSPARENCY DECLARATIONS

None to declare.

REFERENCES

1. Croft SL, Olliaro P. Leishmaniasis chemotherapy - challenges and opportunities. Clin. Microbiol. Infect. 2011;17:1478–83.

2. Chatelain E, Ioset JR. Drug discovery and development for neglected diseases: the DNDi model. Drug Des. Devel. Ther. 2011;5:175–81.

3. Boelaert M, Bhattacharya S, Chappuis F, El Safi SH, Hailu A, Mondal D, et al. Evaluation of rapid diagnostic tests: visceral leishmaniasis. Nat. Rev. Microbiol. 2007;5:S30–9.

4. Chulay JD, Bryceson ADM. Quantitation of amastigotes of *Leishmania donovani* in smears of splenic aspirates from patients with visceral leishmaniasis. Am. J. Trop. Med. Hyg. 1983;32:475–9.

5. Kager PA, Rees PH, Manguyu FM, Bhatt KM, Bhatt SM. Splenic aspiration; experience in Kenya. Trop. Geogr. Med. 1983;35:125–31.

6. Thakur CP. A comparison of intercostal and abdominal routes of splenic aspiration and bone marrow aspiration in the diagnosis of visceral leishmaniasis. Trans. R. Soc. Trop. Med. Hyg. 1997;91:668–70.

7. Sundar S, Rai M. Laboratory diagnosis of visceral leishmaniasis. Clin. Diagn. Lab. Immunol. 2002;9:951–8.

8. González U, Pinart M, Rengifo-Pardo M, Macaya A, Alvar J, Tweed JA. Interventions for American cutaneous and mucocutaneous leishmaniasis. Cochrane Database Syst. Rev. 2009;CD004834.

9. González U, Pinart M, Reveiz L, Alvar J. Interventions for Old World cutaneous leishmaniasis. Cochrane Database Syst. Rev. 2008;CD005067.

10. Gonzalez U, Pinart M, Reveiz L, Rengifo-Pardo M, Tweed J, Macaya A, et al. Designing and Reporting Clinical Trials on Treatments for Cutaneous Leishmaniasis. Clin. Infect. Dis. 2010;51:409–19.

11. Rijal S, Ostyn B, Uranw S, Rai K, Bhattarai NR, Dorlo TPC, et al. Increasing failure of miltefosine in the treatment of kala-azar in nepal and the potential role of parasite drug resistance, reinfection, or noncompliance. Clin. Infect. Dis. 2013;56:1530–8.

12. Biomarkers Definitions Working Group. Biomarkers and surrogate endpoints: preferred definitions and conceptual framework. Clin. Pharmacol. Ther. 2001;69:89–95.

13. Strimbu K, Tavel JA. What are Biomarkers? Curr. Opin. HIV AIDS. 2010;5:463–6.

14. Mary C, Faraut F, Drogoul MP, Xeridat B, Schleinitz N, Cuisenier B, et al. Reference values for *Leishmania infantum* parasitemia in different clinical presentations: quantitative polymerase chain reaction for therapeutic monitoring and patient follow-up. Am. J. Trop. Med. Hyg. 2006;75:858–63.

15. Mary C, Faraut F, Lascombe L, Dumon H. Quantification of *Leishmania infantum* DNA by a real-time PCR assay with high sensitivity. J. Clin. Microbiol. 2004;42:5249–55.

16. De Vries PJ, Van der Meide WF, Godfried MH, Schallig HD, Dinant HJ, Faber WR. Quantification of the response to miltefosine treatment for visceral leishmaniasis by QT-NASBA. Trans. R. Soc. Trop. Med. Hyg. 2006;100:1183–6.

17. Verma S, Kumar R, Katara GK, Singh LC, Negi S, Ramesh V, et al. Quantification of parasite load in clinical samples of leishmaniasis patients : IL-10 level correlates with parasite load in visceral leishmaniasis. PLoS One. 2010;5:e10107.

18. Osman OF, Kager PA, Zijlstra EE, El-Hassan A, Oskam L. Use of PCR on lymph-node samples as test of cure of visceral leishmaniasis. Ann. Trop. Med. Parasitol. 1997;91:845–50.

19. Pizzuto M, Piazza M, Senese D, Scalamogna C, Calattini S, Corsico L, et al. Role of PCR in diagnosis and prognosis of visceral leishmaniasis in patients coinfected with human immunodeficiency virus type 1. J. Clin. Microbiol. 2001;39:357–61.

20. Deborggraeve S, Boelaert M, Rijal S, De Doncker S, Dujardin JC, Herdewijn P, et al. Diagnostic accuracy of a new *Leishmania* PCR for clinical visceral leishmaniasis in Nepal and its role in diagnosis of disease. Trop. Med. Int. Heal. 2008;13:1378–83.

21. Arora SK, Gupta S, Bhardwaj S, Sachdeva N, Sharma NL. An epitope-specific PCR test for diagnosis of *Leishmania donovani* infections. Trans. R. Soc. Trop. Med. Hyg. 2008;102:41–5.

22. Bossolasco S, Gaiera G, Olchini D, Gulletta M, Martello L, Bestetti A, et al. Real-Time PCR assay for clinical management of human immunodeficiency virus-infected patients with visceral leishmaniasis. J. Clin. Microbiol. 2003;41:5080–4.

23. Salotra P, Sreenivas G, Pogue GP, Lee N, Nakhasi HL, Ramesh V, et al. Development of a species-specific PCR assay for detection of *leishmania donovani* in clinical samples from patients with kala-azar and post-kala-azar dermal leishmaniasis. J. Clin. Microbiol. 2001;39:849–54.

24. Antinori S, Calattini S, Longhi E, Bestetti G, Piolini R, Magni C, et al. Clinical use of polymerase chain reaction performed on peripheral blood and bone marrow samples for the diagnosis and monitoring of visceral leishmaniasis in HIV-infected and HIV-uninfected patients: a single-center, 8-year experience in Italy and review. Clin. Infect. Dis. 2007;44:1602–10.

4.1

25. De Doncker S, Hutse V, Rijal S, Man B, Singh Karki BM, Decuypere S, et al. A new PCR — ELISA for diagnosis of visceral leishmaniasis in blood of HIV-negative subjects. Trans. R. Soc. Trop. Med. Hyg. 2005;99:25–31.

26. Salam MA, Khan GM, Mondal D. Urine antigen detection by latex agglutination test for diagnosis and assessment of initial cure of visceral leishmaniasis. Trans. R. Soc. Trop. Med. Hyg. 2011;105:269–72.

27. Khalil EAG, Weldegebreal T, Younis BM, Omollo R, Musa AM, Hailu W, et al. Safety and efficacy of single dose versus multiple doses of AmBisome for treatment of visceral leishmaniasis in Eastern Africa: a randomised trial. PLoS Negl. Trop. Dis. 2014;8:e2613.

28. Sudarshan M, Weirather JL, Wilson ME, Sundar S. Study of parasite kinetics with antileishmanial drugs using real-time quantitative PCR in Indian visceral leishmaniasis. J. Antimicrob. Chemother. 2011;66:1751–5.

29. Dorlo TPC, van Thiel PP, Schoone GJ, Stienstra Y, van Vugt M, Beijnen JH, et al. Dynamics of parasite clearance in cutaneous leishmaniasis patients treated with miltefosine. PLoS Negl. Trop. Dis. 2011;5:e1436.

30. Murray HW, Berman JD, Davies CR, Saravia NG. Advances in leishmaniasis. Lancet. 2005;366:1561–77.

31. de Oliveira CI, Báfica A, Oliveira F, Favali CBF, Correa T, Freitas LAR, et al. Clinical utility of polymerase chain reaction-based detection of *Leishmania* in the diagnosis of American cutaneous leishmaniasis. Clin. Infect. Dis. 2003;37:e149–53.

32. Schönian G, Nasereddin A, Dinse N, Schweynoch C, Schallig HDFH, Presber W, et al. PCR diagnosis and characterization of *Leishmania* in local and imported clinical samples. Diagn. Microbiol. Infect. Dis. 2003;47:349–58.

33. Mendonça MG, de Brito MEF, Rodrigues EHG, Bandeira V, Jardim ML, Abath FGC. Persistence of *leishmania* parasites in scars after clinical cure of American cutaneous leishmaniasis: is there a sterile cure? J. Infect. Dis. 2004;189:1018–23.

34. Schubach A, Haddad F, Oliveira-Neto MP, Degrave W, Pirmez C, Grimaldi GJ, et al. Detection of *Leishmania* DNA by polymerase chain reaction in scars of treated human patients. J. Infect. Dis. 1998;178:911–4.

35. Van der Meide WF, Schoone GJ, Faber WR, Zeegelaar JE, De Vries HJC, Özbel Y, et al. Quantitative nucleic acid sequence-based assay as a new molecular tool for detection and quantification of *leishmania* parasites in skin biopsy samples. J. Clin. Microbiol. 2005;43:5560–6.

36. Kumar R, Bumb RA, Ansari NA, Mehta RD, Salotra P. Cutaneous leishmaniasis caused by *Leishmania tropica* in Bikaner, India: parasite identification and characterization using molecular and immunologic tools. Am. J. Trop.

Med. Hyg. 2007;76:896–901.

37. Van der Meide WF, Peekel I, Van Thiel PPAM, Schallig HDFH, De Vries HJC, Zeegelaar JE, et al. Treatment assessment by monitoring parasite load in skin biopsies from patients with cutaneous leishmaniasis, using quantitative nucleic acid sequence-based amplification. Clin. Exp. Dermatol. 2008;33:394–9.

38. Figueroa RA, Lozano LE, Romero IC, Cardona MT, Prager M, Pacheco R, et al. Detection of *Leishmania* in unaffected mucosal tissues of patients with cutaneous leishmaniasis caused by *Leishmania (Viannia)* species. J. Infect. Dis. 2009;200:638–46.

39. Mimori T, Matsumoto T, Calvopiña MH, Gomez EA, Saya H, Katakura K, et al. Usefulness of sampling with cotton swab for PCR-diagnosis of cutaneous leishmaniasis in the New World. Acta Trop. 2002;81:197–202.

40. Romero I, Téllez J, Suárez Y, Cardona M, Figueroa R, Zelazny A, et al. Viability and burden of *Leishmania* in extralesional sites during human dermal leishmaniasis. PLoS Negl. Trop. Dis. 2010;4:e819.

41. Adams ER, Schoone GJ, Ageed AF, Safi SE, Schallig HDFH. Development of a reverse transcriptase loop-mediated isothermal amplification (LAMP) assay for the sensitive detection of *Leishmania* parasites in clinical samples. Am. J. Trop. Med. Hyg. 2010;82:591–6.

42. Itoh, M, Takagi H. Mass-Survey using urine and confirmation by LAMP for control of visceral leishmaniasis. Kala azar south asia curr. status challenges ahead. 1st ed. New York, Springer; 2011. p. 91–8.

43. Sawyers CL. The cancer biomarker problem. Nature. 2008;452:548–52.

44. Sarkari B, Chance M, Hommel M. Antigenuria in visceral leishmaniasis: detection and partial characterisation of a carbohydrate antigen. Acta Trop. 2002;82:339–48.

45. Hatam GR, Ghatee MA, Hossini SM, Sarkari B. Improvement of the Newly Developed Latex Agglutination Test (Katex) for Diagnosis of Visceral Lieshmaniasis. J. Clin. Lab. Anal. 2009;205:202–5.

46. Attar ZJ, Chance ML, El-Safi S, Carney J, Azazy A, El-Hadi M, et al. Latex agglutination test for the detection of urinary antigens in visceral leishmaniasis. Acta Trop. 2001;78:11–6.

47. Ahsan MM, Islam MN, Mollah AH, Hoque MA, Hossain MA, Begum Z, et al. Evaluation of latex agglutination test (KAtex) for early diagnosis of kala-azar. Mymensingh Med. J. 2010;19:335–59.

48. El-Safi SH, Abdel-Haleem A, Hammad A, El-Basha I, Omer A, Kareem HG, et al. Field evaluation of latex agglutination test for detecting urinary antigens in

visceral leishmaniasis in Sudan. East Mediterr. Heal. J. 2003;9:844–55.

49. Singh DP, Goyal RK, Singh RK, Sundar S, Mohapatra TM. In search of an ideal test for diagnosis and prognosis of kala-azar. J. Heal. Popul. Nutr. 2010;28:281–5.

50. Chappuis F, Rijal S, Jha UK, Desjeux P, Karki BMS, Koirala S, et al. Field validity, reproducibility and feasibility of diagnostic tests for visceral leishmaniasis in rural Nepal. Trop. Med. Int. Health. 2006;11:31–40.

51. Cruz I, Chicharro C, Nieto J, Bailo B, Cañavate C, Figueras MC, et al. Comparison of new diagnostic tools for management of pediatric Mediterranean visceral leishmaniasis. J. Clin. Microbiol. 2006;44:2343–7.

52. Diro E, Techane Y, Tefera T, Assefa Y, Kebede T, Genetu A, et al. Field evaluation of FD-DAT, rK39 dipstick and KATEX (urine latex agglutination) for diagnosis of visceral leishmaniasis in northwest Ethiopia. Trans. R. Soc. Trop. Med. Hyg. 2007;101:908–14.

53. Riera C, Fisa R, Lopez P, Ribera E, Carrió J, Falcó V, et al. Evaluation of a latex agglutination test (KAtex) for detection of *Leishmania* antigen in urine of patients with HIV-*Leishmania* coinfection: value in diagnosis and post-treatment follow-up. Eur. J. Clin. Microbiol. Infect. Dis. 2004;23:899–904.

54. Sundar S, Singh RK, Bimal SK, Gidwani K, Mishra A, Maurya R, et al. Comparative evaluation of parasitology and serological tests in the diagnosis of visceral leishmaniasis in India: a phase III diagnostic accuracy study. Trop. Med. Int. Heal. 2007;12:284–9.

55. Sundar S, Agrawal S, Pai K, Chance M, Hommel M. Detection of leishmanial antigen in the urine of patients with visceral leishmaniasis by a latex agglutination test. Am. J. Trop. Med. Hyg. 2005;73:269–71.

56. Huber C, Batchelor JR, Fuchs D, Hausen A, Lang A, Niederwieser D, et al. Immune response-associated production of neopterin. Release from macrophages primarily under control of interferon-gamma. J. Exp. Med. 1984;160:310–6.

57. Schriefer A, Barral A, Carvalho EM, Barral-Netto M. Serum soluble markers in the evaluation of treatment in human visceral leishmaniasis. Clin. Exp. Immunol. 1995;102:535–40.

58. Hamerlinck FF, van Gool T, Faber WR, Kager PA. Serum neopterin concentrations during treatment of leishmaniasis: useful as test of cure? FEMS Immunol. Med. Microbiol. 2000;27:31–4.

59. Khambu B, Mehta KD, Rijal S, Lamsal M, Majhi S, Baral N. Serum nitrite level and adenosine deaminase activity is altered in visceral leishmaniasis. Nepal Med. Coll. J. 2007;9:40–3.

60. Tripathi K, Kumar R, Bharti K, Kumar P, Shrivastav R, Sundar S, et al. Adenosine deaminase activity in sera of patients with visceral leishmaniasis in India. Clin. Chim. Acta. 2008;388:135–8.

61. Rai AK, Thakur CP, Velpandian T, Sharma SK, Ghosh B, Mitra DK. High concentration of adenosine in human visceral leishmaniasis despite increased ADA and decreased CD73. Parasite Immunol. 2011;33:632–6.

62. Baral N, Mehta KD, Chandra L, Lamsal M, Rijal S, Koirala S. Adenosine deaminase activity in sera of patients with visceral leishmaniasis in Nepal. Trop. Doct. 2005;35:86–8.

63. Erel O, Kocyigit A, Gurel MS, Bulut V, Seyrek A, Ozdemir Y. Adenosine deaminase activities in sera ,lymphocytes and granulocytes in patients with cutaneous leishmaniasis. Mem. Inst. Oswaldo Cruz. 1998;93:491–4.

64. Gasim S, Elhassan AM, Khalil EA, Ismail A, Kadaru AM, Kharazmi A, et al. High levels of plasma IL-10 and expression of IL-10 by keratinocytes during visceral leishmaniasis predict subsequent development of post-kala-azar dermal leishmaniasis. Clin. Exp. Immunol. 1998;111:64–9.

65. Khoshdel A, Alborzi A, Rosouli M, Taheri E, Kiany S, Javadian MH. Increased levels of IL-10, IL-12, and IFN- in patients with visceral leishmaniasis. Braz. J. Infect. Dis. 2009;13:44–6.

66. Cillari E, Vitale G, Arcoleo F, D'Agostino P, Mocciaro C, Gambino G, et al. *In vivo* and *in vitro* cytokine profiles and mononuclear cell subsets in sicilian patients with active visceral leishmaniasis. Cytokine. 1995;7:740–5.

67. Hailu A, van der Poll T, Berhe N, Kager PA. Elevated plasma levels of interferon (IFN)-γ, IFN-γ inducing cytokines and IFN-γ inducible CXC chemokines in visceral leishmaniasis. Am. J. Trop. Med. Hyg. 2004;71:561–7.

68. Hailu A, Van Baarle D, Knol GJ, Berhe N, Miedema F, Kager PA. T cell subset and cytokine profiles in human visceral leishmaniasis during active and asymptomatic or sub-clinical infection with *Leishmania donovani*. Clin. Immunol. 2005;117:182–91.

69. Costa ASA, Costa GC, De Aquino DMC, De Mendonça CRR, Barral A, Barral-Netto M, et al. Cytokines and visceral leishmaniasis: a comparison of plasma cytokine profiles between the clinical forms of visceral leishmaniasis. Mem. Inst. Oswaldo Cruz. 2012;107:735–9.

70. Duthie MS, Guderian J, Vallur A, Bhatia A, Lima dos Santos P, Vieira de Melo E, et al. Alteration of the serum biomarker profiles of visceral leishmaniasis during treatment. Eur. J. Clin. Microbiol. Infect. Dis. 2014;33:639–49.

71. Santos-Oliveira JR, Regis EG, Giacoia-Gripp CBW, Valverde JG, Alexandrino-de-Oliveira P, Lindoso JÂL, et al. Microbial translocation induces an intense

4.1

proinflammatory response in patients with visceral leishmaniasis and HIV type 1 coinfection. J. Infect. Dis. 2013;208:57–66.

72. Santos-Oliveira JR, Regis ER, Leal CRB, Cunha R V, Bozza PT, Da-Cruz AD. Evidence that lipopolisaccharide may contribute to the cytokine storm and cellular activation in patients with visceral leishmaniasis. PLoS Negl. Trop. Dis. 2011;5:e1198.

73. Caldas A, Favali C, Aquino D, Vinhas V, Van Weyenbergh J, Brodskyn C, et al. Balance of IL-10 and Interferon- γ plasma levels in human visceral leishmaniasis : Implications in the pathogenesis. BMC Infect. Dis. 2005;5:113.

74. Ansari NA, Saluja S, Salotra P. Elevated levels of interferon-γ ; , interleukin-10 , and interleukin-6 during active disease in Indian kala azar. Clin. Immunol. 2006;119:339–45.

75. Ansari NA, Sharma P, Salotra P. Circulating nitric oxide and C-reactive protein levels in Indian kala azar patients: Correlation with clinical outcome. Clin. Immunol. 2007;122:343–8.

76. Costa-silva MF, Gomes LI, Martins-filho OA, Rodrigues-silva R, De Moura Freire J, Quaresma PF, et al. Gene expression profile of cytokines and chemokines in skin lesions from Brazilian Indians with localized cutaneous leishmaniasis. Mol. Immunol. Elsevier Ltd; 2014;57:74–85.

77. Peruhype-Magalhães V, Martins-Filho OA, Prata A, De A. Silva L, Rabello A, Teixeira-Carvalho A, et al. Mixed inflammatory/regulatory cytokine profile marked by simultaneous raise of interferon-γ and interleukin-10 and low frequency of tumour necrosis factor-α (+) monocytes are hallmarks of active human visceral Leishmaniasis due to *Leishmania chagasi*. Clin. Exp. Immunol. 2006;146:124–32.

78. Ansari NA, Kumar R, Gautam S, Nylén S, Singh OP, Sundar S, et al. IL-27 and IL-21 are associated with T cell IL-10 responses in human visceral leishmaniasis. J. Immunol. 2011;186:3977–85.

79. Bourreau E, Prévot G, Gardon J, Pradinaud R, Launois P. High intralesional interleukin-10 messenger RNA expression in localized cutaneous leishmaniasis is associated with unresponsiveness to treatment. J. Infect. Dis. 2001;184:1628–30.

80. Louzir H, Melby PC, Ben Salah A, Marrakchi H, Aoun K, Ben Ismail R, et al. Immunologic determinants of disease evolution in localized cutaneous leishmaniasis due to *leishmania major*. J. Infect. Dis. 1998;177:1687–95.

81. Tuon FF, Gomes-Silva A, Da-Cruz AM, Duarte MIS, Neto VA, Amato VS. Local immunological factors associated with recurrence of mucosal leishmaniasis. Clin. Immunol. 2008;128:442–6.

82. Katara GK, Ansari NA, Verma S, Ramesh V, Salotra P. Foxp3 and IL-10 expression correlates with parasite burden in lesional tissues of post kala azar dermal leishmaniasis (PKDL) patients. PLoS Negl. Trop. Dis. 2011;5:e1171.

83. Gama MEA, Costa JML, Pereira JCR, Gomes CMC, Corbett CEP. Serum cytokine profile in the subclinical form of visceral leishmaniasis. Braz. J. Med. Biol. Res. 2004;37:129–36.

84. Cenini P, Berhe N, Hailu A, Mcginnes K, Frommel D. Mononuclear cell subpopulations and cytokine levels in human visceral leishmaniasis before and after chemotherapy. J. Infect. Dis. 1993;168:986–93.

85. Barral-Netto M, Badaró R, Barral A, Almeida RP, Santos SB, Badaró F, et al. Tumor necrosis factor (cachectin) in human visceral leishmaniasis. J. Infect. Dis. 1991;163:853–7.

86. Medeiros IM, Reed S, Castelo A, Salomão R. Circulating levels of sTNFR and discrepancy between cytotoxicity and immunoreactivity of TNF-a in patients with visceral leishmaniasis. Clin. Microbiol. Infect. 2000;6:34–7.

87. De Oliveira FA, Vanessa Oliveira Silva C, Damascena NP, Passos RO, Duthie MS, Guderian JA, et al. High levels of soluble CD40 ligand and matrix metalloproteinase-9 in serum are associated with favorable clinical evolution in human visceral leishmaniasis. BMC Infect. Dis. 2013;13:331.

88. Salomão R, Casterlo Filho A, De Medeiros IM, Sicolo MA. Plasma levels of tumor necrosis factor-alpha in patients with visceral leishmaniasis (kala-azar). Association with activity of the disease and clinical remission following antimonial therapy. Rev. Inst. Med. Trop. 1996;38:113–8.

89. Freitas-Teixeira PM, Silveira-Lemos D, Giunchetti RC, Baratta-Masini A, Mayrink W, Peruhype-Magalhães V, et al. Distinct pattern of immunophenotypic features of innate and adaptive immunity as a putative signature of clinical and laboratorial status of patients with localized cutaneous leishmaniasis. Scand. J. Immunol. 2012;76:421–32.

90. Kurkjian KM, Mahmutovic AJ, Kellar KL, Haque R, Bern C, Secor WE. Multiplex analysis of circulating cytokines in the sera of patients with different clinical forms of visceral leishmaniasis. Cytom. A. 2006;358:353–8.

91. Zijlstra EE, Van der Poll T, Mevissen M. Soluble receptors for tumor necrosis factor as markers of disease activity in visceral leishmaniasis. J. Infect. Dis. 1995;171:498–501.

92. Kocyigit A, Gur S, Gurel MS, Bulut V, Ulukanligil M. Antimonial therapy induces circulating proinflammatory cytokines in patients with cutaneous leishmaniasis. Infect. Immun. 2002;70:12–5.

93. Vouldoukis I, Issaly F, Fourcade C, Paul-Eugène N, Arock M, Kolb JP, et al. CD23 and IgE expression during the human immune response to cutaneous leishmaniasis : possible role in monocyte activation. Res. Immunol. 1994;145:17–27.

94. Kocygit A, Gur S, Erel O, Gurel MS. Associations among plasma selenium, zinc, copper, and iron concentrations and immunoregulatory cytokine levels in patients with cutaneous leishmaniasis. Biol. Trace Elem. Res. 2002;90:47–55.

95. Castes M, Trujillo D, Rojas ME, Fernandez CT, Arava L, Cabrera M, et al. Serum levels of tumor necrosis factor in patients with American cutaneous leishmaniasis. Biol. Res. 1993;26:233–8.

96. Da-cruz AM, De Oliveira MP, De Luca PM, Mendonça SCF, Coutinho SG. Tumor Necrosis Factor- α in Human American Tegumentary Leishmaniasis. Mem. Inst. Oswaldo Cruz. 1996;91:225–9.

97. Gama MEA, De Castro Gomes CM, Silveira FT, Laurenti MD, Da Graça Gonçalves G, Da Silva AR, et al. Severe visceral leishmaniasis in children : the relationship between cytokine patterns and clinical features. Rev. Soc. Bras. Med. Trop. 2013;46:741–5.

98. Ganguly S, Das NK, Panja M, Pal S, Modak D, Rahaman M, et al. Increased levels of Interleukin-10 and IgG3 are hallmarks of Indian post – kala-azar dermal leishmaniasis. J. Infect. Dis. 2008;197:1762–71.

99. Medrano FJ, Rey C, Leal M, Cañavate C, Rubio A, Sánchez-Quijano A, et al. Dynamics of serum cytokines in patients with visceral leishmaniasis and HIV-1 co-infection. Clin. Exp. Immunol. 1998;114:403–7.

100. van den Bogaart E, Talha AB, Straetemans M, Mens PF, Adams ER, Grobusch MP, et al. Cytokine profiles amongst Sudanese patients with visceral leishmaniasis and malaria co-infections. BMC Immunol. 2014;15:16.

101. van der Poll T, Zijlstra EE, Mevissen M. Interleukin 6 during active visceral leishmaniasis and after treatment. Clin. Immunol. Immunopathol. 1995;77:111–4.

102. Melby PC, Andrade-narvaez F, Darnell BJ, Valencia-pacheco G. In situ expression of interleukin-10 and interleukin-12 in active human cutaneous leishmaniasis. FEMS Immunol. Med. Micrbiol. 1996;15:101–7.

103. Noiri E, Hamasaki Y, Negishi K, Sugaya T, Doi K, Fujita T, et al. The potential of urinary tests in the management of kala-azar. Kala Azar South Asia Curr. status challnges ahead. 1st ed. New York, Springer; 2011.

104. Barral-Netto M, Barral A, Santos SB, Carvalho EM, Badaro R, Rocha H, et al. Soluble IL-2 receptor as an agent of serum mediated suppresion in human visceral leishmaniasis. J. Immunol. 1991;147:281–4.

105. Vitale G, Reina G, Mansueto S, Gambino G, Mocciaro C, D'Agostino R, et al. The significance of serum soluble IL-2 receptor as a marker for active visceral leishmaniasis in Sicilian patients. Clin. Exp. Immunol. 1992;90:219–22.

106. Sang DK, Ouma JH, John CC, Whalen CC, King CL, Mahmoud AAF, et al. Increased levels of soluble Interleukin-4 receptor in the sera of patients with visceral leishmaniasis. J. Infect. Dis. 1999;179:743–6.

107. Wasunna KM, Raynes JG, Werel JB, Muigai R, Gachihi G, Carpenter L, et al. Acute phase protein concentrations predict parasite clearance rate during therapy for visceral leishmaniasis. Trans. R. Soc. Trop. Med. Hyg. 1995;89:678–81.

108. Singh UK, Patwari AK, Sinhs RK, Kumar R. Prognostic Value of Serum C-reactive Protein in Kala-azar. J. trop. pediatr. 1999;45:226–8.

109. Gasim S, Theander TG, Elhassan AM. High levels of C-reactive protein in the peripheral blood during visceral leishmaniasis predict subsequent development of post kala-azar dermal leishmaniasis. Acta Trop. 2000;75:35–8.

110. Abebe T, Takele Y, Weldegebreal T, Cloke T, Closs E, Corset C, et al. Arginase activity - a marker of disease status in patients with visceral leishmaniasis in Ethiopia. PLoS Negl. Trop. Dis. 2013;7:e2134.

111. Franca-Costa J, Van Weyenbergh J, Boaventura V, Luz NF, Malta-Santos H, Oliveira MC, et al. Arginase I, polyamine and prostaglandin E2 pathways suppress the inflammatory response and contribute to diffuse cutaneous leishmaniasis. J. Infect. Dis. 2015;211:426–35.

112. Takele Y, Abebe T, Weldegebreal T, Hailu A, Hailu W, Hurissa Z, et al. Arginase activity in the blood of patients with visceral leishmaniasis and HIV infection. PLoS Negl. Trop. Dis. 2013;7:e1977.

113. Mukhopadhyay D, Das NK, Roy S, Kundu S, Barbhuiya JN, Chatterjee M. Miltefosine effectively modulates the cytokine milieu in Indian post kala-azar dermal leishmaniasis. J. Infect. Dis. 2011;204:1427–36.

114. Chappuis F, Sundar S, Hailu A, Ghalib H, Rijal S, Peeling RW, et al. Visceral leishmaniasis: what are the needs for diagnosis, treatment and control? Nat. Rev. Microbiol. 2007;5:873–82.

115. Srividya G, Kulshrestha A, Singh R, Salotra P. Diagnosis of visceral leishmaniasis : developments over the last decade. Parasitol. Res. 2012;110:1065–78.

116. Abass E, Bollig N, Reinhard K, Camara B, Mansour D, Visekruna A, et al. rKLO8, a novel *Leishmania donovani* - derived recombinant immunodominant protein for sensitive detection of visceral leishmaniasis in Sudan. PLoS Negl. Trop. Dis. 2013;7:e2322.

117. Souza AP, Soto M, Costa JML, Boaventura

4.1

VS, De Oliveira CI, Cristal JR, et al. Towards a more precise serological diagnosis of human tegumentary leishmaniasis using *leishmania* recombinant proteins. PLoS One. 2013;8:e66110.

118. Raj VS, Ghosh A, Dole VS, Madhubala R, Myler PJ, Stuart KD. Serodiagnosis of leishmaniasis with recombinant ORFF antigen. Am. J. Trop. Med. Hyg. 1999;61:482–7.

119. Pattabhi S, Whittle J, Mohamath R, El-safi S, Moulton GG, Guderian JA, et al. Design, development and evaluation of rK28-based point-of-care tests for improving rapid diagnosis of visceral leishmaniasis. PLoS Negl. Trop. Dis. 2010;4:e822.

120. Santarém N, Tomás A, Ouaissi A, Tavares J, Ferreira N, Manso A, et al. Antibodies against a *Leishmania infantum* peroxiredoxin as a possible marker for diagnosis of visceral leishmaniasis and for monitoring the efficacy of treatment. Immunol. Lett. 2005;101:18–23.

121. Avila JL, Rojas M, Garcia L. Persistence of elevated levels of galactosyl-alpha (1-3)galactose antibodies in sera from patients cured of visceral leishmaniasis. J. Clin. Microbiol. 1988;26:1842–7.

122. Jensen ATR, Gaafar A, Ismail A, Christensen CB V, Kemp M, El Hassan AM, et al. Serodiagnosis of cutaneous leishmaniasis: assessment of an enzyme-linked immunosorbent assay using a peptide sequence from gene B protein. Am. J. Trop. Med. Hyg. 1996;55:490–5.

123. Bhatia A, Daifalla NS, Jen S, Badaro R, Reed SG, Skeiky YA. Cloning, characterization and serological evaluation of K9 and K26: two related hydrophilic antigens of *Leishmania chagasi*. Mol. Biochem. Parasitol. 1999;102:249–61.

124. Mohapatra TM, Singh DP, Sen MR, Bharti K, Sundar S. Comparative evaluation of rK9 , rK26 and rK39 antigens in the serodiagnosis of Indian visceral leishmaniasis. J. Infect. Dev. Ctries. 2010;4:114–7.

125. Kumar D, Srividya G, Verma S, Singh R, Negi NS, Fragaki K, et al. Presence of anti-Lepp12 antibody: a marker for diagnostic and prognostic evaluation of visceral leishmaniasis. Trans. R. Soc. Trop. Med. Hyg. 2008;102:167–71.

126. Fragaki K, Ferrua B, Mograbi B, Waldispühl J, Kubar J. A novel *Leishmania* infantum nuclear phosphoprotein Lepp12 which stimulates IL1-beta synthesis in THP-1 transfectants. BMC Microbiol. 2003;3:7.

127. Rafati S, Hassani N, Taslimi Y, Movassagh H, Rochette A, Papadopoulou B. Amastin peptide-binding antibodies as biomarkers of active human visceral leishmaniasis. Clin. Vaccine Immunol. 2006;13:1104–10.

128. Sharma V, Chatterjee M, Mandal C, Sen S, Basu D. Rapid diagnosis of indian visceral leishmaniasis using

AchatininH, a 9-O-acetylated sialic acid binding lectin. Am. J. Trop. Med. Hyg. 1998;58:551–4.

129. Bandyopadhyay S, Chatterjee M, Pal S, Waller RF, Sundar S, McConville MJ, et al. Purification, characterization of O -acetylated sialoglycoconjugates-specific IgM , and development of an enzyme-linked immunosorbent assay for diagnosis and follow-up of Indian visceral leishmaniasis patients. Diagn. Microbiol. Infect. Dis. 2004;50:15–24.

130. Menezes-Souza D, Mendes TA de O, Nagem RAP, Santos TT de O, Silva ALT, Santoro MM, et al. Mapping B-cell epitopes for the peroxidoxin of *leishmania* (viannia) braziliensis and its potential for the clinical diagnosis of tegumentary and visceral leishmaniasis. PLoS One. 2014;9:e99216.

131. Hailu A. Pre- and post-treatment antibody levels in visceral leishmaniasis. Trans. R. Soc. Trop. Med. Hyg. 1990;84:673–5.

132. Houghton RL, Petrescu M, Benson DR, Skeiky YA, Scalone A, Badaró R, et al. A cloned antigen (recombinant K39) of *Leishmania chagasi* diagnostic for visceral leishmaniasis in human immunodeficiency virus type 1 patients and a prognostic indicator for monitoring patients undergoing drug therapy. J. Infect. Dis. 1998;177:1339–44.

133. De Almeida Silva L, Romero HD, Prata A, Costa RT, Nascimento E, Carvalho SFG, et al. Immunologic tests in patients after clinical cure of visceral leishmaniasis. Am. J. Trop. Med. Hyg. 2006;75:739–43.

134. Pereira de Oliveira A, Brelaz de Castro MCA, Ferreira de Almeida A, de Assis Souza M, Coutinho de Oliveira B, Reis LC, et al. Comparison of flow cytometry and indirect immuno fluorescence assay in the diagnosis and cure criterion after therapy of American tegumentary leishmaniasis by anti-live *Leishmania (Viannia) braziliensis* immunoglobulin G. J. Immunol. Methods. 2013;387:245–53.

135. Vallur AC, Duthie MS, Reinhart C, Tutterrow Y, Hamano S, Bhaskar KRH, et al. Biomarkers for intracellular pathogens: establishing tools as vaccine and therapeutic endpoints for visceral leishmaniasis. Clin. Microbiol. Infect. 2013;20:O374–83.

136. Singh DP, Sundar S, Mohapatra TM. The rK39 strip test is non-predictor of clinical status for kala-azar. BMC Res. Notes. 2009;2:187.

137. Goswami RP, Das S, Ray Y, Rahman M. Testing urine samples with rK39 strip as the simplest non-invasive field diagnosis for visceral leishmaniasis: an early report from eastern India. J. Postgrad. Med. 2012;58:180–4.

138. Kumar S, Kumar D, Chakravarty J, Sundar S. Identification and characterization of a novel, 37-kilodalton *leishmania donovani* antigen for diagnosis

of Indian visceral leishmaniasis. Clin. Vaccine Immunol. 2011;18:772–5.

139. Zijlstra EE, Nur Y, Desjeux P, Khalil EAG, El-Hassan AM, Groen J. Diagnosing visceral leishmaniasis with the recombinant K39 strip test : experience from the Sudan. Trop. Med. Int. Heal. 2001;6:108–13.

140. Kumar R, Pai K, Pathak K, Sundar S. Enzyme-linked immunosorbent assay for recombinant K39 antigen in diagnosis and prognosis of Indian visceral leishmaniasis. Clin. Diagn. Lab. Immunol. 2001;8:1220–4.

141. Bhattarai NR, Van der Auwera G, Khanal B, De Doncker S, Rijal S, Das ML, et al. PCR and direct agglutination as *Leishmania* infection markers among healthy Nepalese subjects living in areas endemic for Kala-azar. Trop. Med. Int. Heal. 2009;14:404–11.

142. Passos S, Carvalho LP, Orge G, Jerônimo SM, Bezerra G, Soto M, et al. Recombinant *leishmania* antigens for serodiagnosis of visceral leishmaniasis. Clin. Diagn. Lab. Immunol. 2005;12:1164–7.

143. Atta AM, D'Oliveira AJ, Correa J, Atta MLB, Almeida RP, Carvalho EM. Anti-leishmanial IgE antibodies: a marker of active disease in visceral leishmaniasis. Am. J. Trop. Med. Hyg. 1998;59:426–30.

144. Anam K, Afrin F, Banerjee D, Pramanik N, Guha SK, Goswami RP, et al. Immunoglobulin subclass distribution and diagnostic value of *leishmania donovani* antigen-specific immunoglobulin G3 in Indian kala-azar patients. Clin. Diagn. Lab. Immunol. 1999;6:231–5.

145. Afchain D, Desjeux P, La Fuente C, Le Ray D, Cesbron JY, Neyrinck JL, et al. Specific IgE antibodies to *leishmania braziliensis* in patients with mucocutaneous leishmaniasis. Ann. Immunol. 1983;134:311–9.

146. Saha S, Mazumdar T, Anam K, Ravindran R, Bairagi B, Saha B, et al. *Leishmania* promastigote membrane antigen-based enzyme-linked immunosorbent assay and immunoblotting for differential diagnosis of Indian post-kala-azar dermal leishmaniasis. J. Clin. Microbiol. 2005;43:1269–77.

147. Rodriguez B, Beatty R, Belli A, Barreto A, Palacios X, Marin F, et al. Atypical cutaneous leishmaniasis cases display elevated. Parasite Immunol. 2007;29:277–82.

148. Elassad AMS, Younisi SA, Siddig M, Grayson J, Petersen E, Ghalib HW. The significance of blood levels of IgM, IgA, IgG and IgG subclasses in Sudanese visceral leishmaniasis patients. Clin. Exp. Immunol. 1994;95:294–9.

149. Anam K, Afrin F, Banerjee D, Guha SK, Goswami RP, Saha SK, et al. Differential decline in *leishmania* membrane antigen-specific immunoglobulin G (IgG), IgM, IgE, and IgG subclass antibodies in Indian kala-azar patients after chemotherapy. Infect. Immun.

1999;67:6663–9.

150. Gomes IT, Carvalho SFG, Rocha RDR, Peruhype-Magalhães V, Dietze R, Martins-Filho ODA, et al. Anti-*Leishmania chagasi* immunoglobulin G3 detected by flow cytometry for early cure assessment in American visceral leishmaniasis. J. Immunol. Methods. 2010;360:76–83.

151. Fagundes-Silva GA, Vieira-Goncalves R, Nepomuceno MP, de Souza MA, Favoreto S, Oliveira-Neto MP, et al. Decrease in anti-*Leishmania* IgG3 and IgG1 after cutaneous leishmaniasis lesion healing is correlated with the time of clinical cure. Parasite Immunol. 2012;34:486–91.

152. Ghosh AK, Dasgupta S, Ghose AC. Immunoglobulin G subclass-specific antileishmanial antibody responses in Indian kala-azar and post-kala-azar dermal leishmaniasis. Clin. Diagn. Lab. Immunol. 1995;2:291–6.

153. Junqueira Pedras M, Orsini M, Castro M, Passos VMA, Rabello A. Antibody subclass profile against *Leishmania braziliensis* and *Leishmania amazonensis* in the diagnosis and follow-up of mucosal leishmaniasis. Diagn. Microbiol. Infect. Dis. 2003;47:477–85.

154. Mansueto P, Pepe I, Seidita A, Scozzari F, Vitale G, Arcoleo F, et al. Significance of persistence of antibodies against *Leishmania infantum* in sicilian patients affected by acute visceral leishmaniasis. Clin. Exp. Immunol. 2012;12:127–32.

155. Hasker E, Malaviya P, Gidwani K, Picado A, Ostyn B, Kansal S, et al. Strong association between serological status and probability of progression to clinical visceral leishmaniasis in prospective cohort studies in India and Nepal. Satoskar AR, editor. PLoS Negl. Trop. Dis. 2014;8:e2657.

156. Romero HD, Silva LDA, Silva-Vergara ML, Rodrigues V, Costa RT, Guimarães SF, et al. Comparative study of serologic tests for the diagnosis of asymptomatic visceral leishmaniasis in an endemic area. Am. J. Trop. Med. Hyg. 2009;81:27–33.

157. Gangneux JP, Poinsignon Y, Donaghy L, Amiot L, Tarte K, Mary C, et al. Indoleamine 2,3-dioxygenase activity as a potential biomarker of immune supresion during visceral leishmaniasis. Innate Immun. 2013;19:564–8.

158. Kager PA, Hack CE, Hannema AJ, Rees PH, Von dem Borne AEGKR. High C1q levels, low C1s/C1q ratios, and high levels of circulating immune complexes in kala azar. Clin. Immun. and Immunopat. 1982;23:86–93.

159. Sisay Z, Berhe N, Petros B, Tegbaru B, Messele T, Hailu A, et al. Serum chemokine profiles in visceral leishmaniasis, HIV and HIV/ visceral leishmaniasis co-infected Ethiopian patients. Ethiop. Med. J. 2011;49:179–86.

4.1

160. Ansari NA, Ramesh V, Salotra P. Interferon (IFN)– g , Tumor Necrosis Factor – a , Interleukin-6 , and IFN- g receptor 1 are the major immunological determinants associated with post – kala azar dermal leishmaniasis. J. Infect. Dis. 2006;194:958–65.

161. Costa DL, Rocha RL, Carvalho RMA, Lima-neto AS, Harhay MO, Costa CHN, et al. Serum cytokines associated with severity and complications of kala-azar. Pathog. Glob. Heal. 2013;107:78–87.

162. Melby PC, Andrade-narvaez FJ, Darnell BJ, Valencia-pacheco G, Tryon V V, Palomo-cetina A. Increased expression of proinflammatory cytokines in chronic lesions of human cutaneous leishmaniasis. Infect. Immun. 1994;62:837–42.

163. Galdino HJ, Mandaner AE, Pessoni LL, Soriani FM, Pereira LI, Pinto SA, et al. Interleukin 32γ (IL-32γ) is highly expressed in cutaneous and mucosal lesions of American Tegumentary Leishmaniasis patients: association with tumor necrosis factor (TNF) and IL-10. BMC Infect Dis. 2014;14:249.

164. Hoseini SG, Javanmard SH, Hejazi SH, Rafiei L, Zarkesh SH, Karbalaii K, et al. Comparison of immune regulatory factors in acute and chronic lesions of cutaneous leishmaniasis due to *Leishmania major*. J. Res. Med. Sci. 2014;19:S36–40.

165. Milano S, Di Bella G, D'Agostino P, Barbera C, Caruso R, La Rosa M, et al. IL-15 in human visceral leishmaniasis caused by *Leishmania infantum*. Clin. Exp. Immunol. 2002;127:360–5.

166. Rostan O, Gangneux JP, Piquet-pellorce C, Manuel C, McKenzie AN, Guiguen C, et al. The IL-33/ST2 axis is associated with human visceral leishmaniasis and suppresses Th1 responses in the livers of BALB/c mice infected with *Leishmania donovani*. MBio. 2013;4:e00383–13.

167. Sundar S, Reed SG, Sharma S, Mehrotra A, Murray AW. Circulating T Helper 1 (TH1) cell- and TH2 cell-associated cytokines in Indian patients with visceral leishmaniasis. Am. J. Trop. Med. Hyg. 1997;56:522–5.

168. Kumar R, Bumb RA, Salotra P. Correlation of parasitic load with interleukin-4 response in patients with cutaneous leishmaniasis due to *Leishmania tropica*. FEMS Immunol. Med. Micrbiol. 2009;57:239–46.

169. Latifynia A, Khamesipour A, Bokaie S, Khansari N. Antioxidants and proinflamatory cytokines in the sera of patients with cutaneous leishmaniasis. Iran J. Immunol. 2012;9:208–14.

170. Eidsmo L, Wolday D, Berhe N, Sabri F, Satti I, El Hassan AM, et al. Alteration of Fas and Fas ligand expression during human visceral leishmaniasis. Clin. Exp. Immunol. 2002;130:307–13.

171. Zwingenberger K, Harms G, Pedrossa C, Pessoa MC, Scheibenbogen C, Andreesen R. Generation of cytokines in human visceral leishmaniasis: dissociation of endogenous TNF-alpha and IL-1 beta production. Immunobiology. 1991;183:125–32.

172. Amato VS, Andrade HFJ, Amato Neto V, Duarte MIS. Persistence of tumor necrosis factor-alpha in situ after lesion healing in mucosal leishmaniasis. Am. J. Trop. Med. Hyg. 2003;68:527–8.

173. Donaghy L, Gros F, Amiot L, Mary C, Maillard A, Guiquen C, et al. Elevated levels of soluble non-classical major histocompatibility class I molecule human leucocyte antigen (HLA) -G in the blood of HIV-infected patients with or without visceral leishmaniasis. Clin. Exp. Immunol. 2006;147:236–40.

174. Vitale G, Mocciaro C, Gambino G, Spinelli A, Giordano C, Stassi G, et al. Evaluation of serum levels of soluble CD4, CD8 and beta 2-microglobulin in visceral human leishmaniasis. Clin. Exp. Immunol. 1994;97:280–3.

175. Ajdary S, Riazi-rad F, Jafari-shakib R, Mohebbali M. Soluble CD 26 / CD 30 levels in visceral leishmaniasis : markers of disease activity. Clin. Exp. Immunol. 2006;145:44–7.

176. Rai AK, Thakur CP, Kumar P, Mitra DK. Impaired expression of CD26 compromises T-cell recruitment in human visceral leishmaniasis. Eur. J. Immunol. 2012;42:2782–91.

177. Ajdary S, Jafari-Shakib R, Riazi-Rad F, Khamesipour A. Soluble CD26 and CD30 levels in patients with anthroponotic cutaneous leishmaniasis. J. Infect. 2007;55:75–8.

178. Jafari-shakib R, Shokrgozar MA, Nassiri-kashani M, Malakafzali B, Nikbin B, Khamesipour A. Plasma sCD26 and sCD30 levels in cutaneous leishmaniasis. Acta Trop. 2009;109:61–3.

179. Sipsas N, Sfikakist PP, Sfikakist P, Choremi H, Kordossis T. Serum concentrations of soluble intercellular adhesion molecule-1 and progress towards disease in patients infected with HIV. J. Infect. 1994;29:271–82.

180. Abebe T, Hailu A, Woldeyes M, Mekonen W, Bilcha K, Cloke T, et al. Local increase of arginase activity in lesions of patients with cutaneous leishmaniasis in Ethiopia. PLoS Negl. Trop. Dis. 2012;6:e1684.

181. Baccan GC, Oliveira F, Sousa AD, Cerqueira NA, Costa JML, Barral-Netto M, et al. Hormone levels are associated with clinical markers and cytokine levels in human localized cutaneous leishmaniasis. Brain Behav. Immun. 2011;25:548–54.

182. Galindo-Sevilla N, Soto N, Mancilla J, Cerbulo A, Zambrano E, Chavira R, et al. Low serum levels of dehydroepiandrosterone and cortisol in human diffuse

cutaneous leishmaniasis by *Leishmania mexicana*. Am. J. Trop. Med. Hyg. 2007;76:566–72.

183. Bourreau E, Ronet C, Darsissac E, Lise MM, Marie D Sainte, Clity E, et al. In leishmaniasis due to *Leishmania guyanensis* infection, distinct intralesional interleukin-10 and Foxp3 mRNA expression are associated with unresponsiveness to treatment. J. Infect. Dis. 2009;199:576–9.

184. Maretti-Mira AC, de Oliveira-Neto MP, Da-Cruz AM, de Oliveira MP, Craft N, Pirmez C. Therapeutic failure in American cutaneous leishmaniasis is associated with gelatinase activity and cytokine expression. Clin. Exp. Immunol. 2011;163:207–14.

185. Mukhopadhyay D, Das NK, De Sarkar S, Manna A, Ganguly DN, Barbhuiya JN, et al. Evaluation of serological markers to monitor the disease status of Indian post kala-azar dermal leishmaniasis. Trans. R. Soc. Trop. Med. Hyg. 2012;106:668–76.

186. Serarslan G, Yilmaz HR, Söğüt S. Serum antioxidant activities, malondialdehyde and nitric oxide levels in human cutaneous leishmaniasis. Clin. Exp. Dermatol. 2005;30:267–71.

187. Erel O, Kocyigit A, Bulut V, Gurel MS. Reactive nitrogen and oxygen intermediates in patients with cutaneous leishmaniasis. Mem. Inst. Oswaldo Cruz. 1999;94:179–83.

188. Cabrera M, Rodriguez O, Monsalve I, Tovar R, Hagel I. Variations in the serum levels of soluble CD23, nitric oxide and IgE across the spectrum of American cutaneous leishmaniasis. Acta Trop. 2003;88:145–51.

189. Khouri R, Santos GS, Soares G, Costa JM, Barral A, Barral-Netto M, et al. SOD1 plasma level as a biomarker for therapeutic failure in cutaneous leishmaniasis. J. Infect. Dis. 2014;210:306–10.

4.1

Supplementary table 1. Identified potential pharmacodynamic biomarkers for leishmaniasis[a]

Biomarker	Detection techniques	Matrix(ces)	Region(s)	Clinical presen-tation(s)	Biomarker evaluation					Reference(s)
					Time until normalcy	Specificity	Sensitivity (quantitative comparison)	Additional Sensitivity	Geographical applicability	
Direct markers										
Parasite detection										
Parasites in blood	(q)(RT-)PCR, NASBA(-OC), OLIGO-C	Blood	India/France/Netherlands/Nepal/Italy/Sudan	VL	+	++	+	?	++	[14–25,27,28]
Parasites in lesion biopsy	qRT-PCR, QT-NASBA	Lesion biopsy	Netherlands/India/Germany/Israel/Brazil	CL/PKDL	+	++	++	?	++	[17,29–37]
Parasites in skin swab	q(RT-)PCR	(Extra)lesional swab	Colombia/Equador	CL	?	++	+	?	+	[38–40]
Antigen detection										
Carbohydrate antigen	KAtex, ELISA	Urine	Bangladesh/Nepal/Sudan/Brazil/Yemen/Spain/Iran	VL	+	++	+	?	++	[26,44–55]
Indirect markers										
Macrophage-related markers										
IDO	HPLC	Plasma	France	VL	-	?	+	?	?	[157]
ADA	ECM	Serum	India/Nepal	VL	++	+	+	?	+	[59–62]
	ECM	Serum	Turkey	CL	?	+	+	?	?	[63]
MIF	ELISA	Serum	Brazil	VL	?	-	+	?	?	[71,72]
Neopterin	RIA	Serum	Kenya, Brazil,Netherlands	VL	+	?	+	?	++	[57,58]
C1q	RID	Serum	Kenya	VL	+	?	+	?	?	[158]
Cytokines										
CCL3/MIP-1α	ELISA	Serum	Ethiopia	VL	?	+	+	?	?	[159]
CCL4/MIP-1β	ELISA	Serum	Ethiopia	VL	?	+	+	?	?	[159]
CXCL10/IP10	ELISA	Serum	Ethiopia	VL	-	?	+	?	?	[67]
CXCL9/MIg	ELISA	Serum	Ethiopia	VL	-	?	+	?	?	[67]

Biomarker	Detection techniques	Matrix(ces)	Region(s)	Clinical presentation(s)	Time until normalcy	Specificity	Sensitivity (quantitative comparison)	Additional Sensitivity	Geographical applicability	Reference(s)
CD40L	Luminex assay	Serum	Brazil/Bangladesh	VL	+	-	+	?	++	[70,87]
IL-10	CBA/ELISA/MIA	Serum	India/Brazil/Sicily/ Ethiopia	VL/PKDL	+	-	++	+	++	[17,64-69,73, 74,77,82,98, 160,161]
	RT-PCR/qPCR/IHC	Serum/biopsy	French Guiana/Venezue- la/Tunisia/Brazil	CL	?	?	++	++	?	[79–82,162– 164]
IL-12	ELISA	Serum	Iran/Brazil/Ethiopia	VL	++	?	+	?	++	[65,67,69,73, 83,90]
	RT-PCR	Biopsy	Tunisia/Mexico/Brazil	CL	?	?	+	++	++	[76,80,102]
IL-15	ELISA	Serum	Ethiopia, Sicily	VL	?	?	+	?	++	[67,165]
IL-17A	CBA	Serum	Sudan	VL	?	+	+	?	?	[100]
IL-18	ELISA	Serum/Urine	Ethiopia	VL	++	+	+	?	?	[67,103]
IL-27	ELISA	Serum	India	VL	?	?	+	?	?	[78]
IL-32γ	qPCR	Biopsy	Brazil	CL	?	?	+	?	?	[163]
IL-33	ELISA	Serum	France	VL	?	?	+	?	?	[166]
IL-4	ELISA	Serum	Brazil/India	VL	?	?	+	?	-	[17,66,68,69, 83,84,160,167]
	RT-PCR	Biopsy	India/Brazil	CL	?	?	+	++	-	[76,79,81,162 164,168]
IL-6	ELISA/RT-PCR/CBA	Serum	India/Brazil/Sudan/ Ethiopia	VL	++	?	++	-	++	[73,75,77,84, 90,101,160]
	ELISA/RT-PCR/CBA	Biopsy	Europe/Tunesia/Mexico	CL	?	?	+	++	++	[80,92,162, 169]
IL-8/CXCL8	CBA	Serum	Bangladesh/Brazil	VL/CL	?	?	+	?	?	[90,92]
IFN-γ	CBA/ELISA/MIA	Serum	India/Brazil/Sicily/ Ethiopia/Sudan	VL/PKDL	+	+	++	?	++	[65–68,73,74, 77,78,83,97, 99,100,160, 161]

Biomarker evaluation

4.1

Biomarker	Detection techniques	Matrix(ces)	Region(s)	Clinical presen-tation(s)	Biomarker evaluation					Reference(s)
					Time until normalcy	Specificity	Sensitivity (quantitative comparison)	Additional Sensitivity	Geographical applicability	
IFN-γ (cont'd)	RT-PCR	Serum/biopsy	French Guiana/Mexico/Tunisia/Spain	CL	?	?	+	-	?	[79,80,162,164]
sFas/sFasL	ELISA	Serum	Ethiopia/Sudan/India	VL	?	-	+	?	++	[170]
TGF-β	RT-PCR/IHC	Biopsy	India/Brazil/Mexico	CL/PKDL	?	?	+	?	++	[160,162]
TNF-α	CBA/ELISA/IRMA	Serum	Brazil/India/Ethiopia/Sudan	VL/PKDL	++	++	+	?	-	[74,77,83-86,88,90,91,99,100,160,171]
	IRMA/RT-PCR/qPCR/CHL	Serum/biopsy	Brazil/Mexico/Tunisia/Turkey	CL	?	?	+	++	-	[80,92-94,96,160,162,163,169,172]
Cell-surface molecules and circulating receptors										
sHLA-G	ELISA	Serum	French	VL	?	-	+	?	?	[173]
β2-m	ELISA	Serum	Sicily	VL	-	?	+	?	?	[174]
sCD14	ELISA	Serum	Brazil	VL	?	?	+	?	?	[72]
sCD26	ELISA	Serum	Iran/India	VL/CL	?	?	++	?	-	[175–178]
sCD30	ELISA	Serum	Iran	VL/CL	?	?	++	?	?	[175,177,178]
sCD4	ELISA	Serum	Brazil/Sicily	VL	?	?	+	?	++	[57,174]
sCD8	ELISA	Serum	Brazil/Sicily	VL	?	?	++	?	++	[57,174]
sICAM-1	ELISA	Serum	Brazil	VL	?	?	++	?	?	[57,179]
sIL-2R	ELISA	Serum	Brazil/Sicily	VL/PKDL	-	?	++	+	++	[57,70,104–106]
sIL-4R	ELISA	Serum	Kenya	VL	?	+	+	?	?	[106]
sTNFR	ELISA	Serum	Sudan/Brazil	VL	+	?	++	?	++	[86,91]
Acute phase proteins										
AGP	RID	Serum	Kenya	VL	++	?	+	?	?	[107]
CRP	ELISA	Serum	Kenya/India/Sudan	VL	-	?	++	?	++	[75,107–109]

Biomarker	Detection techniques	Matrix(ces)	Region(s)	Clinical presentation(s)	Biomarker evaluation					Reference(s)
					Time until normalcy	Specificity	Sensitivity (quantitative comparison)	Additional Sensitivity	Geographical applicability	
SAA	ELISA	Serum	Kenya	VL	++	?	++	?	?	[107]
Other										
Arginase	ECM	PBMCs/Serum/Lesion biopsy	Brazil/India/Ethiopia	VL/CL/PKDL	++	?	+	-	?	[110–113,180]
Cortisol	RIA	Serum	Brazil/Mexico	CL	?	?	+	?	-	[181,182]
CTLA-4 (CD152)	RT-PCR	Lesion biopcy	India	PKDL	-	?	+	?	?	[82]
DHEA-S	EIA/RIA	Serum	Brazil/Mexico	CL	?	?	+	?	+	[181,182]
Foxp3	RT-PCR	Lesion biopcy	India	PKDL	+	?	+	+	?	[82,183]
MMP2	RT-PCR	Biopsy	Brazil	CL	?	?	++	?	?	[184]
MMP9	Luminex assay	Serum	Brazil/Bangladesh	VL	-	-	+	?	?	[70,87]
NOs	Gries reaction	Serum	India/Turkey/Nepal	VL	?	?	+	?	-	[59,75,185]
	Gries reaction	Serum	Venezuela/Turkey	CL	?	?	+	?	++	[89,186–188]
Prolactin	EIA	Serum	Brazil	CL	?	?	+	++	?	[181]
SOD1	ELISA	Serum	Brazil	CL	+	?	++	?	?	[189]

[a]IDO, indoleamine 2,3-dioxygenase; ADA, adenosine deaminase; MIF, migration-inhibitory factor; CCL, chemokine (C-C motif) ligand; CXCL, chemokine (C-X-C motif) ligand; MIP, macrophage inflammatory protein; Mig, monokine induced by gamma interferon; CD40L, CD40 ligand; IL, interleukin; IFN-, gamma interferon; sFas, soluble Fas; FasL, Fas ligand; TGF-β, transforming growth factor beta; TNF-α, tumor necrosis factor alpha; sHLA, soluble human leukocyte antigen; β2-m, β2-microglobulin; sICAM-1, soluble intercellular adhesion molecule-1; sTNFR, soluble tumor necrosis factor receptor; AGP, alpha-1-acid glycoprotein; CRP, C-reactive protein; SAA, serum amyloid A protein; CTLA-4, cytotoxic T-lymphocyte-associated protein 4; DHEA-S, dehydroepiandrosterone sulfate; MMP, matrix metalloproteinases; NO, nitric oxide; SOD1, superoxide dismutase 1; RT, reverse transcription; NASBA(-OC), nucleic acid sequence-based amplification(-oligochromatography); qPCR, quantitative PCR; QT, quantitative; HPLC, high-performance liquid chromatography; RIA, radioimmunoprecipitation assay; CBA, cytometric bead array; IRMA, immunoradiometric assay; CHL, chemiluminescence; IHC, immunohistochemistry; RID, radial immunodiffusion; RIA, radioimmuneassay; EIA, enzyme immune assay; ECM, enzymatic calorimetric method; KAtex, Latex agglutination test for diagnosis of visceral leishmaniasis; MIA, multiplex immunoassay

4.1

Chapter 4.2

Macrophage activation marker neopterin as a candidate biomarker to predict relapse in visceral leishmaniasis

A.E. Kip
M. Wasunna
F. Alves
J.H.M. Schellens
J.H. Beijnen
A. Musa
E.A.G. Khalil
T.P.C. Dorlo

ABSTRACT

Visceral leishmaniasis (VL) is caused by the *Leishmania* parasite, which replicates within host macrophages, increasing overall macrophage biomass, which subsequently decreases again with waning parasitic infection. The aim of this study was to evaluate neopterin - a macrophage activation marker - as possible pharmacodynamic (PD) marker to monitor VL treatment response, for which recrudescence of parasites (relapse) is a long-term event that is difficult to predict. 497 plasma samples were collected from VL patients in Sudan and Kenya receiving a 28-day miltefosine monotherapy (48 patients) or 11-day combination therapy of miltefosine and liposomal amphotericin B (L-AMB, 48 patients). Neopterin was quantified with ELISA. Values are reported as median (inter-quartile range). Baseline neopterin levels were elevated in all VL patients at 98.8 (63.9-135) nmol/L compared to normal (<10 nmol/L), regressing towards normal levels during treatment. During the first treatment week, levels remained stable for monotherapy patients, but decreased two-fold for combination therapy patients. In combination therapy, neopterin concentrations one day after L-AMB infusion were significantly higher for cured (137 (98.5-197) nmol/L) than for relapsing patients (84.4 (68.9-106) nmol/L), possibly implying an instant immunomodulatory effect of L-AMB on the pro-inflammatory response. The neopterin variable with the highest predictive power of relapse was the increase in neopterin concentration within one month after treatment (ROC AUC of 0.84): at a 1.08 concentration increase ratio, the sensitivity was 93% with a specificity of 65%. This ratio could potentially be used as a surrogate endpoint to identify patients at risk of relapse earlier in the development of new treatment regimens, possibly in a panel of biomarkers to increase its specificity.

INTRODUCTION

Visceral leishmaniasis (VL) is a systemic disease caused by the *Leishmania* parasite. Affecting mostly the poorest of the poor, it remains a high-morbidity neglected tropical disease with over 200,000 new cases and over 20,000 deaths annually [1]. New efficacious, affordable and safe treatments for this devastating disease are urgently needed.

In the last decade, there has been a surge in clinical drug development in VL [2]. As parasite recrudescence occurs in a relatively large proportion of VL patients [3–5], the follow-up period to determine efficacy of new treatment regimens is normally six or even twelve months. To speed up the process of assessing the efficacy of new treatment regimens, sensitive and specific early markers are required that can predict long-term clinical outcomes, to be used in an adaptive trial design with interim analysis. As yet, no longitudinal evaluations of pharmacodynamic markers have been performed in the evaluation of anti-leishmanial therapies [6].

The *Leishmania* parasite resides and replicates within macrophages. Effective control of VL infection is associated with a protective cellular immune response involving interferon-γ (IFN-γ) producing CD4+ and CD8+ cells, activating macrophages to produce free radicals that kill the intracellular *Leishmania* parasites. *Leishmania* infection causes an increase in monocyte load in the infected organs [7,8] and this influx of immature macrophages is required for granuloma formation and the capacity of macrophages to respond to interferon-γ (IFN-γ) [8].

Neopterin, a pteridine biosynthesized from guanosine triphosphate, is excreted by activated macrophages/monocytes and its production therefore mirrors the activation of cellular immunity. The main stimulus for neopterin production is the pro-inflammatory IFN-γ released after T-lymphocyte activation (reviewed in [9,10]). In theory, neopterin release would rise in VL due to macrophage activation and increase in macrophage load during active disease, and subsequently decrease with waning parasitic infection. After its synthesis, neopterin is metabolically stable and excreted via the kidneys by both glomerular filtration and tubular secretion, with a total clearance of 499±79.7 mL/min [11].

Average healthy control neopterin levels (±SD) are 6.78±3.6 nmol/L (n=263) and 5.34±2.7 nmol/L (n=359) for children (<18y) and adults, respectively [12]. In general, 10 nmol/L is taken as the upper limit of normal for healthy control neopterin concentrations. Given that neopterin is released upon macrophage activation, increased neopterin levels are associated with a variety of conditions involving cellular mediated immunity, such as acute viral infections (hepatitis, rubella), intracellular bacterial infections (tuberculosis, leprosy), parasites (malaria) and more (reviewed in [9]). Pre-treatment neopterin levels in VL patients were previously found to be significantly elevated compared to healthy controls with mean concentrations of 32 nmol/L in patients from the *Leishmania chagasi* VL-endemic region Bahia in Brazil [13] and 40 nmol/L in Dutch and Kenyan VL patients [14]. Successful antimonial treatment significantly decreased neopterin levels to healthy control-levels in treatment responders at 30 days post-treatment, but not in refractory patients [13].

The aim of this study was to further evaluate the potential of neopterin as a predictive biomarker in VL in a larger patient population of 96 VL patients by longitudinal neopterin measurements during treatment and up to six months after treatment. In this study, neopterin levels were analysed in VL patients in Kenya and Sudan infected with *Leishmania donovani* receiving either miltefosine monotherapy or a combination therapy of liposomal amphotericin B (L-AMB) and miltefosine. The objective of this study was to characterize neopterin kinetics over time. More importantly, differences in neopterin kinetics between patients that were

4.2

cured and patients that required rescue treatment during or within six months after treatment were evaluated to investigate whether neopterin could be a novel and reliable biomarker for the prediction of treatment relapse in VL patients.

METHODS

Study design and clinical sample collection

Neopterin concentrations were determined as part of a randomized multicentre trial assessing the safety and efficacy of different VL treatments in Eastern Africa [15]. Eligible patients were primary VL cases with parasitological confirmation of VL, aged between 7 and 60 years, HIV negative, and without concomitant severe infection or co-morbidities. Samples originated from patients receiving either a 28-day 2.5 mg/kg/day miltefosine monotherapy (48 patients), or a combination treatment of one dose 10 mg/kg L-AMB on day 1 of treatment, followed by a 10-day 2.5 mg/kg/day miltefosine treatment (48 patients). The study was carried out at three VL treatment centres located in endemic areas: two in Sudan (Dooka and Kassab hospitals) and one in Kenya (Kimalel health center). The study was approved by the national and local Ethics Committees in Kenya (Kenya Medical Research Institute) and Sudan (Institute of Endemic Diseases). The study was explained to all subjects or parents/guardians in their own language and written informed consent was provided before enrollment in the study.

The clinical results and pharmacokinetic analysis of the study are reported elsewhere [15]. Patients that required rescue treatment during treatment or patients who had a fatal outcome before the end of treatment were indicated as "initial treatment failure". Final cure was determined at six months after the end of treatment (day 210). Patients indicated as "relapse" were cured at the end of treatment, but received rescue treatment within six months after treatment due to reappearance of VL clinical signs and symptoms and parasite recrudescence confirmed by microscopy.

To decrease the invasiveness of sampling for patients, neopterin concentrations were quantified in the same samples collected for miltefosine pharmacokinetic analysis [15]. For this reason, baseline samples were taken on the first day of miltefosine treatment before the first miltefosine dose, which in the combination therapy was one day after the L-AMB infusion (study day 2). Real baseline samples were thus only available in the miltefosine monotherapy treatment arm, but were assumed to be equal in the combination therapy arm, since patients were randomized and were balanced with respect to baseline characteristics [15]. Further sampling was performed on study days 4, 7, and 11 (combination therapy), or study days 3, 7, 14 and 28 (monotherapy); and both groups had two samples collected during follow-up at one (day 60) and six months (day 210) after treatment. Plasma was collected from sodium heparin whole blood. Samples were stored and transported at nominally -20°C until analysis.

Analytical method

Neopterin was determined in patient plasma samples with a commercially available ELISA kit (Demeditec, Kiel-Wellsee, Germany), following the manufacturer's instructions. Two calibration curves (0, 1.35, 4.0, 12.0, 37.0, 111 nmol/L) were included in every analysis together with two quality control samples in duplicate. Samples above the upper limit of quantitation were reanalyzed in a 10x dilution with a dilution buffer provided by the manufacturer. The optical density (OD) was measured at 450 nm by an Infinite® M200 Microplate Reader (Tecan,

Männedorf, Switzerland). The OD values were converted to neopterin concentrations from the standard curve using a 4 parameter nonlinear logistic regression model in Prism (version 6.0, GraphPad, La Jolla, CA, USA).

Incurred sample reanalysis was performed for 4% of all samples. The acceptance criterion was adapted from FDA guidelines for bioanalytical method validation [16], and stated that at least two-thirds of the analysed concentrations should be within 20% deviation of the initially analysed concentration.

Neopterin plasma stability at -20°C was reported to be at least six months (in ELISA kit). As incurred sample reanalysis was performed >1.5 years after initial analysis for a proportion of samples, these results were used to assess the influence of long-term storage on neopterin quantification.

Statistical analysis

Data cleaning and interpretation was performed with R (version 3.1.2) and packages "ggplot2", "Hmisc", and "plyr". All values are reported as the median (IQR, interquartile range). In the display of results, nominal time points are depicted instead of actual time points.

Various neopterin variables – absolute neopterin concentrations or relative neopterin concentration changes over time, at different time points during and after treatment - were evaluated for their ability to reliably discriminate between patients that were cured and patients that failed treatment or relapsed. When statistically comparing cured versus relapsed patients, absolute and log-transformed data were checked for normality and equal variances. In general, the two-sided t-test on log-transformed data was used when comparing groups, unless indicated otherwise.

Subsequently, a logistic regression was performed in R to evaluate the significance of the evaluated neopterin variable as a predictor of clinical outcome. Finally, receiver-operating characteristic (ROC) curves were generated with the R package pROC. The interplay between sensitivity and specificity of neopterin as biomarker in isolation was interpreted and the optimal cut-off value was determined with the same package.

RESULTS

Patient population, samples and quality control

A total of 497 plasma samples were available for a total of 96 patients; 48 patients in combination therapy and 48 patients in monotherapy. In both treatment arms, 2 patients experienced initial treatment failure and received rescue treatment before or at the end of treatment. Six patients in the combination therapy arm and nine patients in the monotherapy arm that were initially cured, relapsed within six months of the end of treatment. Samples of patients that received rescue treatment during treatment were only included in the data up to the day they received rescue treatment; subsequent samples were omitted (n=4).

Patient characteristics are depicted in Table 1. Age distribution and gender ratio were comparable between the two treatment arms. When considering initial treatment failure and relapse cases together, treatment failure was more common in children (n=14) than adults (n=5). Patients that relapsed received rescue treatment between day 63 and 217, with the median at day 112, approximately 3 months after treatment.

During treatment, the actual time point for taking samples was within ±15% of the

4.2

Table 1. Demographics of patients included in neopterin analysis.

Parameter	Both arms	Combination therapy arm	Monotherapy arm	Significance
Total no. of patients	96	48	48	n.s.[a]
Female patients [no. (%)]	13 (13.5)	6 (12.5)	7 (14.6)	n.s.[a]
Pediatric patients (≤12 yr) [no. (%)]	47 (49.0)	26 (54.2)	21 (43.8)	n.s.[a]
Age (yr)	15 (7-41)	14 (7-30)	15 (7-41)	n.s.[b]
Body weight (kg)	36 (15-65)	35 (15-59)	37 (16-65)	n.s.[b]
Treatment outcome				
Patients with initial failure [no. (%)]	4 (4.2)	2 (4.2)	2 (4.2)	
Patients with relapse [no. (%)]	15 (15.6)	6 (12.5)	9 (18.8)	n.s.[c]
Patients that cure [no.(%)]	77 (80.2)	40 (83.3)	37 (77.1)	
Treatment centers				
Kimalel, Kenya [no. (%)]	49 (51.0)	25 (52.1)	24 (50.0)	
Kassab, Sudan [no. (%)]	13 (13.5)	6 (12.5)	7 (14.6)	n.s.[c]
Dooka, Sudan [no. (%)]	34 (35.4)	17 (35.4)	17 (35.4)	

All values are given as median (range), unless stated otherwise.
[a]Fisher exact test; [b] Wilcoxon u-test; [c]Chi-square test

nominal time point for taking samples. During follow-up the spread in actual time points was wider, with day 60 at 54-157 days and day 210 at 185-345 days after start of treatment. However, for these time points still >85% of samples were collected within ±15% of the nominal time point.

For all runs, quality control samples were within the acceptable range according to ELISA kit specifications. Incurred sample reanalysis was found to be acceptable (>95% of reanalysed samples were within ±20% deviation of original concentration). Incurred sample reanalysis was also acceptable for the subset (n=12) of samples analysed >1.5 years after initial analysis (11 out of 12 within ±20% deviation). This indicates adequate stability of neopterin in plasma for at least 1.5 years when stored at -20°C.

Baseline neopterin concentrations in active VL patients

As indicated previously, day 1 samples were collected on the first day of miltefosine treatment before the first miltefosine intake, which for the combination therapy was one day after L-AMB infusion (study day 2). True baseline samples were thus only available for the 46 patients in the monotherapy arm. Baseline neopterin levels were above the upper limit of normal (>10 nmol/L) in all VL patients in the monotherapy arm at 98.8 nmol/L (IQR 63.9-135), before the first miltefosine dose (Figure 1). There was a trend towards higher neopterin baseline levels in monotherapy patients cured at the end of treatment (104 nmol/L, IQR 64.9-154) compared to patients requiring rescue therapy during treatment, or within six months after treatment (75.7 nmol/L, IQR 65.4-102) although this was not significant (p=0.448, Table 2). There were no significant differences in baseline neopterin levels between age categories, country and gender.

Table 2. Median neopterin concentration split per treatment arm and treatment outcome.

	Cure		Relapse		Significance (p-value)
	N=	Neopterin concentration (nmol/L)	N=	Neopterin concentration (nmol/L)	
Combination therapy					
Day 2	37	136.6 (98.5-197)	8	84.4 (68.9-106)	0.05395[a]
Day 4	12	123.9 (60.2-305)	2	84.2 (83.6-84.7)	0.5495[b]
Day 7	36	58.2 (38.8-95.1)	6	37.7 (33.1-49.6)	0.1268[a]
Day 11	36	35.0 (25.4-53.3)	7	28.1 (19.4-38.3)	0.3424[a]
Day 60	36	26.3 (14.7-40.2)	5	54.0 (42.0-69.4)	0.01969[a]*
Day 210	28	16.9 (12.0-23.0)	5	15.4 (12.1-17.5)	0.8223[a]
Monotherapy					
Day 1	35	103.6 (64.9-154)	11	75.7 (65.4-102)	0.448[a]
Day 3	14	111.3 (84.6-156)	1	32.0 (N/A)	0.2667[b]
Day 7	36	93.7 (75.8-162)	9	77.8 (60.1-135)	0.2928[b]
Day 14	34	43.5 (28.6-68.1)	10	33.3 (20.6-117)	0.9293[c]
Day 28	35	22.1 (16.5-35.9)	10	21.2 (14.1-42.5)	0.5448[b]
Day 60	36	23.9 (14.2-37.6)	9	40.6 (19.1-61.6)	0.1823[a]
Day 210	30	13.5 (12.0-22.5)	5	10.7 (9.4-72.4)	0.9091[b]

*All values are given as median (inter-quartile range), unless stated otherwise. *p<0.05*
[a]Two-sample t-test on log-transformed neopterin concentrations
[b]Wilcoxon U-test on absolute neopterin concentrations
[c]Welch Two-sample t-test on log-transformed neopterin concentrations with unequal variance
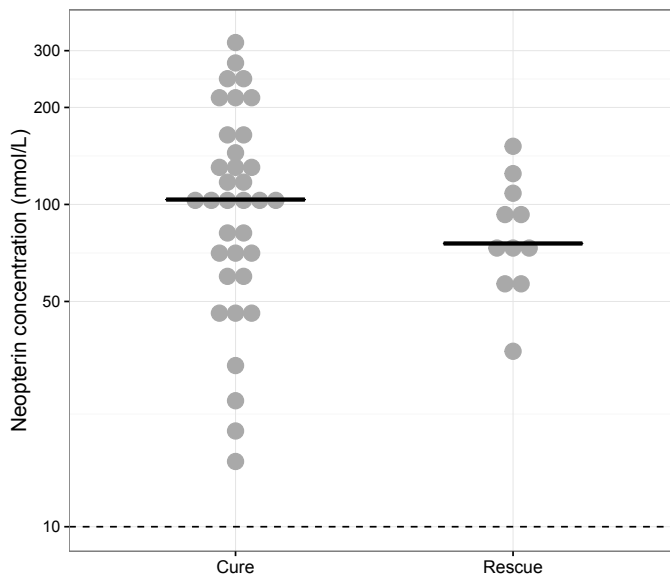

Figure 1. Individual baseline neopterin concentrations (median indicated with horizontal line) in the monotherapy treatment arm - for which baseline samples were available - stratified for patients that were cured ("Cure", n=35) and patients that received rescue treatment during or within six months after treatment ("Rescue", n=11). The dotted line indicates the upper limit of normal in healthy controls (10 nmol/L).

4.2

Neopterin kinetics in two different treatment arms

Interestingly, one day after L-AMB infusion and before the first miltefosine dose, neopterin concentrations in the combination therapy arm were significantly higher (137 nmol/L, IQR 98.5-197) in cured patients, compared to the aforementioned baseline concentration of 98.8 nmol/L in the monotherapy arm (p<0.01). For patients on combination therapy that were initial treatment failures or relapses, neopterin levels were not higher than baseline within one day after L-AMB infusion (84.4 nmol/L, IQR 68.9-106, Table 2).

Figure 2 depicts the differences in neopterin kinetics between the two treatment arms. For both treatment arms neopterin levels regress during treatment to comparable end of treatment concentrations of 33.6 nmol/L (IQR 21.3-52.0, combination therapy, day 11) and 21.9 nmol/L (IQR 16.3-40.0, monotherapy, day 28). There is, however, a difference in the rate of neopterin decline between the two treatment arms. After the aforementioned surge in neopterin concentration during the first treatment day, neopterin concentrations decreased two-fold within the first seven days of treatment in the combination therapy arm to 55.1 nmol/L (IQR 37.2-83.2), while neopterin levels remained unchanged in patients receiving monotherapy with a concentration of 91.3 nmol/L (IQR 65.9-158) after the first week. Interestingly, for both treatment arms, day 210 neopterin concentrations were still elevated (15.5 nmol/L IQR 10.5-22.3, combination therapy, 13.5 nmol/L IQR 11.4-22.9, monotherapy) compared to the normal healthy control levels of <10 nmol/L.
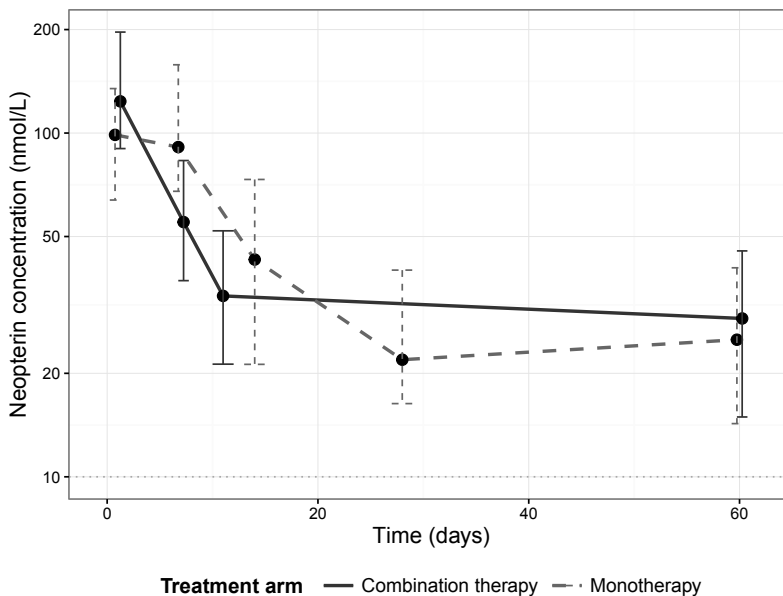

Figure 2. Dynamics of median neopterin concentrations in visceral leishmaniasis patients undergoing a combination therapy of L-AMB and miltefosine (solid line) or miltefosine monotherapy (dashed line). Error bars represent the inter-quartile range (IQR).

Predictive value of neopterin levels for treatment outcome

An important aim of the appraisal of neopterin as a pharmacodynamic biomarker was to relate differences in neopterin levels to clinical outcome using practically evaluable parameters. We

compared absolute neopterin concentrations for treatment cure and failure per treatment arm per time point (Table 2). In addition, we also evaluated relative changes in neopterin dynamics.

<u>Predictive value of absolute neopterin levels for treatment outcome</u>
As described in the previous paragraph, patients on combination therapy that were cured showed significantly higher neopterin concentrations on study day 2 (one day after L-AMB infusion) compared to baseline, which was not observed for patients failing treatment or relapsing. In the same treatment arm, patients that relapsed had a significantly higher neopterin concentration of 54.0 nmol/L at day 60, compared to cured patients (26.3 nmol/L, p<0.05, Table 2). The same trend was observed for the monotherapy treatment arm, though it was not significant (Table 2). When combining the two treatment arms, relapsed patients also showed significantly higher neopterin concentrations (48.0 nmol/L, IQR 29.2-67.5) compared to cured patients (24.9 nmol/L, IQR 14.2-38.9) at day 60 (p<0.05).

Absolute neopterin concentration at day 60 was a significant predictor of relapse in both arms combined and in the combination therapy arm (p<0.05), but not for the monotherapy arm alone.

ROC curves of these parameters are depicted in Figure 3. The area under the curve (AUC) of the ROC was evaluated to assess the parameter's ability to discriminate between patients that were cured and patients that relapsed. In the combination therapy arm, absolute neopterin concentration at day 60 was the best predictor of relapse with an AUC of 0.82 (CI 0.68-0.96) and optimal threshold value of 39.7 nmol/L with corresponding sensitivity of 100% and specificity of 75%. In the monotherapy arm, the absolute neopterin concentration at day 60 was a less reliable predictor of relapse (AUC 0.65), with an optimal cut-off value of 40.2
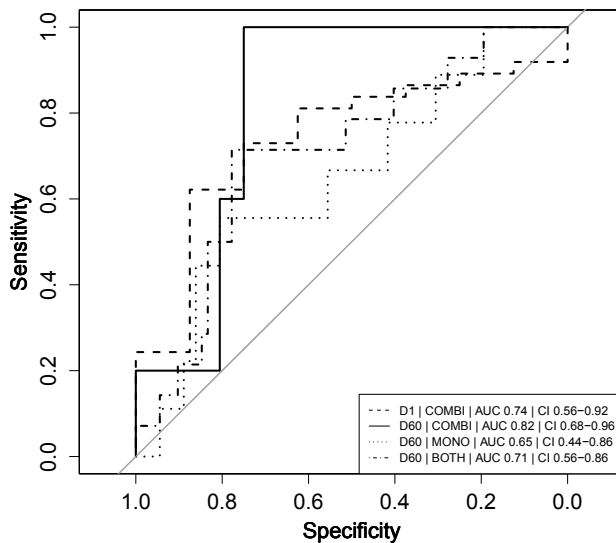

Figure 3. Receiver operator characteristic (ROC) curves of absolute neopterin concentrations as predictors of clinical relapse. Combination therapy is indicated as "COMBI", monotherapy as "MONO" and data of the two arms combined as "BOTH". AUC represents the integrated area under the ROC curve. CI refers to the confidence interval of the calculated AUC. Note that day 1 (D1) neopterin concentrations are evaluated as predictor of cure (cure=1, relapse=0) and day 60 (D60) neopterin concentrations are evaluated as predictor of relapse (relapse=1, cure=0).

4.2

nmol/L and corresponding sensitivity of 56% and specificity of 81%.

Despite the significantly higher neopterin concentrations on study day 2 in combination therapy patients that were cured, this parameter is not a significant predictor of final cure (p=0.0853). The ROC AUC was 0.74 (CI 0.56-0.92) with an optimal threshold value of 122 nmol/L, corresponding to a sensitivity of 62% and specificity of 88%.

Predictive value of relative neopterin levels for treatment outcome
Interestingly, an increase in neopterin concentrations was observed for relapsing patients between end of treatment and day 60 (Table 2), but not for cured patients. Neopterin plasma concentrations at end of treatment and day 60 were available for 80 patients. Relapsing patients (n=14) experienced a significant increase in neopterin levels during the first month after treatment in comparison to patients that remained cured: the ratio of the day 60 neopterin concentration divided by the neopterin concentration at the end of treatment (D60/EoT neopterin concentration ratio) was 2.2 (IQR 1.5-2.8) for patients who relapsed versus 0.78 (IQR 0.53-1.4) for patients who were cured at day 210 (p<0.001, Welch t-test on log-transformed data). For patients that relapsed, there was no correlation between the D60/EoT neopterin concentration ratio and the day they received rescue treatment (linear regression $R^2 = -0.009$).

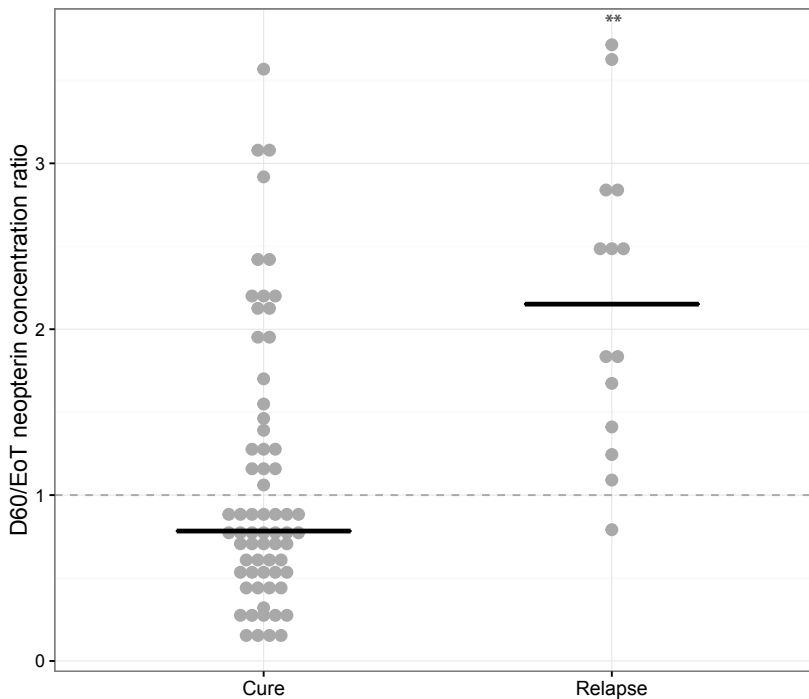The D60/EoT neopterin concentration ratio was a significant predictor of relapse for

Figure 4. D60/EoT neopterin concentration ratio, for cured patients (n=66) and patients that relapsed after treatment (n=14). The dashed line indicates no difference within one month after end of treatment (combination therapy: day 11, monotherapy: day 28). Dots indicate individual observations, the horizontal lines the median per group. ** p<0.001, Welch t-test on log-transformed data.

both arms combined (p<0.001), and the monotherapy (p<0.01) and combination therapy (p<0.05) separately.

ROC curves for the use of the D60/EoT neopterin concentration ratio to predict relapse of disease are depicted in Figure 5. The calculated AUC was 0.84 and the optimal threshold ratio was 1.08 with a sensitivity of 93% and a specificity of 65%. Also, when evaluating the treatment arms separately, AUCs were comparable with optimal threshold values of 0.79 (sensitivity 100%, specificity 56%) for the combination therapy and 1.08 (sensitivity 100%, specificity 65%) for the monotherapy.
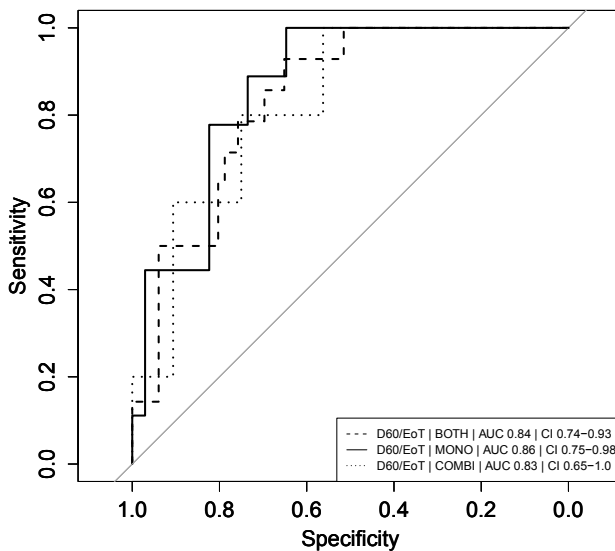

Figure 5. Receiver operator characteristic (ROC) curves of D60/EoT neopterin concentration ratio as predictor for treatment failure (relapse=1, cure=0). Combination therapy is indicated as "COMBI", monotherapy as "MONO" and data of the two arms combined as "BOTH". AUC represents the integrated area under the ROC curve. CI refers to the confidence interval of the calculated AUC.

DISCUSSION

This study is the first to investigate the kinetics of neopterin, a known macrophage activation marker, during treatment and follow-up of VL. Longitudinal analysis of neopterin concentrations during and after miltefosine monotherapy or L-AMB + miltefosine combination therapy, revealed a different profile of neopterin kinetics for the two treatment arms, implying a difference in the drug elicited immune reaction.

Increased neopterin concentrations in VL patients: issue of specificity

This study confirms the increased plasma neopterin concentrations of VL patients prior to treatment, though at a higher baseline neopterin level of 98.8 nmol/L as compared to the previously reported levels of 32 nmol/L [13] and 40 nmol/L [14]. One possible explanation could be that patients in this study were infected with a different *Leishmania* subtype (*L. donovani*), compared to the patients included in previous studies (*L. chagasi* [13], not documented [14]). Neopterin is a nonspecific marker of activated cell-mediated immunity and therefore its

4.2

concentrations are elevated in a large range of infectious diseases [17]. This is an important drawback of its applicability as a pharmacodynamic marker in clinical practice at an individual patient level. The 98.8 nmol/L baseline neopterin level in VL before treatment, however, was higher than observed in other infectious diseases, such as HIV (depending on the stage 16.9-50.0 nmol/L [18]), tuberculosis (21-37.3 nmol/L [19–21]), malaria (21-58 nmol/L [22,23]) and schistosomiasis (17.8 nmol/L [24]). Even HIV co-infected tuberculosis patients had lower baseline neopterin levels (54 nmol/L [19], 24 nmol/L [20]). However, neopterin concentrations at end of treatment and on day 60 were generally at lower concentration levels, comparable to observed concentrations in other infectious diseases. Therefore, the D60/EoT concentration ratio analysis might be more prone to specificity issues in the case of co-infections.

Depending on the purpose of use, the minimally acceptable characteristics of pharmacodynamic biomarkers concerning sensitivity and specificity will differ. Requirements for specificity are less strict in a clinical trial setting, as concomitant disease is often an exclusion criteria. This means neopterin would still be applicable in a well-controlled clinical setting.

Possible differences in immune dynamics between treatment arms
In VL, the activation of CD4$^+$ T cells and differentiation into Th1 cells is crucial for the production of pro-inflammatory IFN-γ and the subsequent promotion of parasite killing in infected macrophages [25]. CD4$^+$ cells produce IL-12 to activate IFN-γ production in T cells. The increased baseline neopterin concentration in VL patients indicates an activation of the Th1 response, as neopterin is a product of pro-inflammatory Th1 activation.

Amphotericin B and its lipid formulation have been found to have differential immunomodulatory properties *in vitro* [26]. While amphotericin B deoxycholate is associated with a strong pro-inflammatory effect, L-AMB has been found to downregulate pro-inflammatory cytokines by diverting signalling from TLR2 to TLR4 *in vitro* [27,28]. The initial surge in neopterin levels within one day after the L-AMB infusion in cured patients, however, suggests that a direct immunomodulatory effect of L-AMB on the pro-inflammatory Th1 response is implicated in cure. A significant rise in pro-inflammatory cytokines was also observed in mice with *Aspergillus flavus* infection treated with L-AMB (AmBisome) [29]. One possible explanation could be that L-AMB positively reinforces and amplifies already persisting immune reactions. The subsequent steep decline in neopterin levels could indicate a decrease in macrophage load and thus neopterin production due to successful activation of intracellular parasite killing and apoptosis.

Many anti-leishmanial modes of action have been described for miltefosine, *inter alia* the alteration of lipid metabolism and membrane lipid composition and the direct stimulation of apoptotic cell death (reviewed in [30]). Besides the direct antileishmanial activity of miltefosine, the drug also has indirect host cell-dependent immunomodulatory properties. Miltefosine enhances the IFN-γ induced elimination of the parasite *in vitro* by increasing the expression of IFN-γ receptors and hereby restoring the IFN-γ responsiveness of macrophages [31]. Additionally the Th1/Th2 balance was restored in infected macrophages *in vitro* by the dose-dependent induction of IL-2 and IL-12 production [31,32], which both induce the pro-inflammatory response. In this study, no increase in pro-inflammatory neopterin upon miltefosine monotherapy was observed, other than the increased neopterin baseline levels.

Miltefosine accumulates in plasma due to its long half-life during the first weeks of treatment, until it reaches a steady-state concentration around 4th week of treatment [33]. The stable neopterin concentration from day 1 to day 7 implies that a certain miltefosine

threshold concentration has to be reached before neopterin levels start to decline after day 7. However, the sparse sampling scheme does not permit more elaborate explanations of the observed effects.

Neopterin concentration elevation at six months post-treatment
Six months post-treatment, neopterin concentrations were still elevated in comparison to the 10 nmol/L that is generally referred to as the upper limit of normal in healthy controls. Healthy endemic control levels were not available in this study. A possible explanation could be a generally higher neopterin level in populations from VL-endemic regions, e.g. due to a higher incidence of other concomitant infections. No studies have been found investigating endemic control levels in Kenya and Sudan, but a recent study in Ethiopia found a healthy control level of 3.8 nmol/L (IQR, 1.6-5.5 nmol/l) [19], which does not support this hypothesis. Lingering immune activation could be an alternative explanation. In patients with chronic infection such as HIV, elevated neopterin concentrations have been found. In HIV patients treated for 3-13 months with zidovudine or didanosine, neopterin concentrations remained elevated above normal levels at approximately 19 nmol/L [34].

Neopterin as a pharmacodynamic biomarker to predict VL relapse
In this study we identified neopterin characteristics that could potentially be used as early predictors of clinical relapse. To accurately discriminate between patients that cure and patients that relapse, the AUC of the ROC was evaluated as a description of sensitivity and specificity. As a general rule, AUCs of 0.7-0.8 are considered acceptable, 0.8-0.9 are considered excellent and >0.9 are considered outstanding [35].

The neopterin variable with the highest predictive power was the D60/EoT neopterin concentration ratio, with an AUC of 0.84. A big advantage of the D60/EoT neopterin concentration over the absolute day 60 neopterin concentration was its high AUC in both treatment arms, and thus the marker can be applied in both therapies. A possible explanation for the difference in predictive ability of relapse of the absolute day 60 neopterin concentration between treatment arms – significant only for the combination therapy - could be that the time period between end of treatment (day 11 for the combination therapy, day 28 for the monotherapy) and the follow-up time point at day 60 is longer for the combination therapy.

The neopterin concentration of a proportion of cured patients also increased within one month after treatment (Figure 4), leading to a relatively low specificity. No explanation could be found in clinical data for this increase: there were no consistent trends in fever, haematological or clinical chemistry parameters, nor were there more co-infections or co-medications reported in cured patients who showed an increase in neopterin concentration within one month after treatment, versus patients that did not show this increase.

Additionally, the initial surge in the neopterin concentration after L-AMB infusion could hold predictive potential, but was not a significant predictor of final cure in this study. Prospective studies will have to confirm its potential, during which more extensive sampling in the first days of treatment will be valuable to better describe kinetics of neopterin before and after initial days of treatment and its potential correlation with long term outcome.

Practical application of neopterin as biomarker
Currently there are no biomarkers to identify patients at risk of relapse when monitoring treated VL patients, nor to establish final cure in the follow-up of clinical trials; this lack of early markers

4.2

of cure is slowing down the development of new antileishmanial treatment regimens. The application of the D60/EoT neopterin concentration ratio could potentially help clinical staff in identifying patients who have an increased risk of relapse and merit further monitoring. For example, if the neopterin surge within one month post treatment exceeds a factor 1.08, the patient could be more intensively and closely followed up, possibly using qPCR to quantify parasite loads in the blood and/or tissue to possibly discover relapse earlier.

As mentioned previously, issues with sensitivity and specificity are less of a problem in clinical trials than in monitoring treatment at an individual patient level in clinical practice. Solutions for a lack of specificity could be to use a panel of biomarkers and to exclude co-infections, as is the case in clinical trials. The implementation of the D60/EoT neopterin concentration ratio marker in routine clinical care is not feasible due to the sampling point one month after treatment.

An advantage of neopterin as pharmacodynamic biomarker is that ELISA kits for its analysis are relatively low cost: a commercial kit costs around 3 euro per sample. A basic laboratory infrastructure is required, however, which is not always available in health centers in disease-endemic regions where VL is being treated.

A simple dipstick assay is available for the semi-quantitative detection of neopterin in serum in resource-limited settings, and has also been tested in VL patients [36], though this assay is possibly not sensitive enough to pick-up the relatively low difference in concentration between end of treatment and day 60. Additionally, a method has been developed to quantify neopterin extracted from dried blood spots with HPLC and fluorescence detection [37,38]. This would significantly reduce the costs of sample storage and shipment. Additionally, neopterin is generally detectable in urine and therefore this non-invasive sample collection method could be further investigated, although its quantitative interpretation remains difficult and it has not yet been evaluated in VL patients.

CONCLUSION & FUTURE PERSPECTIVES

This study is the first evaluation of the clinical relevance of neopterin as a predictor of relapse in VL patients treated with miltefosine monotherapy or a combination therapy with L-AMB. It is the first longitudinal exploration of the kinetics of neopterin in VL patients and the differences in kinetics upon successful treatment or treatment failure. The ratio in neopterin concentration between day 60 and end of treatment was found to be a significant predictor of relapse. At a 1.08 concentration increase ratio, the sensitivity was 93% with a specificity of 65%. In a clinical trial setting, this marker could be used as a surrogate endpoint to identify patients at risk of relapse earlier in the development of new treatment regimens, possibly with a panel of biomarkers to increase its sensitivity and specificity. The use of neopterin as a predictive biomarker for relapse in VL should be formally evaluated in a prospective trial. Due to the sampling point at one month post-treatment, and specificity issues, this marker is not feasible for application in routine clinical care.

ACKNOWLEDGEMENTS

4.2

REFERENCES

1. Alvar J, Vélez ID, Bern C, Herrero M, Desjeux P, Cano J, et al. Leishmaniasis worldwide and global estimates of its incidence. PLoS One. 2012;7.

2. Croft SL, Olliaro P. Leishmaniasis chemotherapy-challenges and opportunities. Clin. Microbiol. Infect. 2011;17:1478–83.

3. Rijal S, Ostyn B, Uranw S, Rai K, Bhattarai NR, Dorlo TPC, et al. Increasing failure of miltefosine in the treatment of Kala-azar in Nepal and the potential role of parasite drug resistance, reinfection, or noncompliance. Clin. Infect. Dis. 2013;56:1530–8.

4. Sundar S, Singh A, Rai M, Prajapati VK, Singh AK, Ostyn B, et al. Efficacy of miltefosine in the treatment of visceral leishmaniasis in India after a decade of use. Clin. Infect. Dis. 2012;55:543–50.

5. Collin S, Davidson R, Ritmeijer K, Keus K, Melaku Y, Kipngetich S, et al. Conflict and Kala-Azar: determinants of adverse outcomes of kala-azar among patients in southern Sudan. Clin. Infect. Dis. 2004;38:612–9.

6. Kip AE, Balasegaram M, Beijnen JH, Schellens JHM, de Vries PJ, Dorlo TPC. Systematic review of biomarkers to monitor therapeutic response in leishmaniasis. Antimicrob. Agents Chemother. 2015;59:1–14.

7. Murray HW, Stern JJ, Welte K, Rubin BY, Carriero SM, Nathan CF. Experimental visceral leishmaniasis: production of interleukin 2 and interferon-gamma, tissue immune reaction, and response to treatment with interleukin 2 and interferon-gamma. J. imm. 1987;138:2290–7.

8. Cervia JS, Rosen H, Murray HW. Effector role of blood monocytes in experimental visceral leishmaniasis. Infect. Immun. 1993;61:1330–3.

9. Hamerlinck FF. Neopterin: a review. Exp. Dermatol. 1999;8:167–76.

10. Hoffmann G, Wirleitner B, Fuchs D. Potential role of immune system activation-associated production of neopterin derivatives in humans. Inflamm. Res. 2003;52:313–21.

11. Estelberge W, Weiss G, Petek W, Paletta B, Wächter H, Reibnegger G. Determination of renal clearance of neopterin by a pharmacokinetic approach. FEBS Lett. 1993;329:13–6.

12. Werner ER, Bichler A, Daxenbichler G, Fuchs D, Fuith LC, Hausen A, et al. Determination of neopterin in serum and urine. Clin. Chem. 1987;33:62–6.

13. Schriefer A, Barral A, Carvalho EM, Barral-Netto M. Serum soluble markers in the evaluation of treatment in human visceral leishmaniasis. Clin. Exp. Immunol. 1995;102:535–40.

14. Hamerlinck FF, van Gool T, Faber WR, Kager PA. Serum neopterin concentrations during treatment of leishmaniasis: useful as test of cure? FEMS Immunol. Med. Microbiol. 2000;27:31–4.

15. Wasunna M, Njenga S, Balasegaram M, Alexander N, Omollo R, Edwards T, et al. Efficacy and safety of AmBisome in combination with sodium stibogluconate or miltefosine and miltefosine monotherapy for African visceral leishmaniasis: phase II randomized trial. PLoS Negl. Trop. Dis. 2016;10:e0004880.

16. US Food and Drug Administration FDA. Guidance for Industry: Bioanalytical Method Validation. 2001. http://www.fda.gov/downloads/Drugs/Guidances/ucm070107.pdf. Accessed 13 Jan 2015.

17. Murr C, Widner B, Wirleitner B, Fuchs D. Neopterin as a marker for immune system activation. Curr. Drug Metab. 2002;175–87.

18. Fuchs D, Jaeger H, Popescu M, Reibnegger G, Werner ER, Kaboth W, et al. Comparison of serum and urine neopterin concentrations in patients with HIV-1 infection. Clin. Chim. Acta. 1990;187:125–30.

19. Skogmar S, Schön T, Balcha TT, Sturegård E, Jansson M, Björkman P. Plasma levels of neopterin and C-reactive protein (CRP) in tuberculosis (TB) with and without HIV coinfection in relation to CD4 cell count. PLoS One. 2015;10:e0144292.

20. Hosp M, Elliott a M, Raynes JG, Mwinga a G, Luo N, Zangerle R, et al. Neopterin, beta 2-microglobulin, and acute phase proteins in HIV-1-seropositive and -seronegative Zambian patients with tuberculosis. Lung. 1997;175:265–75.

21. Cesur S, Aslan T, Hoca NT, Çimen F, Tarhan G, Çifçi A, et al. Clinical importance of serum neopterin level in patients with pulmonary tuberculosis. Int. J. Mycobacteriology. 2014;3:5–8.

22. Thuma PE, Weiss G, Herold M, Gordeuk AR. Serum neopterin, interleukin-4 , and interleukin-6 concentrations in cerebral malaria patients and the effect of iron chelation therapy. Am. J. Trop. Med. Hyg. 1996;54:164–8.

23. Biemba G, Gordeuk VR, Thuma P, Weiss G. Markers of inflammation in children with severe malarial anaemia. Trop. Med. Int. Heal. 2000;5:256–62.

24. Zwingenberger K, Richter J, Siqueira Vergetti JG, Feldmeier H. Praziquantel in the treatment of hepatosplenic schistosomiasis: biochemical disease markers indicate deceleration of fibrogenesis and diminution of portal flow obstruction. Trans. R. Soc. Trop. Med. Hyg. 1990;84:252–6.

25. Kaye P, Scott P. Leishmaniasis: complexity at the host-pathogen interface. Nat. Rev. Microbiol. 2011;9:604–15.

26. Ben-Ami R, Lewis RE, Kontoyiannis DP. Immunocompromised hosts: immunopharmacology of modern antifungals. Clin. Infect. Dis. 2008;47:226–35.

27. Bellocchio S, Gaziano R, Bozza S, Rossi G, Montagnoli C, Perruccio K, et al. Liposomal amphotericin B activates antifungal resistance with reduced toxicity by diverting Toll-like receptor signalling from TLR-2 to TLR-4. J. Antimicrob. Chemother. 2005;55:214–22.

28. Simitsopoulou M, Roilides E, Dotis J, Dalakiouridou M, Dudkova F, Andreadou E, et al. Differential expression of cytokines and chemokines in human monocytes induced by lipid formulations of amphotericin B. Antimicrob Agents Chemother. 2005;49:1397–403.

29. Olson JA, Schwartz J, Hahka D, George A, Proffitt RT, Adler-Moore JP. Differences in efficacy and cytokine profiles following echinocandin or liposomal amphotericin B monotherapy or combination therapy for murine pulmonary or systemic *Aspergillus flavus* infections. Antimicrob. Agents Chemother. 2012;56:218–30.

30. Dorlo TPC, Balasegaram M, Beijnen JH, de Vries PJ. Miltefosine: a review of its pharmacology and therapeutic efficacy in the treatment of leishmaniasis. J. Antimicrob. Chemother. 2012;67:2576–97.

31. Wadhone P, Maiti M, Agarwal R, Kamat V, Martin S, Saha B. Miltefosine promotes IFN-γ-dominated anti-leishmanial immune response. J. Immunol. 2009;182:7146–54.

32. Ghosh M, Roy K, Roy S. Immunomodulatory effects of antileishmanial drugs. J. Antimicrob. Chemother. 2013;68:2834–8.

33. Dorlo TPC, van Thiel PPAM, Huitema ADR, Keizer RJ, de Vries HJC, Beijnen JH, et al. Pharmacokinetics of miltefosine in Old World cutaneous leishmaniasis patients. Antimicrob. Agents Chemother. 2008;52:2855–60.

34. Gisslen M, Norkrans G, Svennerholm B, Hagberg L. The effect on human immunodeficiency virus type 1 RNA levels in cerebrospinal fluid after initiation of zidovudine or didanosine. J. Infect. Dis. 1997;175:434–7.

35. Hosmer DWH, Lemeshow SL. Assessing the fit of the model; Hosmer DWH; Lemeshow SL; editors. Applied logistic regression. New York; 2000. pp. 162. 2nd Editio. New York: Wiley : New York;

36. Bührer-Sekula S, Hamerlinck FF V, Out TA, Bordewijk LG, Klatser PR. Simple dipstick assay for semi-quantitative detection of neopterin in sera. J. Immunol. Methods. 2000;238:55–8.

37. Opladen T, Abu Seda B, Rassi A, Thöny B, Hoffmann GF, Blau N. Diagnosis of tetrahydrobiopterin deficiency using filter paper blood spots: Further development of the method and 5 years experience. J. Inherit. Metab. Dis. 2011;34:819–26.

38. Zurflüh MR, Giovannini M, Fiori L, Fiege B, Gokdemir Y, Baykal T, et al. Screening for tetrahydrobiopterin deficiencies using dried blood spots on filter paper. Mol. Genet. Metab. 2005;86:96–103.

4.2

Chapter 5

| Conclusions & perspectives
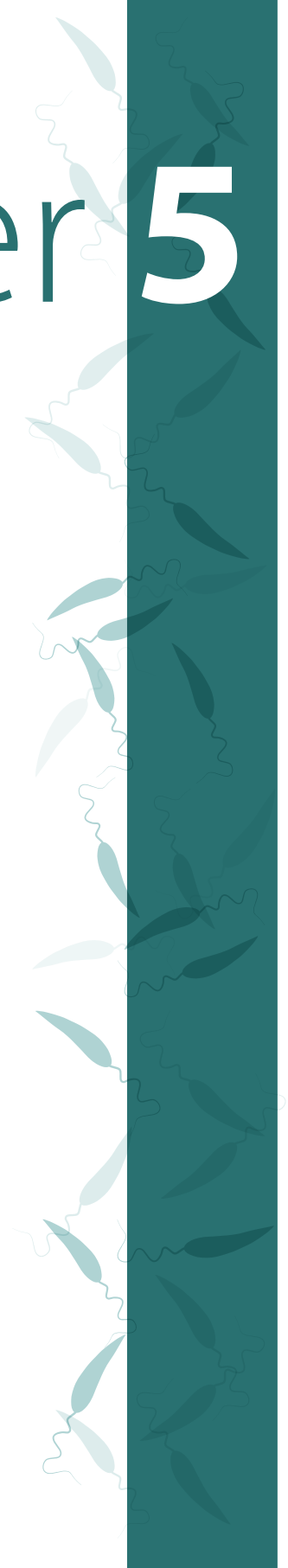
CONCLUSIONS AND PERSPECTIVES

Despite an increase in research efforts in developing more efficacious and less toxic (combination) treatments against the neglected disease leishmaniasis, the efficacy and safety of currently available regimens are not sufficient. Treatment options are especially limited for vulnerable neglected patient populations, such as HIV co-infected and pediatric patients. Though several new chemical entities against leishmaniasis are in various phases of drug development, the process to drug approval and registration of these compounds is slow, expensive and unpredictable, with a high level of attrition [1]. To expand the therapeutic options for leishmaniasis patients it is of utmost importance to optimize treatment with the currently available drugs, either by changing the dosage or length of current regimens of existing monotherapies, or by administering these drugs in combination. Studying the clinical pharmacology of these new regimens is crucial in rationalizing the choice of drugs and dosage and can provide new information on how to further improve treatment.

Especially for tropical neglected diseases, clinical pharmacokinetic studies are often omitted during drug development, or are only performed in small patient populations [2]. For instance, the pharmacokinetics of liposomal amphotericin B, a key component of antileishmanial therapy, has never been evaluated in leishmaniasis patients (**chapter 1**). In addition, pharmacokinetic studies focusing on specific patient populations are generally lacking. For instance, only 11% of pharmacokinetic studies in neglected tropical diseases involved pediatric patients, while children are particularly affected by infection with these diseases. In leishmaniasis, approximately half of the global disease burden is in children between the age of 0 and 14 [3].

This thesis describes the clinical pharmacokinetics of antileishmanial drugs, miltefosine in particular, across endemic regions and in three clinical presentations of leishmaniasis: visceral leishmaniasis, cutaneous leishmaniasis and post-kala-azar dermal leishmaniasis. The clinical studies described in this thesis are focused on the optimization of antileishmanial treatment with existing drugs in pediatric and HIV co-infected leishmaniasis patients, for whom efficacies of antileishmanial treatments are generally lower and pharmacokinetic studies are urgently needed.

In **chapter 1**, we identified that though underexposure in pediatric compared to adult patients has been reported for pentavalent antimony, miltefosine and liposomal amphotericin B, modified dosages for children have only been clinically evaluated for miltefosine. Furthermore, out of the five antileishmanial drugs only pentamidine pharmacokinetics was evaluated in HIV infected patients, while in certain endemic regions up to 40% of visceral leishmaniasis patients is co-infected with HIV [4]. Further pharmacokinetic research has the potential to improve antileishmanial treatment efficacies, specifically in these patient populations.

The development and validation of bioanalytical methods employing less-invasive sampling methods

The reason for the limited number of clinical pharmacokinetic studies for antileishmanial drugs is the challenge of conducting these studies in the resource-poor areas of endemicity of leishmaniasis. Drug quantification in plasma is still the gold standard in pharmacokinetic research to approximate drug exposure at the target site. Venous blood sampling, however, requires an appropriate laboratory set-up, including uninterrupted -20°C storage capacity,

which is logistically complicated, expensive and often not available in these remote areas. In addition, venous sampling is often too invasive for the weakened visceral leishmaniasis patient population, especially for HIV co-infected patients. In these patients, but also for pediatric patients, (extensive) pharmacokinetic sampling is often not ethically acceptable. Dried blood spot (DBS) sampling, on the other hand, is an attractive and less invasive alternative, as DBS samples can be collected by a simple finger-prick and only require a small volume of blood. An additional advantage is the easy and inexpensive storage at room temperature, making it applicable in remote low resource settings. **Chapter 2.1** describes the successful validation of an analytical method to accurately and precisely analyze miltefosine concentrations in DBS.

The influence of hematocrit on method accuracy is the most widely discussed hurdle in the implementation of DBS sampling. Due to variation in hematocrit values, varying blood volumes are collected in sub-punches used for analysis. This could be particularly problematic in visceral leishmaniasis patients, who are typically anemic and for whom hematocrit values generally increase during treatment with clinical improvement. An hematocrit effect on method accuracy could be observed during the bioanalytical validation of the DBS method, which urged the exploration of alternative sampling methods (**chapter 2.2**). However, no effect of hematocrit was observed in the clinical validation for an hematocrit level range of 23.4% to 44.0%. The method was successfully applied in the clinical pharmacokinetic studies described in **chapters 3.3** and **3.4**. This novel sampling technology contributes to easier conduct of pharmacokinetic studies in remote areas and might allow for richer sampling in leishmaniasis patients.

In bioanalysis, one strategy to overcome the hematocrit influence on drug quantification is to collect a volumetrically controlled whole blood sample that is analyzed as a whole, instead of a sub-punch. Volumetric absorptive microsampling (VAMS) was explored as an alternative dried blood sampling method in **chapter 2.2**. The impact of hematocrit on assay accuracy was reduced compared to conventional DBS sampling, although recovery declined with increasing hematocrit, resulting in a reversed but diminished hematocrit effect. The VAMS method performed better than DBS sampling in the bioanalytical validation, introducing less variability when selecting dried blood as a matrix over plasma. No clinical validation of the VAMS method has been performed up to date. Whether VAMS is also performing better in clinical practice, should be investigated by analyzing paired VAMS, DBS and plasma samples. Furthermore, its cost-effectiveness and ease to use in the clinic should be explored.

To facilitate the conduct of future clinical trials investigating new antileishmanial treatment regimens, bioanalytical methods employing the less-invasive, logistically less complicated and more affordable DBS or VAMS sampling, should be developed for other antileishmanial drugs as well. To our best knowledge, these methods have not been developed for paromomycin and amphotericin B, which will be evaluated in future clinical (combination) therapies.

Evaluating the intracellular miltefosine pharmacokinetics
As mentioned, drug quantification in plasma is still the gold standard in pharmacokinetic analysis. The *Leishmania* parasite, however, resides intracellularly within macrophages in the liver, spleen, bone marrow or skin, depending on the subspecies and clinical presentation. The exact mechanism of action of miltefosine is not fully clarified, but multiple hypotheses exist. Though indirect immunomodulatory effects have been described, the direct site of action

of miltefosine is within the cell or cell membrane [5]. Up to now it was unknown if plasma miltefosine concentrations are an appropriate proxy of intracellular miltefosine exposure.

Miltefosine concentrations in peripheral blood mononuclear cells (PBMCs) could possibly be considered a closer approximation of the parasite's miltefosine exposure. With a validated bioanalytical method (**chapter 2.3**), miltefosine concentrations were determined in PBMCs to evaluate the intracellular pharmacokinetics of miltefosine. Interestingly, the intracellular to plasma concentration ratio was 2.17, with a delay in intracellular accumulation. Considering the high protein binding of miltefosine (96-98% [5]), the accumulation of miltefosine in the cell or cell membrane implies high affinity of miltefosine with the membrane or any other intracellular components.

A population pharmacokinetic model was developed simultaneously describing plasma and intracellular miltefosine concentrations (**chapter 3.1**). A lower miltefosine plasma exposure in pediatric compared to adult visceral leishmaniasis patients has previously been reported [6,7] and was recently confirmed and extended to intracellular exposure in PBMCs in cutaneous leishmaniasis patients [8]. With the population PK model, no distinct differences could be identified in the mentioned intracellular accumulation ratio between adults and children. For the first time in cutaneous leishmaniasis patients, exposure-response relationships were explored for miltefosine using a population modelling approach. All miltefosine exposure measures were significantly related to treatment outcome, which could be expected due to their high correlations. In future exposure-response studies, intracellular concentrations can be derived from plasma concentrations with the developed population pharmacokinetic model. Subsequently, derived individual intracellular exposure can be linked to individual *in vitro* susceptibility values (IC_{50}) of clinically isolated strains, to gain a better understanding of the contribution of *Leishmania* susceptibility and miltefosine exposure to treatment outcome.

While drug exposure in PBMCs could be considered a closer approximation of target site exposure than plasma, the parasite's exposure to antileishmanial drugs can more accurately be determined in cutaneous leishmaniasis by quantifying drug concentrations in lesion biopsies. Up to now, this has only been reported for pentavalent antimony (**chapter 1**). Bioanalytical methods could be developed to determine drug concentrations of other antileishmanial drugs, such as miltefosine or paromomycin, in lesion biopsies to facilitate exposure-response studies in cutaneous leishmaniasis.

Pharmacokinetic evaluation of allometric miltefosine dose in children

During the development of miltefosine as an antileishmanial drug, limited pharmacokinetic studies were performed in children and the standard adult 2.5 mg/kg/day linear dosing regimen for 28 days was extrapolated to the pediatric population. As previously mentioned, this resulted in an underexposure in children compared to adults, across endemic areas and clinical presentations [6,8,9]. Clinical efficacy of the 2.5 mg/kg/day miltefosine dose in pediatric compared to adult visceral leishmaniasis patients was lower [10,7,11]. Lower miltefosine exposure contributed to the lower efficacy levels in children, given that miltefosine exposure has been found to be predictive of treatment failure in visceral leishmaniasis [9,12].

After previous simulation studies, an allometric miltefosine dose was proposed in pediatric leishmaniasis patients, administering a higher mg/kg/day dose to children with a low fat-free mass than the linear 2.5 mg/kg/day dosing. In this thesis, two clinical pharmacokinetic evaluations of this allometric miltefosine dosing regimens have been described: in 4 to 12 year

old East African visceral leishmaniasis patients (**chapter 3.2**) and 4 to 17 year old Bangladeshi post-kala-azar dermal patients (**chapter 3.3**).

Both these studies identified an increase in miltefosine exposure in terms of the area under the plasma concentration-time curve from start to day 28 of treatment (AUC_{0-D28}) and an increase in the proportion of pediatric patients reaching the previously described 17.9 µg/mL miltefosine threshold deployed in assessing probability of cure in Nepalese visceral leishmaniasis patients [12]. However, the pharmacokinetic evaluations of this novel miltefosine dosing regimen also showed divergent outcomes between studies. Pediatric Bangladeshi post-kala-azar dermal patients receiving the allometric miltefosine dose achieved accumulated end of treatment concentrations in line with those previously reported in adults and predicted exposure values. In pediatric East African visceral leishmaniasis patients, miltefosine exposure increased in the first weeks of treatment but end of treatment concentrations were considerably lower than in Bangladeshi children and 30% lower than predicted. This illustrates the importance of conducting pharmacokinetic studies in different endemic regions.

A stagnation in miltefosine accumulation in the third week of treatment was observed in East Africa in 37% of patients, which most likely contributed to the lower than predicted miltefosine exposure after allometric dosing, but no explanation for this non-linearity could be found. Furthermore, in accordance with a previous study on the pharmacokinetics of miltefosine after conventional dosing, bioavailability was decreased in the first week of treatment in East African visceral leishmaniasis patients. Both these non-linearities could not be evaluated for the study in Bangladeshi PKDL patients, due to its sparse sampling scheme and descriptive non-compartmental analysis.

While a significant difference in miltefosine exposure was found between male and female patients in the Bangladeshi post-kala-azar dermal patient population (**chapter 3.3**), no such difference was observed in East African visceral leishmaniasis patients. This is in line with the hypothesis that this gender difference could potentially be caused by differences in fat-free mass approximations, which can be expected to differ between regions. A future pooled population analysis of collected pharmacokinetic data from all conducted miltefosine pharmacokinetic studies might improve our understanding and provide us with more reliable body size descriptors to finally update the allometric dose to reach similar exposure levels in male and female pediatric patients, in line with adult exposure.

As expected, the efficacy of allometric miltefosine dosing in pediatric East African visceral leishmaniasis patients is higher than previously observed for conventional 2.5 mg/kg/day dosing. Evaluating the median end of treatment miltefosine concentration - often applied as a simple metric of miltefosine exposure – as a predictor of cure is probably not appropriate due to the observed pharmacokinetic non-linearities. This emphasizes the need to get a better understanding of what determines parasitic response. Identification of the most relevant miltefosine exposure measure is crucial in establishing a relationship with outcome. Pooled population analyses could contribute to identifying the pharmacokinetic targets that determine or influence treatment response.

Pharmacokinetic evaluation of miltefosine and liposomal amphotericin B in HIV co-infected patients

Visceral leishmaniasis has emerged as an important opportunistic infection of HIV in visceral leishmaniasis areas of endemicity. Research on rationalizing treatment of visceral leishmaniasis

patients co-infected with HIV is limited and **chapter 3.4** describes the first pharmacokinetic study performed in this specific patient population. HIV co-infected patients generally react less well to antileishmanial treatment with higher fatality rates [4]. Especially in this specific patient population, relapse frequencies are high, urging the administration of adequate antileishmanial drug dosages to reduce relapse rates and avoid drug resistance.

Miltefosine exposure (AUC_{0-D28}) was 37% lower in HIV co-infected patients compared to previously published data on adult East African visceral leishmaniasis patients not co-infected with HIV. This could have contributed to the observed low cure levels at day 28, considering the established exposure-response relationship of miltefosine in visceral leishmaniasis patients. The 50 mg bi-daily dose could be increased at least to the conventional 2.5 mg/kg daily dose, as patients now received a median dose of 2.1 mg/kg.

A lower miltefosine exposure was observed in patients receiving antiretroviral treatment containing efavirenz, compared to patients who did not receive efavirenz. Further research on the possible influence of efavirenz on miltefosine exposure is required to investigate whether this is a clinically relevant drug-drug interaction.

The lack of amphotericin B pharmacokinetic studies in visceral leishmaniasis patients complicates interpretation of pharmacokinetic results obtained for this drug, given that nothing is known about exposure in non HIV-infected visceral leishmaniasis patients after liposomal amphotericin B administration. Further research on this compound's clinical pharmacokinetics is pivotal for treatment optimization, considering the lower than expected exposure identified in this study compared to amphotericin B exposure in patients treated for other clinical indications.

Additionally, there is little knowledge about what composes the active fraction of liposomal amphotericin B (free fraction or liposome encapsulated). Total amphotericin B exposure in blood plasma is possibly not an appropriate approximation of the (intracellular) parasites' exposure to amphotericin B and free fraction could be more representative. Bioanalytical methods have been developed to analyze the free fraction of amphotericin B, however the free fraction sample isolation is laborious and its application in remote visceral leishmaniasis areas of endemicity complicated.

No significant exposure-response relations could be identified in this study, possibly due to the large variability in amphotericin B drug exposure or the heterogeneity of the HIV co-infected population. These patients receive a multitude of drugs, have compromised and variable immune responses due to HIV infection and are experiencing other co-infections such as malaria or tuberculosis. In the future, a more comprehensive approach to identify a pharmacokinetic-pharmacodynamic relationship should consider CD4 counts or viral load data as covariates.

Identification of potential biomarkers in the monitoring of leishmaniasis treatment response

The last part of this thesis focused on the identification of potential biomarkers as surrogate endpoints to predict final treatment outcome in leishmaniasis. In visceral leishmaniasis, establishing final cure requires long follow-up periods of six or even up to twelve months, slowing down the development of new antileishmanial regimens. The majority of patients cures at the end of a 28-day miltefosine regimen, defined as clinical improvement and negative parasitology in a spleen, liver or bone marrow biopsy. The follow-up period is needed to monitor parasite recrudescence which is observed as relapse of active disease.

Chapter 4.1 provides a systematic overview and discussion of possible markers in monitoring treatment response in leishmaniasis. The need for further longitudinal evaluation of potential pharmacodynamic biomarkers during treatment was emphasized. Longitudinal evaluation of neopterin, one of the markers that we identified as a promising pharmacodynamic biomarker in the systematic literature analysis, was performed in patients either treated with miltefosine in monotherapy or in combination with liposomal amphotericin B (described in **chapter 4.2**). The neopterin-increase between end of treatment and one month after the end of treatment was identified as a potential predictive biomarker for relapse in visceral leishmaniasis, on a population level. To increase specificity, neopterin could be used within a panel of biomarkers. Future efforts should concentrate on identifying the most appropriate markers to increase specificity. A semi-mechanistic population pharmacodynamic model could be developed with the neopterin concentration data, describing the rates of neopterin production and metabolism possibly altered due to active visceral leishmaniasis disease and treatment. This pharmacodynamic model could give a simplified representation of the underlying physiological processes and would allow us to more accurately predict the risk of relapse for visceral leishmaniasis patients.

In addition to investigating neopterin as a biomarker indicating cure or relapse, this chapter also adds to the knowledge on the host immune response to miltefosine and liposomal amphotericin B in visceral leishmaniasis. In the combination therapy, a significant neopterin elevation within one day after liposomal amphotericin B infusion was observed in patients that cure, but not patients that fail treatment. This could indicate that a direct immunomodulatory activity of liposomal amphotericin B on pro-inflammatory neopterin production would be required for cure.

On the other hand, neopterin levels remained stable for one week after start of miltefosine monotherapy, after which levels started to decrease. This coincides with a previous report describing at least a three day lag in the clearance of blood parasite RNA for the miltefosine monotherapy treatment arm, compared to an instant 1 log-decrease in parasite loads for patients treated with a miltefosine combination therapy with liposomal amphotericin B [7]. Combined with the known accumulation of miltefosine due to its long elimination half-life, these results could indicate that a certain miltefosine concentration threshold needs to be reached before miltefosine exerts antileishmanial activity.

The research described in this thesis contributes to the optimization of antileishmanial treatment by describing the clinical pharmacokinetics and pharmacodynamics of miltefosine and liposomal amphotericin B. Moreover, it also provides directions for future research to further rationalize leishmaniasis treatment strategies.

The development of novel bioanalytical assays is of utmost importance in respect to prospective pharmacokinetic studies for leishmaniasis. To facilitate the conduct of these studies, non-invasive and feasible drug quantification methods in DBS could be developed for amphotericin B and paromomycin. Furthermore, bioanalytical assays to quantify antileishmanial drugs in skin lesion tissue can be developed to support future exposure-response studies in cutaneous leishmaniasis.

Several challenges remain to be overcome in the characterization of the clinical pharmacokinetics of miltefosine. What is the best body size descriptor in determining

the optimal miltefosine dose in pediatric patients? How can we explain the differences in miltefosine exposure between East Africa and the Indian subcontinent? What causes the decreased bioavailability at start of treatment observed in East Africa? What is the cause of the observed non-linear stagnation in miltefosine accumulation? Why are HIV co-infected patients relatively lower exposed to miltefosine? Addressing these questions is crucial in the dose optimization for miltefosine, especially in pediatric and HIV co-infected patient populations. Pooling of all available pharmacokinetic data from different leishmaniasis regions of endemicity and for different clinical manifestations, in a population pharmacokinetic analysis, could be an effective method to further characterize and possibly explain the observed non-linearities and geographical disparities.

Future research should focus on establishing appropriate miltefosine exposure targets related to parasitic response and treatment outcome, which could differ per clinical presentation. The proposed pharmacokinetic exposure target for cutaneous leishmaniasis should be investigated in a larger patient cohort. The miltefosine pharmacokinetics in post-kala-azar dermal leishmaniasis patients after allometric dosing could be studied by population pharmacokinetic/pharmacodynamic modelling to more accurately estimate exposure. In assessing exposure-response relations, potential biomarkers should be further evaluated.

In addition to refining our understanding of miltefosine pharmacokinetics, it is key to intensify the clinical pharmacological research on other antileishmanial drugs such as liposomal amphotericin B and paromomycin. A better understanding of the pharmacokinetic and pharmacodynamic properties of antileishmanial drugs will lead to improved and more rational (combination) treatment regimens for the profoundly marginalized leishmaniasis patients.

REFERENCES

1. Chatelain E, Ioset JR. Drug discovery and development for neglected diseases: the DNDi model. Drug Des. Devel. Ther. 2011;5:175–81.

2. Verrest L, Dorlo TPC. Lack of clinical pharmacokinetic studies to optimize the treatment of neglected tropical diseases: a systematic review. Clin. Pharmacokinet. 2016. doi:10.1007/s40262-016-0467-3.

3. Institute for Health Metrics and Evaluation (IHME). GBD Results Tool. Seattle, WA: IHME, University of Washington, 2016. Available from http://ghdx.healthdata.org/gbd-results-tool (Accessed 7 Feb 2017).

4. Alvar J, Aparicio P, Aseffa A, Den Boer M, Cañavate C, Dedet JP, et al. The relationship between leishmaniasis and AIDS: The second 10 years. Clin. Microbiol. Rev. 2008;21:334–59.

5. Dorlo TPC, Balasegaram M, Beijnen JH, de vries PJ. Miltefosine: A review of its pharmacology and therapeutic efficacy in the treatment of leishmaniasis. J. Antimicrob. Chemother. 2012;67:2576–97.

6. Dorlo TPC, Huitema ADR, Beijnen JH, De Vries PJ. Optimal dosing of miltefosine in children and adults with visceral leishmaniasis. Antimicrob. Agents Chemother. 2012;56:3864–72.

7. Wasunna M, Njenga S, Balasegaram M, Alexander N, Omollo R, Edwards T, et al. Efficacy and safety of AmBisome in combination with sodium stibogluconate or miltefosine and miltefosine monotherapy for African visceral leishmaniasis: phase II randomized trial. PLoS Negl. Trop. Dis. 2016;10:e0004880.

8. Castro MM, Gomez MA, Kip AE, Cossio A, Ortiz E, Navas A, et al. Pharmacokinetics of miltefosine in children and adults with cutaneous leishmaniasis. Antimicrob Agents Chemother. 2017; 61(3): e02198-16.

9. Dorlo TPC, Kip AE, Younis BM, Ellis SE, Alves F, Beijnen JH, et al. Reduced miltefosine exposure in East African visceral leishmaniasis patients affects the time to relapse of infection. 2017; Submitted for publication.

10. Ostyn B, Hasker E, Dorlo TPC, Rijal S, Sundar S, Dujardin J, et al. Failure of miltefosine treatment for visceral leishmaniasis in children and men in South-East Asia. PLoS One. 2014;9:e100220.

11. Bhattacharya SK, Sinha PK, Sundar S, Thakur CP, Jha TK, Pandey K, et al. Phase 4 trial of miltefosine for the treatment of Indian visceral leishmaniasis. J. Infect. Dis. 2007;196:591–8.

12. Dorlo TPC, Rijal S, Ostyn B, De Vries PJ, Singh R, Bhattarai N, et al. Failure of miltefosine in visceral leishmaniasis is associated with low drug exposure. J. Infect. Dis. 2014;210:146–53.

Appendix
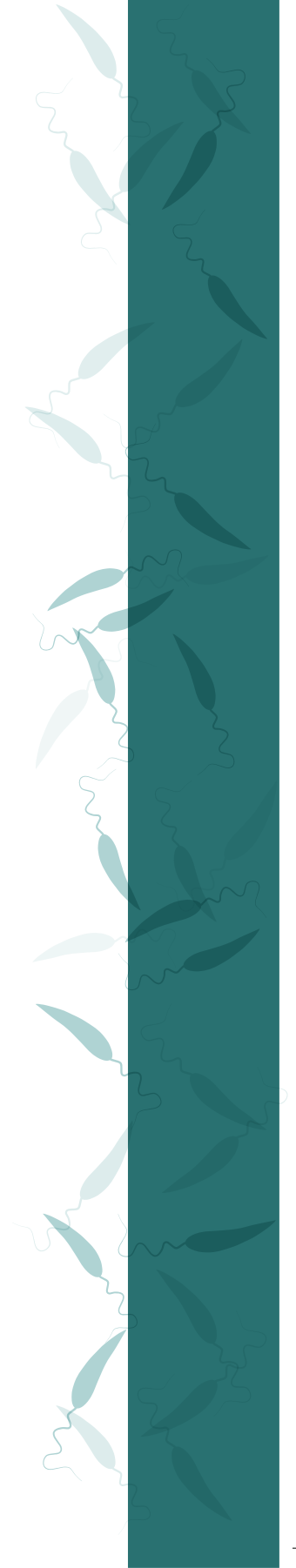
SUMMARY

Leishmaniasis is a tropical infectious disease caused by the *Leishmania* parasite, which is transmitted by the bite of a sand-fly. Its clinical presentation has two main manifestations: an infection of the inner organs spleen and liver (visceral leishmaniasis) or an infection of the skin (cutaneous leishmaniasis). As the disease almost exclusively affects low-income populations in developing countries, with limited availability and access to treatment and research funding, leishmaniasis is referred to as a neglected tropical disease. Treatment options for leishmaniasis are scarce and it is therefore crucial to optimize treatment regimens with the currently available drugs. This thesis focuses on the optimization of antileishmanial therapy by investigating the exposure of patients to antileishmanial drugs (pharmacokinetics, or "what the body does to the drug", **chapter 3**) and the effects of the drug on both the patient's body and parasite (pharmacodynamics, **chapter 4**). In order to explore the pharmacokinetics of drugs, bioanalytical methods were developed, as described in **chapter 2**.

In **chapter 1**, the clinical pharmacokinetics of systemically administered antileishmanial drugs are reviewed, including their absorption, distribution, metabolism and excretion, potential drug-drug interactions, with a focus on special patient populations particularly relevant for leishmaniasis. This review provides a perspective on knowledge gaps in the clinical pharmacokinetics of antileishmanial drugs and could be used to guide future studies in this area.

For decades, the pharmacokinetics of drugs in blood plasma has been considered the gold standard as an approximation for target site exposure of the drug. **Chapter 2** of this thesis describes the development and validation of novel bioanalytical methods to quantify the drug miltefosine, currently the only oral drug in the treatment of leishmaniasis, in other human matrices, either to simplify blood sampling in the remote areas where leishmaniasis is endemic (**chapters 2.1** and **2.2**), or to more accurately approximate the target site exposure (**chapter 2.3**).

Chapter 2.1 describes the bioanalytical and clinical validation of an analytical method to quantify miltefosine in dried blood spots (DBS). The DBS sampling method is a more patient-friendly alternative to the conventional plasma sampling, as only a small volume of blood is collected with a finger-prick. Furthermore, DBS sampling is much simpler and cheaper than plasma sampling due to the storage and shipment at room temperature, making it applicable in the remote regions where leishmaniasis is endemic. The method was successfully validated and the clinical validation showed that plasma and DBS concentrations correlated well. The bioanalytical validation showed an effect of haematocrit on the accuracy of miltefosine quantification in DBS, most probably due to blood volume variation in the sub-punches collected for the analysis. However, no haematocrit effect could be observed in the clinical validation and therefore the method can be implemented in clinical studies without haematocrit correction.

Chapter 2.2 describes the validation of a bioanalytical assay using a very novel alternative dried blood sampling method: volumetric absorptive microsampling (VAMS), a technique with which a precise volume of 10 μL can be sampled from a patient's finger-prick using a sampling device with an absorbent tip, which can be processed as a whole. As expected due

to the fixed volume collection, the effect of haematocrit on the accuracy of the assay in the bioanalytical validation was reduced. However, a decline in recovery could be observed with increased haematocrit levels. In order to consider VAMS as an appropriate and cost-effective alternative to conventional plasma sampling, a clinical validation will be required in the future.

Chapter 2.3 reports the validation of a bioanalytical method to quantify miltefosine in peripheral blood mononuclear cells (PBMCs). The quantification of intracellular miltefosine is particularly of interest as the *Leishmania* parasite resides and replicates within macrophages once it has entered the human host and intracellular miltefosine concentrations are therefore expected to more closely resemble the parasite's exposure to miltefosine. With this successfully validated method, intracellular miltefosine concentrations were determined in cutaneous leishmaniasis patients up to one month after treatment.

The overall theme of **chapter 3** is the pharmacokinetics of antileishmanial drugs in leishmaniasis patients, in particular in vulnerable patient populations such as children and HIV co-infected patients. **Chapter 3.1** describes both the plasma and intracellular pharmacokinetics of miltefosine in Colombian adults and children with cutaneous leishmaniasis. A population pharmacokinetic model was developed describing both the plasma and intracellular miltefosine exposure. Both intracellular and plasma exposure were significantly related to probability of cure in this patient population. An exposure target was proposed, which should be further evaluated in future clinical studies. Furthermore, this study confirmed a significant underexposure to miltefosine in children compared to adults after receiving the conventional dose of 2.5 mg mg/kg/day, proportional to body weight.

Chapters 3.2 and **3.3** describe the evaluation of a novel miltefosine dosing regimen for children, aimed to increase miltefosine exposure to adult levels. In **chapter 3.2**, a new dosing regimen of miltefosine is investigated in paediatric visceral leishmaniasis patients between 4 and 12 years old from Kenya and Uganda, in which patients with a smaller body size received a relatively higher mg/kg dose (between 2.7 and 3.9 mg/kg/day) as opposed to the conventionally administered standardized 2.5 mg/kg/day. A population pharmacokinetic model was developed which identified a decreased bioavailability - fraction of the administered dose that reaches the blood stream from the gut after oral intake - in the first week of treatment. Nevertheless, miltefosine concentrations accumulated to higher levels in the first weeks of treatment, contributing to an increase in total exposure. In addition, variability in exposure declined in comparison to exposure with the conventional mg/kg dose. Both these factors most probably contributed to the observed increase in efficacy of miltefosine in children with this new dosing regimen.

In **chapter 3.3**, the same novel miltefosine dosing regimen is evaluated in 80 children between 4 and 17 years old from Bangladesh with a post-kala-azar-dermal leishmaniasis infection, a skin infection which develops within three years after visceral leishmaniasis infection in 10 to 20% of cases in Southeast Asia. Paediatric miltefosine exposure was increased to adult levels in this patient population after receiving the new dosing regimen. However, female patients reached a significantly lower exposure than males. This disparity in exposure between male and female patients has not been identified previously and could imply that different body size descriptors should be evaluated in determining the appropriate dosing regimen to

overcome these differences.

The pharmacokinetics of the antileishmanial drugs miltefosine and liposomal amphotericin B were evaluated in 30 adult HIV co-infected visceral leishmaniasis patients in Ethiopia, which is described in **chapter 3.4**. In this first description of liposomal amphotericin B pharmacokinetics in visceral leishmaniasis patients, we identified a two-fold lower exposure in patients with visceral leishmaniasis as opposed to previously published data of patients without this infection. Miltefosine exposure was 35% lower in patients with an HIV-visceral leishmaniasis co-infection in comparison to visceral leishmaniasis patients without HIV, only partly explained by the 19% lower dose administered to these patients.

The focus of **chapter 4** is pharmacodynamics in leishmaniasis patients. In visceral leishmaniasis, final cure can only be determined six to twelve months after treatment, as there is a relatively high chance clinical symptoms recur during this period. Therefore there is an urgent need for reliable pharmacodynamic biomarkers to monitor and compare therapies in order to predict clinical outcome earlier during treatment.

The systematic review described in **chapter 4.1**, gives an overview of the markers that have been studied in leishmaniasis patients up to now and that could potentially be used as pharmacodynamic markers. A total of 53 biomarkers were identified and further evaluated based on five criteria: time to normalcy, specificity, sensitivity, association to clinical parameters (such as spleen/liver size) and geographical applicability.

Chapter 4.2 describes the dynamics of one of these markers, the macrophage activation marker neopterin, in a longitudinal analysis amongst 96 visceral leishmaniasis patients in Kenya and Sudan. Neopterin levels are increased in all visceral leishmaniasis patients at start of treatment, compared to healthy human levels. Differences in neopterin concentrations over time were observed between patients enrolled in the miltefosine monotherapy compared to patients receiving a combination treatment of miltefosine with liposomal amphotericin B. Furthermore, patients that experienced a relapse of visceral leishmaniasis in the follow-up period of six months, showed a significantly higher increase in neopterin concentrations within one month after end of treatment than patients that remained cured. Therefore this parameter of neopterin recovery could potentially be used as a surrogate endpoint to identify patients at risk of relapse earlier in the development of new treatment regimens, possibly in a panel of biomarkers to increase its specificity.

In conclusion, this thesis includes the successful validation of various bioanalytical methods to quantify miltefosine in different matrices, applied in several of the described pharmacokinetic studies. We provided a description of intracellular miltefosine accumulation, which could be considered a closer approximation of target site exposure in comparison to plasma. We gained more insight into the pharmacokinetics of miltefosine, especially in particularly vulnerable patient populations such as pediatric and HIV patients. In addition, we provided a first description of the pharmacokinetics of liposomal amphotericin B in visceral leishmaniasis patients. In combination with the clinical pharmacodynamic research conducted, these studies contributed to the further optimization of antileishmanial therapy.

NEDERLANDSE SAMENVATTING

Leishmaniasis is een tropische infectieziekte die wordt veroorzaakt door de *Leishmania* parasiet, welke overgedragen wordt door de beet van een zandvlieg. Er zijn twee typische verschijningsvormen van leishmaniasis: een infectie van de inwendige organen lever en milt (viscerale leishmaniasis) en een infectie van de huid (cutane leishmaniasis). Omdat de ziekte bijna exclusief voorkomt in ontwikkelingslanden en er zeer weinig financiering beschikbaar is voor behandeling van en onderzoek naar deze ziekte, wordt leishmaniasis ook wel een "neglected" of "verwaarloosde" ziekte genoemd. Behandelopties voor patiënten met leishmaniasis zijn beperkt en het is daarom cruciaal om de behandeling met de beschikbare geneesmiddelen te optimaliseren. Dit proefschrift richt zich op de optimalisatie van antileishmaniale behandelingen door het onderzoeken van de blootstelling van patiënten aan geneesmiddelen tegen deze infectieziekte (farmacokinetiek, of "wat het lichaam doet met een geneesmiddel", **hoofdstuk 3**) en het effect van het geneesmiddel op de parasiet of het lichaam van de patiënt (farmacodynamiek, **hoofdstuk 4**). Om de farmacokinetiek van geneesmiddelen te bestuderen, zijn bioanalytische methoden ontwikkeld, welke beschreven zijn in **hoofdstuk 2**.

In **hoofdstuk 1** wordt een overzicht gegeven van de klinische farmacokinetiek van systemisch toegediende antileishmaniale geneesmiddelen, samen met de absorptie, de distributie, het metabolisme en de excretie van de middelen en potentiële geneesmiddelinteracties. Hierbij ligt de focus op speciale patiëntenpopulaties die vooral relevant zijn bij behandeling van leishmaniasis. Dit hoofdstuk geeft inzicht in de hiaten in onze kennis over de klinische farmacokinetiek van deze middelen en kan als richting voor toekomstig onderzoek functioneren.

Hoofdstuk 2 beschrijft de ontwikkeling en validatie van bioanalytische methoden voor de kwantificatie van miltefosine, op dit moment het enige orale geneesmiddel in de behandeling van leishmaniasis, in patiëntenmonsters. Decennialang is de bepaling van geneesmiddelconcentraties in bloedplasma al de gouden standaard ter benadering van de blootstelling aan het geneesmiddel op de plaats van de werking. In **hoofdstuk 2** worden de validaties van drie nieuwe methoden beschreven waarbij miltefosine concentraties bepaald worden in verschillende matrices: ofwel om bloedafname simpeler, goedkoper en patiëntvriendelijker te maken (**hoofdstukken 2.1** en **2.2**), ofwel om tot een betere benadering te komen van de miltefosine concentraties waaraan de parasiet wordt blootgesteld (**hoofdstuk 2.3**).

Hoofdstuk 2.1 beschrijft de bioanalytische en klinische validatie van een methode om miltefosine te kwantificeren in 'dried blood spots' (DBS). De afname van DBS monsters is een patiëntvriendelijker alternatief voor conventionele bloed afname middels een venapunctie, omdat er maar een klein bloedvolume afgenomen wordt met een vingerprik. Verder is een DBS afname makkelijker en goedkoper, omdat opslag en vervoer plaats kan vinden bij kamertemperatuur, waardoor de methode beter toepasbaar is in de afgelegen gebieden waar leishmaniasis heerst. De ontwikkelde methode was accuraat en precies en een goede correlatie tussen plasma en DBS concentraties werd aangetoond. In de bioanalytische validatie werd een effect van hematocriet op de nauwkeurigheid van de methode geïdentificeerd, waarschijnlijk door variatie in het bloedvolume dat wordt uitgeponst bij het opwerken van

de bloedmonsters. Echter, omdat dit effect niet werd geobserveerd in de klinische validatie, kan de DBS methode geïmplementeerd worden in klinische studies zonder correctie voor hematocriet waarde.

Hoofdstuk 2.2 beschrijft de validatie van een bioanalytische methode waarbij gebruik gemaakt wordt van een alternatieve manier van bloedafname, namelijk 'volumetric absorptive microsampling' (VAMS). Daarbij wordt een precies bloedvolume van 10 µL afgenomen uit een vingerprik met een daarvoor speciaal ontwikkeld bloedafnamesysteem en deze 10 µL wordt vervolgens in zijn totaal opgewerkt. In de bioanalytische methode ontwikkeling werd hiermee het effect van hematocriet op de nauwkeurigheid van de methode sterk verminderd. Een afname van extractie opbrengst van miltefosine met toenemende hematocriet waarden, was echter zichtbaar. Of VAMS een geschikt en kosteneffectief alternatief is voor het afnemen van plasmamonsters zal in de toekomst moeten blijken uit een klinische validatie.

Hoofdstuk 2.3 beschrijft de validatie van een bioanalytische methode om miltefosine te kwantificeren in perifere bloed mononucleaire cellen (PBMCs, specifieke witte bloedcellen). Het bepalen van de intracellulaire miltefosine concentratie is vooral interessant omdat de *Leishmania* parasiet zich bevindt in macrofagen en zich daar ook vermenigvuldigt. Intracellulaire miltefosine concentraties zouden daarom een betere benadering kunnen zijn voor de blootstelling van de parasiet aan miltefosine. Met deze methode kunnen intracellulaire miltefosine concentraties tot één maand na behandeling aangetoond worden.

Het centrale thema van **hoofdstuk 3** is de farmacokinetiek van antileishmaniale geneesmiddelen in leishmaniasis patiënten. **Hoofdstuk 3.1** beschrijft de intracellulaire en plasma farmacokinetiek van miltefosine in Colombiaanse volwassenen en kinderen met cutane leishmaniasis. Een wiskundig-statistisch model is ontwikkeld waarin zowel de plasma als de intracellulaire miltefosine blootstelling beschreven wordt. Miltefosine blootstelling was significant gerelateerd aan de kans op genezing in deze patiëntenpopulatie. Een grenswaarde voor blootstelling wordt in dit hoofdstuk voorgesteld, maar zal verder bestudeerd moeten worden in toekomstige prospectieve klinische studies. Verder bevestigt deze studie eerdere bevindingen dat kinderen een lagere blootstelling bereiken dan volwassenen wanneer de conventionele dosering wordt toegediend welke proportioneel aan lichaamsgewicht is (2.5 mg/kg/dag).

Hoofdstukken 3.2 en **3.3** beschrijven de evaluatie van een nieuwe miltefosine dosering in kinderen, gericht op het verhogen van de miltefosine blootstelling naar hetzelfde niveau als in volwassenen. **Hoofdstuk 3.2** beschrijft de farmacokinetiek van deze nieuwe dosering in pediatrische viscerale leishmaniasis patiënten tussen de 4 en 12 jaar oud in Kenia en Oeganda, waarbij patiënten met een kleinere lichaamsgrootte een relatief hogere mg per kg dosering toegediend kregen (tussen de 2.7 en 3.9 mg/kg/dag) in tegenstelling tot de conventionele 2.5 mg/kg/dag. Een populatie farmacokinetisch model werd ontwikkeld waarmee een verlaagde biologische beschikbaarheid – de fractie van de toegediende dosis die uiteindelijk terechtkomt in de bloedstroom vanuit de darmen na orale inname – werd geïdentificeerd gedurende de eerste week van behandeling. Desondanks accumuleerden de miltefosine concentraties naar een hoger niveau in de eerste weken van behandeling dan voorheen geobserveerd na de conventionele dosering, wat bijgedragen heeft aan de verhoging van de totale blootstelling.

Verder was de variabiliteit in blootstelling verlaagd in vergelijking met vorige studies. Beide observaties hebben waarschijnlijk bijgedragen aan de waargenomen verhoogde effectiviteit van de nieuwe miltefosine dosering in kinderen met viscerale leishmaniasis.

In **hoofdstuk 3.3** wordt dezelfde miltefosine dosering geëvaluaeerd in tachtig kinderen uit Bangladesh tussen de 4 en 17 jaar met post-kala-azar dermale leishmaniasis, een huidinfectie die zich ontwikkeld binnen drie jaar na een viscerale leishmaniasis infectie in 10 tot 20% van de patiënten in Zuidoost Azië. De nieuwe miltefosine dosering resulteerde in deze populatie in een verhoging van de blootstelling vergeleken met de conventionele dosering. Vrouwen bereikten echter een significant lagere miltefosine blootstelling dan mannen. Een dergelijk verschil in blootstelling tussen mannen en vrouwen is nog niet eerder beschreven en zou kunnen impliceren dat alternatieve indicatoren voor lichaamsgrootte geëvalueerd moeten worden om tot een adequate dosering te komen die deze verschillen elimineert.

De farmacokinetiek van miltefosine en een ander geneesmiddel tegen leishmaniasis, liposomale amfotericine B, is bestudeerd in dertig volwassen viscerale leishmaniasis patiënten gecoïnfecteerd met HIV in Ethiopië, beschreven in **hoofdstuk 3.4**. Naar ons weten is dit de eerste beschrijving van de farmacokinetiek van liposomale amfotericine B in viscerale leishmaniasis patiënten. De blootstelling aan dit geneesmiddel in deze patiëntenpopulatie was circa tweevoud lager dan eerder gemeten in patiënten zonder viscerale leishmaniasis. Daarbij was ook de miltefosine blootstelling in deze populatie 35% lager dan in viscerale leishmaniasis patiënten zonder HIV, gedeeltelijk te verklaren door de 19% lagere dosis die ze toegediend kregen. In nader onderzoek naar de farmacokinetiek van de geneesmiddelen toegediend in behandeling van HIV, werden geen veranderingen gezien door de simultane toediening van antileishmaniale geneesmiddelen.

De focus van **hoofdstuk 4** ligt op de farmacodynamiek bij leishmaniasis patiënten. Bij viscerale leishmaniasis kan uiteindelijke genezing pas zes tot twaalf maanden na behandeling vastgesteld worden, omdat er een grote kans is dat de klinische symptomen in deze periode weer terugkeren. Er is hierdoor dringend behoefte aan betrouwbare farmacodynamische biomarkers om de uitkomst van behandeling te kunnen voorspellen mede om zo verschillende therapiën met elkaar te kunnen vergelijken in klinische ontwikkeling.

In **hoofdstuk 4.1** wordt een systematisch literatuuroverzicht gegeven van de biomarkers die tot nu toe zijn bestudeerd in leishmaniasis patiënten en dit hoofdstuk geeft richting voor toekomstig onderzoek. In totaal werden er 53 biomarkers geïdentificeerd en geëvalueerd op basis van vijf criteria: tijd tot normaliteit, specificiteit, sensitiviteit, relatie tot andere klinische parameters (zoals milt/lever grootte) en geografische toepasbaarheid.

Hoofdstuk 4.2 beschrijft de dynamiek van één van deze markers, namelijk de macrofaag activatie marker neopterine, in een longitudinale analyse bij 96 viscerale leishmaniasis patiënten in Kenia en Soedan. Neopterine concentraties zijn verhoogd in alle viscerale leishmaniasis patiënten aan het begin van behandeling wanneer deze vergeleken worden met een gezonde populatie. Er bleken verschillen te zijn in neopterine concentraties over tijd tussen patiënten in verschillende behandelarmen (een monotherapie met miltefosine of een combinatie therapie van miltefosine met liposomale amfotericine B). Bij patiënten

waarbij klinische symptomen terugkeerden binnen zes maanden na behandeling, kon een significante stijging in neopterine concentratie vastgesteld worden binnen één maand na behandeling. Deze toename was niet zichtbaar voor patiënten die gedurende deze periode geen klinische symptomen ondervonden. Deze neopterine variabele zou daarom mogelijk kunnen dienen als een biomarker om uitkomst van behandeling te voorspellen, waarschijnlijk in combinatie met andere markers ter verhoging van de specificiteit.

Concluderend kan worden vastgesteld dat in dit proefschrift verschillende bioanalytische methoden succesvol zijn ontwikkeld, welke bijgedragen hebben aan verder farmacokinetisch onderzoek in leishmaniasis. Wij hebben de intracellulaire miltefosine accumulatie beschreven, die beschouwd kan worden als een betere benadering van de miltefosine blootstelling op de plaats van werking dan de bloedconcentratie. Met de farmacokinetische studies beschreven in dit proefschrift hebben we een beter inzicht gekregen in de farmacokinetiek van miltefosine in specifieke patiëntenpopulaties zoals kinderen en HIV patiënten, en hebben we een eerste beschrijving gegeven van de liposomale amfotericine B farmacokinetiek in viscerale leishmaniasis patiënten. In combinatie met het klinische farmacodynamische onderzoek beschreven in dit proefschrift, hebben deze studies bijgedragen aan de verdere optimalisatie van antileishmaniale therapie.

DANKWOORD | ACKNOWLEDGEMENTS

De afgelopen maanden heb ik gewacht op dat ene moment waar velen mij voor waarschuwden: het "Ik ben er he-le-maal klaar mee" moment. Maar ik kan eerlijk zeggen dat zelfs in de laatste maanden van mijn promotietraject, ik vooral weemoedig werd van de gedachte dat deze mooie vier jaren tot een einde zouden komen. En hier heb ik vele mensen voor te danken!

Thomas, ik vond het een eer om jouw eerste PhD student te mogen zijn. Ik heb veel bewondering voor jouw drijvende kracht in het klinisch farmacologisch onderzoek in leishmaniasis en voor je onstuitbare ambitie en motivatie. Ik ben ontzettend dankbaar voor het vertrouwen dat je me hebt gegeven om terug te kunnen keren naar het onderzoek. Naast je onmisbare inhoudelijke ondersteuning hebben we ook veel gelachen. Je stond altijd voor me klaar: ook al woonde je een tijd in Zweden, ik kon bij je terecht. Ik weet zeker dat jouw steun gedurende de laatste maanden van mijn promotie voor een - voor menigeen onverwachte – soepele en stressloze afronding van mijn proefschrift heeft gezorgd. Ergens voelt het vreemd om "ons onderzoek" nu te verlaten, maar het is tijd voor een nieuwe fase. Thomas, bedankt voor alles!

Mijn promotoren prof. dr. Jos Beijnen en prof. dr. Jan Schellens wil ik hartelijk bedanken voor hun begeleiding: ik heb veel van jullie geleerd. Jos, ik ben onder de indruk van jouw passie voor onderzoek en sta versteld van de hoeveelheid werk die je in korte tijd kan verrichten. En het is waar: het komt uiteindelijk allemaal goed! Jan, ik wil je vooral hartelijk danken voor je kritische blik rondom de klinische aspecten van mijn onderzoek. Je gedrevenheid in klinisch onderzoek is bewonderingswaardig.

Hilde, ook al ben ik niet één van "jouw OIOs", je hebt je altijd over mij ontfermd op het lab. Ik wil je bedanken voor alle wijze raad en ondersteuning. Weer een koppige OIO die alles op haar eigen manier wilde doen, maar ik verlaat toch zeker GLP-minded dit lab!

During my PhD project I was very fortunate to have been involved in clinical trials across the globe and I would like to thank everybody that has contributed to the realisation of this thesis.

First and foremost, I want to express my gratitude and appreciation for the patients who were willing to participate in the clinical studies, and their parents/guardians. Despite the sometimes invasive procedures they had to undergo, they contributed to further optimization of antileishmanial therapy, without any self-interest.

I would like to thank the Drugs for Neglected Diseases *initiative* (DND*i*) for the opportunity to be involved in the clinical trials performed in Eastern Africa and the support provided during the past years. Especially these lasts months I could count on the help of many people, providing large amounts of data and feedback in a short time span, for which I am genuinely grateful. At DND*i* Geneva, I especially would like to thank: Fabiana Alves, Jorge Alvar, Séverine Blesson, Alexandra Solomos, Séverine Monnerat. At DND*i* Africa I want to thank: Monique Wasunna, Robert Kimutai, Lilian Were, Peninah Menza, Truphosa Omollo, Brian Mutinda, Josephine Kesusu, Raymond Omollo, and many more. My thanks also goes out to all other members of the LEAP platform – Asrat Hailu, Ermias Diro, Joseph Olobo, Ahmed Musa, Eltahir Khalil, Jane Mbui and the late Rashid Juma. I have learned a lot from you. Thanks all for the pleasant collaboration and the critical appraisal of the manuscripts. I am grateful for your kindness and hospitality during site initiation visits and meetings: I instantly felt that I was part of the team. Who knows what the future brings and I hope to see you again sometime.

At the CIDEIM in Cali, Colombia, I would like to thank Maria Adelaida Gomez, María

del Mar Castro, Nancy Gore Saravia and Alexandra Cossio for the scientific discussions and critical appraisal of the manuscripts. I really appreciate the interest you took in my work and hope to meet you all "in person" someday.

Grateful acknowledgements go out to icddr,b (international centre for diarrhoeal disease research, Bangladesh) for the opportunity to take part in the allometric miltefosine dosing in PKDL study. Dinesh Mondal, thanks for the freedom you gave us in this collaboration and I especially appreciate your responsiveness in the writing of this manuscript.

A special word of thanks I would like to express to the clinical and laboratory teams of the clinical sites: Gondar (Ethiopia), Kacheliba and Kimalel (Kenya), Dooka and Kassab (Sudan), Amudat (Uganda), CIDEIM Cali and Tumaco (Colombia), Mymensingh Medical College Hospital and local upazila hospitals (Bangladesh). Without your precise work in the collection and handling of the clinical samples, the analyses in this thesis would lose all their value.

Mats Karlsson, I want to thank you for the opportunity of spending a month at your research group and for your support during this time. The Uppsala Pharmacometrics group truly is an inspiring group of scientists from whom I learned a lot.

Henk, bedankt dat ik welkom was op het lab van het Koninklijk Instituut voor de Tropen – Biomedical Research. Gerard, het was altijd gezellig om een middagje op het KIT door te brengen. Bedankt voor al je hulp, ik heb veel van je mogen leren.

Lieve keet-familie en "overkant", promoveren dat is één groot feest, maar vooral dankzij jullie: wat ga ik jullie missen. Bedankt voor alle gezellige koffie-pauzes, vrimibo's, kerstdiners, ijspauzes, OIO-weekenden, vier-uurtjes, surprise dansjes etc.

Lotte, het begon allemaal met een avondje Jenga en een verloren fiets, en na drie jaar samen op een kamer is het zo'n vreemde gedachte je niet meer elke dag te zien: wat leuk dat je mijn paranimf (/styliste) wil zijn! Cynthia, bedankt voor al je wijze raad en gezelligheid, heerlijke baksels en treinselfies. Met al je antwoorden op vragen over einde-promotie-traject, leer ik zelfs op afstand nog veel van je. Merel, superleuk dat ik nog een jaartje van je brabantse gezelligheid heb mogen genieten. Ook heb je me ontzettend geholpen in de laatste maanden als ik even een tweede stel hersens nodig had voor de soms onverwachte data, thanks!

Emilie, bedankt voor je luisterend oor tijdens de vele koffiepauzes of etentjes. Ik ben blij dat ik zo vastberaden was je een keer mee te krijgen naar de surprise, want je danst ons er allemaal uit! Bedankt dat je ook tijdens de verdediging als paranimf een extra steun voor mij wil zijn. Ellen, ik mis je nog steeds hoor: vier-uurtjes, verkleedfeestjes maar ook een klankbord de afgelopen jaren (hoe druk je nou een intracellulaire LLOQ uit?..). Reel, computer-camp buddie! Page, Uppsala, wat hebben we eigenlijk veel gedaan samen de afgelopen jaren. Nynke, ik heb veel van je geleerd, bedankt voor je geduld in onze matrix-effect-discussies en voor de gezelligheid op ons kamertje 2. Remy, bedankt dat ik de afgelopen jaren vaak bij je binnen kon lopen voor een ongezouten mening: een goede voorbereiding op de verdediging van mijn proefschrift! ps: je had vast wel eens gelijk. Sven, bedankt voor de vrijdagmiddag-organisatie en al je schouderdansjes. Huixin, thanks for always being helpful and patient with my modelling questions. Vincent en Emilia, wat hebben we een mooi OIO-weekend georganiseerd! Mondharmonica spelen is gewoon niet aan iedereen besteed.. Bedankt ook Jeroen R (oh de nachttrein gaat nu al?), straatgenootje Julie (thanks voor de post!), DE Linda (mede-project-manager), Rose (snel weer ladiesnight?), Markiemark, Maikel, Carla, Willeke, Jill, Sanne, Kimberley, Marit, Hedvig, Semra: THANKS! Ook oud-gedienden Jeroen H, Anita, Nalini, Iris, Afrouz, Jolanda, Jelte, Rik, Geert, Coen, Bart, Bojana, Robin, Didier, Ruud, en de vele

stagiaires de afgelopen jaren: bedankt voor de gezelligheid. Karen, ik wil je daarbij speciaal bedanken voor al je hulp met het Mitra-project.

Met veel plezier ging ik de afgelopen vier jaar naar het lab, en kon zelfs een af en toe falende API3 nog wel aan door de goede sfeer daar. Michel, bedankt voor de vele runs en delen bioanalytisch proza die je hebt nagekeken. Abadi en Niels, het is maar goed dat ik jullie te vriend heb gehouden! Abadi, het turbogas staat uit toch? Niels, ik heb veel van je geleerd en je wist me altijd op te beuren als ik lichtelijk wanhopig werd (dat, en uilensokken). Luc, bedankt voor je hulp (en geduld!) als de API3 het weer eens begaf (waarom gaat de naald nu opeens dóór de well-plate?). Joke, bedankt voor je hulp bij het ontcijferen van de vele samples, altijd gezellig om vakantieverhalen te delen. Bas en Matthijs, bedankt voor jullie contributies in mijn GLP-training. Helaas raken jullie nu een groot-pepernoot-eter kwijt! Lianda, Dieuwke, Ciska, Joke, Nikkie, Bas B, Kees: ik moet echt honderden dingen gevraagd hebben: bedankt voor jullie steun en gezelligheid. Roel, Denise en Yvonne bedankt voor de ondersteuning bij van alles rondom al mijn lab-bezigheden!

Team Sweden! Although I only spend six weeks in Uppsala, I managed to squeeze in 2xUPSS, 2 defense parties, and many more fun evenings. Eva, Anne-Gaëlle, João, Elin, Stein, Philippe, Nebojša, Erik, Flavia, Gunnar, Robin, Anders, Marina, Brendan, and definitely forgetting many: thanks for the great times! Most of all, I want to thank everybody for their help and for letting me pick your brain for a little while. Still waiting for that mug though…

Bedankt lieve vrienden voor jullie interesse in mijn onderzoek en het toleceren van mijn afwezigheid de afgelopen maanden. We maken er een feestje van de 21e! Tamara, een groot deel van onze promotie pieken en dalen hebben we samen gedeeld, vooral in ons huisje in de Boothstraat. Dit heeft onze vriendschap zeker versterkt. Bedankt dat je altijd voor me klaarstaat. Special thanks also to my dear llama family for making me love science and the lab and providing an endless supply of nerdy science jokes.

Opa, u heeft me altijd gemotiveerd om te schrijven. Dat het zo'n dik en ingewikkeld boek zou worden hadden we toen niet gedacht. Oma, u hield altijd goed mijn publicatie-scores bij, een extra stok achter de deur om door te werken!

Lieve pap en mam, bedankt voor de onvoorwaardelijke steun die jullie mij altijd hebben gegeven, ondanks de soms voor anderen onlogische keuzes op mijn carrière-pad. Jullie hebben me altijd gestimuleerd om het meeste en beste uit mijzelf naar boven te halen. In mijn werk, maar zeker ook als persoon, zou ik niet zijn wie en waar ik nu ben zonder jullie.

Lieve Mirjam en Nelleke, ook al zien we elkaar zeker niet zo vaak als ik zou willen, jullie staan altijd voor me klaar. Jullie kennen me door en door en weten altijd de goede dingen te zeggen of te zorgen voor de nodige afleiding. Bedankt zusjes!

Lieve Ruud, bedankt voor je steun en voor het vertrouwen dat je gedurende dit hele traject in mij en mijn kunnen hebt gehad. Ik kan me niemand bedenken met wie ik dit moment beter kan vieren dan met jou.

AFFILIATIONS

F. Alves   Drug for Neglected Diseases *initiative*, Geneva, Switzerland

J. Baker   Centre for Nutrition and Food Security (CNFS), International Centre for Diarrhoeal Disease Research, Bangladesh (ICDDR,B), Dhaka, Bangladesh

M. Balasegaram   Drug for Neglected Diseases *initiative*, Geneva, Switzerland

J.H. Beijnen   Department of Pharmacy & Pharmacology / Department of Clinical Pharmacology, Antoni van Leeuwenhoek Hospital/MC Slotervaart, Amsterdam, the Netherlands Division of Pharmacoepidemiology & Clinical Pharmacology, Utrecht Institute for Pharmaceutical Sciences (UIPS), Utrecht University, Utrecht, the Netherlands

S. Blesson   Drug for Neglected Diseases *initiative*, Geneva, Switzerland

M.M. Castro   Centro Internacional de Entrenamiento e Investigaciones Medicas (CIDEIM), Cali, Colombia

A. Cossio   Centro Internacional de Entrenamiento e Investigaciones Medicas (CIDEIM), Cali, Colombia

E. Diro   Department of Internal Medicine, University of Gondar, Gondar, Ethiopia

T.P.C. Dorlo   Department of Pharmacy & Pharmacology, Antoni van Leeuwenhoek Hospital/MC Slotervaart, Amsterdam, the Netherlands Pharmacometrics group, department of Pharmaceutical Biosciences, Uppsala University, Uppsala, Sweden

M.A. Gomez   Centro Internacional de Entrenamiento e Investigaciones Medicas (CIDEIM), Cali, Colombia

A. Hailu   Department of Microbiology, Immunology, and Parasitology, School of Medicine, Addis Ababa University, Addis Ababa, Ethiopia

M.G. Hasnain   Centre for Nutrition and Food Security (CNFS), International Centre for Diarrhoeal Disease Research, Bangladesh (ICDDR,B), Dhaka, Bangladesh Centre for Clinical Epidemiology and Biostatistics (CCEB), School of Medicine and Public Health, The University of Newcastle (UoN), New South Wales, Australia

M.J.X. Hillebrand   Department of Pharmacy & Pharmacology, Antoni van Leeuwenhoek Hospital/MC Slotervaart, Amsterdam, the Netherlands

R. Juma †   Centre for Clinical Research, Kenya Medical Research Institute, Nairobi, Kenya

E.A.G. Khalil   Institute of Endemic Diseases, University of Khartoum, Sudan

K.C. Kiers	Department of Pharmacy & Pharmacology, Antoni van Leeuwenhoek Hospital/MC Slotervaart, Amsterdam, the Netherlands
R. Kimutai	Drug for Neglected Diseases *initiative*, Nairobi, Kenya
A.E. Kip	Department of Pharmacy & Pharmacology, Antoni van Leeuwenhoek Hospital/MC Slotervaart, Amsterdam, the Netherlands
J. Mbui	Centre for Clinical Research, Kenya Medical Research Institute, Nairobi, Kenya
B. Mengesha	Leishmaniasis Research and Treatment Center, University of Gondar, Gondar, Ethiopia
P. Menza	Drug for Neglected Diseases *initiative*, Nairobi, Kenya
D. Mondal	Centre for Nutrition and Food Security (CNFS), International Centre for Diarrhoeal Disease Research, Bangladesh (ICDDR,B), Dhaka, Bangladesh
M.A. Mural	Centre for Nutrition and Food Security (CNFS), International Centre for Diarrhoeal Disease Research, Bangladesh (ICDDR,B), Dhaka, Bangladesh
A.M. Musa	Institute of Endemic Diseases, University of Khartoum, Sudan
J. Olobo	Makerere University, Kampala, Uganda
H. Rosing	Department of Pharmacy & Pharmacology, Antoni van Leeuwenhoek Hospital/MC Slotervaart, Amsterdam, the Netherlands
N.G. Saravia	Centro Internacional de Entrenamiento e Investigaciones Medicas (CIDEIM), Cali, Colombia
J.H.M. Schellens	Department of Clinical Pharmacology, Antoni van Leeuwenhoek Hospital/MC Slotervaart, Amsterdam, the Netherlands Division of Pharmacoepidemiology & Clinical Pharmacology, Utrecht Institute for Pharmaceutical Sciences (UIPS), Utrecht University, Utrecht, the Netherlands
A. Solomos	Drug for Neglected Diseases *initiative*, Geneva, Switzerland
P.J. de Vries	Division of Internal Medicine, Tergooiziekenhuizen, Hilversum, the Netherlands
M. Wasunna	Drug for Neglected Diseases *initiative*, Nairobi, Kenya
L. Were	Drug for Neglected Diseases *initiative*, Nairobi, Kenya

LIST OF PUBLICATIONS

Kip AE, Kiers KC, Rosing H, Schellens JHM, Beijnen JH, Dorlo TPC. Volumetric absorptive microsampling (VAMS) as an alternative to conventional dried blood spots in the quantification of miltefosine in dried blood samples. Journal of Pharmaceutical & Biomedical Analysis 2017; 135:160-166.

Castro MM, Gomez MA, **Kip AE**, Cossio A, Ortiz E, Navas A, Dorlo TPC, Saravia NG. Pharmacokinetics of miltefosine in children and adults with cutaneous leishmaniasis. Antimicrobial Agents & Chemotherapy 2017; 61(3): e02198-16.

Wasunna M, Njenga S, Balasegaram M, Alexander N, Omollo R, Edwards T, Dorlo TPC, Musa B, Ali MHS, Elamin MY, Kirigi G, Juma R, **Kip AE**, Schoone GJ, Hailu A, Olobo J, Ellis S, Kimutai R, Wells S, Khalil EAG, Strub Wourgaft N, Alves F, Musa A. Efficacy and safety of AmBisome in combination with sodium stibogluconate or miltefosine and miltefosine monotherapy for African visceral leishmaniasis: phase II randomized trial. PLoS Neglected Tropical Diseases 2016; 10(9): e0004880.

Dohmen LCT, Navas A, Vargas DA, Gregory DJ, **Kip AE**, Dorlo TPC, Gomez MA. Functional validation of ABCA3 as a miltefosine transporter in human macrophages: impact on intracellular survival of leishmania (viannia) panamensis. Journal of Biological Chemistry 2016; 291(18): 9638-9647.

Kip AE, Rosing H, Hillebrand MJX, Blesson S, Mengesha B, Diro E, Hailu A, Schellens JHM, Beijnen JH, Dorlo TPC. Validation and clinical evaluation of a novel method to measure miltefosine in leishmaniasis patients using dried blood spot sample collection. Antimicrobial Agents & Chemotherapy 2016; 60(4): 2081-2089.

Kip AE, Rosing H, Hillebrand MJX, Castro MM, Gomez MA, Schellens JHM, Beijnen JH, Dorlo TPC. Quantification of miltefosine in peripheral blood mononuclear cells by high-performance liquid chromatography-tandem mass spectrometry. Journal of Chromatography B 2015; 998-999: 57-62.

Kip AE, Balasegaram M, Beijnen JH, Schellens JHM, de Vries PJ, Dorlo TPC. Systematic review of biomarkers to monitor therapeutic response in leishmaniasis. Antimicrobial Agents & Chemotherapy 2015; 59(1):1-14.
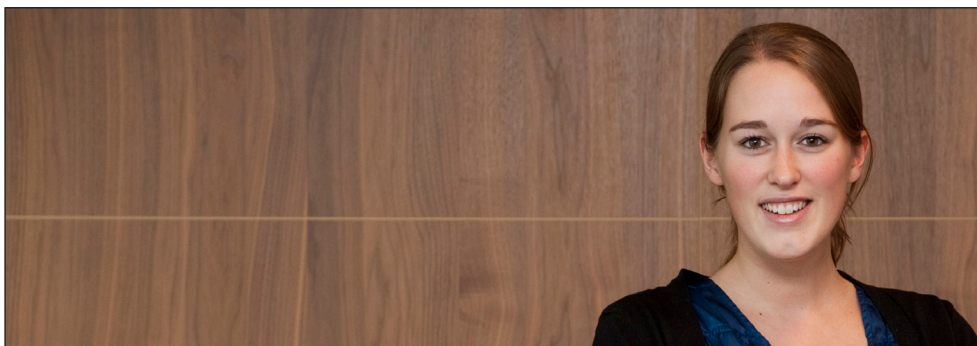
CURRICULUM VITAE

Anke Kip was born June 27th 1987 in Eindhoven and grew up in Limbricht, in the south of the Netherlands. Following high school in 2005, she first got her propaedeutic diploma in chemical engineering from the Technical University of Eindhoven. Subsequently, she continued her bachelor studies at University College Maastricht where she studied life sciences. As part of her bachelors program, she spend a semester at the University of California in Los Angeles (UCLA), focusing on immunology and microbiology. She started the master studies Drug Innovation at Utrecht University in 2009 with a major research elective at the Cellular Architecture and Dynamics department of Utrecht University. Her research focussed on the identification and characterization of llama heavy chain only antibody fragments (VHH) against the CD4 and CCR5 binding site of HIV-1.

After graduating in 2011, Anke worked as a strategy consultant at Boston Consulting Group (BCG). She started her PhD in February 2013 at the Slotervaart hospital, later Antoni van Leeuwenhoek hospital, supervised by dr. T.P.C. Dorlo, prof. dr. J.H. Beijnen and prof. dr. J.H.M Schellens. In parallel, she also followed the Drug Innovation PhD training program of Utrecht University. She received the EPASG grant for a one-month elective training period at the Pharmacometrics group of prof. dr. Mats Karlsson at Uppsala University, Sweden.

Her PhD project resulted in this thesis which she will defend on June 21st 14:30.